Enhanced Oil Recovery by Carbonated (CO_2-Enriched) Water Injection

Seyyed Mojtaba Seyyedi Nasooh Abad

Submitted for the degree of Doctor of Philosophy

Heriot-Watt University

School of Energy, Geoscience, Infrastructure and Society,

Institute of Petroleum Engineering

Oct 2016

ABSTRACT

Different enhanced oil recovery (EOR) scenarios have been developed to recover the residual oil remain in the reservoirs after waterflooding. Carbonated (CO2-enriched) water injection (CWI) is one of the currently emerging EOR scenarios which was thoroughly investigated in this study. The main objectives of this thesis are to: (1) quantify the level of additional oil recovery by CWI, and (2) identify the underlying mechanisms by which the additional oil is recovered. The above objectives are investigated via a series of integrated experimental studies.

The results of high-pressure high-temperature micromodel experiments revealed a novel oil recovery mechanism by CWI. CO_2 partitioning between carbonated water (CW) and ‘’live’’ oil leads to rapid formation and growth of a gaseous new phase inside the oil which would hugely boost the performance of CWI and represents a game-changer for this EOR technique. Furthermore, the results of contact angle measurements revealed carbonated water has a significant impact on the rock wettability state.

Next, a series of coreflood experiments were performed to study the potential of CWI for improving oil recovery at core scale. The results of coreflood experiments revealed the promising potential of CWI for improving oil recovery either as a secondary or tertiary injection scenario. A series of high-pressure imbibition experiments were performed in this thesis, to investigate the potential of CW on spontaneous imbibition. Results revealed that CW has a significant potential for increasing the amount of imbibed water and consequently oil recovery.

Finally, a series of multiple-contact (PVT) experiments were performed to study the phase behaviour of the crude oil, when contacts with the injected CW. The results of these experiments revealed that the new phase forms immediately, when ‘’live’’ oil contacts with the CW with further growth at subsequent contacts. The new phase is composed of a multi-component hydrocarbon mixture starting with CH4 and CO2 in earlier stages and becoming richer towards the latter contacts. Furthermore, the performance of CWI in a long porous medium was studied to investigate the effectiveness of CWI and its displacement front propagations away from the injection point. The outcomes of this integrated investigation would help us in better understanding the oil recovery mechanisms of CWI and its true potential under realistic reservoir conditions. This would enable us to identify and target suitable oil reservoirs for this EOR technique.

DEDICATION

To my lovely parents and sisters for their continuous support throughout my study

Acknowledgment

I would like to express my sincere appreciation to my supervisors Prof. Mehran Sohrabi for his outstanding technical guidance and support throughout my study. His extensive knowledge on this area and constant encouragement has been invaluable for the successful completion of this thesis.

The financial support of Heriot-Watt University during my study through a full scholarship is highly appreciated. This work was carried out as part of the ongoing Enhanced Oil Recovery by Carbonated Water Injection (CWI) joint industry project (JIP) in the Institute of Petroleum Engineering of Heriot-Watt University. The project is equally sponsored by ADCO, BG Group, Eni, Galp Energia, Oil India, and the UK DECC, which is gratefully acknowledged.

I would like to thank my good friend Dr. Pedram Mahzari for his invaluable technical support and motivation throughout my study. I would like also to tank my good friend Dr. Reza Haghi for his support and motivation during my PhD.

I also want to thank Mr. Shaun Ireland, Mr. Adam Sisson, Dr. Amir Farzaneh, and everyone in the Institute of Petroleum Engineering of Heriot-Watt University for helping me with lab equipment related and study issues, which made my research possible.

Thank you very much to Dr. Morteza Haghighatsefat and Dr. Nejat Rahmanian for accepting to be my examiners and also for their constructive comments.

Finally, my deepest and special thanks go to my parents and my sisters who support me throughout my study from undergraduate until now.

DECLARATION STATEMENT

(Research Thesis Submission Form should be placed here)

TABLE OF CONTENTS

TABLE OF CONTENTS i

LISTS OF FIGURES iv

LISTS OF Tables x

LISTS OF PUBLICATIONS BY THE CANDIDATE xi

Chapter 1: Introduction 12

1.1 Introduction 12

1.2 Sweep Efficiency 14

1.3 Carbonated Water Injection 14

1.3.1 Literature Review of CWI (Experimental Studies) 14

1.3.2 CWI Field Experience 19

1.4 Thesis Content 21

Chapter 2: Pore Scale Investigations of CWI 25

2.1 Introduction 25

2.2 Experimental Setup and Procedure 25

2.2.1 Micromodel Rig 25

2.2.2 Fluids Properties 29

2.2.3 Image Analysis of the Micromodel Experimental Results 31

2.2.4 Methodology 33

2.3 Experimental Results and Discussion 34

2.3.1 Dead Oil System 34

2.3.2 Live Oil System 37

2.4 Conclusion 52

Chapter 3: Wettability Alteration by Carbonated Water-Contact Angle Measurements 55

3.1 Introduction 55

3.2 Experimental Setup and Procedure 56

3.2.1 Contact Angle Rig 56

3.2.2 Fluids 58

3.2.3 Solid Substrates 59
3.2.4 Experimental Procedure 59
3.3 Results and Discussion 61
3.3.1 Un-aged System 61
3.3.2 Aged System 69
3.4 Conclusion 74
Chapter 4: Coreflooding Studies 76
4.1 Introduction 76
4.2 Experimental Setup and Procedure 77
4.2.1 Coreflood Rig 77
4.2.2 Fluids Properties 78
4.2.3 Core Properties 78
4.2.4 Methodology 82
4.3 Coreflood Experiments Results 84
4.3.1 Coupling Impacts of New Phase Formation and Wettability Alteration 84
4.3.2 Impact of Carbonation Level of CW 98
4.3.3 CWI Potential in a Heterogeneous and Longer Porous Media 100
4.3.4 Repeatability of Coreflood Experiments 111
4.4 Conclusion 112
Chapter 5: Enhancing Water Imbibition Rate and Oil Recovery by Carbonated Water 114
5.1 Introduction 114
5.2 Experimental Setup and Procedure 115
5.2.1 Imbibition Rig 115
5.2.2 Fluids Properties 117
5.2.3 Core Properties 118
5.2.4 Methodology 119
5.3 Results and Discussion 120
5.3.1 Spontaneous Imbibition in Carbonate Rock 120

5.3.2 Spontaneous Imbibition in Sandstone Rock 129
5.4 Conclusion 134
Chapter 6: Characterization of Fluids-Fluids Interactions Leading to EOR by Carbonated Water Injection 136
6.1 Introduction 136
6.2 Experimental Setup and Procedure 137
6.2.1 PVT and Slim Tube Rigs 137
6.2.2 Fluids Properties 139
6.2.3 Methodology 140
6.3 Experimental Results and Discussion 143
6.3.1 PVT Experiments 143
6.3.2 Slim Tube Experiments 156
6.3.3 Displacement Front Propagation 159
6.3.4 Discussion 160
6.4 Conclusions 161
Chapter 7: Conclusions and Recommendations 164
7.1 Conclusions 164
7.1.1 Recovery Mechanisms by CWI 164
7.1.2 Potential of CWI for Enhancing Oil Recovery at Core-Scale 166
7.2 Recommendations 167
7.2.1 Effect of Dissolved Gases Type 168
7.2.2 Coupling the Low Salinity Brine Injection with CWI 168
7.2.3 Improving the Carbonation Level of CW by using Co-solvent 169
7.2.4 Investigating Performance of CWI in Heterogeneous Carbonate Rocks 169
7.2.5 Using a Nano-CT scanner 170
7.2.6 Developing a Numerical Model 170
References: 171

LISTS OF FIGURES

Figure 1-1 Solubility of CH_4 and CO_2 in brine with the salinity of 54,540 ppm at temperature of 100 °F 15
Figure 2-1 Schematic of micromodel rig 26
Figure 2-2 Schematic diagram of the optical system of micromodel rig 27
Figure 2-3 Optical system of micromodel rig in the laboratory 27
Figure 2-4 Schematic of glass plates of the micromodel 28
Figure 2-5 Micromodel when it is fully saturated with water 29
Figure 2-6 Schematic of the rocking cell used for preparing ‘’live’’ fluids 30
Figure 2-7 Carbon number distribution of crude J 31
Figure 2-8 A simple example of fluids distribution 32
Figure 2-9 Image analysis in Adobe Photoshop CS media 32
Figure 2-10 Full scan of the model after A) initial oil saturation was established. B) 24 hours of waterflooding C) 24 hours of CWI in the dead oil system and D) final waterflooding period to strip the dissolved CO_2 out of the remained oil and reach to its actual volume (Image dimensions: 768*1002 pixels) 36
Figure 2-11 Oil swelling during CWI in the dead oil system 37
Figure 2-12 Colour of the oil after A) waterflooding period and B) 24 hours CWI in the dead oil system (Image dimensions: 1024*305 pixels) 37
Figure 2-13 Full scan of the model after A) initial oil saturation was established, B) 24 hours of waterflooding, C) 24 hours of CWI in live oil system and D) final waterflooding period to strip the dissolved CO_2 out of the remained oil and reach to its actual volume (Image dimensions: 745*1024 pixels) 40
Figure 2-14 Nucleation of new gaseous phase inside the oil after 21 min of tertiary CWI in a system where live crude J was used (Image dimensions: 552*497 pixel) 41
Figure 2-15 Recovery factor (%OOIP) during both secondary waterflooding (WF) and tertiary CWI for live oil system 41
Figure 2-16 Residual oil saturations at the end of WF and tertiary CWI and new phase saturation at the end of tertiary CWI for live oil system 43
Figure 2-17 Comparison of the oil swelling during CWI in dead oil and live oil systems 43
Figure 2-18 Colour of the oil after A) waterflooding period and B) 24 hours of CWI in live oil system (Image dimensions: 1024*370 pixels) 44

Figure 2-19 Full scan of the model after A) initial oil saturation was established, B) 1 hour of CWI, C) 24 hours of CWI in live oil system and D) final waterflooding period to strip the dissolved CO_2 out of the remained oil and reach to its actual volume (Image dimensions: 743*1024 pixels).....46
Figure 2-20 Nucleation of the new phase inside the oil just after CW breakthrough (Image dimensions: 431*746 pixels) 47
Figure 2-21 Recovery factor (%OOIP) during secondary WF and secondary and tertiary CWI.....47
Figure 2-22 Residual oil saturations at the end of secondary CWI and counterpart secondary WF and new gaseous phase saturation at the end of secondary CWI.....48
Figure 2-23 Reconnection of an isolated oil in a dead-end pore due to formation and growth of the gaseous new phase (Image dimensions: 1024*698 pixels) 49
Figure 2-24 Total enlargement of an isolated oil ganglia during CWI period.....50
Figure 2-25 Effect of new phase on restricting the path of CW and diverting it to unswept area of porous media (Image dimensions: 778*768 pixels) 51
Figure 2-26 Flow of new gaseous phase inside the oil that creates a favourable three phase flow region (Image dimensions: 1024*517 pixels).....52
Figure 3-1 Contact angle measurement rig 57
Figure 3-2 Position of the needle and substrate inside the visual cell 58
Figure 3-3 Schematic of a captive drop contact angle system. Needle diameter is 0.793 mm (droplet size 15 µL).....60
Figure 3-4 Measured equilibrium contact angles of the crude oil-un-aged Quartz in plain brine (DB) and carbonated water (CW) versus pressure at temperature of 100 ^{0}F 62
Figure 3-5 Measured equilibrium contact angles of the crude oil-un-aged Mica in plain brine (DB) and carbonated water (CW) versus pressure at temperature of 100 ^{0}F 64
Figure 3-6 Cation bridging on Mica surface 65
Figure 3-7 Measured equilibrium contact angles of the crude oil-un-aged Calcite in plain brine (DB) and carbonated water (CW) versus pressure at temperature of 100 ^{0}F66
Figure 3-8 Mechanism of Calcite wettability alteration [71].....67
Figure 3-9 Calcite surface, A) Before introducing CO_2 into brine and B) 24 hours after submerging it in carbonated water 68
Figure 3-10 Effect of CW on the surface of calcite. A and B) Smooth, clean calcite. C and D) The same substrate after exposing to carbonated water for 24 hr.....68
Figure 3-11 Reproducibility of contact angle measurements at pressure and temperature of 2500 psi and 100 ^{0}F respectively.....69

Figure 3-12 Measured equilibrium contact angles of the crude oil-Aged Quartz and crude oil-Un-aged Quartz systems in plain brine (DB) and carbonated water (CW) at pressure and temperature of 2500 psi and 100 ^{0}F respectively.....70
Figure 3-13 Measured equilibrium contact angles of the crude oil-Aged Mica and crude oil-Un-aged Mica systems in plain brine (DB) and carbonated water (CW) at pressure and temperature of 2500 psi and 100 ^{0}F respectively.....71
Figure 3-14 Measured equilibrium contact angles of the crude oil-Aged Calcite and crude oil-Un-aged Calcite systems in plain brine (DB) and carbonated water (CW) at pressure and temperature of 2500 psi and 100 ^{0}F respectively.....73
Figure 3-15 Reproducibility of contact angle measurements for the aged system at pressure and temperature of 2500 psi and 100 ^{0}F respectively.....74
Figure 4-1 Schematic of the rig.....77
Figure 4-2 EDS map of Berea sandstone rock (mag 10000 x) 80
Figure 4-3 Results of the Lithium tracer test in a heterogeneous sandstone core.....81
Figure 4-4 CT-Scan results of the heterogeneous sandstone core (30 cm*4.9 cm).....81
Figure 4-5 Recovery during both conventional waterflooding and secondary CWI in un-aged Berea cores 84
Figure 4-6 Recovery during both conventional waterflooding and secondary CWI in un-aged Berea cores 85
Figure 4-7 Differential pressure across the core during both conventional waterflooding and secondary CWI in un-aged Berea rocks. The increase in dP across the core during CWI period reveals the formation and growth of the new phase.....87
Figure 4-8 Differential pressure across the core during the first pore volume of conventional waterflooding and secondary CWI in un-aged Berea rocks.....88
Figure 4-9 Comparison of water cut during secondary CWI with its secondary waterflooding counterpart in water-wet systems 89
Figure 4-10 Comparison of water cut during secondary CWI with its secondary waterflooding counterpart in water-wet systems 89
Figure 4-11 Recovery during both conventional waterflooding and secondary CWI in aged Berea (mixed-wet) cores.....91
Figure 4-12 Recovery during both conventional waterflooding and secondary CWI in aged Berea (mixed-wet) cores.....91
Figure 4-13 Differential pressure across the cores during both conventional waterflooding and secondary CWI in aged Berea (mixed-wet) rocks 92

Figure 4-14 Differential pressure across the cores during both conventional waterflooding and secondary CWI in aged Berea (mixed-wet) rocks 93
Figure 4-15 Comparison of water cut during secondary CWI with its secondary waterflooding counterpart in mixed-wet system 94
Figure 4-16 Comparison of water cut during secondary CWI with its secondary waterflooding counterpart in mixed-wet system 94
Figure 4-17 Gas rate during secondary CWI and its secondary waterflooding counterpart in water-wet system 96
Figure 4-18 Gas rate and CO_2 rate during secondary CWI in water-wet system 97
Figure 4-19 Gas rate and CO_2 rate during secondary CWI in water-wet system 98
Figure 4-20 Oil recovery through secondary conventional waterflooding, CWI, and CW with 27% higher carbonation level at pressure and temperature of 2500 psi and 100 °F 99
Figure 4-21 Measured cumulative oil recovery in the tertiary carbonated water injection (CWI) in a heterogeneous sandstone core at 100 °F and 2500 psia 102
Figure 4-22 Comparison of the performance of the secondary CWI in an aged heterogeneous sandstone core with its secondary water injection counterpart 104
Figure 4-23 Oil recovery through experiments 6 and 7 in an aged heterogeneous sandstone core 104
Figure 4-24 Comparison of the water cut during secondary CWI in the heterogeneous core with its secondary water injection counterpart 105
Figure 4-25 Comparison of the water cut during secondary CWI in the heterogeneous core with its secondary water injection counterpart around water breakthrough time . 106
Figure 4-26 Gas rate during water injection in the heterogeneous sandstone core 107
Figure 4-27 Rate of gas production and calculated rate of CO_2 production during WI and tertiary CWI in the heterogeneous sandstone core 108
Figure 4-28 Rate of gas production and calculated rate of CO_2 production during tertiary carbonated water injection in the heterogeneous sandstone core 108
Figure 4-29 Gas rate during secondary carbonated water injection in a heterogeneous sandstone core 110
Figure 4-30 Gas rate during secondary carbonated water injection in a heterogeneous sandstone core 110
Figure 4-31 Reproducibility of experiment number 1 (waterflooding in un-aged Berea core) 111
Figure 4-32 Reproducibility of experiment number 2 (CWI in un-aged Berea core) ... 112

Figure 5-1 Schematic of the high-pressure spontaneous imbibition rig 116
Figure 5-2 Conventional imbibition cell 117
Figure 5-3 Cumulative oil production during spontaneous imbibition of brine and CW into an aged carbonate rock at room temperature and pressure of 2500 psi. CW improved the rate of spontaneous imbibition and led to 13.3% additional oil recovery 121
Figure 5-4 Inlet of a reservoir carbonate core A) before and after B) CWI..... 123
Figure 5-5 ICP analysis of the effluent brine samples taken during spontaneous imbibition of brine and CW into an aged carbonate rock 124
Figure 5-6 Cumulative oil production during spontaneous imbibition of brine into an un-aged carbonate rock at room temperature and pressure of 2500 psi..... 126
Figure 5-7 Cumulative oil production during spontaneous imbibition of brine and CW into an un-aged carbonate rock at room temperature and pressure of 2500 psi..... 126
Figure 5-8 Cumulative oil production during spontaneous imbibition of brine and CW into aged and un-aged carbonate rocks at room temperature and pressure of 2500 psi 128
Figure 5-9 Tertiary spontaneous imbibition of CW in aged rock system and un-aged rock system at pressure of 2500 psi and room temperature 129
Figure 5-10 Cumulative oil production during spontaneous imbibition of brine and CW into an aged sandstone rock at room temperature and pressure of 2500 psi..... 130
Figure 5-11 Cumulative oil production during spontaneous imbibition of brine and CW into aged sandstone and carbonate rocks at room temperature and pressure of 2500 psi 132
Figure 5-12 ICP analysis of the effluent brine samples taken during spontaneous imbibition of brine and CW into an aged sandstone rock 133
Figure 5-13 Changes in concentration of Silica in the effluent brine samples collected during spontaneous imbibition studies on aged sandstone rock 134
Figure 6-1 Schematic of PVT rig 138
Figure 6-2 Schematic of slim tube rig..... 139
Figure 6-3 CO_2 and CH_4 contents of equilibrated CW in each contact. The dashed lines represent the original (initial) conditions of the fluid before it comes in contact with any other fluid. The sharp drop in the CO_2 content of CW indicates strong CO_2 partitioning 144
Figure 6-4 GOR of equilibrated CW in each contact. The strong decline in the GOR of CW indicates strong CO_2 partitioning between CW and live oil..... 145

Figure 6-5 GOR of the equilibrated liv oil in each contact. CO_2 exchange between CW and live oil led to an increase in the GOR of live oil by around 2.6 times 146
Figure 6-6 CH_4 and CO_2 contents of the gas separated from equilibrated live oil in each contact. CO_2 exchange between CW and live oil led to decrease in the CH_4 content of live oil and increase in its CO_2 content 147
Figure 6-7 Composition of the condensate. Presence of CO_2 in the new gaseous phase led to an insignificant extraction of the light components of oil..... 149
Figure 6-8 Composition of the new gaseous phase versus pore volumes of CW that brought in contact with live oil. The gaseous phase is mainly composed of CH_4 at the first contact and it became richer with CO_2 in subsequent contacts 151
Figure 6-9 Changes in the density of dead oil taken out in each contact. Multiple contacts between the carbonated water and the live oil would not adversely affect the main oil properties..... 152
Figure 6-10 Changes in the viscosity of dead oil taken out in each contact. Multiple contacts between the carbonated water and the live oil would not adversely affect the oil main properties..... 153
Figure 6-11 Swelling factor (SF) of the oil in each contact..... 154
Figure 6-12 Swelling factor (SF) of the oil versus the CO_2 content of oil. The SF increases as the CO_2 content of oil increases until the CO_2 content of oil reaches to around 90 scc CO_2/scc oil. From that point onward the swelling factor is almost constant 154
Figure 6-13 CO_2 pseudo-partition coefficient in each contact. The increase in the value of CO_2 pseudo-partition coefficient indicates the growth in CO_2 content of the new phase..... 156
Figure 6-14 Comparison of oil recovery obtained by CWI with the one from conventional waterflood..... 158
Figure 6-15 Differential pressure behaviour during both conventional waterflooding (blue curve) and secondary CWI (orange curve). Although the residual oil saturation at the end of CWI was 24% lower than the one in WF, the differential pressures were the same..... 159
Figure 6-16 Breakthrough times of water and CO_2 during secondary CWI. The water breakthrough happened at earlier times compared to CO_2 breakthrough 160

LISTS OF Tables

Table 1-1 Ionic composition of sea brine 16
Table 2-1 Micromodel dimensions 29
Table 2-2 Properties of crude J 30
Table 2-3 Brine composition 31
Table 2-4 Saturations and porosity that obtained by (A) image analysis technique and (BA) simple geometrical equations and (B) image analysis technique 33
Table 3-1 Brine components 58
Table 3-2 Crude B properties 59
Table 3-3 List of experiments 61
Table 4-1 Crude J properties 78
Table 4-2 Sea brine components 78
Table 4-3 Summary of coreflood experiments and their conditions 79
Table 4-4 Dimensions and properties of the cores used in this study 82
Table 5-1 Crude oil properties 118
Table 5-2 Sea brine Components 118
Table 5-3 Dimensions and properties of the cores used in this study 118
Table 6-1 Crude J properties 139
Table 6-2 Sea brine components 140
Table 6-3 Ratio of the volume of CW to live oil in each contact 141
Table 6-4 Dimensions and properties of the slim tube 142
Table 6-5 Gas composition results of new phase 148
Table 6-6 Predicted and actual values of composition of the new gaseous phase 150

LISTS OF PUBLICATIONS BY THE CANDIDATE

1. Seyyedi, M., Sohrabi, M. and Farzaneh, A., *Investigation of Rock Wettability Alteration by Carbonated Water through Contact Angle Measurements.* Energy & Fuels, 2015: p. 5544-5553.

2. Seyyedi, M., and Sohrabi, M., *Enhancing Water Imbibition Rate and Oil Recovery by Carbonated Water in Carbonate and Sandstone Rocks.* Energy & Fuels, 2016: p. 285–293.

3. Seyyedi, M., Sohrabi, M. and Farzaneh, A., *Investigation of Rock Wettability Alteration by Carbonated Water - Contact Angle Measurement.* Presented at IOR 2015 - 18th European Symposium on Improved Oil Recovery, Germany.

4. Seyyedi, M., Mahzari, P., and Sohrabi, M., *An integrated study of the dominant mechanisms leading to improved oil recovery by carbonated water injection.* Journal of Industrial and Engineering Chemistry, 2016: p. 22-32.

5. Seyyedi, M., Sohrabi, M., and Sisson, A., *Experimental investigation of the coupling impacts of new gaseous phase formation and wettability alteration on improved oil recovery by CWI.* Journal of Petroleum Science and Engineering, 2016.

6. Seyyedi, M., and Sohrabi, M., *Pore scale Investigation of Crude Oil/CO_2 Compositional Effects on Oil Recovery by Carbonated Water Injection*. Submitted to Fuel.

Chapter 1: Introduction

1.1 Introduction

An oil reservoir is an underground hydrocarbon pool contained in a porous or fractured rock formation. Petroleum reservoirs are classified as conventional and unconventional reservoirs. In the case of conventional reservoirs, the oil or gas inside the porous or fractured rock formation is trapped by a sealing rock called cap-rock. On the other hand, for the case of unconventional hydrocarbon reservoirs the formation rock have a low permeability which leads to the trap of hydrocarbons in place, therefore, no need for any cap-rock and therefore different production mechanism is required. The focus of this study is on conventional oil reservoirs.

In general, the life of oil production from an oil reservoir can be divided into three parts including, primary, secondary and tertiary oil recovery. In the primary recovery period, the reservoir has sufficient pressure to push the oil. The main driving forces in this period are solution gas drive, aquifer inflow, expansion of the gas cap and gravity segregation. However, as time passes and the hydrocarbon fluids are produced, the pressure will often decline, and production will falter. At this stage, the secondary recovery operation is implemented in which usually waterflooding or gas injection are applied to maintain the pressure of the reservoir.

One of the most commonly used methods for increasing oil production from oil reservoirs is waterflooding. Waterflooding is a ‘’secondary recovery’’ method. In this method water, as the injection fluid displaces oil from the pore spaces, but the efficiency of such displacement depends on several factors such as oil viscosity and rock wettability state and characteristics. Over the past 40 years, three important and in-depth books written by Craig [1], Willhite [2], and Rose et al. [3] address waterflooding (WF) technology and the parameters that affect its performance.

The average global oil recovery by waterflooding is around 30%-35% of the original oil in place (OOIP), as a result, a significant amount of oil remain in place. The main reason for such a poor performance of waterflooding is unfavourable mobility ratio of the displacing fluid (brine) and the displaced fluid (oil) [1]. Mobility is defined as the ratio of effective permeability to phase viscosity and mobility ratio is defined as the

mobility of the injection fluid (water) divided by that of the fluid it is displacing, such as oil. For the case of waterflood, the mobility ratio is defined as:

$$M = \frac{\mu_o}{\mu_w}\frac{K_{rw,or}}{K_{ro,cw}} \quad \text{Eq.1}$$

Where μ_o is the oil viscosity, μ_w is water viscosity, and $K_{rw,or}$, $K_{ro,cw}$ are water and oil endpoint relative permeabilities. Furthermore, the reservoir properties such as reservoir heterogeneity could adversely affect the performance of waterflooding.

As a result, to recover the residual oil after conventional waterflooding, an enhanced oil recovery (EOR) method is needed. Enhanced oil recovery is the implementation of various techniques for increasing the amount of crude oil that can be extracted from an oil field.

The major EOR methods can be classified into three categories [4] including; (i) thermal such as steam injection, in-situ combustion, and hot water injection, (ii) chemical such as micellar-polymer flooding, polymer flooding, and alkaline injection and (iii) solvent such as hydrocarbon miscible, CO_2 miscible, CO_2 immiscible, nitrogen, and flue gas injections. The efficiency of an EOR scenario could be different for different reservoirs depend on the reservoir conditions, rock and oil types. As a result, to achieve the most benefit of an EOR method the conditions of the target, i.e. unrecovered oil, as well as the oil production mechanisms of the EOR processes should be well understood and studied.

At the same time with the continued increase in the use of fossil fuels (as one of the main sources of energy), there is an increase in undesired CO_2 emission from burning of the fossil fuels. Increase in the atmospheric concentration of CO_2 leads to global warming that is now recognised as one of the most serious problems facing humanity [5]. To control the trend of global warming, an efficient method that can mitigate the CO_2 emission is needed. One of the effective methods that can lead to a reduction in the atmospheric concentrations of CO_2 is CO_2 storage in oil reservoirs [5].

As a result, significant interest exists in improving recovery from oil reservoirs while addressing concerns about increasing CO_2 concentrations in the atmosphere. The combination of Enhanced Oil Recovery (EOR) and safe geologic storage of CO_2 in oil reservoirs is appealing and can be achieved by carbonated water injection (CWI) which is the main focus of this study.

The main objective of this thesis is to thoroughly investigate the underlying oil recovery mechanisms by CWI and feasibility of this method as an EOR technique. In this chapter, some of the basic concepts, past experiences related to this oil recovery method and the needs for and benefits of this study are discussed.

1.2 Sweep Efficiency

The effectiveness of an enhanced oil recovery process depends on the total sweep efficiency which is divided into three different sweep efficiencies called areal sweep efficiency (Ea), vertical sweep efficiency (Ev) and microscopic displacement efficiency (Em). Areal sweep efficiency is the fraction of the reservoir area from which the injected fluid displaces reservoir fluid at the time of breakthrough (BT). Parameters such as formation dip angle and dip azimuth, the presence of fractures, mobility ratio, injection pattern and directional permeability affect areal displacement efficiency (Ea). Some parts of the oil reservoir will not be invaded by the injected fluid if there are vertical heterogeneities within the reservoir, so a vertical sweep efficiency (Ev), which is less than unity, should be considered to account for the vertical heterogeneity as well. Alongside these two factors, microscopic displacement efficiency (Em) describes the displacement efficiency at the pore scale. Parameters such as gravity, capillary, and viscous forces and also pore size distribution, geometry and aspect ratio of pores (i.e. pore to throat effective diameter ratio) in the porous medium have effects on the microscopic displacement efficiency.

Based on the above definitions, the total sweep efficiency can be defined as:

$$Et = Ea.\ Ev.\ Em \qquad \text{Eq.2}$$

One of the objectives of this study is to comprehensively investigate the sweep efficiency of CWI method at the pore level and to find an in-depth understanding of oil recovery mechanisms of this EOR method.

1.3 Carbonated Water Injection

1.3.1 Literature Review of CWI (Experimental Studies)

Carbonated water injection (CWI) is a CO_2-augmented waterflood (WF) process, in which relatively small quantities of CO_2 are used efficiently to enhance oil recovery

from oil reservoirs without the need for a vast source of CO_2. Depends on the reservoir conditions, CWI can be carried out either as a secondary or tertiary recovery method. If the reservoir was already waterflooded, then CWI can be implemented as a tertiary injection scenario, but if the reservoir was not waterflooded, then CWI can be used as a secondary injection scenario. Compared to hydrocarbon gases the solubility of carbon dioxide in brine, at normal reservoir pressure and temperature, is higher. Figure 1-1 depicts the measured solubility of CO_2 and CH_4 in a specific type of sea brine at different pressures and a constant temperature of 100 °F. The brine composition is shown in Table 1-1, and it has a total salinity of 54,540 ppm. As can be seen from Figure 1-1, the solubility of CO_2 in the brine is much higher than the solubility of CH_4. This higher solubility of CO_2 in brine makes the brine a suitable carrier fluid for CO_2 in oil reservoirs for both EOR and additionally safe CO_2 storage.

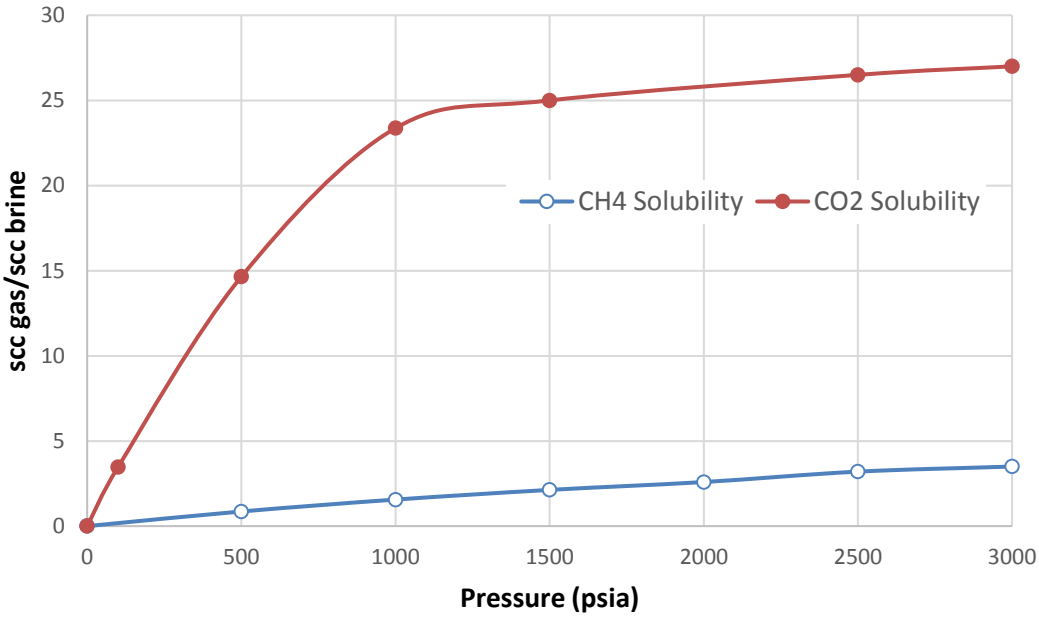

Figure 1-1 Solubility of CH_4 and CO_2 in brine with the salinity of 54,540 ppm at temperature of 100 °F

Table 1-1 Ionic composition of sea brine

ion	ppm
Na	16844
Ca	664
Mg	2279
SO_4^{-2}	3560
Cl	31107
HCO_3^{-1}	193

Initially, potential of CWI for enhancing oil recovery was studied by Martin [6] through a series of coreflood experiments. He reported 12% additional oil recovery during CWI compared to waterflooding. He conducted a further study [7], through performing several coreflood experiments, he showed that CWI reduced the initial oil saturation from 30%OOIP (original oil in place) to 8%OOIP. Johnson [8] also studied the potential of CWI for enhancing oil recovery through conducting coreflood experiments. Substantial oil recovery was obtained when CW was injected. Further coreflood experiments were carried out by Holm [9]. His results showed that the injection of CW can modify the permeability of dolomite core.

Oil recovery mechanisms of CWI at pore scale were first studied by Sohrabi et al. [10]–[14] through performing a series of high-pressure high-temperature direct flow visualisation (micromodel) experiments. n-Decane and mineral oil were used in these studies. The experiments were carried out at pressure and temperature of 2000 psia and 100 °F. Their results revealed the good potential of CWI for both secondary and tertiary injection scenarios, with the performance of secondary CWI better than tertiary. They concluded that the main oil recovery mechanisms were: (i) oil swelling that causes coalescence of trapped oil ganglia leading to local flow diversion to unswept area of the porous medium, and (ii) oil viscosity reduction due to CO_2 partitioning between the CW and oil. The first mechanism was more pronounced in the case of light oils with the second mechanism more dominant for the case of medium to heavy oils.

Further high-pressure high-temperature micromodel experiments were performed by Riazi et al. [15], [16] using n-Decane in their studies. Their results were consistent with the results of Sohrabi et al. [10]–[14]. They studied potential benefit of a subsequent

depressurization period on oil recovery after the CWI period. Sohrabi et al. [13], [17], [18] also investigated the performance of CWI at core scale through performing several coreflood experiments at high-pressure (2500 psia) and high-temperature (100 °F) using dead crude oil (without dissolved gas) or light oil (n-decane). Their results showed good potential for CWI either as a secondary or tertiary injection method. As with their high-pressure micromodel results, their coreflood experiments confirmed the better performance of secondary CWI compared to the tertiary CWI.

Yang et al. [19] studied the performance of both secondary and tertiary CWI by performing a series of coreflood experiments in sand packs which were not aged and using dead crude oil. The experiments were conducted at 600 psig and 104 °F. Further experiments in sand packs were carried out by Torabi and Mosavat [20]. They studied the performance of both secondary and tertiary CWI. Dead crude oil was used in this study, and the sand packs were not aged. Their results showed better performance of secondary CWI compared to tertiary CWI. They demonstrated that increase in injection pressure or decrease in test temperature led to better performance of CWI, which was attributed to the higher concentration of CO_2 in CW at higher pressures or lower temperatures. Their results showed that around 40.7% to 61.1% of the total injected CO_2 was stored during CWI.

Kechut et al. [21], [22] conducted a series of high-pressure flow visualisation (micromodel) and coreflood experiments, as well as compositional simulation, studying the performance of both secondary and tertiary CWI. Their results showed good delivery of CO_2 from CW front to the oil front. In their coreflood experiments, they used n-Decane and dead crude oil and were using un-aged cores. They showed that CWI had high potential as CO_2 storage strategy with around 50% of the total volume of the injected CO_2 being stored by the end of their test. Shakiba et al. [23] conducted a series of coreflood experiments to study the performance of both secondary and tertiary CWI which also used dead crude oil with an un-aged core. Their results showed good performance of both secondary and tertiary CWI; however, the performance of secondary CWI was better.

Guanli et al. [24] studied the potential of CWI on improving the CO_2 EOR performance in water-wet Berea using a light crude oil as the oil phase. They observed that injecting one pore volume CW (CO_2-enriched water) before CO_2 flooding can alleviate the

adverse effect of water shielding and thereby led to a better recovery during CO_2 injection in water-wet oil reservoirs. Zuo et al. [25], [26] studied gas exsolution from CW using micromodel investigations. Mineral oil was used as the oil phase in this study which showed a pressure drop that led to CO_2 exsolution from CW, leading to water flow blockage and local flow diversion into oil-filled pores and therefore better oil recovery. A 10% incremental oil recovery was achieved by lowering the pressure 2 Mpa below the CO_2 liberation pressure. Mosavat et al. [27] studied the potential of CWI at pore scale through running micromodel experiments at a low pressure of 304 psia and low temperature of 19 °C with dead oil used in the study. They studied the possibility of wettability alteration by CWI. A summary of all these previously published works, as well as their main outputs and limitations, are brought in Table 1-2.

Table 1-2 Methodology, outputs and limitations from the previous publications in the area of CWI

Previous works	Methodology	Outputs	Limitations
Martin [6]	Coreflood experiments	12% additional oil recovery by CWI compared to waterflooding	Using dead oil
Martin [7]	Coreflood experiments	22% additional oil recovery by CWI compared to waterflooding	Using dead oil
Johnson [8]	Coreflood experiments	Good oil recovery by CWI	Using dead oil
Holm [9]	Coreflood experiments	CW can modify the permeability of dolomite core	Using dead oil
Sohrabi et al. [10-14]	Micromodel experiments	Oil recovery mechanisms by CWI including oil swelling and oil viscosity reduction	Using dead n-Decane
Riazi et al. [15, 16]	Micromodel experiments	Oil recovery mechanisms by CWI including oil swelling and oil viscosity reduction	Using dead n-Decane
Sohrabi et al. [13, 17, 18]	Coreflood experiments	i. Good potential for CWI either as a secondary or tertiary injection method. ii. Better performance of secondary CWI compared to the tertiary CWI	Using dead crude oil or light oil (n-decane).
Yang et al. [19]	Coreflood experiments	The good potential of CWI either as a secondary or tertiary injection method.	Using un-aged sand pack and dead crude oil
Torabi and Mosavat [20]	Coreflood experiments	i. The good potential of CWI either as a secondary or tertiary injection method. ii. Better performance of	Using un-aged sand pack and dead crude oil

		secondary CWI compared to the tertiary CWI. iii. Better performance of CWI at higher pressure and lower temperature	
Kechut et al. [21, 22]	Coreflood and micromodel experiments, plus compositional simulations	i. Good performance of both secondary and tertiary CWI. ii. High potential of CWI as a CO_2 storage strategy	Using n-Decane and dead crude oil and using un-aged cores
Shakiba et al. [23]	Coreflood experiments	Good performance of both secondary and tertiary CWI; however, the performance of secondary CWI was better	Using dead crude oil with an un-aged core
Guanli et al. [24]	Coreflood experiments	Injecting one pore volume of CW before CO_2 flooding can alleviate the adverse effect of water shielding and lead to a better oil recovery during CO_2 injection.	Using dead crude oil with an un-aged core
Zuo et al. [25, 26]	Micromodel experiments	A 10% incremental oil recovery was achieved by lowering the pressure 2 Mpa below the CO_2 liberation pressure	Using mineral oil
Mosavat et al. [27]	Micromodel experiments	Possibility of wettability alteration by CWI	The low pressure of 304 psia and low temperature of 19 °C with dead oil

1.3.2 CWI Field Experience

The better performance of CWI compared to conventional waterflooding has been shown through coreflood as well as micromodel experiments [6]–[27]. Despite some encouraging experimental results, only a few EOR field applications were found in the literature. Some of its applications were for well stimulation; i.e. improving the permeability of the area around the wellbore, while others were applied to clean up the groundwater from oil-based contamination. In the following sections, details of some of these experiences are mentioned.

1.3.2.1 CWI for EOR Purposes

The first reported CWI field trial happened in Allegany County near Richburg, New York in 1947 [7]. The production data for this field showed a significant improvement

in the production rate from 92 barrels/acre/year to 1260 barrels/acre/year as a result of carbonated water injection instead of plain water.

The other carbonated water injection field experience took place in a field located ten miles north of Bartlesville, Oklahoma. Carbonated water injection in this field, which is known as the K&S project, was started in 1958 [28]. A significant improvement in water injectivity was observed in all injection wells of this field during carbonated water injection period. It was also reported that the additional oil production obtained in 1959 was more than the oil production during the entire primary production life, i.e. 29 years, of the field.

Increases in oil recovery and water injectivity and also shorter flood life have been reported for CWI application compared to plain water injection in Oklahoma, Texas and Kansas and projects elsewhere [29]–[31].

In another field scale application [32], the oil recovery improvement by CWI compared to conventional waterflooding was reported to be 14 to 16% of the original oil in place. The effect of water saturation, at the start of CWI, was experimentally studied by the same authors demonstrating that water saturation had an unfavourable effect on the performance of CWI.

1.3.2.2 CWI for Well Stimulation

As a result of CO_2 dissolution in water, carbonic acid (H_2CO_3) will be formed. Therefore, low pH carbonated water (CW) can react with rock minerals and in particular carbonate materials and from bicarbonates that are much more soluble especially in the vicinity of the wellbore. Mineral dissolution by CW leads to improved permeability near the wellbore thus improving water injectivity [29], [33]. Therefore, in some fields, CWI was applied with the aim of well stimulation [34]. The results of this application in the Aleksandrovsk field, for instance, show a noticeable improvement in the water intake rate of wells after CWI [35].

1.3.2.3 CWI for Cleaning Up the Ground Water from Contaminations

The other application of carbonated water (CW) is cleaning up the groundwater from oil-based contamination. Nelson et al. [36] conducted a pilot field scale trial to evaluate the recovery of volatile, light non-aqueous phase liquids from ground water using CW.

In this method, CW is injected into the subsurface resulting in the nucleation of CO_2 bubbles at and away from the injection point. The nucleating bubbles coalesce, rise and volatilize residual oil ganglia. This method removed 78% of the pentane and 50% of the less volatile hexane.

1.4 Thesis Content

As it was shown in Table 1-2, CWI has the potential to improve oil recovery in oil reservoirs. However, all the previous studies [6]–[27] neglected to consider the following points:

(i) The use of ‘’live’’ oil (with dissolved gas) rather than dead or refined oil. Reservoir oils normally have a significant amount of dissolved gases. The presence of dissolved gas may affect the performance of CWI.

(ii) Establishing the native wettability state of the reservoir. Initial wettability state of oil reservoirs controls the performance of waterflooding. Most of the oil reservoirs in particular carbonate reservoirs are mixed-wet to oil-wet. Therefore, to study the performance of CWI at real reservoir conditions, the cores must be aged with the reservoir crude oil to mimic the initial wettability state of the reservoir as much as possible. However, as mentioned earlier, in most of the above studies the cores were not aged. CWI might have effects on the wettability state of the rock and causes wettability alteration which can directly affect its performance.

In this study, the main objectives are; (i) to address these lack of information, (ii) to achieve an in-depth understanding of the underlying oil recovery mechanisms by CWI, (iii) to study CW-oil phase behaviour under realistic reservoir conditions and (iv) to quantify the level of additional oil recovery by CWI. For these aims, a series of high-pressure high-temperature micromodel, contact angle, coreflood, imbibition, multiple-contact (PVT) and slim tube experiments were carried out. Detailed descriptions of these exercises are discussed in five chapters as described below.

Chapter 2 address the lack of pore level information on CWI at realistic reservoir conditions. It should be noted that although conventional coreflood experiments are very useful for quantification of the performance of CWI and the level of additional oil recovery due to this injection strategy, the black-box nature of coreflood experiments means that the underlying physical processes involved in CWI cannot be easily

identified and studied by these experiments. High-pressure visualisation (micromodel) experiments of CWI provide a very useful tool to visualise and investigate directly the pore-scale mechanisms and events taking place during the flooding process. For this purpose, a series of high-pressure high-temperature micromodel experiments have been conducted to comprehensively study the oil recovery mechanisms by CWI at the pore-scale. In this chapter, the results of CWI as both secondary (pre-waterflood) and tertiary oil recovery (post-waterflood) processes are discussed. To understand the impact of dissolved gas in oil two different systems were used, dead oil and ''live'' (CH_4-saturated) oil. The results were compared with each other to better understand the actual behaviour of CWI under realistic reservoir conditions where reservoir oil has a significant amount of dissolved gases. Reservoir crude oil have been used in these experiments and the experiments have been performed at a pressure and temperature of 2500 psia and 100 °F, respectively.

Having visually studied (Chapter 2) the complex fluid-fluid interactions happening during CWI at pore-scale, Chapter 3 addresses the lack of sufficient understanding of the possibility of wettability alteration of minerals by CWI. One of the factors that control the performance of waterflood is wettability of the oil reservoirs. In oil-wet reservoirs, water being a non-wetting phase would preferentially flow through the larger pores bypassing a significant number of the smaller pores filled with oil. This result in an early water breakthrough and lower oil recovery compared to the water-wet case. Hence, a favourable wettability alteration can significantly affect the oil displacement efficiency and the recovery factor. In this chapter, the aim is to assess the impact of CW (carbonated water) on changing the wettability of oil reservoirs. For this objective, a series of high-pressure high-temperature contact angle experiments have been conducted to thoroughly investigate the effect of low pH of CW on wettability alteration of three different minerals, including quartz, mica, and calcite, at two distinct wettability states (oil-wet and water-wet). Reservoir crude oil have been used in these measurements and the experiments have been performed in a wide range of pressure from 100 psia to 2500 psia and at a constant temperature of 100 °F.

After reaching an in-depth understanding of the complex fluid-fluid (Chapter 2) and fluid-fluid-rock (wettability study, Chapter 3) interactions happening during CWI, in Chapter 4, a series of high-pressure high-temperature coreflood experiments have been conducted to study the potential of CWI at core scale and to quantify the level of

additional oil recovery by CWI. Cores with different lengths have been used. The aim of this chapter was to understand; (i) the potential of CWI under realistic reservoir conditions and to further study the oil recovery mechanisms by CWI, (ii) the effect of carbonation level of CW on its performance and (iii) the effect of rock heterogeneity on CWI performance. Both secondary and tertiary CWI have been studied. To mimic the realistic reservoir conditions CH_4-saturated crude oil (live oil) have been used. The experiments have been performed at pressure and temperature of 2500 psia and 100 °F. CWI potential in both water-wet and mixed-wet systems was studied.

In addition to coreflood experiments (Chapter 4), to study the potential of CWI for improving oil recovery from fractured reservoirs or heterogeneous ones, where viscous forces are very poor and oil recovery is mainly happening due to spontaneous imbibition, in Chapter 5 a series of high-pressure imbibition experiments were conducted. Spontaneous imbibition refers to the process of a wetting fluid being spontaneously drawn into a porous medium by the capillary forces and displacing a non-wetting fluid. The resultant displacement could be counter-current (in the opposite direction) or co-current (in the same direction). The active role of this mechanism during waterflood has been recognised, in particular, in heterogeneous and fractured reservoirs where large permeability variations usually make the direct displacement of oil by water inefficient. To investigate the potential of carbonated water (CW) for speeding up the rate of water imbibition from high permeability zones into low permeability parts a series of high-pressure imbibition experiments have been carried out using reservoir crude oil. Two different types of rock (sandstone and carbonate) have been used. The results of six high-pressure imbibition experiments were presented to support the benefits of CWI on water imbibition rate and oil recovery on two different rock types. All the experiments were conducted at a pressure of 2500 psia.

Having comprehensively studied the oil recovery mechanisms by CWI (Chapters 2 and 3) and the potential of CWI for improving oil recovery (Chapters 4 and 5), in Chapter 6, a series of high-pressure high-temperature multiple-contact (PVT) experiments have been carried out to thoroughly understand CW-oil phase behaviour under realistic reservoir conditions. The phase behaviour of the CW-oil system has not been studied yet in literature. For this aim, multiple batches of CW was sequentially brought into contact with a specific volume of a ‘’live’’ oil using a PVT cell. After each contact, the resultant phases were analysed to track the CO_2 partitioning and consequent changes in

properties and compositions of phases. Furthermore, in all previously reported studies [6]–[9], [13], [17]–[23] either small cores or cores with the maximum length of 30 cm were used to examine CWI potential. CWI potential and CO_2-water front movements at such short length porous mediums cannot be the best representative of CWI behaviour in a reservoir at a considerable distance from the injection well. Also, displacement tests performed in core plugs can be influenced by heterogeneities which may control the propagation of carbonated water and hence CO_2 transfer. In this chapter, a 60 ft slim tube packed with 80-140 Ottawa sand was used to study the behaviour of CW at long distances from injection point inside the oil reservoir. The behaviour of CW at noticeable distances from the injection well has not been investigated yet. The water-CO_2 propagation front was also studied at such a noticeable long porous medium.

The major findings of this study with some suggestions for future work are given in Chapter 7.

Chapter 2: Pore Scale Investigations of CWI

2.1 Introduction

As it was discussed in Chapter 1 (Section 1.3.1, Table 1-2), in all the reported direct flow visualization (micromodel) experiments [10]–[16], [21], [22], [25]–[27] either mineral oil or dead crude oil was used which cannot represent the condition of real oil reservoirs where oil has normally a significant amount of dissolved gases. The presence of associated gas in oil might affect the performance of CWI.

In this chapter, by using a high-pressure micromodel system, the author will comprehensively investigate the underlying oil recovery mechanisms by CWI, at pore scale, for both dead and ‘’live’’ (CH_4-saturated) oil systems. More importantly, the impact of dissolved gas in oil on the performance of CWI will be investigated. Reservoir crude oil had been used in this study. The experimental conditions were 2500 psia and 100 °F.

2.2 Experimental Setup and Procedure

2.2.1 Micromodel Rig

Figure 2-1 shows the schematic of the micromodel rig used in this study for performing CWI and waterflooding. The rig can operate at pressures as high as 5000 psia and temperatures as high as 160 °F. To avoid the corrosion problem when working with the CW acidic fluid, different elements of this high-pressure rig were made of titanium instead of steel. The rig consists of a number of major components as described below.

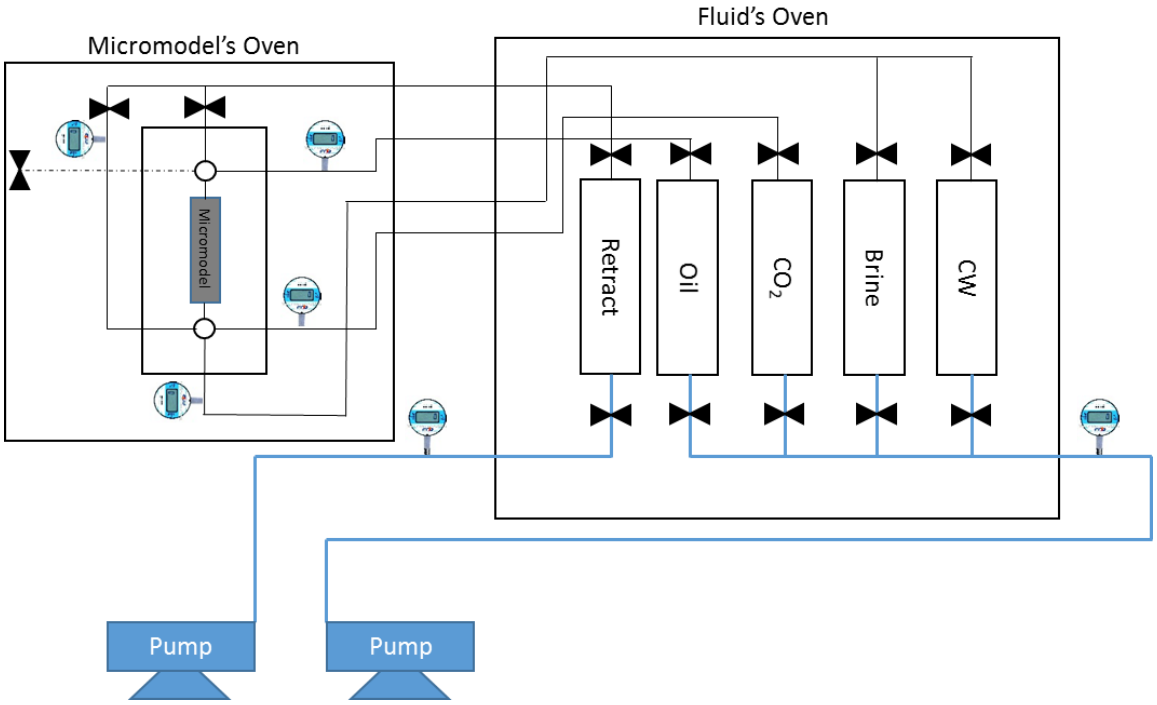

Figure 2-1 Schematic of micromodel rig

2.2.1.1 Fluid Storage Oven

As can be seen from Figure 2-1, all fluids are kept inside fluid storage oven at test temperature and pressure (100 °F and 2500 psia). Inside the fluid storage oven, there are five storage cells including; (i) CW, (ii) brine, (iii) oil, (iv) CO_2 and (v) the remaining one is used to retract the fluids from the bypass and micromodel outlet.

2.2.1.2 Micromodel Oven

The micromodel is inside the overburden chamber which is placed in a separate oven at same experimental conditions. This chamber can be turned to allow flow tests to be performed at any desired degree of orientation, including vertical and horizontal.

2.2.1.3 High Accuracy Pumps

Two sets of high accuracy pumps have been used to inject and retract the fluids in the micromodel. The pumps are capable of working at pressures up to 10,000 psia with a flow rate in the range 0.001 to 450 cc/hr.

2.2.1.4 High-Resolution Digital Camera

A high-resolution digital camera has been used to capture high-quality images and videos during flooding periods. A manual camera mount and positioning system is used, which allows the camera and its magnifying lens to be positioned at any part of the micromodel. Figure 2-2 and Figure 2-3 show a schematic diagram of the optical system of the rig and an illustration of a part of this system in the laboratory, respectively.

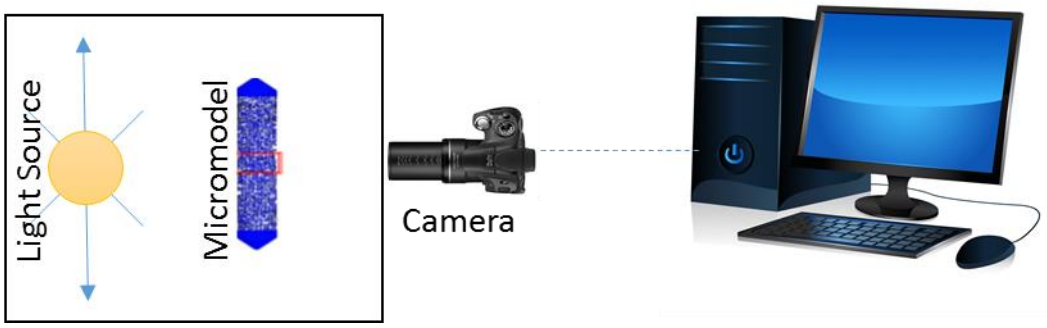

Figure 2-2 Schematic diagram of the optical system of micromodel rig

Figure 2-3 Optical system of micromodel rig in the laboratory

2.2.1.5 Glass Micromodel

The micromodel is a transparent porous media made of two glass plates. Initially, on the surface of one of the glass plates, a two-dimensional (2D) pore pattern that was generated by random sampling from a normal pore size distribution was etched. Then,

the second glass plate that is entirely flat was placed on top of the first plate, covering the etched pattern and thus creating an enclosed pore space. This covering plate has inlet and outlet holes at either end which allow fluids to flow inside the porous pattern (Figure 2-4). Since the solid walls of the micromodel are all made of glass, the fluids flow in the porous pattern and their interactions with each other can be clearly observed. The effects of geometry of the pore network on the patterns of flow and trapping can also be observed. Figure 2-5 shows the micromodel when it is fully saturated with water. The illustration shows the pore pattern as well as the triangular sections at both ends of the porous section, which have been designed to evenly distribute the fluids in the porous medium. The micromodel dimensions are shown in Table 2-1. As can be seen from this table, the range of pore diameters, which controls the aspect ratio, is relatively wide. Aspect ratio is the ratio of the pore to throat effective diameter. Aspect ratio is an indication of the degrees of heterogeneity of the porous medium at the pore-scale. This ratio is quite important as it can promote the snap-off mechanisms which in turn lead to higher oil trapping (residual oil saturation) during water and carbonated water injection.

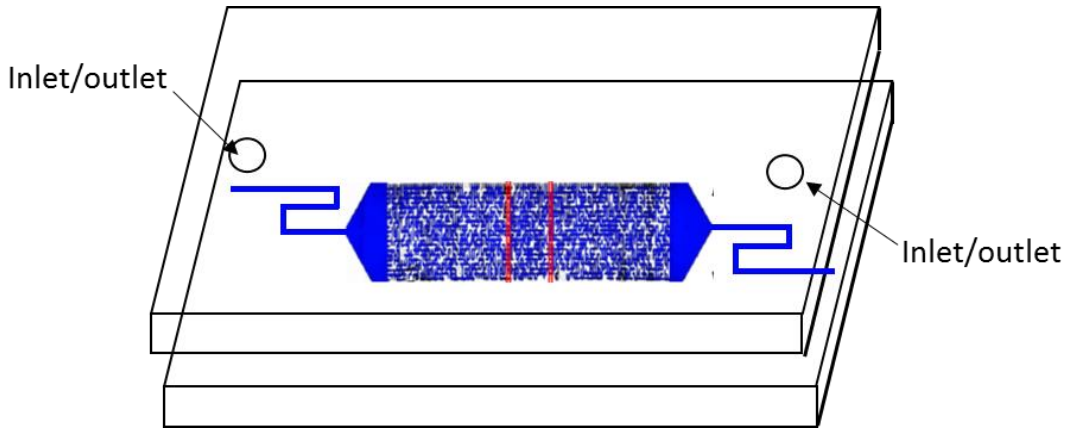

Figure 2-4 Schematic of glass plates of the micromodel

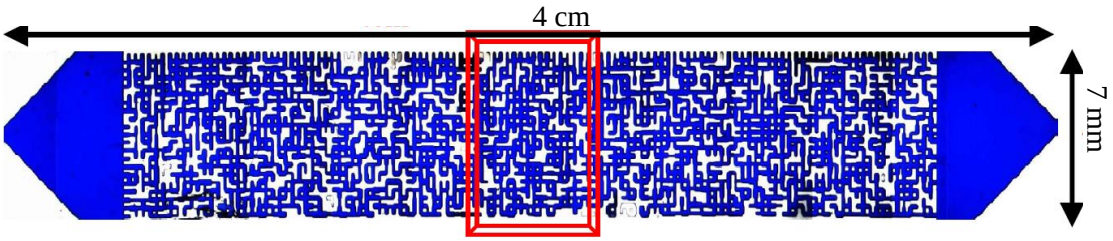

Figure 2-5 Micromodel when it is fully saturated with water

Table 2-1 Micromodel dimensions

height (cm)	width (cm)	pore volume (cm^3)	porosity	average pore depth (µm)	pore dia. range(µm)
4	0.7	0.01	0.5109	50	30-500

2.2.2 Fluids Properties

The properties of crude oil used in this study are shown in Table 2-2. To prepare ‘’live’’ oil, the crude oil was fully saturated with CH_4 at the experimental conditions, i.e. the pressure of 2500 psia and temperature of 100 °F, inside a rocking cell. Figure 2-6 shows the schematic of the rocking cell used for preparing any live fluids in this study. The bottom side of the rocking cell is connected to a pump that keeps the pressure inside the cell constant. The rocking cell is equipped with a heating jacket that enables to provide the live fluids in the desired temperature. The fluids inside the cell were mixed for an extended period of time, and the pressure of the cell was constantly monitored. One good indication that equilibrium had been achieved was the stable pressure of the pump connected to the bottom of the cell. As long as mass transfer between the phases is happening, the pressure inside the rocking cell would change, and the pump would continue injecting or retraction to keep the pressure constant at the test pressure. When equilibrium is achieved, there would be no further mass transfer and the pump would not inject or retract anymore.

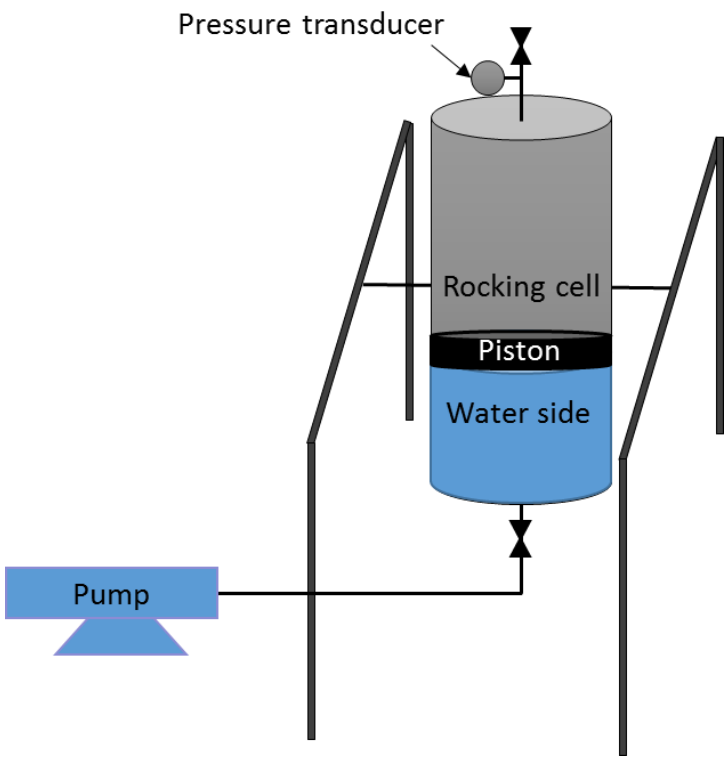

Figure 2-6 Schematic of the rocking cell used for preparing ‘’live’’ fluids

As can be seen from Table 2-2, the live oil viscosity is much less than dead oil viscosity. The viscosities of both dead and live crude ‘’J’’ were measured at test pressure and temperature of 100 °F. Figure 2-7 depicts the carbon number distribution of crude J obtained by high-resolution gas chromatograph (HRGC) with flame ionisation detector (FID). The vertical axis in this figure shows the weight percent (wt%) of components, and the horizontal axis shows the components name. As can be seen from this figure, Crude J is mainly made of medium to heavy components.

Table 2-3 presents the compositions of the brine used in this study. The total brine salinity is 54,500 ppm. CW was made at test conditions by mixing brine with CO_2.

Table 2-2 Properties of crude J

crude ID	API	dead oil viscosity (cp)	live oil viscosity (cp)	GOR (scc CH_4/scc oil)
Crude J	20.87	86	14	50

Table 2-3 Brine composition

ion	ppm
Na	16844
Ca	664
Mg	2279
SO_4^{-2}	3560
Cl	31107
HCO_3^{-1}	193

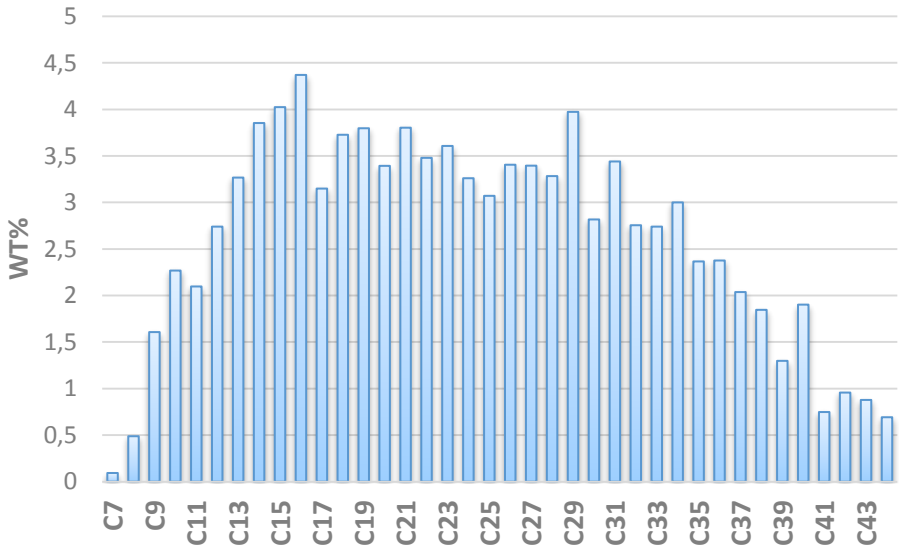

Figure 2-7 Carbon number distribution of crude J

2.2.3 Image Analysis of the Micromodel Experimental Results

The main output of high-pressure high-temperature micromodel experiments is some important qualitative information about fluid flow mechanisms in the porous medium. However, to achieve some quantitative information the results have been processed using image analysis techniques.

To measure the oil saturation in the porous pattern of the micromodel an image analysis computer program, i.e. Adobe Photoshop CS5, have been used. In this method, the fluid saturation was estimated based on the number of pixels representing each phase. In this procedure, the depth of pores in the entire micromodel was assumed uniform.

The accuracy of this model was measured by using a simple example of fluid distribution shown in Figure 2-8. Figure 2-9 illustrates the analysis of this image in Adobe Photoshop software. Having analysed the image by this method, the obtained saturation, and porosity values were compared to the ones obtained by simple geometrical equations. The results are shown in Table 2-4. Comparisons of the results reveal the high accuracy of this image analysis technique.

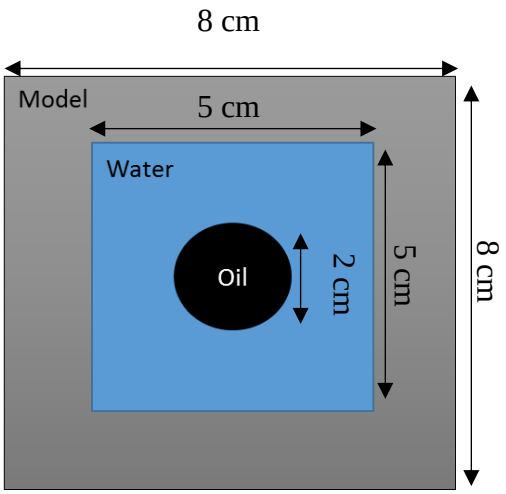

Figure 2-8 A simple example of fluids distribution

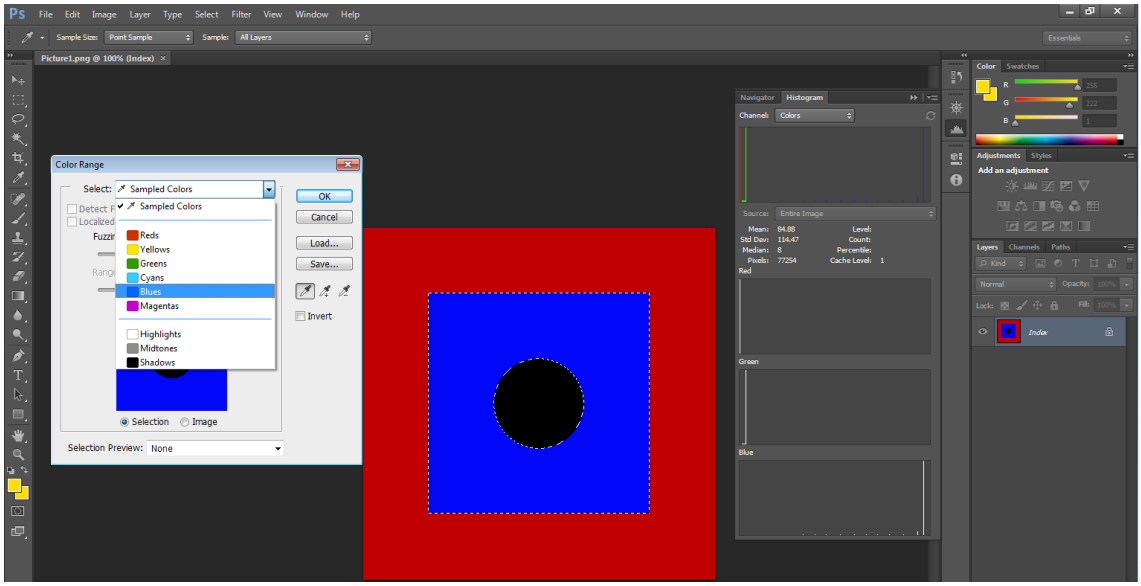

Figure 2-9 Image analysis in Adobe Photoshop CS5 media

Table 2-4 Saturations and porosity that obtained by (A) image analysis technique and (B) simple geometrical equations

	A (pixel)	**B** (cm^2)
Grain (grey)	223729	39
water (blue)	77254	21.86
Oil (black)	11122	3.14
Porosity %	39.5	39
Water saturation %	87.42	87.44
Oil saturation %	12.58	12.56

2.2.4 Methodology

In all the experiments conducted in this chapter a two-dimensional (2D) glass micromodel with a semi-geometrical pore pattern has been used. As the pore volume of the micromodel is extremely low; i.e. 0.01 cc, and it is quite fragile, performing micromodel experiments compared to coreflood experiments need more attention in the operational procedure. Before setting up the micromodel, the glass plates were thoroughly cleaned by merging them in an ultrasonic n-Decane bath and then rinsed them with plenty of distilled water. Having cleaned the plates, the flat glass plate was placed on the top of etched one, and the inlet and outlet holes of the flat plate were connected to the inlet and outlet lines of the etched plate. To seal the groove between the plates, Silicon rubber compound-flowable fluid was used. At this stage, extra care should be taken since the failure to achieve a perfect seal will cause overburden failure and therefore leakage of the overburden fluid into the porous medium. Next, the sealed glass plates were placed inside the overburden chamber, and the overburden pressure of around 300-400 psia was applied. Then, the pressure inside the porous pattern was increased by injection of water while the overburden pressure was increased. Care should always be taken to keep the pressure of the overburden 400 psia above the pore pressure within the micromodel. This process was continued until the desired pore pressure, i.e. 2500 psia, was reached. Next, the temperature was increased to 100 °F while the pressures were kept constant. Having established the desired pressure and temperature, the water was displaced by brine.

Next, the oil was injected to displace the brine and establish initial water saturation (Swi). The injection of oil was continued for several pore volumes to be sure that no

more brine would be produced and also to age the model's surface. After establishing the initial water saturation, for dead oil system, the performance of tertiary CWI was studied. For this purpose, the model was flooded by plain brine with the rate of 0.05 cc/hr. The injection continued until the distribution of fluids in the model stabilised. Next, CW was injected into the model at the same rate as plain water was injected. The injection of CW continued for 24 hours during which the model was scanned by a high-resolution camera to detect any possible oil redistribution in the model. After 24hrs of CWI, since the remained oil in the model was swelled due to CO_2 dissolution, the model was flooded by plain brine to strip CO_2 out of the oil and determine actual residual oil saturation after CWI.

For the case of the live oil system, as oil was fully saturated with CH_4, to minimise the CH_4 mass transfer between brine and oil during experiments, the brine was fully saturated with CH_4 at the conditions of the experiment. The test procedure was same as the one used in tertiary CWI for the dead oil system with the only difference being that CH_4-saturated oil and CH_4-saturated brine were used instead of dead oil and plain brine. The experiments were performed at a pressure of 2500 psia and temperature of 100 °F. Finally, for the case of live oil systems, the performance of secondary CWI has been studied. The procedure was the same as the one used in the tertiary CWI experiment with the only difference being that CWI replaces waterflood (WF).

2.3 Experimental Results and Discussion

Two systems were considered, (i) dead oil and (ii) live oil. First, the results of tertiary CWI in dead oil systems were analysed and next the results of the live oil system.

2.3.1 Dead Oil System

To investigate the potential of CWI for the dead oil system first, the model was flooded by plain water. Figure 2-10A demonstrates the model at its initial oil saturation, and Figure 2-10B depicts the model after the waterflood (WF) period. Based on the image analysis results, the recovery factor of waterflooding for dead oil system was around 38% of the original oil in place (OOIP). Significant amounts of oil remained in place after waterflood period which is attributed to adverse viscosity ratio between the water and dead crude J which in turn leads to earlier water breakthrough and poor sweep efficiency. The injection was continued until no further redistribution of fluids inside

the model was observed. The main oil production during waterflood period took place before the water breakthrough. After the breakthrough, the injected water was passed through the water film that had already been formed and as a result left the model without any further oil production. To produce the bypassed oil, either the injection rate should significantly be increased, which is not possible in a real reservoir case, or find a way to reconnect the bypassed oil ganglia to each other. The later can be achieved by tertiary CWI. Therefore, CW was injected into the model from the same head as water was injected. The direction of injection is from the bottom of the model toward its top. CWI was continued for 24 hours. Figure 2-10C shows the model after 24 hours of CWI in the dead oil system. To have a realistic volume of the remaining oil in the model, having finished CWI, a period of waterflood was carried out to strip CO_2 out of the remained oil and reach to its actual volume. It should be noted that we did not have oil production through this step. Figure 2-10D shows actual residual oil saturation after the remained oil was deprived of CO_2. Comparison of Figure 2-10B with 2-10D clearly indicates a reduction in the saturation of the remaining oil and improved oil recovery by CWI in the dead oil system. Based on the image analysis, tertiary CWI led to the production of 17.7% of the remaining oil in place. Ultimate oil recovery at the end of CWI period in dead oil system was 47 %OOIP.

As CW comes in contact with the bypassed oil, due to CO_2 concentration contrast between the phases (CW and oil) and higher solubility of CO_2 in oil than in water, carbon dioxide transfers from CW into the oil. This mass exchange leads to oil swelling which in turn leads to reconnection of some bypassed oil ganglions and oil displacement. The oil swelling of a bypassed oil ganglion was tracked over 12 hours of CWI. Figure 2-11 depicts the swelling versus time. As can be seen from this figure, CO_2 transfer from CW into the dead oil led to the oil swelling of around 14.4%.

In addition to oil swelling, the colour of the oil during CWI period gets lighter. The change in the colour of the oil can be seen in both Figure 2-10B and Figure 2-10C and also Figure 2-12. In the micromodel, the colour of a crude oil is an indication of its composition or in another word its viscosity. The heavier the oil, the darker its colour and vice versa. Therefore, changes in the colour of the oil indicate oil viscosity reduction due to CO_2 mass transfer during CWI.

Based on the direct visualisation results (Figure 2-11 and Figure 2-12), in the case of the dead oil system, the main oil recovery mechanisms were oil swelling, which leads to oil reconnection, redistribution and displacement, and oil viscosity reduction.

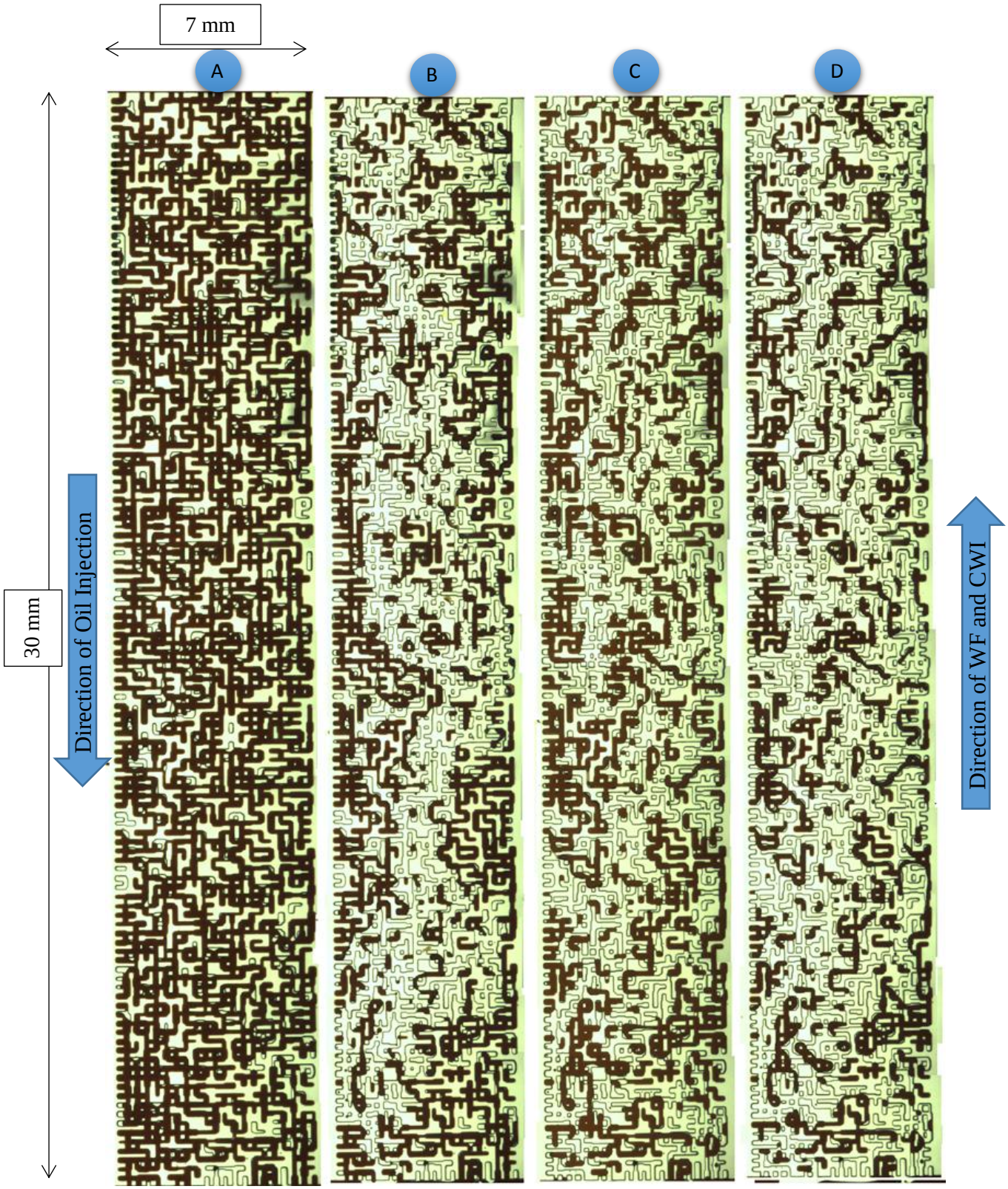

Figure 2-10 Full scan of the model after A) initial oil saturation was established. B) 24 hours of waterflooding C) 24 hours of CWI in the dead oil system and D) final waterflooding period to strip the dissolved CO_2 out of the remained oil and reach to its actual volume (Image dimensions: 768*1002 pixels)

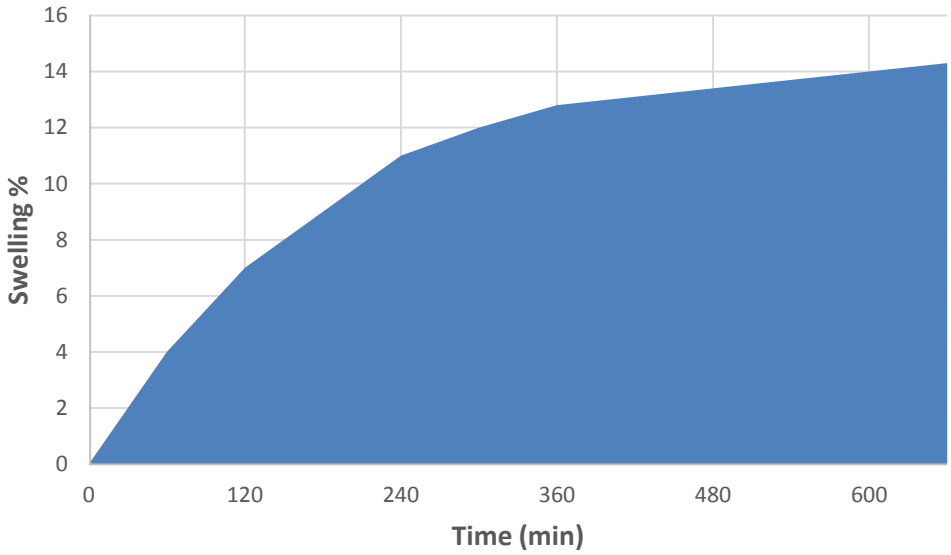

Figure 2-11 Oil swelling during CWI in the dead oil system

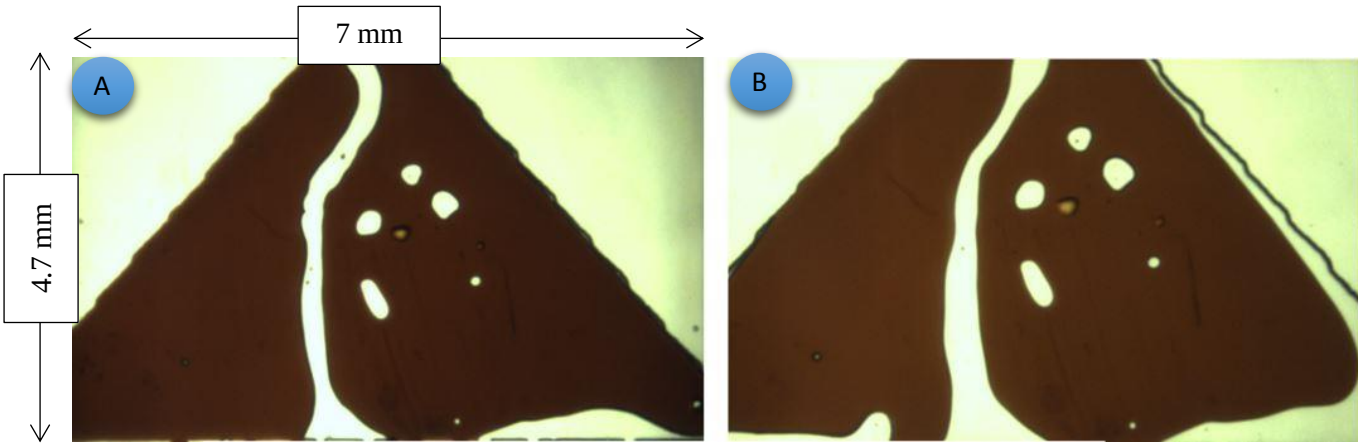

Figure 2-12 Colour of the oil after A) waterflooding period and B) 24 hours CWI in the dead oil system (Image dimensions: 1024*305 pixels)

2.3.2 Live Oil System

2.3.2.1 Tertiary CWI

So far, oil recovery mechanisms by CWI for live oil systems, at pore scale, have not been studied. In all previous studies either dead oil or mineral oil have been used that cannot be the representative of a reservoir oil that has normally a significant amount of dissolved gases. To comprehensively study the underlying oil recovery mechanisms by CWI, at pore scale in the ‘’live’’ oil system, a tertiary CWI was carried out in a system where live (CH_4-saturated) oil was used. Having established the initial oil saturation (Figure 2-13A), the model was flooded by CH_4-saturated brine. As mentioned above,

the brine was pre-equilibrated with CH_4 at experimental conditions, i.e. pressure and temperature of 2500 psia and 100 °F, to minimise any CH_4 mass transfer between the live oil (CH_4-saturated oil) and brine. Figure 2-13B shows the model after waterflood period. Conventional waterflooding in live oil system led to an oil recovery of 46% of the OOIP (original oil in place). The obtained oil recovery during waterflood period in the live oil system is around 8% higher than the one achieved in the dead oil system. This is because of better viscosity ratio for live oil system than dead oil system. The viscosity of the live oil is much less than dead oil, which in turn favours the water sweep efficiency and leads to better oil displacement and recovery. As a result, the residual oil saturation at the end of waterflood period in live oil system was around 8% of the original oil in place less than that in the dead oil system. The lower residual oil saturation in live oil system adversely affects the performance of tertiary CWI since CW will meet less remaining oil in the model and the remaining oil is more disconnected and dispersed. Therefore, its production will be even more challenging.

Having no more oil redistribution and production during waterflood (WF) period, CW was injected from the same head as water was injected (from the bottom of the model toward its top). The injection of CW was continued for 24 hours, same as the one for dead oil system. It was noticed that after 21 min of CWI in the live oil system, a gaseous new phase nucleates inside the oil at the interface of oil and CW. This phenomenon did not happen during 24 hours of CWI in the dead oil system. Nucleation of the new phase for the live oil system indicates the great importance of dissolved gases in oil during CWI. Figure 2-14 shows a section of the micromodel after 21 minutes of tertiary CWI in the live oil system. As CWI continued, the saturation of the new phase increased. Figure 2-13C shows the distribution of phases inside the micromodel after CWI period. The yellow colour, in this figure and the next figures, indicates the gaseous new phase that evolves during CWI in the live oil system. The gas saturation at this stage was around 10%. To have the realistic volume of the remaining oil in the model, after CWI period, a period of waterflood was carried out to strip the CO_2 out of the remained oil. Figure 2-13D shows the actual residual oil saturation in the model. Comparison of Figure 2-13B with Figure 2-13D reveals the significant potential of CWI for producing the bypassed live oil from waterflood period (Figure 2-15). Based on the imaging analysis results, CWI led to the production of 18.6% of the remaining oil in place. The ultimate oil recovery by CWI in live oil system was around 55% of the

OOIP, which is 7% higher than the one in the dead oil system. Although lower oil saturation at the start of CWI in live oil system compared to the dead oil system (8% lower) adversely affects the performance of CWI, the additional oil recovery by CWI in live oil system was higher than dead oil system. Based on the observation results, the reason for such a good performance of CWI in live oil system was formation and growth of the gaseous new phase inside the live oil.

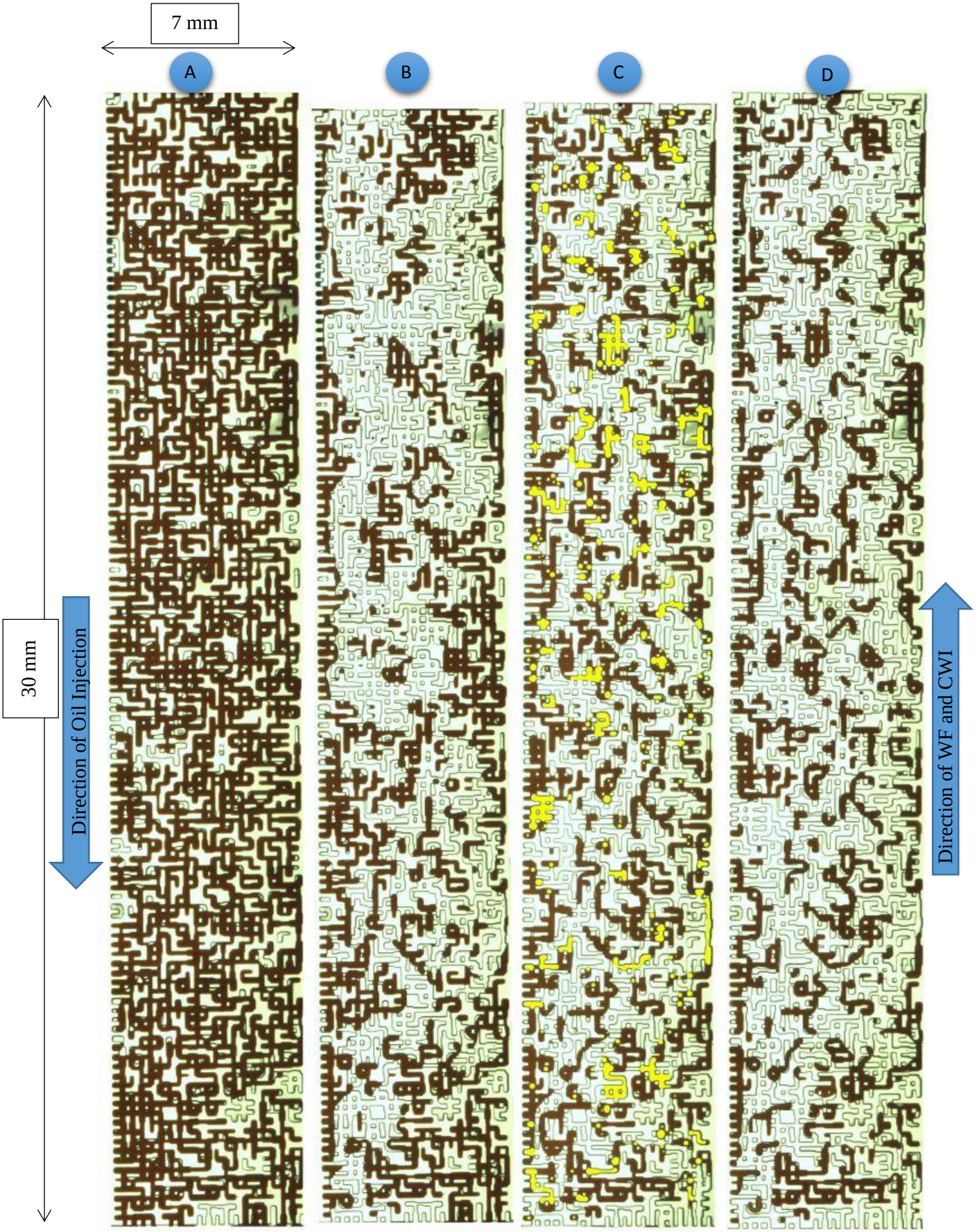

Figure 2-13 Full scan of the model after A) initial oil saturation was established, B) 24 hours of waterflooding, C) 24 hours of CWI in live oil system and D) final waterflooding period to strip the dissolved CO_2 out of the remained oil and reach to its actual volume (Image dimensions: 745*1024 pixels)

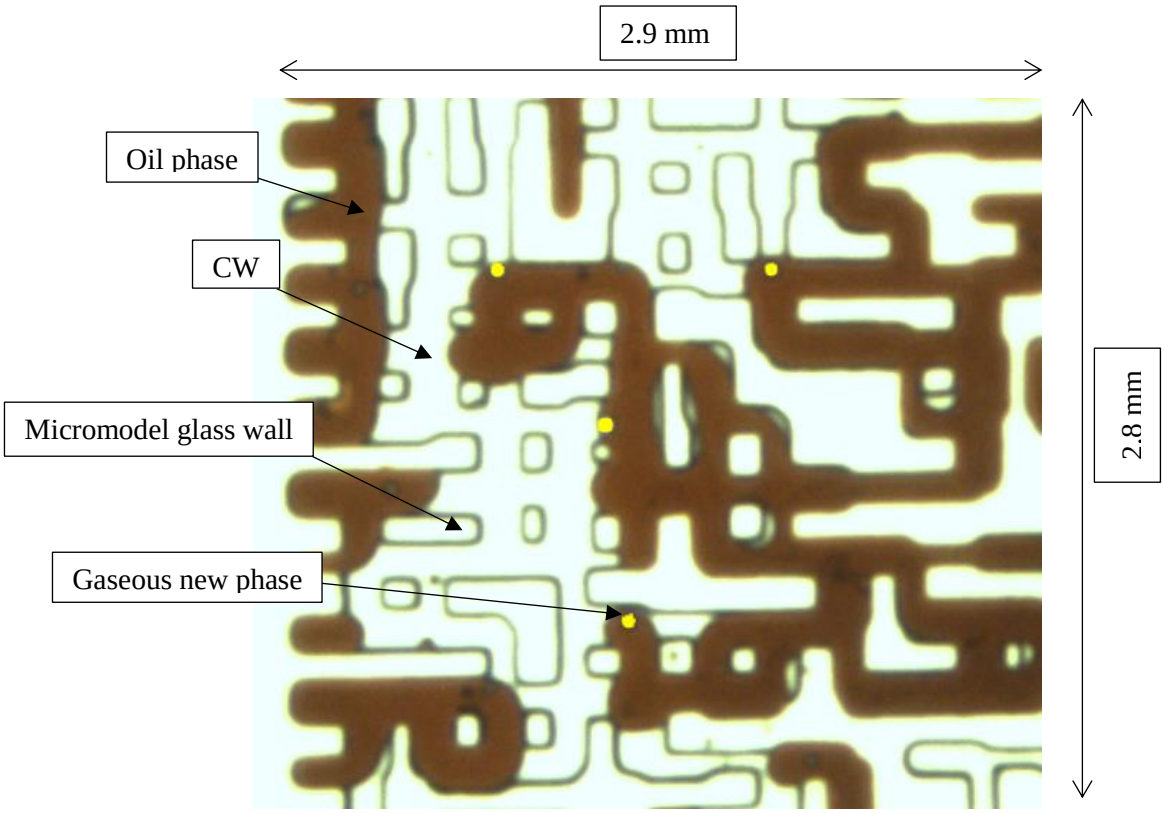

Figure 2-14 Nucleation of new gaseous phase inside the oil after 21 min of tertiary CWI in a system where live crude J was used (Image dimensions: 552*497 pixel)

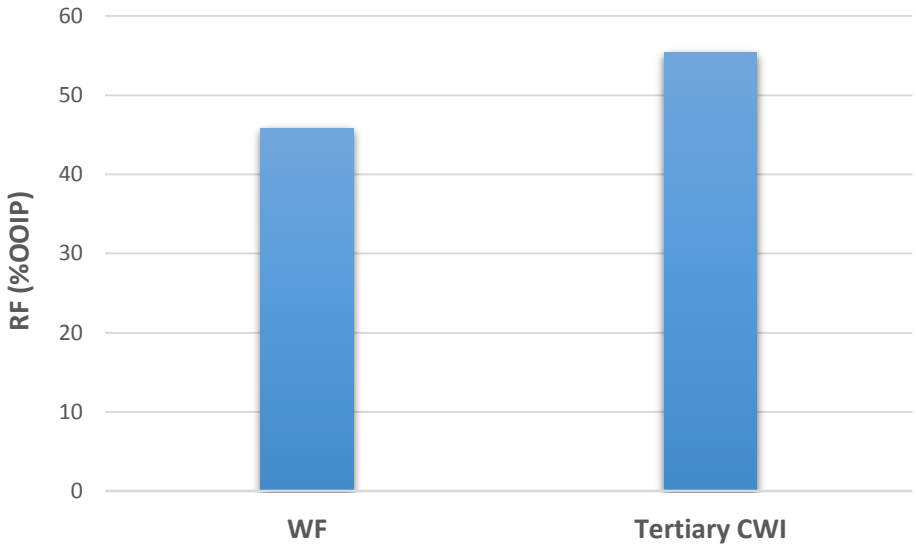

Figure 2-15 Recovery factor (%OOIP) during both secondary waterflooding (WF) and tertiary CWI for live oil system

As CW comes in contact with live oil, due to CO_2 concertation contrast between the live oil and CW and also higher solubility of CO_2 in oil than in water, CO_2 starts to dissolve in CH_4-saturated oil (Live oil). Since the solubility of CH_4 in the oil phase is lower than CO_2, at initial times CO_2 dissolution from CW into the oil phase liberates the CH_4 out of the solution that triggers the formation of the new phase. The presence of CH_4 in the new phase triggers the exsolution of dissolved CO_2 from the oil phase that leads to the growth of the new phase as it was observed in the micromodel test. The characteristic of the new phase and how it evolves during CWI in live oil system will be explained in details in Chapter 6.

The saturation of the new phase at the end of CWI period in live oil system was around 10% of the original oil in place which is almost equal to the obtained additional oil recovery by CWI (9% OOIP, Figure 2-16).

Based on the observations, nucleation and growth of the gaseous new phase inside the oil lead to much stronger oil swelling compared to the dead oil system. Figure 2-17 shows the total oil swelling measured in a separated oil ganglion during CWI period in both live oil and dead oil systems. As can be seen from this figure, for live oil system CWI led to much stronger oil swelling (around 2.3 times higher) in a shorter period. The reasons for stronger and earlier oil swelling in live oil system compared to dead oil systems are: (i) nucleation and growth of the gaseous new phase inside the live oil as it comes in contact with CW. Based on the pore scale observations, the total increase in the volume of oil in live oil system was around 35%, and more than 60% of that was due to the formation of the gaseous new phase. (ii) Stronger CO_2 diffusivity in live oil than dead oil system. The CO_2 diffusion coefficient in oil is a direct function of oil viscosity, i.e. the lower the oil viscosity, the stronger the CO_2 diffusivity. Since the viscosity of the live oil is much less than dead oil (Table 2-2), the CO_2 diffusion in live oil system is stronger than dead oil system which in turn directly affects the rate of oil swelling.

Later on in this chapter, the impact of formation and growth of the gaseous new phase on the oil recovery by CWI in live oil system will be discussed in details.

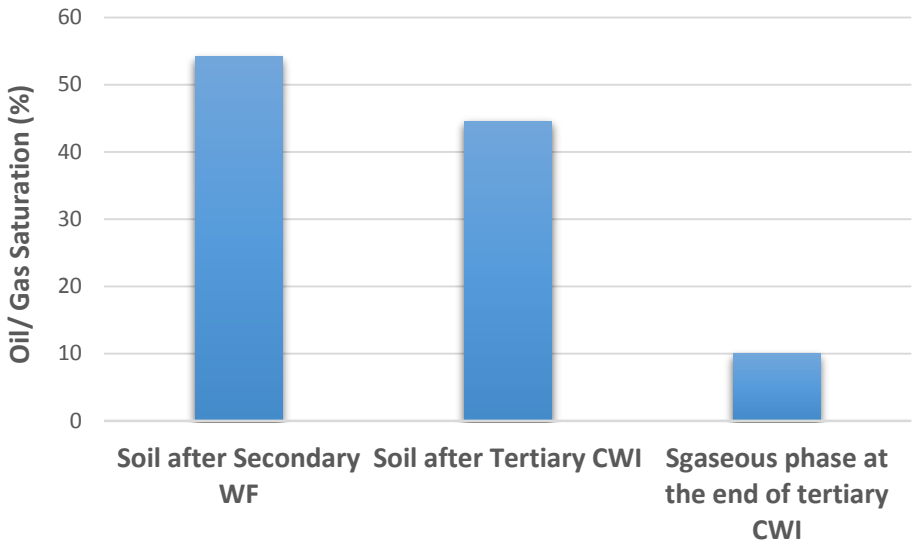

Figure 2-16 Residual oil saturations at the end of WF and tertiary CWI and new phase saturation at the end of tertiary CWI for live oil system

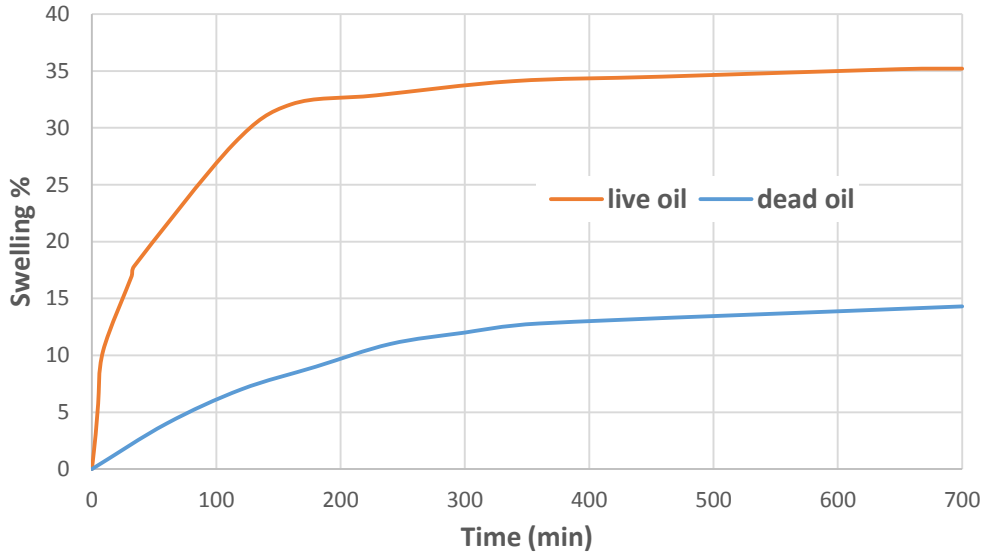

Figure 2-17 Comparison of the oil swelling during CWI in dead oil and live oil systems

Same as dead oil system some indications of oil viscosity reduction was observed. Figure 2-18 shows the change in the colour of oil before and after CWI period. The observed change in the colour of oil is attributed to dissolution of CO_2 into the oil. As CW comes in contact with oil due to the partitioning of CO_2 between the CW and oil, CO_2 transfers into the oil, which causes a reduction in the oil density and viscosity.

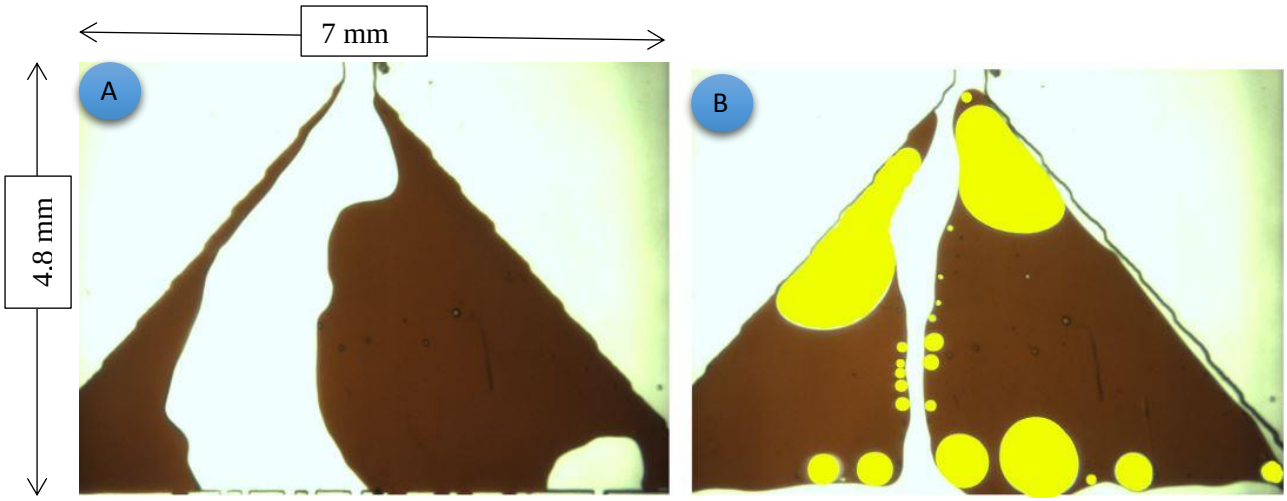

Figure 2-18 Colour of the oil after A) waterflooding period and B) 24 hours of CWI in live oil system (Image dimensions: 1024*370 pixels)

Based on the high-pressure high-temperature observation results, the main oil recovery mechanisms for the case of live oil system was formation and growth of the gaseous new phase that leads to better oil recovery. The rapid formation of the new phase can be a game-changer in our understanding of CWI true potential under realistic reservoir conditions where oil has normally a significant amount of dissolved gases.

2.3.2.2 Secondary CWI

As it was shown above, CWI showed a better performance in live oil system than dead oil system which was attributed to rapid formation and growth of the new phase inside the live oil as CO_2 from CW transfers into the oil. As a result, to have an in-depth understanding of this mechanism that only happened for live oil system a secondary CWI in live oil system was carried out. For this purpose, after establishing the initial water and oil saturations (Figure 2-19A), CW was injected into the model for 24 hrs. Figure 2-19B shows the model after one hour of CWI and Figure 2-19C shows the model at the end of CWI period. The yellow areas in this image show the gaseous new phase formed inside the oil. The gas saturation at the end of CWI was around 11% which is around 1% higher than the gas saturation at the end of tertiary CWI. Furthermore, it was noticed that almost immediately after CW breakthrough, the new phase started to nucleate inside the oil which was faster than the time it took for the formation of the new phase during tertiary CWI (Figure 2-20). The reason for the observed later formation of the gaseous new phase inside oil during tertiary CWI was the presence of a large volume of plain water in the model which had been injected

during the preceding conventional waterflooding. As a result, this large volume of plain water in the model needs to be replaced by CW, so that CW can come in contact with the remained oil. This process takes some time and therefore it delayed the formation of new gaseous phase during the tertiary CWI compared to the secondary CWI. Figure 2-20 shows the new phase formed inside the oil just after the breakthrough of CW. The oil recovery during the secondary CWI was 58% of the OOIP, which was around 3% higher than the recovery during tertiary CWI in live oil system and around 12% higher than the oil recovery obtained by secondary WF in live oil system (Figure 2-21). Although both secondary and tertiary CWI in live oil system were effective in improving oil recovery compared to plain (conventional) waterflood, the secondary CWI was more efficient. This is because of the higher oil saturation and better oil connectivity during secondary CWI compared to tertiary CWI. Furthermore, the saturation of the gaseous new phase at any given time during CWI was higher in secondary CWI than in tertiary CWI. The reason for the observed stronger and faster formation of gaseous new phase during secondary CWI is the lower saturation of water in the model during secondary CWI compared to tertiary where the model had been flooded with plenty of plain water beforehand.

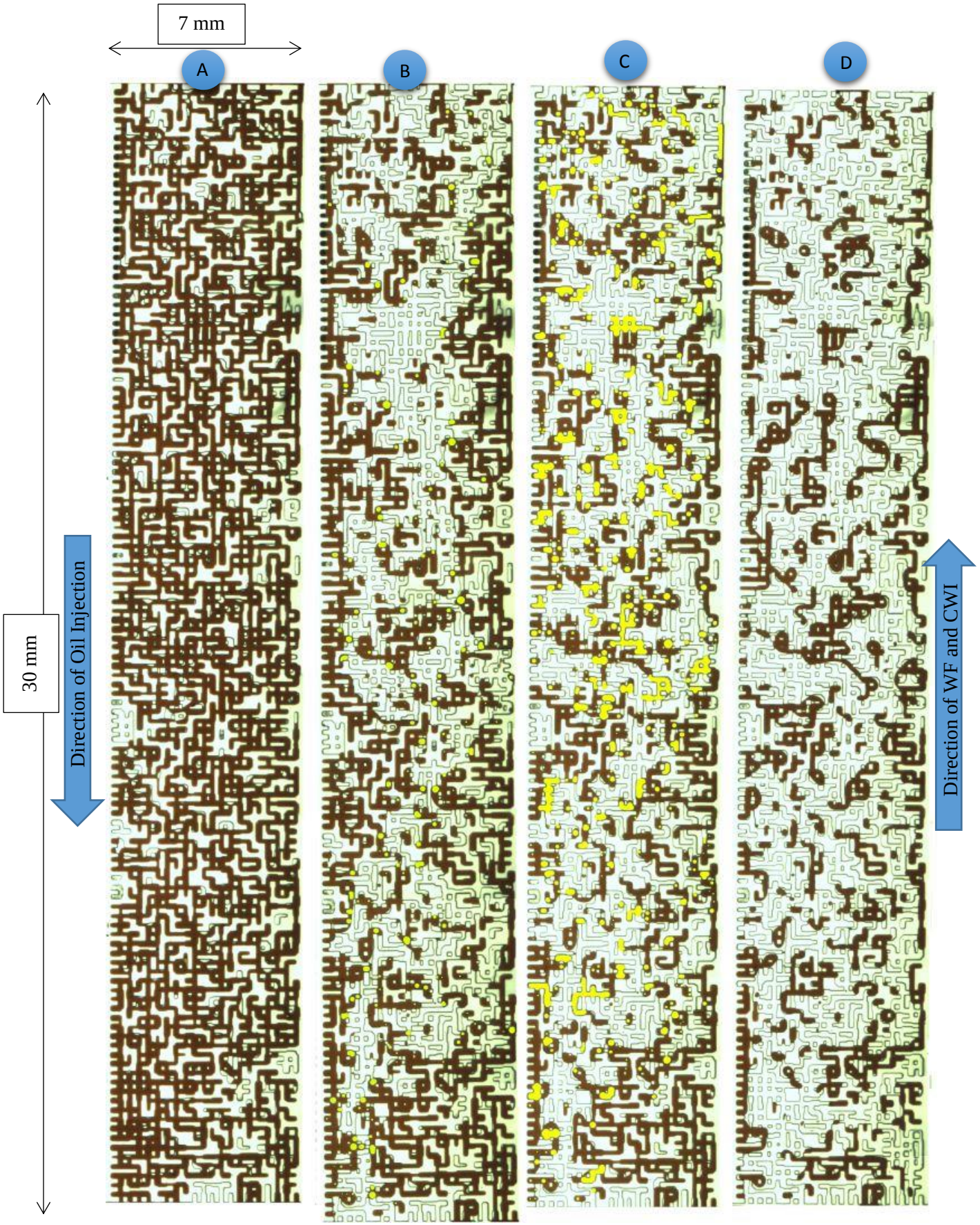

Figure 2-19 Full scan of the model after A) initial oil saturation was established, B) 1 hour of CWI, C) 24 hours of CWI in live oil system and D) final waterflooding period to strip the dissolved CO_2 out of the remained oil and reach to its actual volume (Image dimensions: 743*1024 pixels)

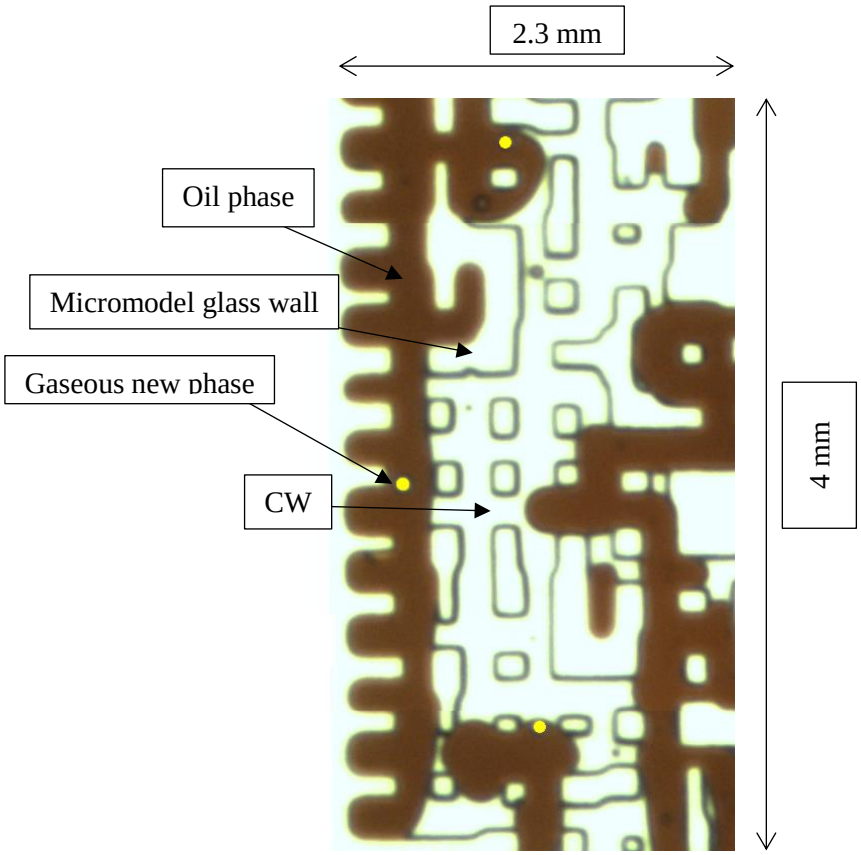

Figure 2-20 Nucleation of the new phase inside the oil just after CW breakthrough (Image dimensions: 431*746 pixels)

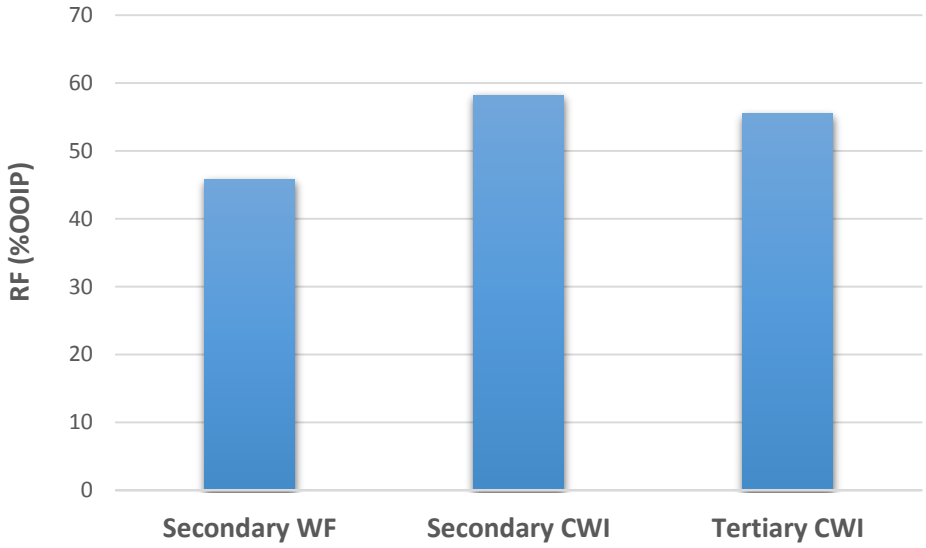

Figure 2-21 Recovery factor (%OOIP) during secondary WF and secondary and tertiary CWI

Figure 2-22 shows the residual oil saturations at the end of secondary CWI and its secondary WF counterpart in the live oil system. Furthermore, it demonstrates the saturation of the gaseous new phase at the end of secondary CWI. Interestingly, the saturation of the gaseous new phase at the end of CWI is close to the difference between the oil saturations at the end of secondary CWI and secondary WF. This result indicates the great importance of formation and growth of the new phase on additional oil recovery by CWI in oil reservoirs where oil has a significant amount of dissolved gases.

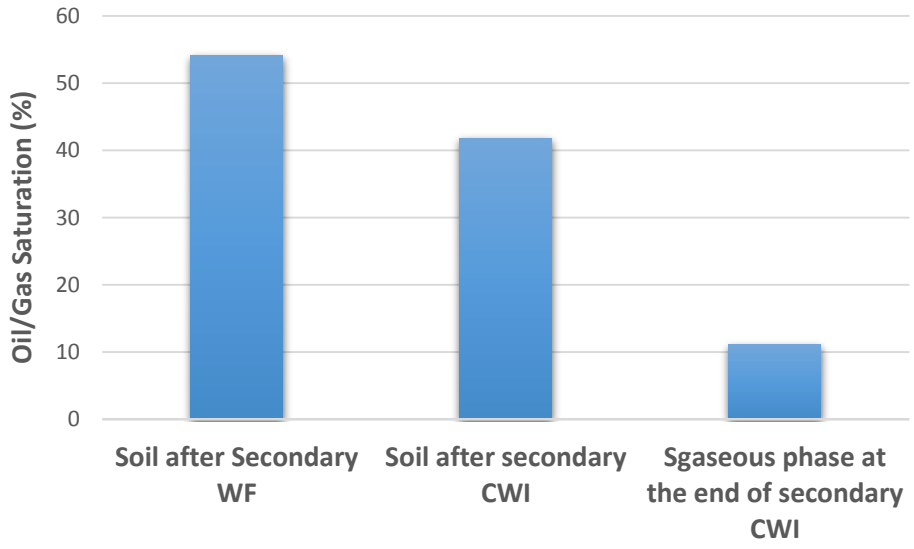

Figure 2-22 Residual oil saturations at the end of secondary CWI and counterpart secondary WF and new gaseous phase saturation at the end of secondary CWI

2.3.2.3 Effects of Nucleation and Growth of the New Phase on Oil Recovery

As it was shown in Figure 2-14 and Figure 2-20, as soon as CW comes in contact with ‘’live’’ crude oil, a gaseous new phase nucleates inside the oil at the interface between the oil and CW and with time the saturation of this new phase increases. Based on the direct observations, the formation and growth of the gaseous new phase were the main reason for the additional oil recovery during CWI in the micromodel when live oil was used. Formation and growth of the new phase inside the oil can help improve oil recovery through:

1) Reconnection of isolated oil ganglia. Formation of the new phase leads to a much larger effective overall oil swelling (compared to the normal swelling of oil) and thereby the isolated oil ganglia are reconnected and redistributed. In this study, overall oil swelling (or total enlargement) is defined as:

$$\frac{\text{Final volume of the hydrocarbon phase (oil + new phase)} - \text{initial volume of the oil}}{\text{initial volume of the oil}}$$

This reconnection and redistribution leads to movements of some of the bypassed oil ganglia and hence, additional oil recovery. Figure 2-23 demonstrates how CW can result in the reconnection of an isolated oil ganglion. This figure also shows how the gaseous new phase grows with time. Shortly after CW comes in contact with live crude oil, small bubbles of gas forms inside the oil at the interface of the oil and CW (Figure 2-14 and Figure 2-20). With time and as CWI continues, more of these gas bubbles are formed inside the oil and as they grow, they merge with their surrounding bubbles and form a larger bubble as can be seen from Figure 2-23. When the saturation of the gaseous new phase passes a critical value, it can flow inside the oil and brings about a favorable three phase flow (Figure 2-26).

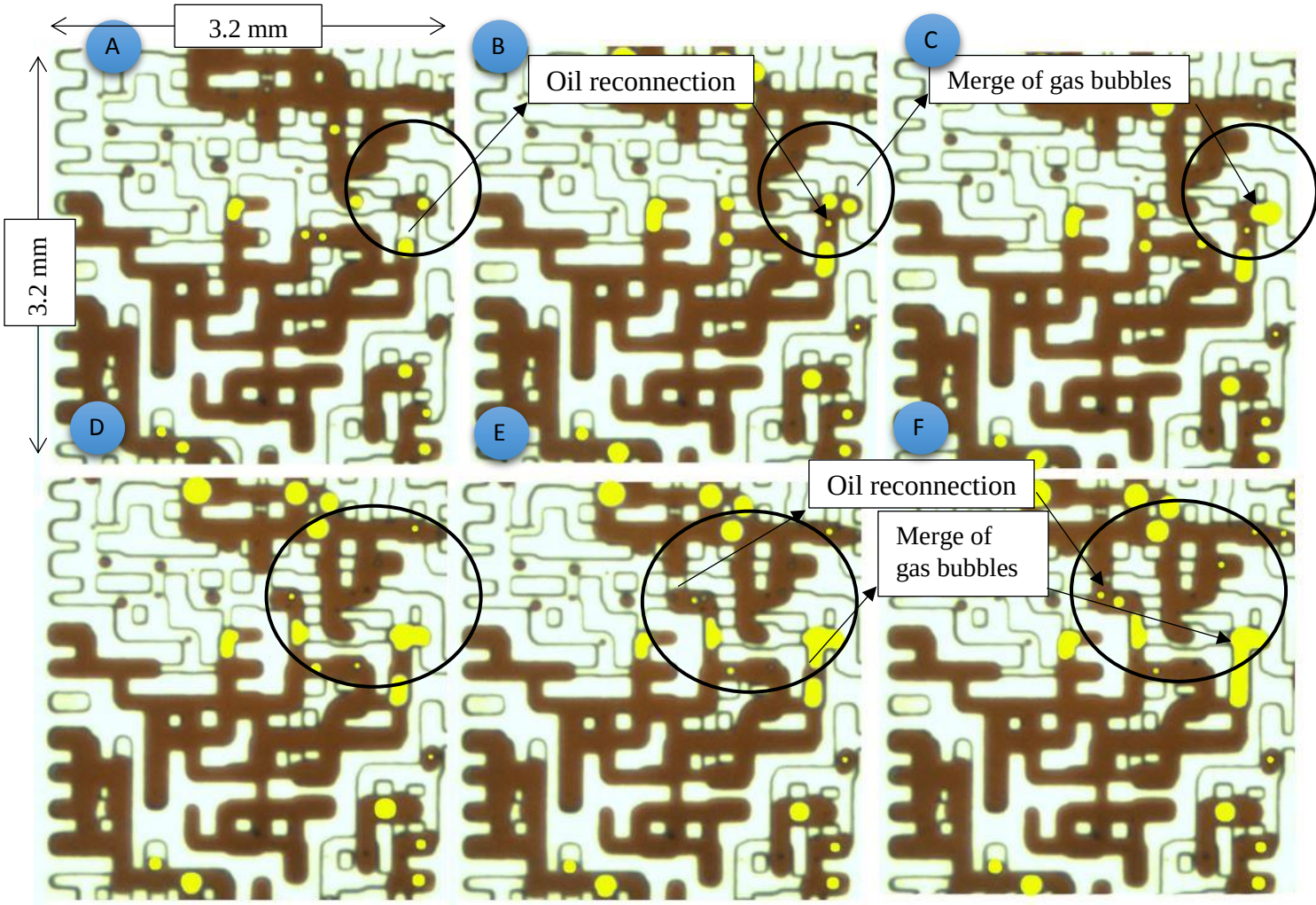

Figure 2-23 Reconnection of an isolated oil in a dead-end pore due to formation and growth of the gaseous new phase (Image dimensions: 1024*698 pixels)

To quantify the effect of the formation and growth of the new phase on the total enlargement of oil, the change in the volume of an isolated oil ganglion was measured during CWI. As can be seen from Figure 2-24, the total increase in the volume of oil in this example was around 35%, and more than 60% of that was due to the formation of the new phase. As can be seen, shortly after the start of CWI, there is some (normal) oil swelling which stops relatively quickly but the increase in the oil volume due to the formation of the new phase continues.

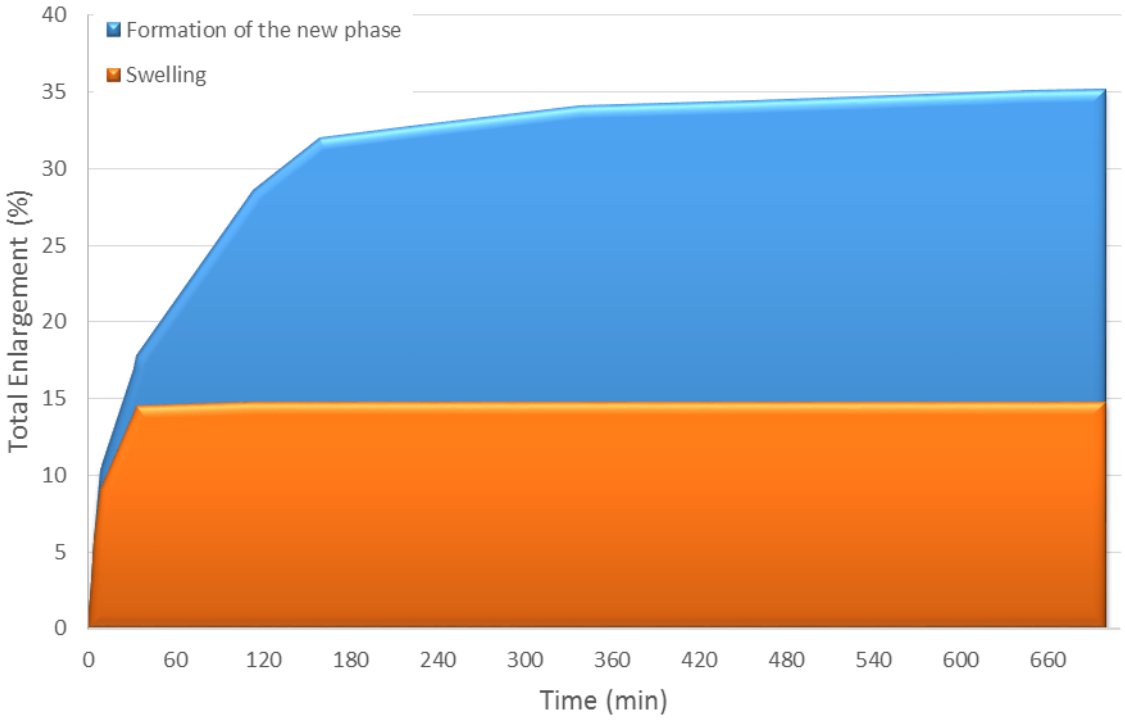

Figure 2-24 Total enlargement of an isolated oil ganglia during CWI period

2) Restricting the path of CW and diverting it to unswept areas of the porous medium. As it is shown in Figure 2-25, the formation and growth of the new phase can restrict the flow path of flowing water and thereby divert it to unswept areas of the porous medium. The reason for such behavior is the lower relative permeability of CW when we have the new gaseous phase in the system. Therefore, instead of having a two-phase relative permeability; we have a three-phase relative permeability. The area highlighted by the circle in Figure 2-25 shows how the growth of the new gaseous phase can block the water path and lead to reconnection of two isolated oil ganglia.

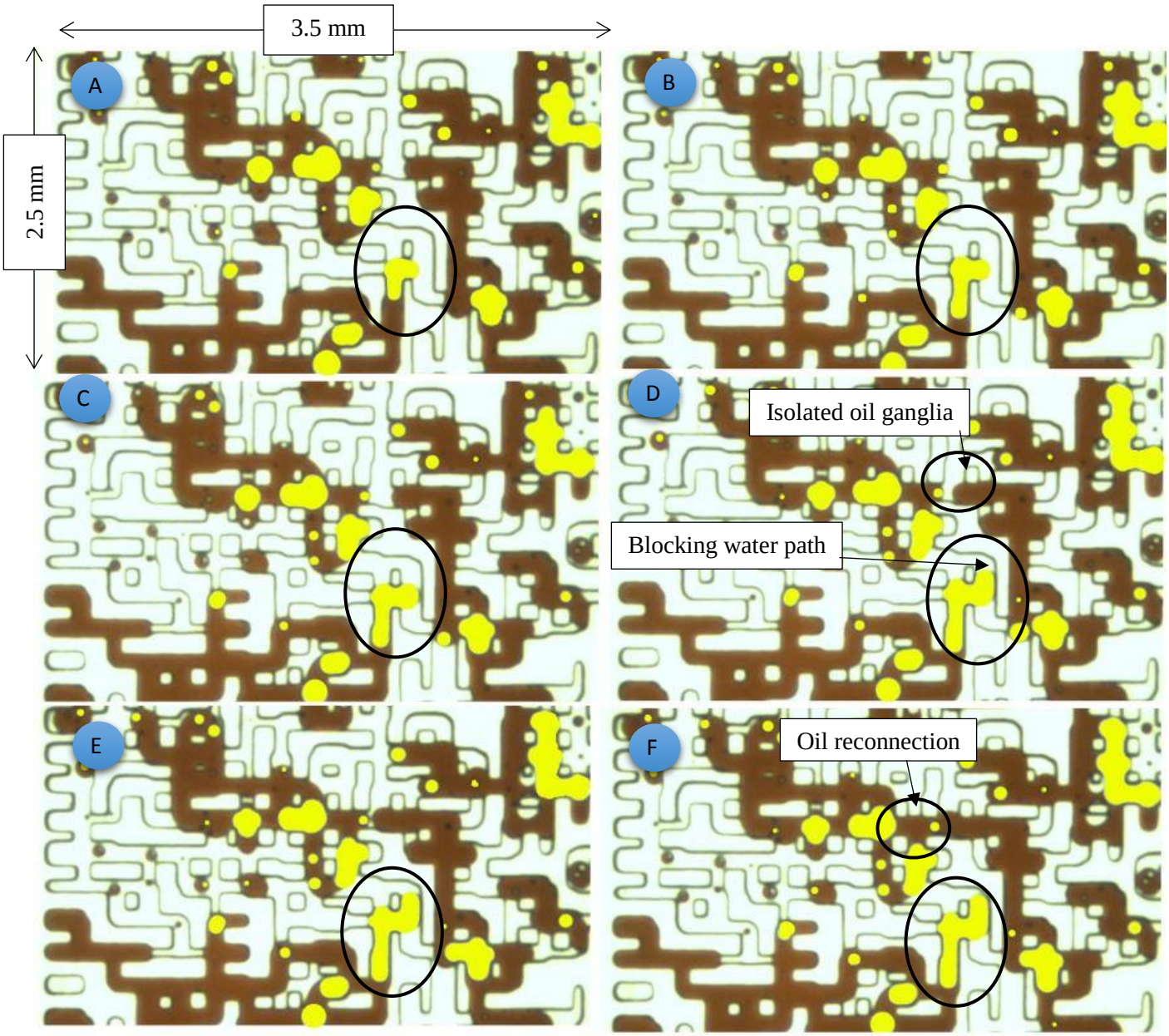

Figure 2-25 Effect of new phase on restricting the path of CW and diverting it to unswept area of porous media (Image dimensions: 778*768 pixels)

3) Formation of the new phase results in a favourable three phase flow condition. As mentioned earlier, as the injection of CW continues, the gaseous new phase formed inside the oil grows in volume and its saturation increases, and when its saturation reaches a critical saturation, it starts to flow (Figure2-26). However, it only flows inside the oil. The flow of this new phase creates a favourable three phase flow region which leads to lower residual oil saturation. Figure 2-26 demonstrates how the movement of the gaseous new phase inside the oil will affect the oil displacement and leads to lower residual oil saturation.

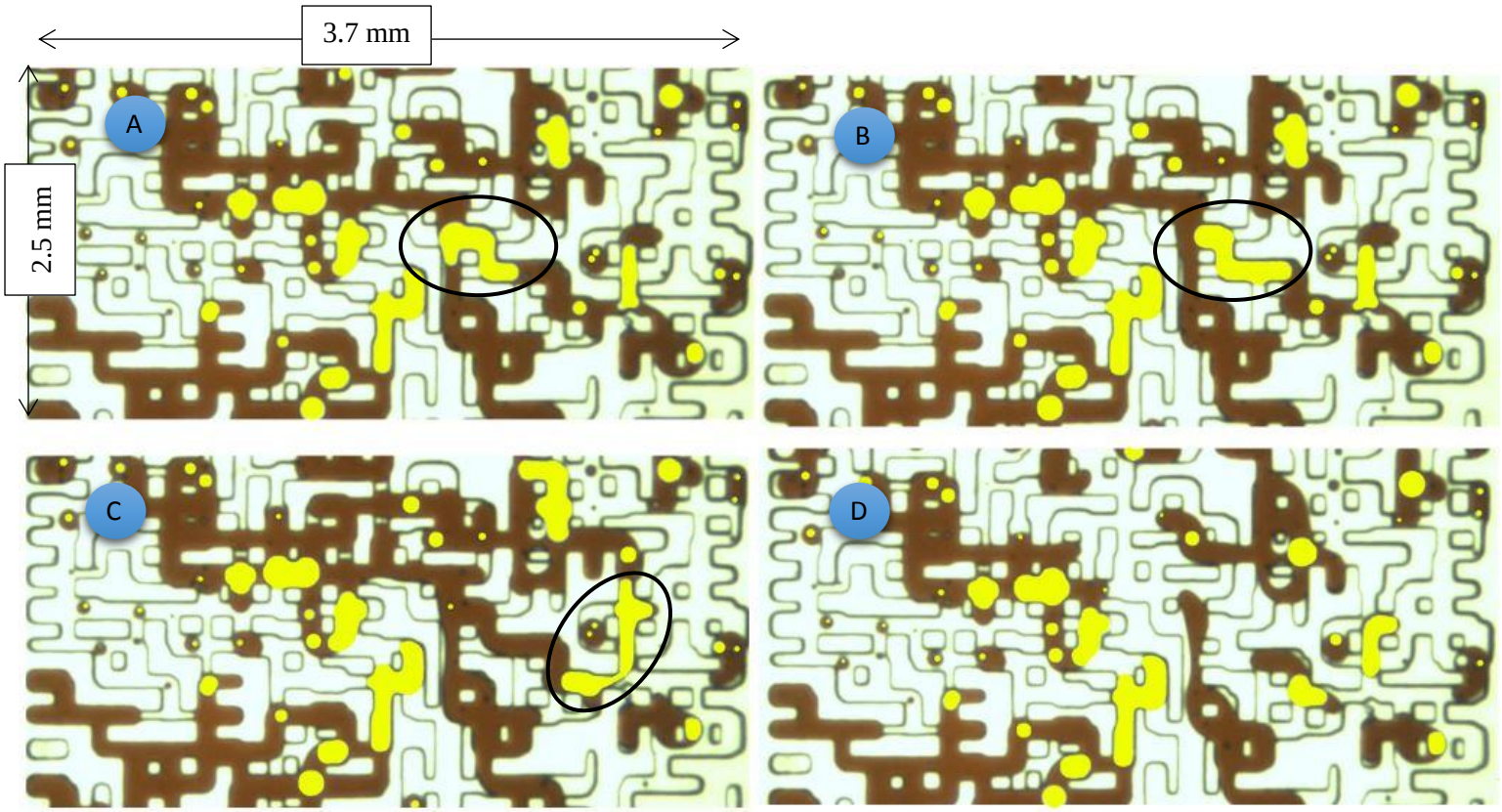

Figure 2-26 Flow of new gaseous phase inside the oil that creates a favourable three phase flow region (Image dimensions: 1024*517 pixels)

It should be noted that among the three phenomenons explained above the last one; i.e. the three phase flow condition, happened at later times and the first one, i.e. reconnection of isolated oil ganglia due to high overall oil swelling, happened at earlier times. This is because for having a three phase flow system the saturation of the new gaseous phase should pass a critical saturation and this will take some time. On the other hand, as soon as CW comes in contact with the live oil, we have the rapid formation of the new gaseous phase inside the oil which leads to instantaneous oil swelling that can lead to oil reconnection.

2.4 Conclusion

A series of high-pressure high-temperature micromodel experiments have been performed to comprehensively study the underlying oil recovery mechanisms by CWI at pore scale for two different systems, dead oil, and CH_4-satuerated (live) oil. The following conclusion can be made from this study:

1. CO_2 partitioning between CW and live oil trigger the rapid formation and growth of a gaseous new phase inside the oil. The new phase always remained inside the oil surrounded by a thin oil layer. This phenomenon was not observed in the case of the dead oil system.
2. For both dead and live oil systems CWI shows good potential for producing the bypassed oil; however, the performance of CWI for live oil system, where oil has dissolved gas, was better than dead oil system which was attributed to nucleation and growth of the gaseous new phase.
3. Based on the direct visualization results, for both dead oil and live oil systems CO_2 exchange from CW into the oil phase leads to oil swelling. However, oil swelling (total oil enlargement) for live oil system is much stronger and takes place at much earlier times compared to dead oil. This is due to nucleation of the new phase in the live oil system.
4. Formation and growth of the gaseous new phase is a new oil recovery mechanism by CWI for live oil systems that would boost the performance of CWI significantly and represents a game-changer for this EOR technique and a massive improvement in our understanding of the mechanisms of oil recovery by CWI at real reservoir conditions.
5. Formation of the new phase led to better oil recovery by; (i) reconnection of the trapped oil and oil displacement, (ii) creating a favourable three phase flow region with less residual oil saturation, and (iii) restricting the flow path of CW and diverting CW toward unswept areas of the porous medium.
6. Secondary CWI shows better performance than tertiary CWI. This is because of the higher oil saturation and better oil connectivity during secondary CWI compared to tertiary CWI.
7. The formation and growth of the new phase were stronger for the case of secondary CWI compared to tertiary CWI in the live oil system. The reason for the observed stronger and faster formation of the new phase during secondary CWI is the lower saturation of water in the model during secondary CWI compared to tertiary where the model had been flooded with plenty of plain water beforehand.
8. The colour of the oil became lighter when it came in contact with CW. This is an indication of oil viscosity reduction due to CO_2 transfer from CW to crude oil.

9. More than 60% of the total enlargement of the oil volume during CWI period in live oil system was due to the formation of the new gaseous phase inside the oil.

Chapter 3: Wettability Alteration by Carbonated Water-Contact Angle Measurements

3.1 Introduction

One of the factors that control the performance of waterflooding is wettability of the oil reservoirs. In oil-wet reservoirs, water being a non-wetting phase would preferentially flow through the larger pores bypassing a significant number of the smaller pores filled with oil. This result in an early water breakthrough and lower oil recovery compared to the water-wet case. Hence, a favourable wettability alteration can significantly affect the oil displacement efficiency and the recovery factor. In this chapter, the aim is to assess the impact of CW (carbonated water) on changing the wettability of oil reservoirs.

The dissolution of CO_2 in water reduces its pH, which can affect the electric charges on water-rock interfaces and hence, may change the wettability characteristics of the surface. This wettability alteration would have a direct effect on electrical properties of porous media [37], capillary pressure [38], [39], relative permeability [38], and flooding behaviour [40], [41]. Wettability is recognised as one of the controlling parameters of the amount of remaining oil in place and oil recovery [42].

Wettability alteration during CO_2 flooding in core samples has been studied by several researchers [43], [44]. Through using coreflood experiments, they proved that wettability alteration can happen because of CO_2 flooding. Furthermore, wettability alteration by CO_2 dissolution in brine has already been investigated for the systems of CO_2-water-coal [45]–[47], CO_2-brine-Mica [48], [49], CO_2-brine-Quartz [48], [50], CO_2-reservoir brine-reservoir rock [51]–[54], and CO_2-water-glass [55], [56]; however, very limited study focus on the wettability alteration of oil-brine-rock system with dissolution of CO_2 [52].

Yang et al. [52] performed several contact angle measurements to determine the wettability of a crude oil-brine-rock system with the dissolution of CO_2. They found that wettability alteration is likely to happen when CO_2 is injected into an oil reservoir and is expected to significantly affect the rate and amount of oil recovery. Sad et al. [57] investigated wettability alteration during CO_2 immiscible flooding through contact angle measurements. They found that exposing a carbonate rock to brine including CO_2

led to wettability alteration from oil-wet to intermediate wet. The amount of this wettability alteration was higher at higher CO_2 concentrations in brine.

Very limited direct information and measured data currently exist in the literature on the impact of CWI on the wettability of minerals. In this chapter, to assess and quantify the extent of possible wettability alteration due to carbonation of water, a series of high-pressure high-temperature contact angle measurements have been performed. The captive bubble method was used for measuring the contact angles. Three different minerals namely; Quartz, Mica, and Calcite were exposed to plain and then carbonated water under a wide range of pressures between 100 and 3500 psi. The temperature of the measurements was kept constant at 100 ^{0}F. For each mineral, two situations were considered; an un-aged (clean) system and an aged system.

3.2 Experimental Setup and Procedure

3.2.1 Contact Angle Rig

A high-pressure, high-temperature Drop Shape Analyser (DSA) rig was used for performing contact angle measurements. The rig can operate at pressures as high as 7500 psi and temperatures up to 356 °F. The metal components of the rig are made of Hastelloy C 276 to make the rig compatible with high salinity brine and CO_2 at high pressure and temperature conditions. The determination of contact angle is based on visual observation. The schematic of the rig and its principal components is shown in Figure 3-1.

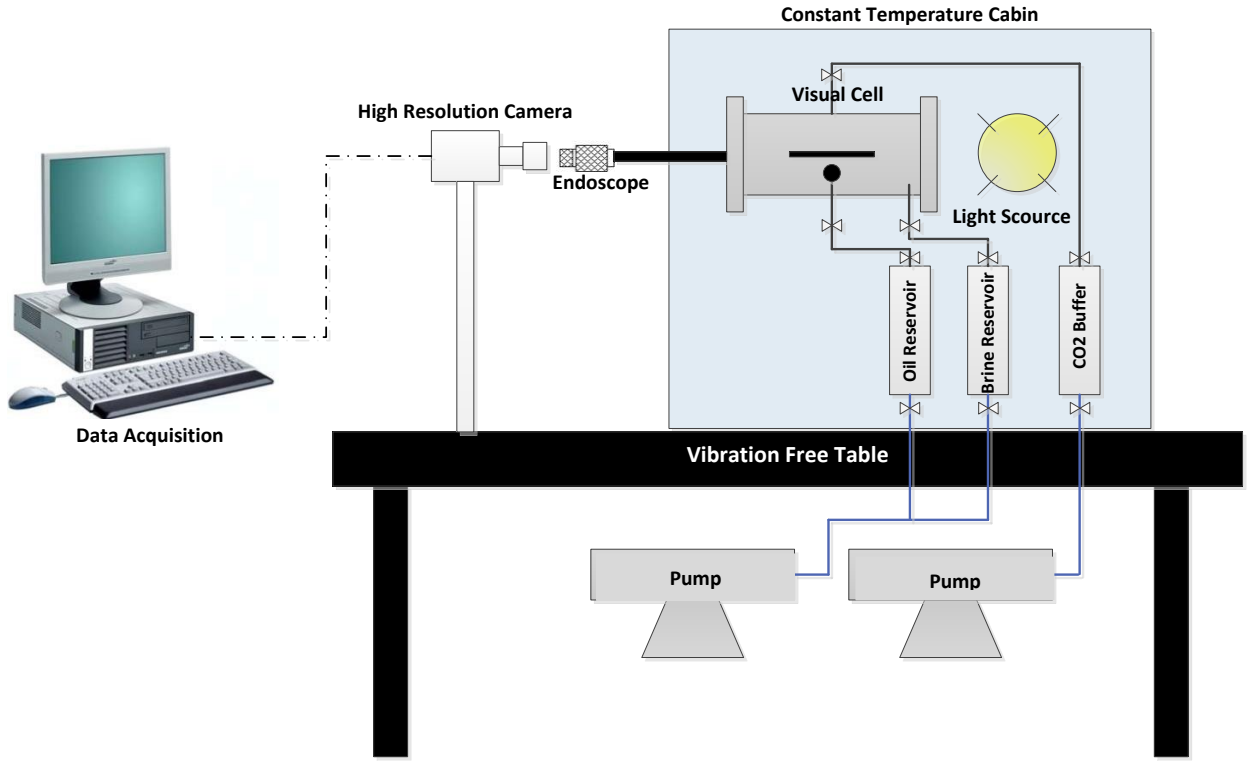

Figure 3-1 Contact angle measurement rig

Both sides of the visual cell have high-pressure sight glass windows, which make visual observation possible on one side and a light source on the other side. The rock sample is positioned inside the cell with a holder (Figure 3-2). Around the visual cell, there is a heat jacket to keep the temperature at desired value. A high-resolution digital camera was used to capture high-quality digital images of the drop on a vibration-free table.

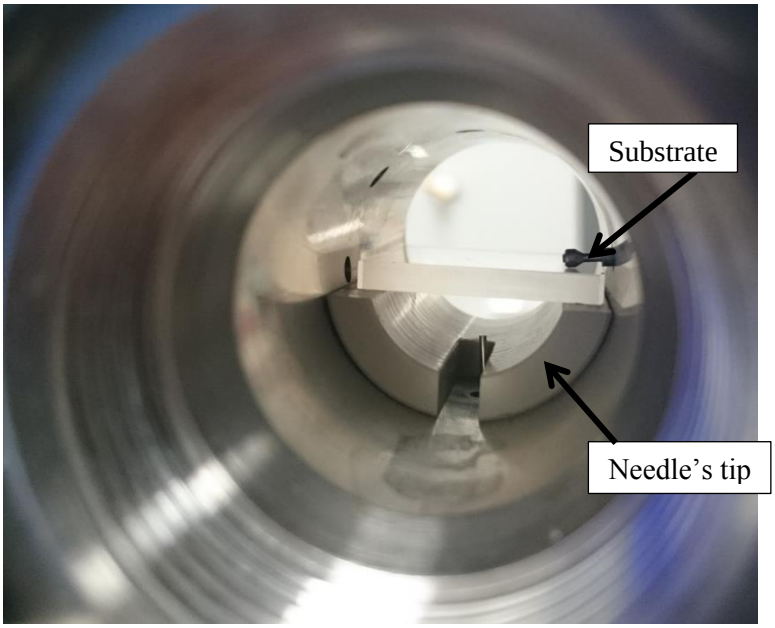

Figure 3-2 Position of the needle and substrate inside the visual cell

3.2.2 Fluids

A synthetic sea brine sample was prepared and degassed. The brine was a mixture of monovalent and divalent ions and was relatively high salinity sea brine (54,597 ppm) as shown in Table 3-1. CO_2 with purity of 99.99 mol% was used for the measurements. Reservoir crude "B" was used for the contact angle measurements. The properties of crude B are shown in Table 3-2. The viscosity and density were measured at the temperature of 100 ^{0}F which was the test temperature.

Table 3-1 Brine components

Ion	ppm
Na	16844
Ca	664
Mg	2279
SO_4^{-2}	3560
Cl	31107
HCO_3^{-1}	193

Table 3-2 Crude B properties

Crude ID	API	viscosity (cp)	density (gr/cm^3)	saturates (%wt.)	aromatics (%wt.)	resins (%wt.)	asphaltene (%wt.)
B	28.9	31.25	0.8757	43.8	25.86	29.94	0.4

3.2.3 Solid Substrates

Three different minerals were used as substrates which were Quartz, Mica, and Calcite. Quartz is one of the main minerals of sandstone rocks. The Quartz slides were provided by UQG Ltd (UK optical manufacturer) with dimensions of 30*30*1 mm.

Mica can be found in some shale and clay materials. High-quality optical grade Mica sheets (Ruby V-1 Mica Scratch free) were provided by S&J Trading Company with dimensions of 25 mm*25mm*300 Microns.

Calcite is the main constituent of carbonate rocks. High quality and smooth Calcite plates were obtained from UKGE Company with dimensions of 30*30*1 mm.

3.2.4 Experimental Procedure

Before each experiment, the high-pressure visual cell and all the connection lines were cleaned and then dried by N_2. A brand new substrate was used for each of the performed measurements. After cleaning, the substrate was placed inside the high-pressure visual cell and levelled horizontally. Figure 3-3 shows the position of the needle, with the substrate placed above it, within the high-pressure visual cell.

Subsequently, the cell's sight glasses were closed and made leak-free. Next, the cell was vacuumed to make it air free. Then, the cell was filled with the brine. During this stage, care should be taken not to move the substrate out of its position. At the start of this stage, the test temperature was adjusted by switching the heater and the temperature controller on. The system was then pressurised to the pressure of the measurement by injection of brine. Having reached the desired pressure and temperature, an oil droplet was slowly introduced onto the substrate surface to analyse its shape and measure the corresponding contact angle.

The contact angle was determined using the captive-drop technique such as depicted in Figure 3-3. A smaller contact angle indicates stronger tendency for the aqueous phase to wet the substrate.

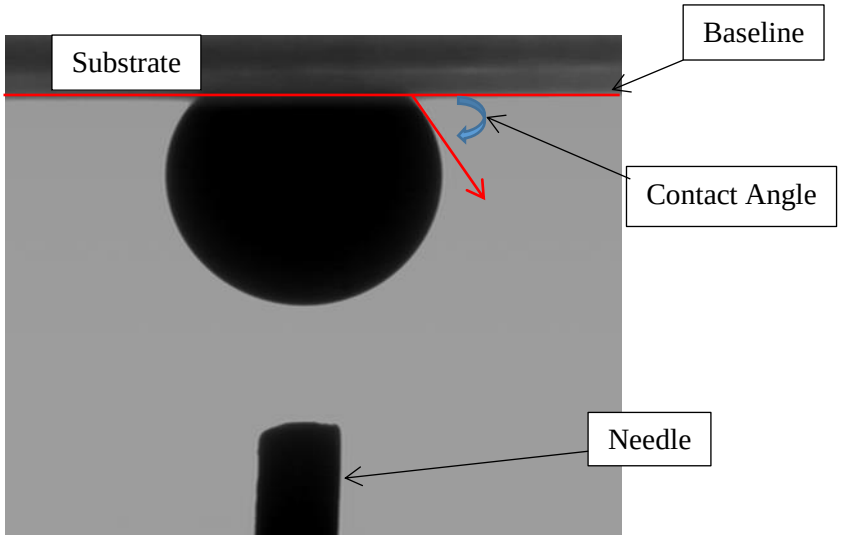

Figure 3-3 Schematic of a captive drop contact angle system. Needle diameter is 0.793 mm (droplet size 15 µL)

The contact angle measurement rig is equipped with DSA image processing software that determines the actual shape of the drop by the analysis of the image pixels. The contact line (baseline) with the surface can also be determined by the same method or manually by the user. The drop shape is fitted to a general conic section equation. The derivative of this equation at the intersection point of the contour line with the baseline gives the slope at the 3-phase contact point and thereby the contact angle. The measurement resolution is 0.1^0. For each droplet, contact angle has been measured for 24 hr to ensure that the equilibrium contact angle has been reached.

Having completed the measurement with plain brine or dead brine (DB), CO_2 was gradually introduced to the top of the brine and at the same time brine was retracted very slowly from the bottom port. After putting the CO_2 as a gas cap on top of the brine, brine retraction was stopped, and the bottom port was closed. Next, the system was allowed to achieve equilibrium. It should be noted that since the CO_2 cap over the brine was connected to a CO_2 buffer, the pressure of the CO_2 cap would always remain at the desired (test) pressure and the water would always have access to CO_2 to become saturated with CO_2 during the measurement. Depending on the test pressure, the time for achieving equilibrium between the CO_2 cap and brine would vary. One good indication that equilibrium had been reached was the pressure of the pump connected to the CO_2 buffer. As long as CO_2 continues dissolving in the brine, the pressure of the CO_2 buffer would be dropping, and the pump would continue injecting CO_2 to keep the pressure of the CO_2 cap constant at the test pressure. When equilibrium is achieved,

there would be no further mass transfer and the pump would not inject anymore. During the whole time that the test was in progress, the shape of the droplet was analysed, and the contact angle was measured. The main advantage of this method is that it captures the dynamic process of CO_2 transfer from carbonated water into the oil and possible alteration of the water-oil contact angle due to carbonated water.

After completing the test at first pressure level, the visual cell was cleaned again, and the same procedure was followed for the next pressure. This has been done for each substrate. Table 3-3 shows the list of experiments.

Table 3-3 List of experiments

Contact Angle Experiments			
No.	Pressure (psi)	Temperature (^{0}F)	Substrate
1	100	100	Clean Quartz
2	600	100	Clean Quartz
3	1500	100	Clean Quartz
4	2500	100	Clean Quartz
5	600	100	Clean Mica
6	2500	100	Clean Mica
7	3500	100	Clean Mica
8	600	100	Clean Calcite
9	2500	100	Clean Calcite
10	3500	100	Clean Calcite
11	2500	100	Aged Quartz
12	2500	100	Aged Mica
13	2500	100	Aged Calcite

3.3 Results and Discussion

3.3.1 Un-aged System

The results of contact angle measurements between crude oil and clean (un-aged) substrates in plain brine (DB) and carbonated water will be presented and discussed in this section. Based on these measurements, the effect of pressure on contact angle in

plain brine and carbonated water and more importantly effect of carbonated water on wettability alteration of clean minerals will be analysed.

3.3.1.1 Crude Oil-Un-aged Quartz Contact Angle Measurements

In the first set of experiments, contact angles were measured between crude oil B and plain brine (DB) on clean brand new Quartz substrates at 100 ^{0}F. The values of these contact angles as a function of pressure are shown in Figure 3-4. The experimental conditions of these tests are shown in Table 3-3 as experiments number 1, to 4. As Figure 3-4 shows, for the plain brine (DB) system the contact angle between the Quartz plate and crude B was almost pressure independent. Moreover, it shows that clean Quartz was water-wet in this experimental condition. However, after CO_2 was introduced to the system, the wettability was affected by the dissolution of CO_2 in water and altered towards more neutral wet (Figure 3-4). The extent of this wettability alteration was higher at higher CO_2 concentrations in brine or in another word at higher pressures (>1000 psi).

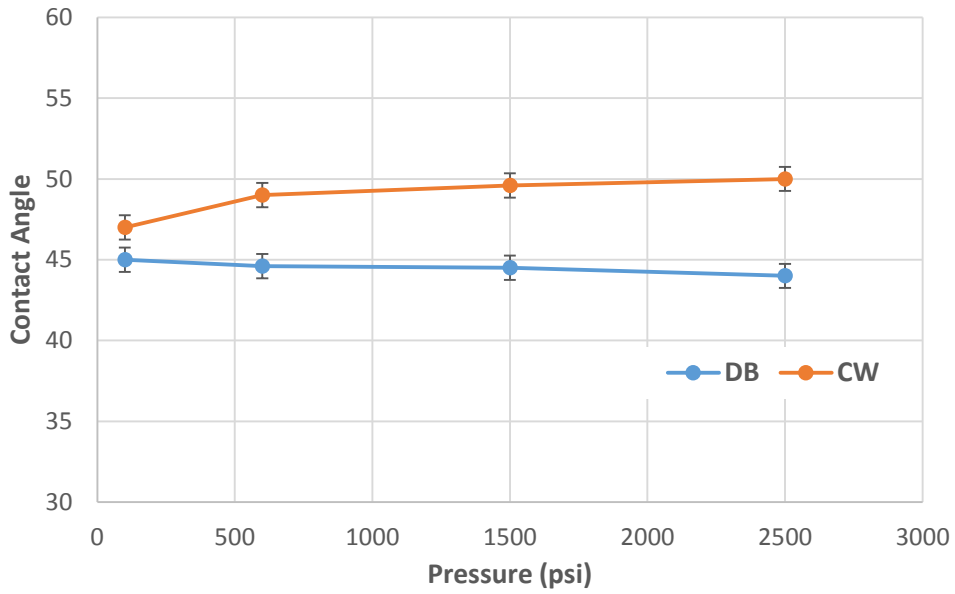

Figure 3-4 Measured equilibrium contact angles of the crude oil-un-aged Quartz in plain brine (DB) and carbonated water (CW) versus pressure at temperature of 100 ^{0}F

Quartz is in the category of Silica minerals and has negative charges above the pH values in the range of 2-3 [58], [59]. The main chemical groups on Silica surfaces in aqueous solutions are silanol and silicilic acid groups. The hydrophilicity of silica depends on the surface density of these functional groups [60]. At near neutral pH,

some silica surfaces such as Quartz are negatively charged through deprotonation of silanol sites as in reaction 1. The measured pKa values for reaction 1 are in the range of 5.7 and 7.7 [61]. When CO_2 dissolves into the brine, the brine pH reduces. Thus, reaction 1 shift to the left and the surface charge of silica is diminished. The pH effect on silica wettability was reported by Gribanova [62]. Gribanova mentioned when pH was decreased from 6 to 3; the contact angle increased from 19° to 23° in the air-brine-silica system at ambient pressure and temperature [62]. Chiquet et al. [48] explained that the decreased surface charge with decreased pH results in destabilizing the water film, therefore increasing contact angles.

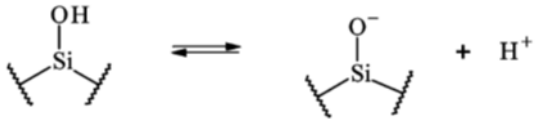

(1)

In the plain brine (DB) measurements, since the pH of the brine at test condition was around 7.5, the Quartz plate had a negative surface charge. This negatively charged Quartz showed water-wet behaviour in plain brine measurements. This means that oil-brine interface had a negative charge too. After CO_2 was introduced to the system, wettability of Quartz changed towards neutral wet. This contact angle variation is mainly due to the change in brine pH that occurs due to the dissolution of CO_2 in brine (reaction 2). The decrease in pH leads to decrease in the negative surface charge density carried by the Quartz-brine and brine-oil interfaces. As a result, the repulsive electrostatic forces between the Quartz-brine and brine-oil interfaces, which favour stabilizing the brine film and favour water-wet behaviour, are less efficient at low pH and therefore the Quartz became neutral wet.

3.3.1.2 Crude Oil-Un-aged Mica Contact Angle Measurements

Clean brand new Mica was used as the second mineral examined in this work. The measurements were performed at three different pressures of 600, 2500, and 3500 psi and a constant temperature of 100 ^{0}F. The results of these measurements are shown in Figure 3-5. As it is demonstrated in this figure, after introducing CO_2 to brine from the top of the cell, the wettability of Mica changed toward more water-wet (as CO_2 dissolved in the brine and carbonated water was produced). Based on Figure 3-5, at high pressures (>1000 psi) carbonated water caused the system to become more water-wet.

However, at low pressures (<1000 Psi) the effect of carbonated water on changing wettability of Mica was almost negligible.

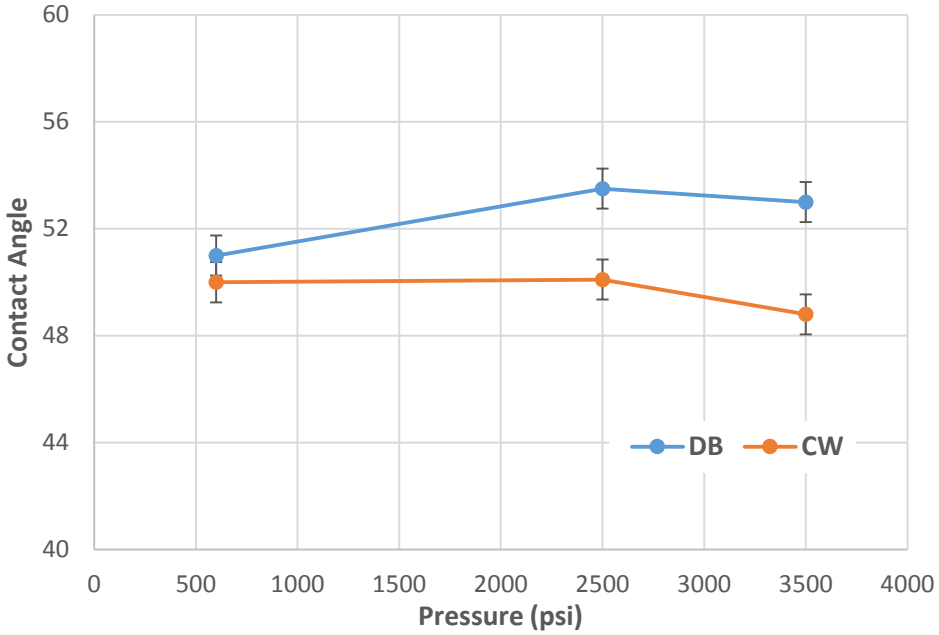

Figure 3-5 Measured equilibrium contact angles of the crude oil-un-aged Mica in plain brine (DB) and carbonated water (CW) versus pressure at temperature of 100 ^{0}F

Mica, like Quartz, is negatively charged except at very low pH [63]. Thus, it might be expected that the interactions with brine and oil should be similar for Mica and Quartz. However, the above measurements showed that Mica did not behave similarly to Quartz. This is because; the total surface charge of Mica consists of 90% to 95% of its structural charge, so the effect of pH on Mica surface charge is weak. Therefore, ion exchange can take place on the surface of Mica, and that should be considered in the studies of their surface properties [64].

The composition of the brine used in the measurements includes multivalent metal cations such as Ca^{2+} and Mg^{2+}. Such cations are believed to act as bridges between the negatively charged oil and Mica mineral; this process is named cation bridging (Figure 3-6). When CO_2 is introduced to the top of the brine, reactions 2, 3, and 4 take place. In reaction 2, $H_2CO_3{}^*$ is the sum of $CO_2(aq)$ and H_2CO_3. As a result of reactions 3 and 4, the amount of H^+ ions increases in brine and as a consequence the mineral surface exchanged H^+ ions, existed in brine, with cations previously adsorbed. This mechanism is called ion exchange. Through this process, the bond between oil and the surface becomes weaker as Mica becomes slightly more water-wet. This mechanism is also active for Quartz minerals but to a much lesser extent [65].

$$CO_2\ (g) + H_2O \longrightarrow H_2CO_3^{*} \quad (2)$$

$$H_2CO_3 \longrightarrow H^+ + CO_3^{2-} \quad (3)$$

$$H_2CO_3 \longrightarrow H^+ + HCO_3^- \quad (4)$$

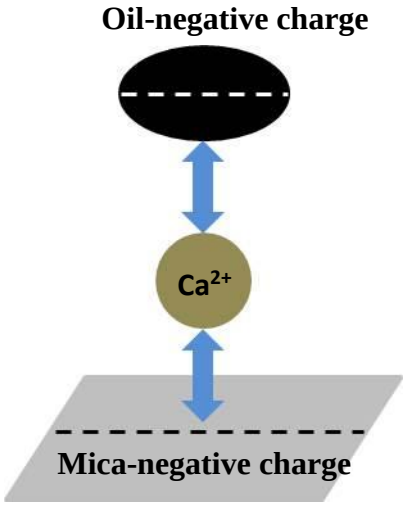

Figure 3-6 Cation bridging on Mica surface

3.3.1.3 Crude Oil-Un-aged Calcite Contact Angle Measurements

The third series of contact angle measurements were carried out using clean brand new polished Calcite substrates. The measurements were performed at three different pressures of 600, 2500, and 3500 psi and the constant temperature of 100 ^{0}F. Figure 3-7 shows the results of these measurements. As can be seen, for the plain brine (DB) system, the change in contact angle with pressure was very small, and Calcite showed water-wet behaviour. However, after introducing CO_2 to the brine, the wettability of Calcite changed toward more water-wet. This change in the wettability towards more water-wet increased with pressure and was more profound when the pressure was above 1000 psi.

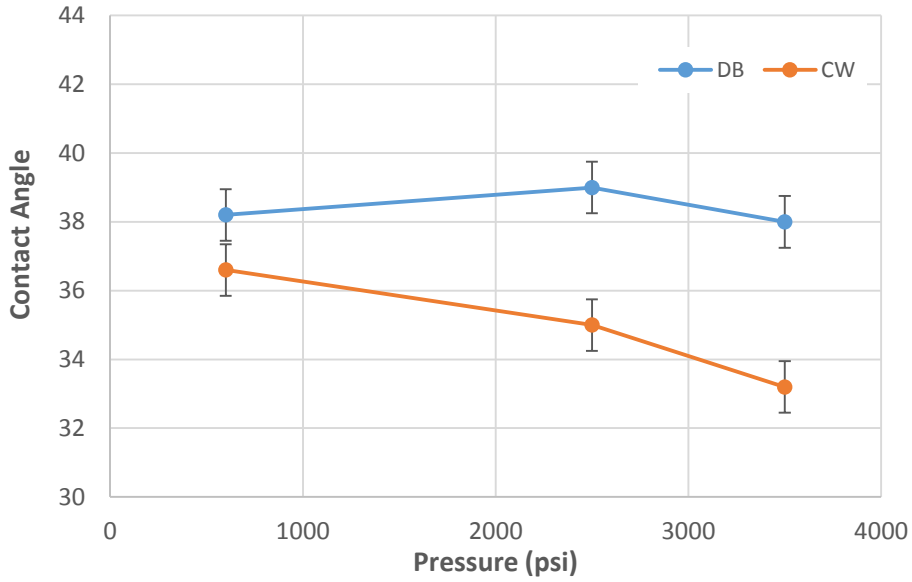

Figure 3-7 Measured equilibrium contact angles of the crude oil-un-aged Calcite in plain brine (DB) and carbonated water (CW) versus pressure at temperature of 100 ^{0}F

Calcite surface is positively charged below a pH of about 9.5 [41], [66]. Therefore, in the measurements positively charged Calcite has a tendency toward attracting negatively charged oil; however, due to the presence of Potential Determining Ions such as Ca^{2+}, SO_4^{2-} and Mg^{2+} in the surrounding brine, Calcite showed water-wet behaviour. The concentrations of these Potential Determining Ions have a significant effect on the surface chemistry and wettability alteration of Calcite. These ions have the ability to change rock surface charges, released adsorbed carboxylic oil component from the rock surface and alter rock wettability and eventually improve oil recovery [67]–[71].

Based on published research on imbibing sea water into a chalk rock samples, it is expected that SO_4^{2-} ions will be adsorbed on positively charged chalk surfaces and as a result, the bond between a negative oil component and rock surface will deteriorate. Due to the decrease in the positive surface charges of chalk, more Ca^{2+} ion will be able to attach to the rock surface releasing negatively charged oil components (Figure 3-8). Since the brine used in these measurements contains these Potential Determining Ions, a stable film of water will be present between the oil droplet and Calcite surface and hence, Calcite shows water-wet behaviour.

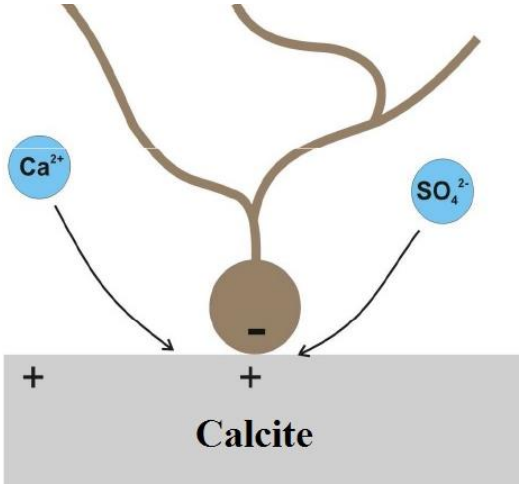

Figure 3-8 Mechanism of Calcite wettability alteration [71]

Now, when CO_2 is added to the brine, the following reaction can take place and therefore the concentration of Ca^{2+} ions increases and, as a result, more Ca^{2+} ion is able to be adsorbed onto the calcite surface releasing more negatively charged oil components and making the surface more water-wet.

$$CaCO_3 + H_2O + CO_2 \longrightarrow 2HCO_3^- + Ca^{2+} \quad (5)$$

It should be noted that at lower pressures (<1000 psi), since the amount of dissolved CO_2 is less than that at higher pressures (>1000 psi), the degree of wettability change is expected to be less as was observed in the measurements.

During Calcite contact angle measurements, some dissolution of Calcite was observed. Figure 3-9 shows a Calcite surface before introducing CO_2 in the system (plain brine) and also 24 hours after submerging it in carbonated water. This Figure shows some changes (increased in surface roughness) happening on the surface of Calcite when it was submerged in CW. In order to observe these changes in more detail, ESEM images were taken from the Calcite substrate before running the experiment and after the same substrate had been exposed to CW at a pressure of 2500 psi. Figure 3-10A and Figure 3-10B show the Calcite surface in the test before adding CO_2 to brine. As it is depicted in these figures, Calcite substrate's surface was initially very smooth; however, after it was exposed to CW (Figure 3-10C and Figure 3-10D), its surface became rough due to reactions with CO_2-enriched brine causing uneven dissolution of the surface. The dissolution rate of Calcite is a function of brine pH that is a function of CO_2 pressure on

top of the brine [72]. We believed that the observed dissolution of Calcite surface could also be a mechanism responsible for desorption of organic acid groups, increased water wetness and improved oil recovery by carbonated water.

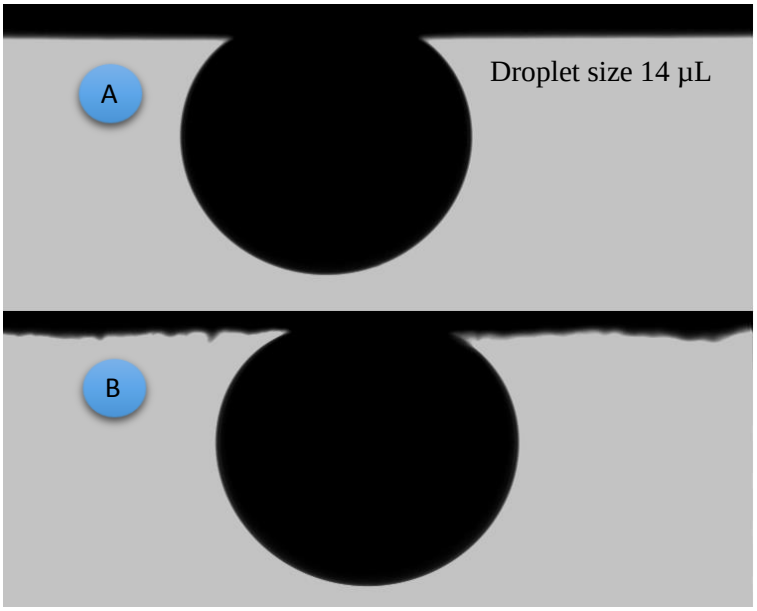

Figure 3-9 Calcite surface, A) Before introducing CO_2 into brine and B) 24 hours after submerging it in carbonated water

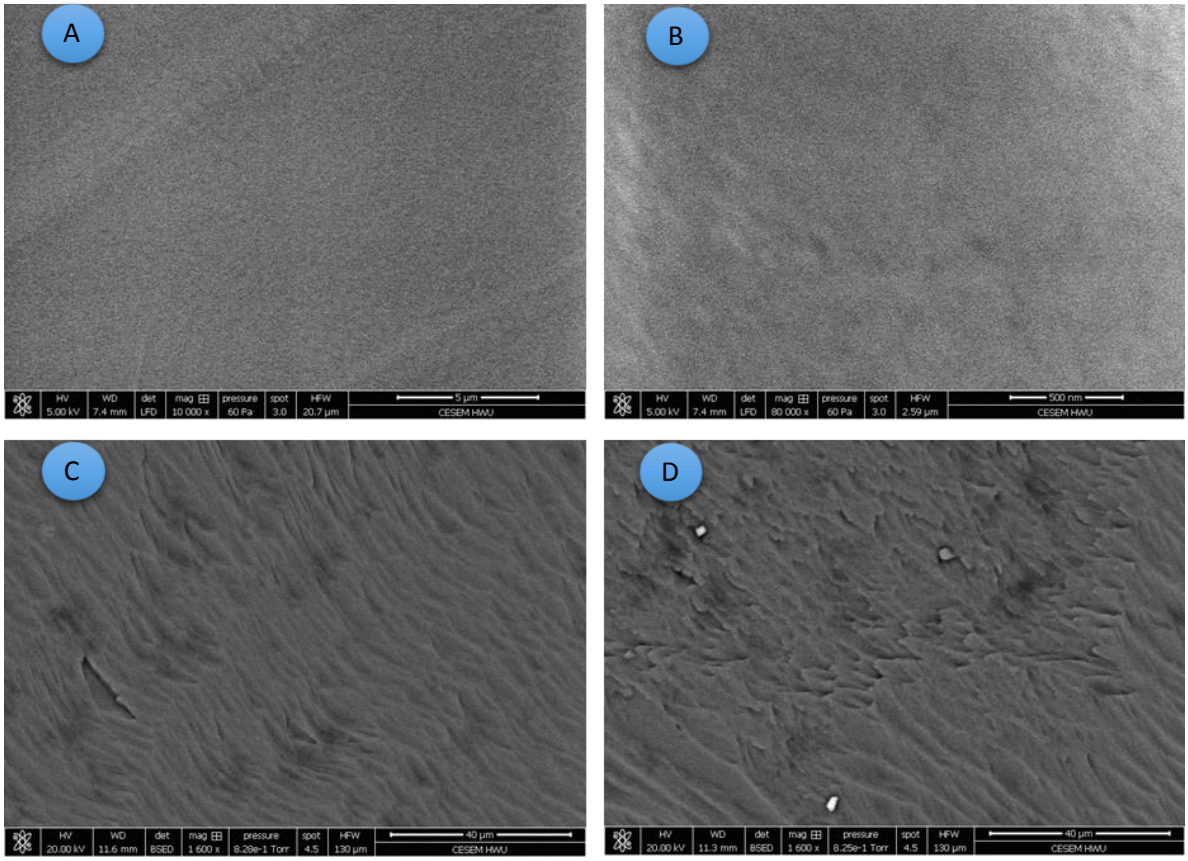

Figure 3-10 Effect of CW on the surface of calcite. A and B) Smooth, clean calcite. C and D) The same substrate after exposing to carbonated water for 24 hr

3.3.1.4 Repeatability of Un-Aged Measurements

To examine the repeatability of the measurements, the experiments performed at 2500 psi for different substrates have been repeated. Figure 3-11 shows the results of repeat measurements at a pressure of 2500 psi and temperature of 100 ^{0}F. As can be seen from this figure, a reasonably good level of repeatability was obtained for the measurements. Furthermore, the error bars in Figure 3-4, Figure 3-5, and Figure 3-7 were set based on the repeatability of the measurements.

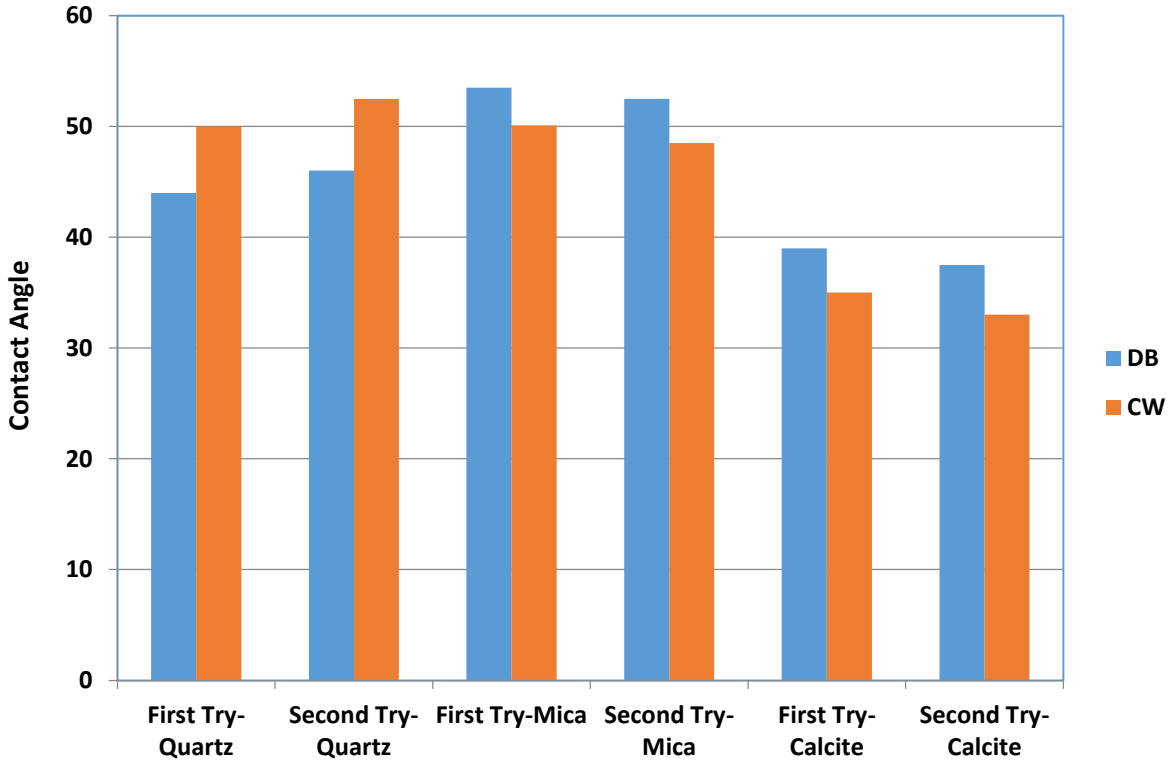

Figure 3-11 Reproducibility of contact angle measurements at pressure and temperature of 2500 psi and 100 ^{0}F respectively

3.3.2 Aged System

So far in this chapter, the effect of CW on the wettability of three different un-aged minerals at different pressures have been investigated and discussed. In order to mimic reservoir conditions as closely as possible, in the following series of measurements the substrates (Quartz, Mica, and Calcite) were aged in a crude oil (Crude B) for different time periods. For this purpose, first, the brand new clean substrates were allowed to attain ionic equilibrium in the brine (see Table 3-1) for three days. Next, the substrates were removed from the brine and were submerged in a beaker filled with crude B. The

beaker was kept inside a temperature controlled oven at a temperature of 140 ^{0}F for a period of time. A higher temperature was chosen to improve the aging process.

After the aging process, the bulk oil was removed from the surface of the substrates. For this purpose, the substrates were moved to a centrifuge tube filled with the sea brine (see Table 3-1) and centrifuged at 3000 rpm for 20 min. Having removed the bulk oil, the substrates were used for contact angle measurements.

Aged experiments were performed at a pressure of 2500 psi and temperature of 100 ^{0}F. This pressure was chosen because of two reasons. First, as it was observed in the aforementioned experiments, the maximum contact angle change had been observed at this pressure. Second, the pressure of 2500 psi represents a real reservoir pressure compared to the lower pressures tested in this study.

3.3.2.1 Aged Quartz

A Quartz substrate was aged in crude B for 32 days using the procedure explained above and was then used in contact angle measurements. Figure 3-12 compares the results of this test with the results of the un-aged Quartz test at the same pressure (2500 psi) and temperature (100 ^{0}F).

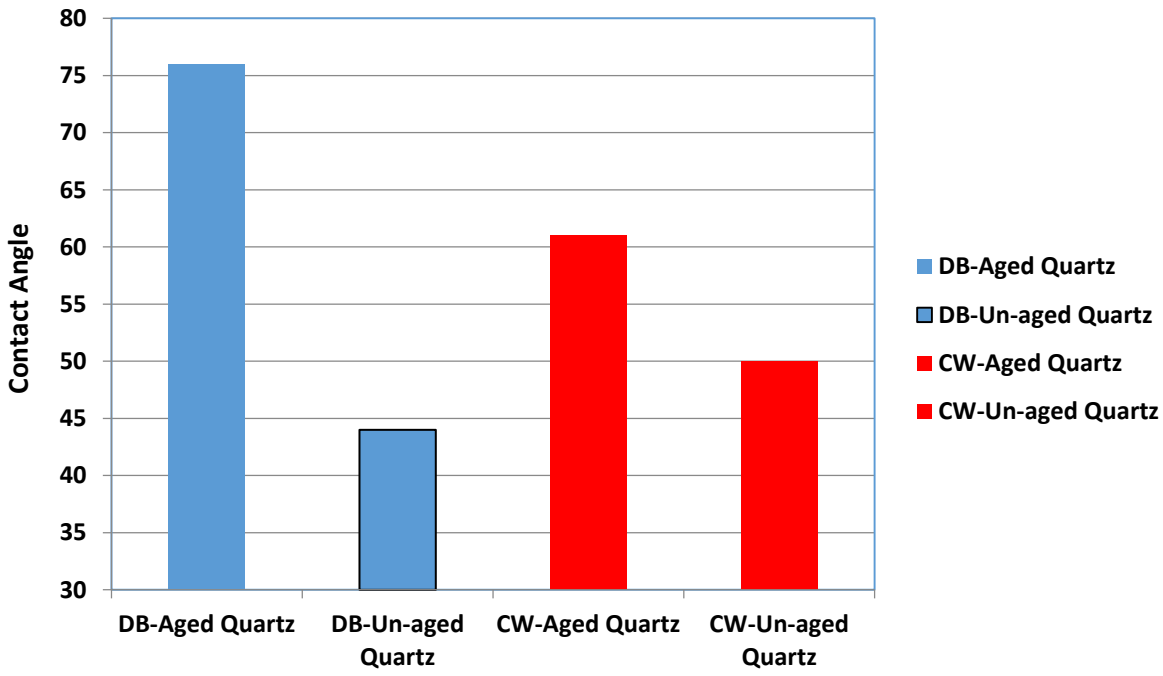

Figure 3-12 Measured equilibrium contact angles of the crude oil-Aged Quartz and crude oil-Un-aged Quartz systems in plain brine (DB) and carbonated water (CW) at pressure and temperature of 2500 psi and 100 ^{0}F respectively

It can be observed from Figure 3-12 that aging process caused that wettability of quartz in plain brine (DB) atmosphere changed toward more oil-wet. The contact angle changed from 44 to 76. Based on this figure, for the aged Quartz, after CO_2 was introduced into the brine, contact angle reduced by around 15 degrees and wettability changed toward more water-wet. This trend of wettability alteration is opposite to what had been observed for the effect of CO_2 in the un-aged Quartz measurements. During the aging period, heavy components of the oil are adsorbed on the substrate's surface resulting in the surface to become oil-wet. When CO_2 is added to the brine, it dissolves into the brine and as a result, the pH of the brine reduces. This acidic nature of CW may cause the oil aggregates adsorbed on the substrate during aging in oil to be detached from the surface changing the wettability toward more water-wet.

3.3.2.2 Aged Mica

A brand new and clean Mica substrate was aged in crude B for 32 days before being used for these measurements. Figure 3-13 shows the results of this test in comparison with the results of the un-aged Mica test performed at the same pressure (2500 psi) and temperature (100 ^{0}F).

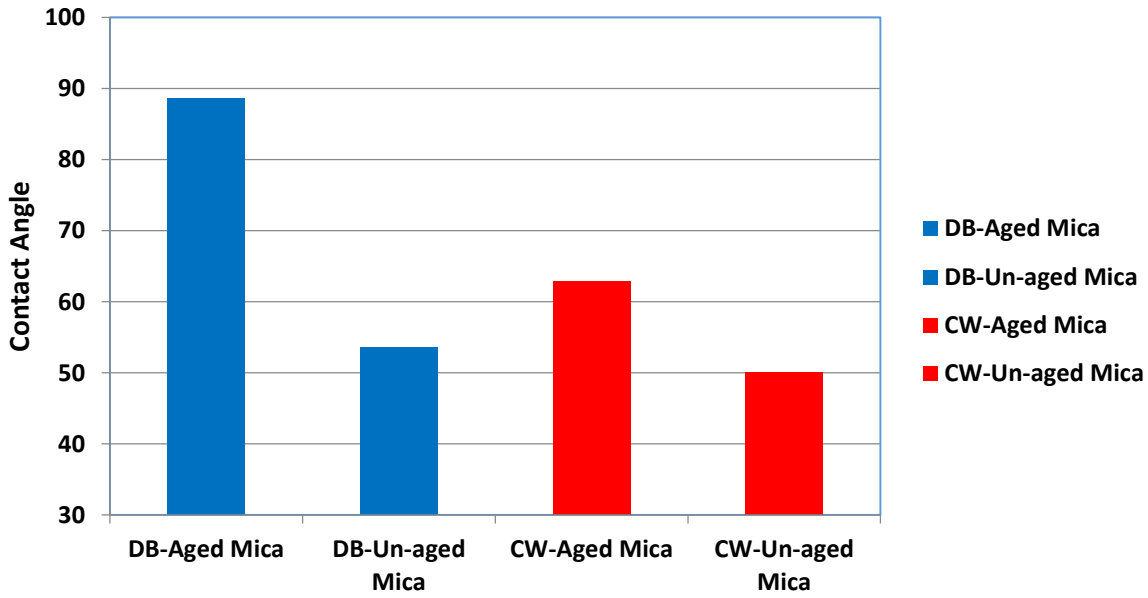

Figure 3-13 Measured equilibrium contact angles of the crude oil-Aged Mica and crude oil-Un-aged Mica systems in plain brine (DB) and carbonated water (CW) at pressure and temperature of 2500 psi and 100 ^{0}F respectively

As can be seen from Figure 3-13, due to the aging process, the aged Mica exhibited higher contact angle for plain brine (DB) compared to the un-aged one which indicates that the aged Mica was more oil-wet than the un-aged one. The results also show that when CO_2 was introduced to the system, the wettability of the aged Mica changed toward more water-wet. This trend of wettability alteration is consistent with what was observed for the un-aged one. However, the amount of this wettability alteration for the aged Mica is much more than that of the un-aged Mica. The reason for wettability alteration of aged Mica in the presence of CO_2 in brine would be the same reason that was mentioned for the wettability alteration of aged Quartz.

3.3.2.3 Aged Calcite

A polished calcite substrate was aged in crude B for 14 days and then was centrifuged for 20 min to remove the crude oil. However, for Calcite contrary to the other two minerals, even after centrifuging the sample, there was still oil remaining on the surface. This indicates the strong effect of aging on the wettability of Calcite which shifts its wettability toward strongly oil-wet. Therefore, in order to remove this remaining oil, the aged calcite substrate was rinsed thoroughly with cyclohexane until no colour could be seen in the rinse fluid. This has to be done before running the test since if a continuous oil film exists on the surface, the probe oil can merge with the bulk oil and the contact angle would be 180. This angle would not be the contact angle reflecting the chemical properties of the surface after aging.

Having removed the bulk oil from the aged Calcite, it is ready for the test. The results of this test were compared with the results of un-aged Calcite test at a pressure of 2500 psi and brought in Figure 3-14.

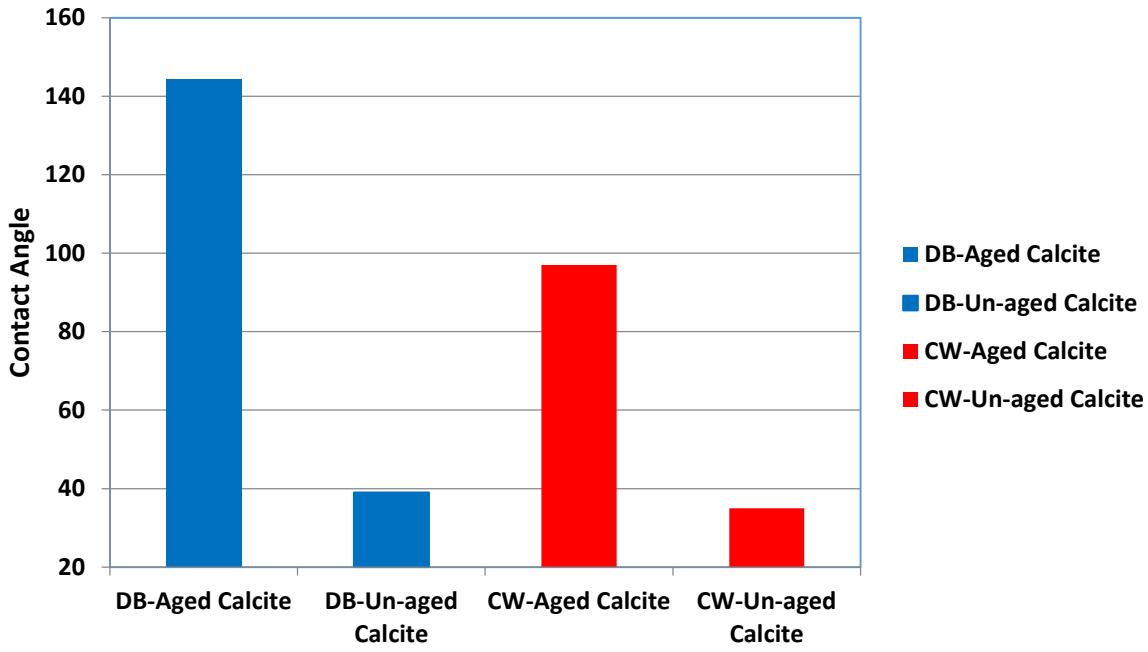

Figure 3-14 Measured equilibrium contact angles of the crude oil-Aged Calcite and crude oil-Un-aged Calcite systems in plain brine (DB) and carbonated water (CW) at pressure and temperature of 2500 psi and 100 ^{0}F respectively

As demonstrated in Figure 3-14, aging had a noticeable effect on the wettability of Calcite and made it oil-wet. Although the aging time for Calcite substrate was almost half of the aging time of Quartz and Mica, it became significantly more oil-wet than the two latter minerals. This shows that the aging process, at a specific period of time, with crude B is more effective on carbonate rocks compare to sandstones.

When CO_2 was introduced to the system, the wettability of Calcite changed toward water-wet. This trend of wettability alteration is consistent with what was observed for un-aged Calcite. However, the extent of wettability alteration for the aged Calcite was much higher than the un-aged Calcite. The observed wettability alteration of Calcite is crucial since Calcite is the main element of carbonate reservoirs and most carbonate reservoirs tend to be oil-wet. Oil-wet behaviour generates significant problems in oil recovery from these reservoirs since oil will have a stronger tendency to remain attached to the rock surface rather than move toward the production well. It also decreases the efficiency of waterflooding.

Based on the observation and measured data on wettability alteration of aged calcite sample, it is expected that injection of CW can favourably alter the wettability of carbonate reservoirs from oil-wet toward water-wet and hence, improve oil recovery.

By comparing Figure 3-12, Figure 3-13 and Figure 3-14, it can be seen that the amount of wettability alteration in aged Calcite due to the presence of CW is higher than that of the aged Mica and Quartz. This is because, in addition to desorption of oil aggregates from the surface due to pH reduction, there is another factor for wettability alteration of Calcite, which is the dissolution of Calcite in the presence of CW (see Figure 3-10). This mechanism will cause the fresh surface of the Calcite to come in contact with oil resulting in a more wettability alteration for Calcite.

3.3.2.4 Repeatability of Aged Measurements

Figure 3-15 shows the results of repeated measurements for two different experiments at pressure and temperature of 2500 psi and 100 ^{0}F. This figure confirms the repeatability of the reported contact angle measurements.

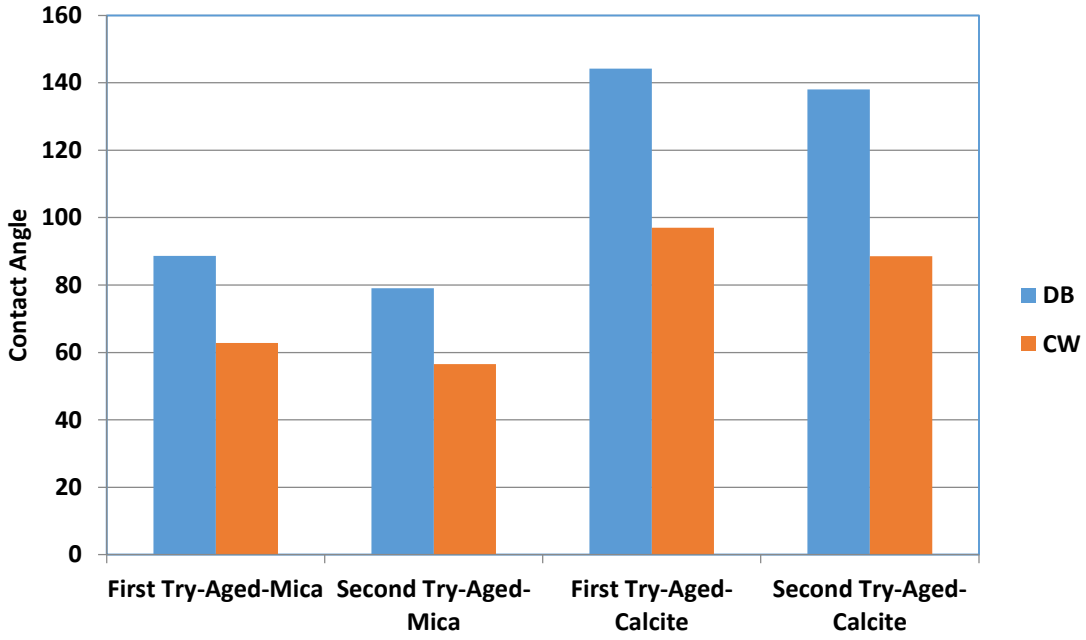

Figure 3-15 Reproducibility of contact angle measurements for the aged system at pressure and temperature of 2500 psi and 100 ^{0}F respectively

3.4 Conclusion

It is well-documented that wettability alteration has a significant effect on recovery factor of oil reservoirs. Since CO_2 injection under various injection strategies (including plain CO_2 flood, CO_2-WAG or Carbonated Water Injection) is widely considered for

and applied to oil reservoirs, it is very important to understand the impact of dissolved CO_2 in the water on the wettability of reservoir rock. A series of high-pressure high-temperature contact angle measurements have been performed and analysed in this chapter to comprehensively investigate the effect of CO_2-enriched water on wettability alteration for different minerals. Two systems were considered, un-aged and aged minerals. The following conclusions were reached in this study:

1. Carbonated (CO_2-enriched) water has a significant impact on wettability. The extent of wettability alteration is a direct function of CO_2 concentration in brine (or in another word saturation pressure) and also initial wettability stage of the rock.

2. One important cause of wettability alteration in un-aged Quartz is the decrease of brine pH that follows CO_2 dissolution. This caused the wettability of un-aged Quartz to change toward neutral wet.
3. Due to the dissolution of CO_2 in brine, the amount of H^+ in brine increases and ion exchange between multivalent metal cations (Mg^{2+} and Ca^{2+}) and H^+ takes place. Due to this ion exchange, the un-aged Mica became slightly more water-wet.
4. The difference in wettability alteration observed for different minerals demonstrates that each mineral behaves differently in the presence of CW.
5. Dissolved CO_2 in brine on un-aged Calcite caused some dissolution of Calcite as well as wettability alteration towards more water-wet conditions.
6. The results reveal that wettability alteration by CW has a stronger effect on aged minerals compared to unaged ones. This shows that under real reservoir conditions, where the reservoir rock is usually mixed-wet or oil-wet, the dissolved CO_2 in water can have a major impact on the wettability of the reservoir, which in turn will affect the oil displacement recovery factor.
7. The extent of wettability alteration on the aged Calcite was higher than that of the aged Mica and Quartz. This is attributed to the dissolution of Calcite by the low-pH carbonated water as well as the desorption of the adsorbed oil wetting layer that also took place in the Quartz and Mica measurements.

Chapter 4: Coreflooding Studies

4.1 Introduction

Having comprehensively investigated the fluid-fluid (Chapter 2) and rock-fluid-fluid (wettability studies, Chapter 3) interactions during CWI in oil reservoirs, to study the potential of this EOR scenario and impacts of these interactions on oil recovery at core scale, in this chapter, a series of high-pressure high-temperature coreflood experiments were conducted using a representative live oil. The aims of this chapter are as follows;

(i) Comprehensively studying the effects of new oil recovery mechanisms of CWI, i.e. formation and growth of the new gaseous phase and wettability alteration, and to find the degree of importance of each of them. For this aim, a series of carefully designed coreflood experiments were performed at pressure and temperature of 2500 psia and 100 °F. To study the potential of CWI on wettability alteration of the oil-brine-rock system, two separate systems were considered, water-wet system and mixed-wet system. ‘’Live’’ crude oil was used in all the experiments to study the effect of third phase (new phase) formation on oil recovery by CWI. For each system, a secondary waterflood and a secondary CWI were conducted, and their results were compared with each other. Additionally, to study the potential of CWI as a CO_2 storage strategy in oil reservoirs, the CO_2 storage capacity was determined.
(ii) Investigating the effect of carbonation level of CW on its performance. For this aim, a secondary CWI with 27% higher CO_2 content was performed and the results were compared with a coreflood experiment in which CO_2 content of CW was less. In both experiments, the cores were aged and ‘’live’’ reservoir oil was used.

(iii) Investigating the potential of secondary and tertiary CWI in a heterogeneous and long porous medium. For this purpose, two experiments have been carried out using CW in a heterogeneous core with the length of 30 cm, and the results were compared with the results of conventional waterflooding. To mimic the real reservoir conditions, the core was aged and live reservoir oil was used.

It should be noted that in order to keep the consistency between the coreflood and micromodel experiments, the same type of fluids and experimental conditions have been used in all of the performed coreflood and micromodel experiments in this thesis.

4.2 Experimental Setup and Procedure

4.2.1 Coreflood Rig

The coreflood rig used for the experiment has been designed to conduct flooding experiments at high-pressure and high-temperature. To minimize the gravity effect, the core holder was placed horizontally. The experimental apparatus is shown in Figure 4-1 and consists of the following components: a Hassler-type core holder, two pumps, injection cells, two pressure transducers, back pressure regulator, a separator and a gasometer. The core holder, injection cells, and back pressure regulator (BPR) are placed inside the oven and are maintained at constant temperature (100 °F). While running an experiment, the core effluent would pass through a backpressure regulator where the pressure would drop to atmospheric pressure and hence, any dissolved gas will be liberated and measured. The separated liquid would then be collected in a graduated cylinder while the gas will pass through a gasometer.

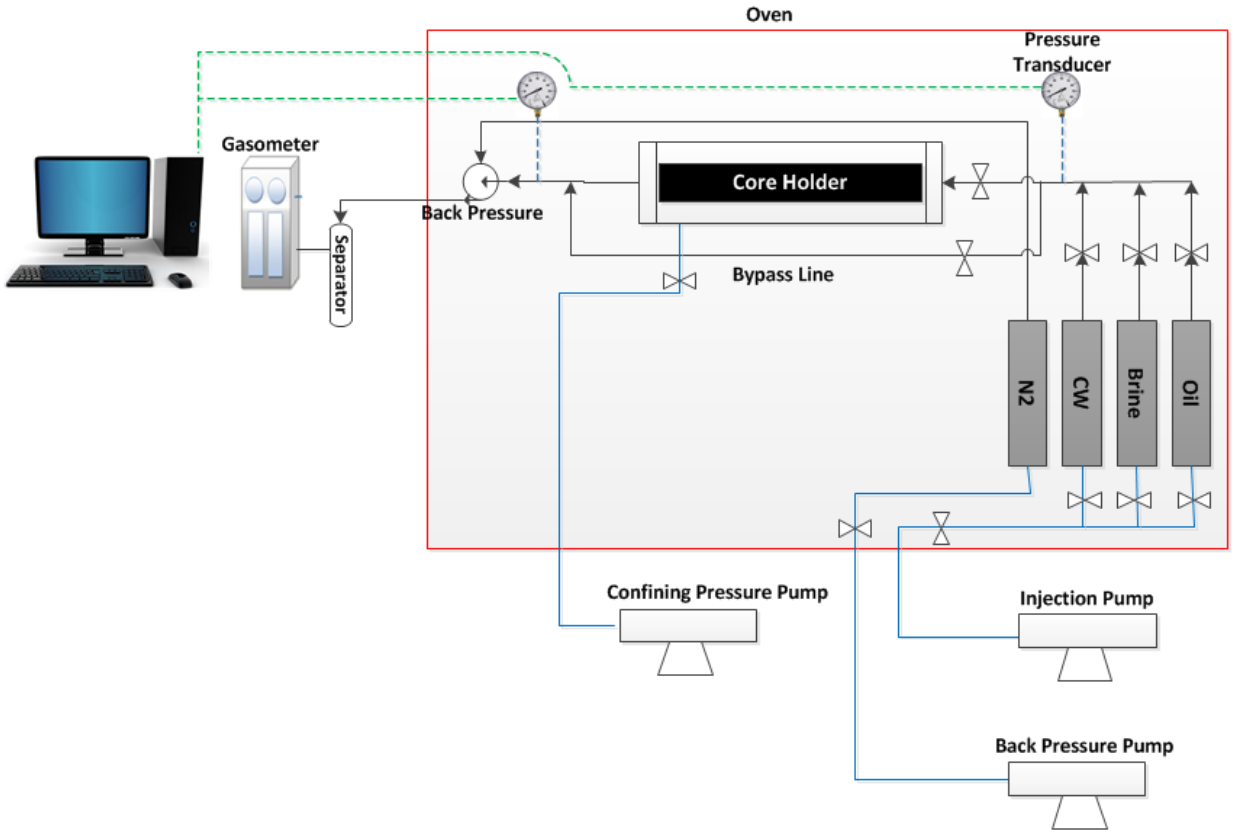

Figure 4-1 Schematic of the rig

4.2.2 Fluids Properties

It should be noted that to have a consistency with the micromodel experiments reported in Chapter 2, the same type of fluids under same experimental conditions were used in this chapter. Therefore, ‘’live’’ reservoir crude oil (J) was used in all of the coreflood experiments have been reported in this chapter. The API and density of this crude oil in dead conditions and temperature of 100 °F are respectively 20.87° and 0.9247 gr/cm^3. The other properties of the crude oil are shown in Table 4-1. To prepare the live oil used in the experiments, crude J was mixed with CH_4 at test pressure and temperature of 2500 psia and 100 °F. To prepare the CW, CO_2 was mixed with the high salinity sea brine at test pressure and temperature (2500 psi and 100 °F). The CO_2 content of CW at experimental conditions was 26 scc CO_2/scc brine. The sea brine has the salinity of 54,540 ppm and viscosity of 0.789 cp at test conditions. The brine composition is shown in Table 4-2.

Table 4-1 Crude J properties

crude ID	API	saturates (wt. %)	aromatics (wt. %)	resins (wt. %)	asphaltenes (wt. %)
Crude J	20.87	30.00	40.10	24.20	5.70

Table 4-2 Sea brine components

Ion	ppm
Na	16844
Ca	664
Mg	2279
SO_4^{-2}	3560
Cl	31107
HCO_3^{-1}	193

4.2.3 Core Properties

As discussed earlier, the main objectives of this chapter are to comprehensively investigate; (i) the new oil recovery mechanisms by CWI, (ii) the impact of carbonation level of CW on its performance and (iii) finally the potential of both secondary and tertiary CWI in a heterogeneous and long porous medium. For this aim, seven series of

coreflood experiments have been conducted at pressure and temperature of 2500 psia and 100 °F. Table 4-3 summarizes the coreflood experiments and their conditions. The aim of the first four experiments is to address the lack of understanding about impacts of new oil recovery mechanisms by CWI, i.e. wettability alteration and formation of the new phase, on its performance. In experiment number 5 the aim is to understand the effects of carbonation level of CW on its oil displacement potential. Finally, experiments number 6 and 7 were carried out with this objective to comprehensively study the potential of both secondary and tertiary CWI in a 30 cm long and heterogeneous porous medium.

Table 4-3 Summary of coreflood experiments and their conditions

Exp.	Injection Scenario	Wettability state	Oil	T (°F)	P (psia)
1	WF	water-wet	Crude J (live – Fully Saturated)	100	2500
2	CWI	water-wet	Crude J (live – Fully Saturated)	100	2500
3	WF	mixed-wet	Crude J (live – Fully Saturated)	100	2500
4	CWI	mixed-wet	Crude J (live – Fully Saturated)	100	2500
5	CW with higher carbonation level	mixed-wet	Crude J (live – Fully Saturated)	100	2500
6	WF ⟶ CWI	mixed-wet	Crude J (live – Fully Saturated)	100	2500
7	CWI	mixed-wet	Crude J (live – Fully Saturated)	100	2500

For the first five experiments, to achieve the same properties of all cores, five homogenous Berea sandstone cores were drilled from an outcrop. The dimensions and other physical properties of these cores are given in Table 4-4. In all experiments, the porosities of the cores were determined by helium porosity test and then reconfirmed by brine. The pore volumes of the cores were determined as the total volume of fluid used

to saturate the core. The porosity was calculated as the ratio of the pore volume and the bulk volume of the core. The permeabilities of the cores were measured at the test pressure and temperature using brine (Table 4-2). To have a complete understanding of the mineralogy of the Berea sandstone cores used, ESEM analysis was performed on a slice of the rock. Figure 4-2 shows the EDS map of a slice of Berea. As can be seen from this figure, the rock is mainly made of silica oxide (Quartz). It also has feldspar, clay, mica and some Fe and Ti rich minerals.

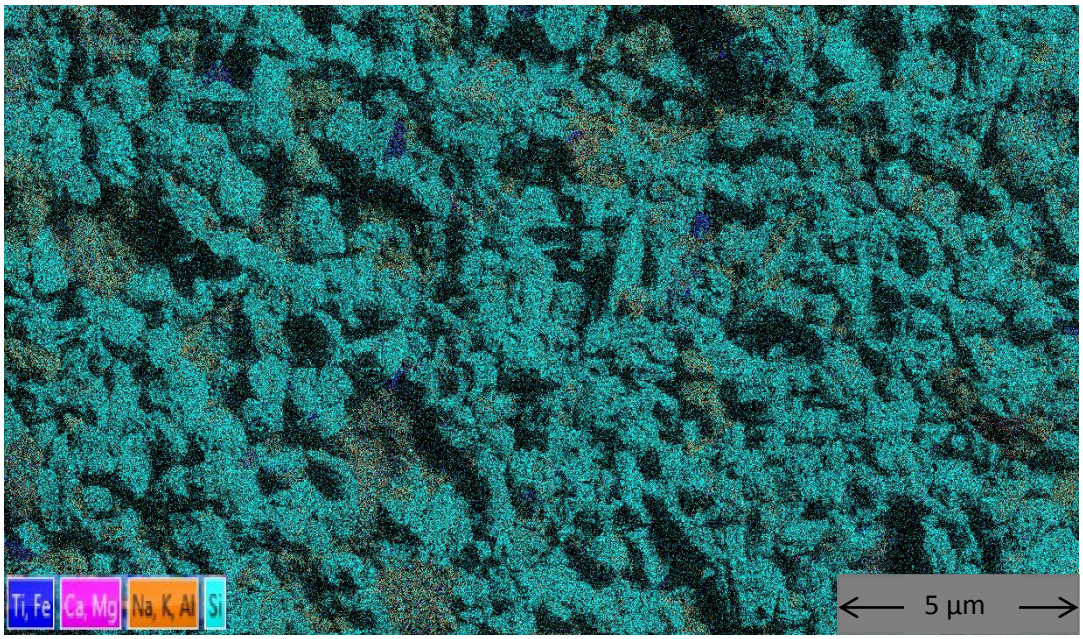

Figure 4-2 EDS map of Berea sandstone rock (magnification 10000 x)

To study the performance of CWI in a heterogeneous and long porous media, a 30 cm long heterogeneous sandstone outcrop was used (experiments 6 and 7 in Table 4-3). The dimensions and other physical properties of this core are given in Table 4-4. To be sure that the core is heterogeneous, miscible tracer test was performed. Lithium was used as the tracer. Figure 4-3 shows the change in lithium concentration during the tracer test. The y-axis in this figure shows the ratio of lithium concentration in the effluent fluid to the original concentration of the lithium in the injected fluid. Based on this figure, the gradual rise in lithium concentration and the long decreasing tail in the lithium concentration profile reveals that the core is heterogeneous. Furthermore, the core was sent for CT-scanning analysis to see heterogeneities, such as permeability layers were present in the core. The results of core scanning (Figure 4-4) shows the heterogeneity of the core. Figure 4-4 shows the bedding. The scan was performed along the long axis of

the core. Figure 4-4A shows the long axis of the core when it was normally viewed, and Figure 4-4B shows the long axis of the core when the data were levelled.

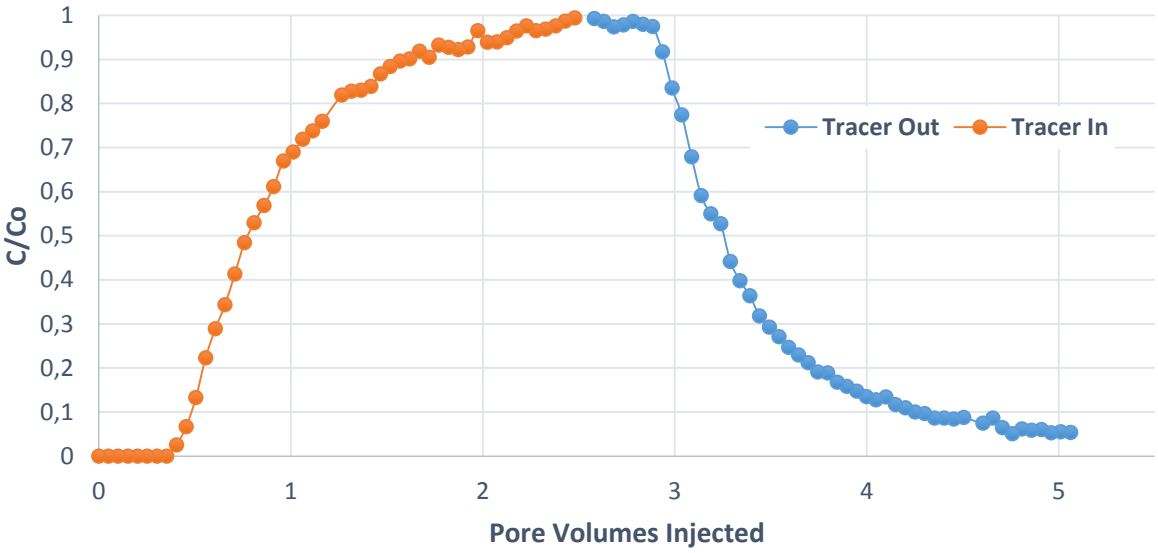

Figure 4-3 Results of the Lithium tracer test in a heterogeneous sandstone core

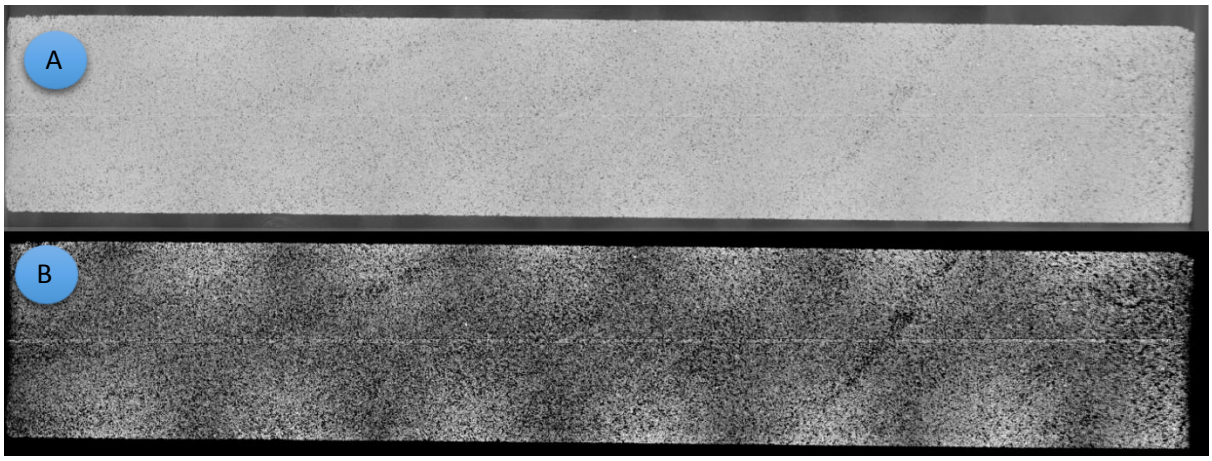

Figure 4-4 CT-Scan results of the heterogeneous sandstone core (30 cm*4.9 cm)

To have a complete understanding of the mineralogy of the sandstone used, XRD analysis was performed on a slice of the rock. The results of the XRD analysis shows that 99.7% of the rock is mainly made of silica oxide (Quartz), and the rest is Greenalite ($Fe_6Si_4O_{10}(OH)_8$).

Table 4-4 Dimensions and properties of the cores used in this study

Exp.	length (cm)	diameter (cm)	porosity%	**brine** permeability (mD)	pore volume (cc)
1	14.8	3.8	23.7	142	39.58
2	14.8	3.8	23.1	158	38.778
3	14.5	3.8	27.8	160	38.824
4	15	3.8	27.8	132	37.365
5	14.9	3.8	27.55	127	37.56
6	30	4.9	17.68	98.7	102.108
7	30	4.9	17.68	98.7	102.108

4.2.4 Methodology

For each core, first, the pore volume (porosity) and permeability were measured. Next, initial water saturation (Swi) was established through a drainage process of the brine-saturated core with injecting several heavy mineral oils and finally crude oil (i.e., displacement of brine with oil). After establishing initial water saturation, for experiments number 3 to 7 the cores were aged in dead crude J for three weeks at a temperature of 194 °F. This altered their wettability towards a mixed-wet to the oil-wet system. The higher temperature was chosen to accelerate the aging process. For experiments number 1 and 2 the cores were not aged, leaving them as water-wet systems. Next, ‘’live’’ oil was injected into the cores to displace the dead oil. The live oil is a mixture of methane and crude J. Before injecting the live oil to the core, its gas oil ratio (GOR) was measured through injecting it into the bypass. The GOR of the live oil was 50 scc CH_4/ scc oil. Once the live oil had completely displaced the dead oil, the cores were ready for the experiments.

For the case of water-wet system (experiments number 1 and 2), one core was flooded by secondary conventional waterflooding and the other by secondary CWI. The same procedure was followed for the experiments number 3 and 4 in which the cores were aged and had a mixed-wet to oil-wet wettability state.

For experiment number 5 to prepare CW with higher CO_2 concentration, the sea brine used in all other experiments (Table 4-2) was diluted by adding distilled water until its salinity reached to 500 ppm. It is well documented that the solubility of gases in lower

salinity brine is higher than high salinity brine. The CO_2 content of prepared CW under this condition was 33 scc CO_2/scc brine which was 27% higher than the one of high salinity CW (26 scc CO_2/scc brine). Having prepared the CW with higher carbonation level, it was injected into the core, and the volumes of effluent fluids were recorded to calculate the recovery. Finally, the results were compared with experiment number 4 in which the CO_2 content of injected CW was 26 scc CO_2/scc brine.

Experiment number 6 was a secondary conventional waterflooding (WF) followed by a tertiary carbonated water injection (CWI). To simulate conventional waterflooding (WF) in an oil reservoir, a period of methane-saturated brine injection (WF) was conducted until no more oil was produced. Through this stage, the volume of effluent fluids was recorded to calculate the recovery of WF as a secondary recovery method. The conditions of the core at this stage of the test would represent a waterflooded heterogeneous oil reservoir in which significant amounts of oil still exist in the form of immobile disconnected patches of oil. Most oil reservoirs are abandoned at this stage (after waterflood) unless an EOR (enhanced oil recovery) method can be justified on both technical and economic grounds. Next, to examine the potential of CWI as the tertiary injection scenario, at the end of WF period, CWI began with the same injection rate and from the same end of the core as the preceding WF. Experiment number 7 was a secondary CO_2-saturated brine injection (CWI). CWI continued until no more oil was produced.

It should be noted that all experiments were performed at pressure and temperature of 2500 psi and 100 °F with an injection rate of 5 cm^3/hr. Furthermore, since in all performed experiments the oil was saturated with CH_4 in order to minimise any CH_4 mass transfer between the brine and oil during WF periods in experiments number 1, 3 and 6, the brine was pre-equilibrated with CH_4 before the waterflooding. The GOR of the CH_4-saturated brine was measured 3 scc CH_4/scc brine at laboratory conditions.

4.3 Coreflood Experiments Results

4.3.1 Coupling Impacts of New Phase Formation and Wettability Alteration

To assess the impacts of nucleation and growth of the new phase and wettability alteration on oil recovery by CWI, four coreflood experiments were performed. Two systems were considered, water-wet (WW) system (un-aged system) and mixed-wet system (aged system). First, the results of un-aged rocks are discussed followed by aged results.

4.3.1.1 Un-Aged Berea System

In the first set of coreflood experiments, the performance of CWI against conventional waterflooding was compared in un-aged (water-wet) Berea cores. For this aim, one core was flooded by CH_4-saturated brine and the other by CW. Figure 4-5 shows the oil recovery (RF) versus pore volume of injection (PVI) for both conventional waterflooding and secondary CWI in this system.

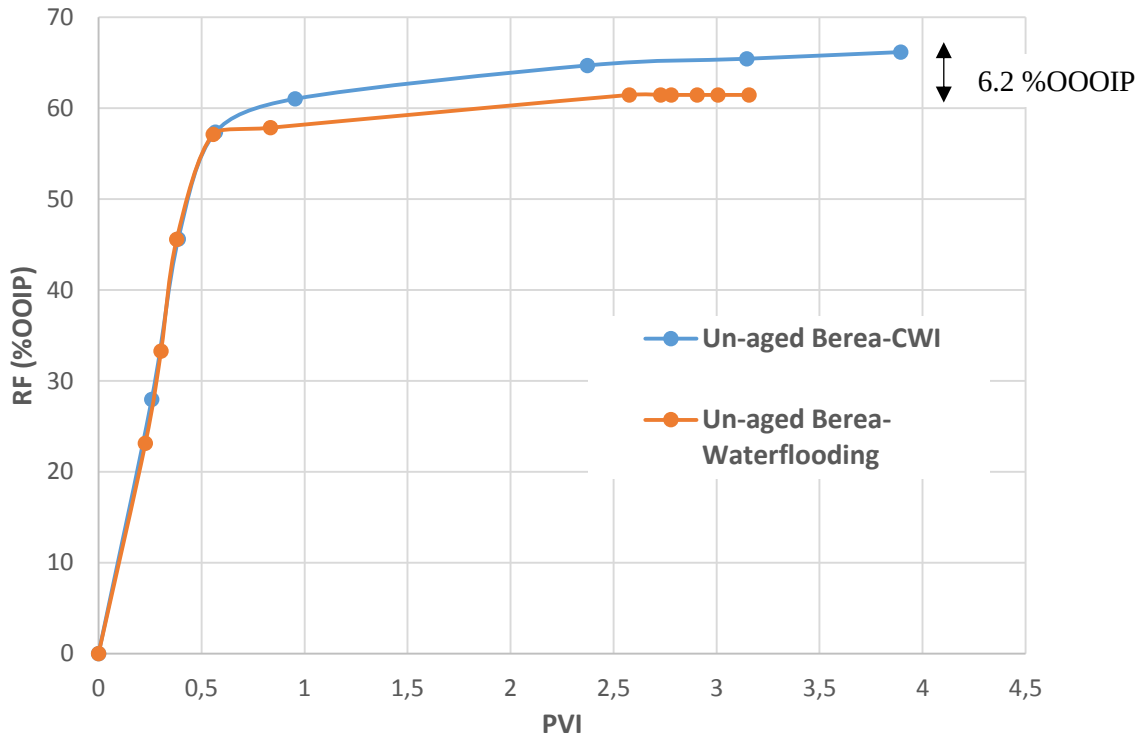

Figure 4-5 Recovery during both conventional waterflooding and secondary CWI in un-aged Berea cores

As can be seen from Figure 4-5, the oil recovery by secondary CWI is 6.2% OOIP higher than the recovery obtained from conventional waterflooding. Figure 4-6 shows a

magnified section of Figure 4-5. Based on this figure, the breakthrough (BT) for both CWI and WF in the un-aged Berea took place at the same time with the additional recovery by CWI was obtained after BT. Since the rocks were not aged, it is expected their wettability states to be water-wet. This can be confirmed by the recovery curve trend of conventional waterflooding (Figure 4-5). For conventional waterflooding, the main recovery happened before the BT with small amounts of oil produced after the BT. This behaviour represents water-wet conditions. Based on the performed wettability studies in Chapter 3 (section 3.3.1), CW has a small effect on wettability state of a water-wet system. Therefore, additional oil recovery due to wettability alteration by CW can be neglected for the water-wet system.

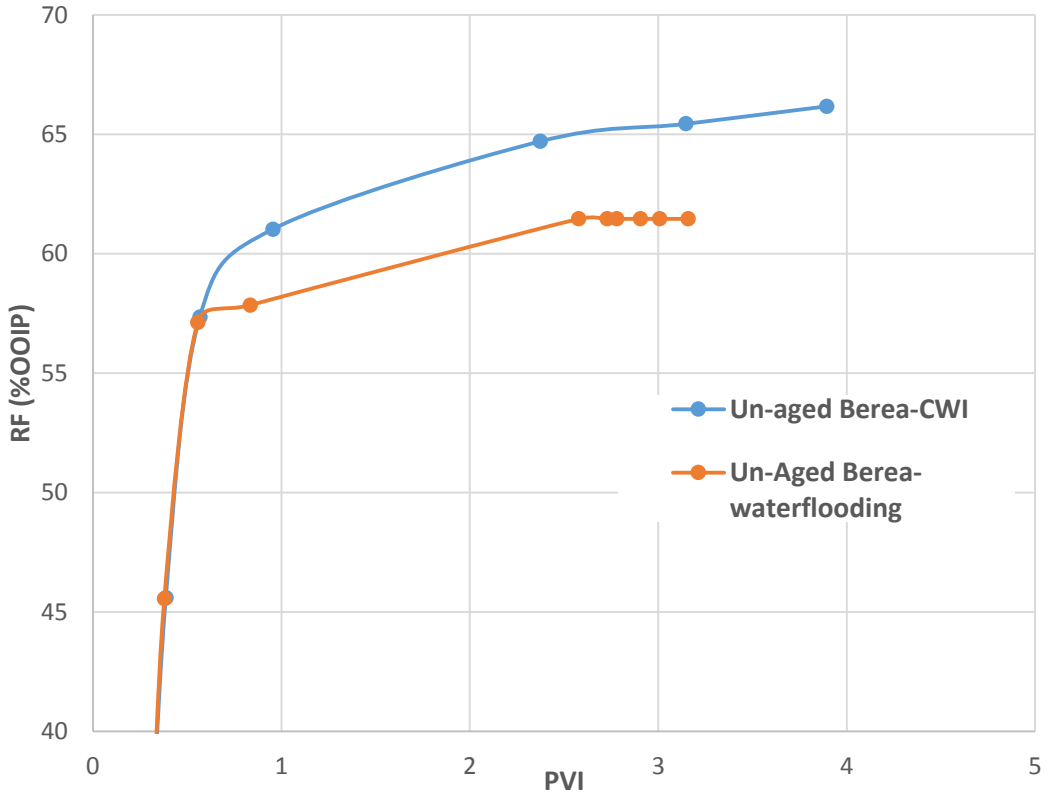

Figure 4-6 Recovery during both conventional waterflooding and secondary CWI in un-aged Berea cores

In early studies [6]–[14], [16]–[24], [27], [73], in which refined oil or dead oil had been used, the observed additional oil recovery by CWI was attributed to only oil swelling and oil viscosity reduction due to CO_2 transferring from CW into the oil. However, under more realistic reservoir conditions, where oil has a significant amount of dissolved gases, these two mechanisms are not the most dominant oil recovery

mechanisms by CWI. Results of the performed high-pressure high-temperature micromodel experiments in Chapter 2 (section 2.3.2), with the same crude oil (Crude J), under same experimental conditions, revealed that fluid/fluid interaction happening at the interface of ‘’live’’ oil and CW triggers the formation and growth of the new gaseous phase that boosts the performance of CWI significantly and represents a game-changer for this EOR technique. As it was shown in Chapter 2 (section 2.3.2.3), formation and growth of the new phase leads to much stronger oil swelling. As can be seen from Figure 2-24, the total increase in the volume of live crude oil J was around 35% with greater than 60% of that due to the formation of the new phase. As can be seen, shortly after the start of CWI, there is (normal) oil swelling which stops relatively quickly but the increase in the oil volume due to the formation of the new phase continues. Furthermore, oil recovery due to viscosity reduction is more dominant for medium to heavy oils. However, the live oil used in this study has the viscosity of around 14 cp. At this viscosity range, slight viscosity reduction by CO_2 dissolution from CW into the oil can be neglected. It should also be noted that the potential of this mechanism (oil viscosity reduction) depends on the amount of transferred CO_2 which is reliant on the CO_2 supply or in other words, the CO_2 content of CW. As the CO_2 content of CW is relatively low, this mechanism is generally slow, and oil recovery through this mechanism will be observed after an extended period of CWI. Therefore, the predominant recovery mechanism here was formation and growth of the new gaseous phase which led to 6.2% additional oil recovery.

The differential pressure (dP) across the core confirms the formation and growth of the new phase. Figure 4-7 presents the differential pressure across the core during both coreflood experiments. The dP trend during waterflood confirms our assumption regarding the wettability state of the cores. As can be seen, although there was oil production, dP across the core during waterflooding did not drop until around one pore volume. This behaviour represents the water-wet conditions in which water, the wetting phase, would travel through smaller pores which leads to higher dP.

Based on Figure 4-7, up to the time of BT, both differential pressure curves are virtually identical, however, after the BT, the dP of the CWI test started to increase. In contrast, the dP of waterflooding test decreased after one pore volume. The observed increase in dP during CWI is an indication of formation and growth of the new phase inside the live oil when it comes in contact with CW. As it was revealed in micromodel experiments

performed in Chapter 2 (Section 2.3.2.3), the third phase (new phase) is forming next to the water path, where CW contacts the live oil. Thereby, even small amounts of the new phase can cause a reduction in relative permeability of water and thereby increase in dP across the core. Although the formation of the new phase led to small injectivity loss, it helped to increase the oil recovery by diverting the water to unswept areas of the porous medium and redistributing and reconnecting the isolated oil ganglia. Figure 4-8 shows the dP across the core during the first pore volume of injection. Based on Figure 4-8, both water and CW have near identical entry pressure for the case of the water-wet system.

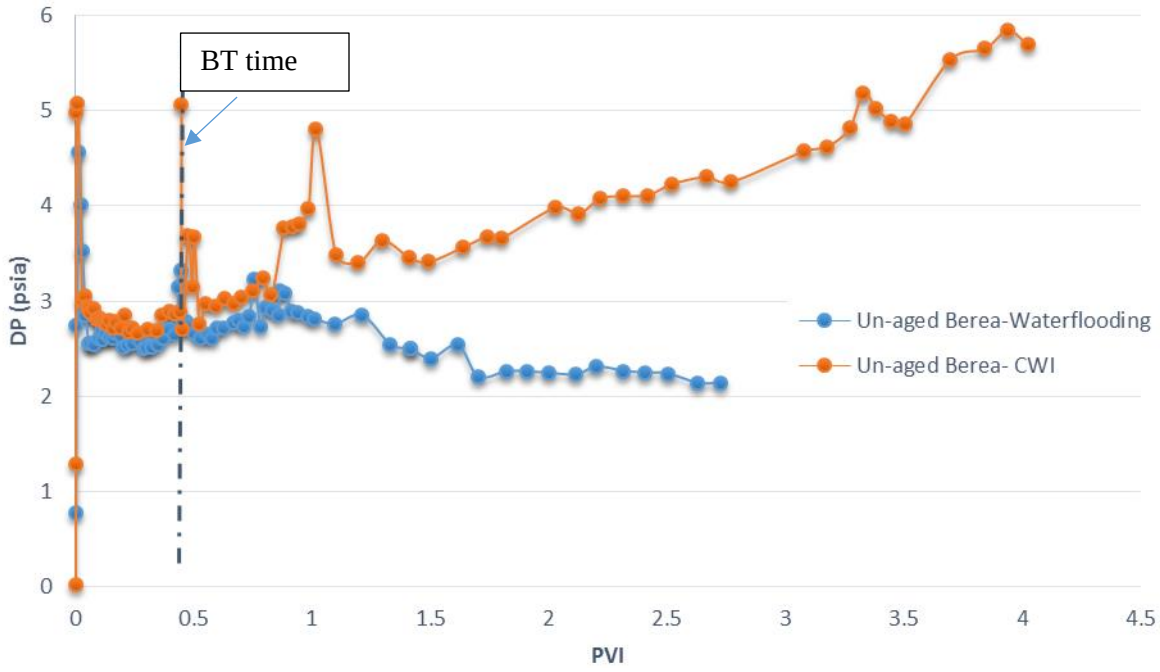

Figure 4-7 Differential pressure across the core during both conventional waterflooding and secondary CWI in un-aged Berea rocks. The increase in dP across the core during CWI period reveals the formation and growth of the new phase

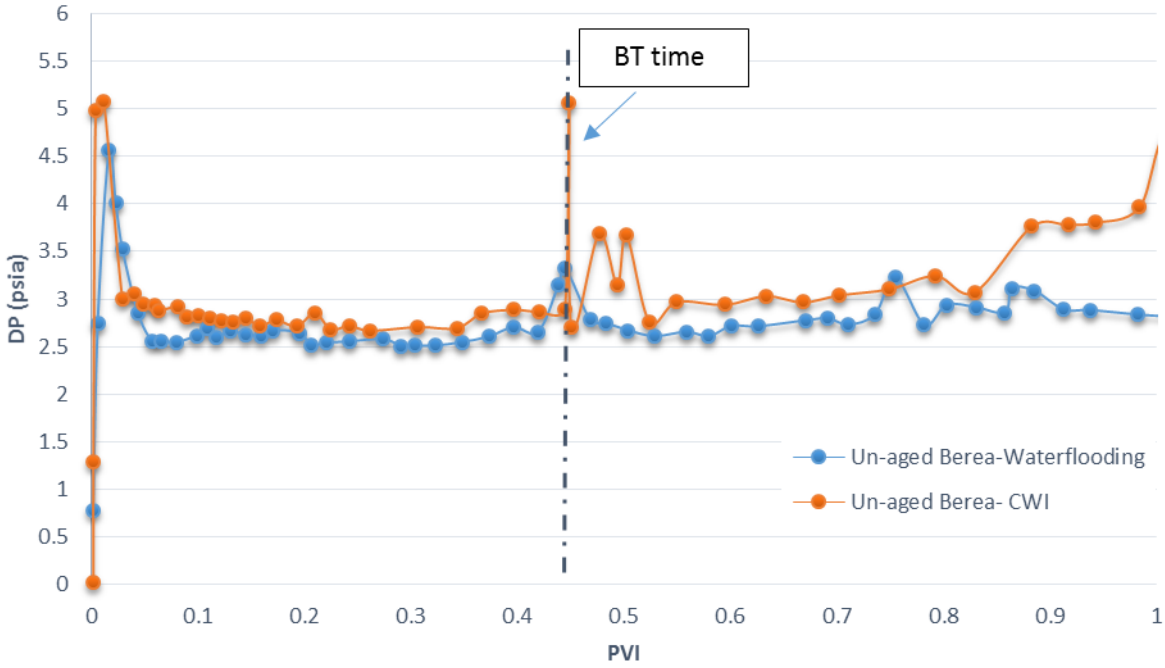

Figure 4-8 Differential pressure across the core during the first pore volume of conventional waterflooding and secondary CWI in un-aged Berea rocks

Figure 4-9 compares water cut during secondary CWI with its secondary water injection counterpart. As depicted in this figure, the water cut during CWI is less than that during waterflooding. This shows better conformance control of CWI compared to the conventional waterflood. Figure 4-10 shows a blown up version of the data presented in Figure 4-10 which highlights the differences between water cuts during CWI and WF after the water BT. This figure clearly shows better conformance control for the case of CWI.

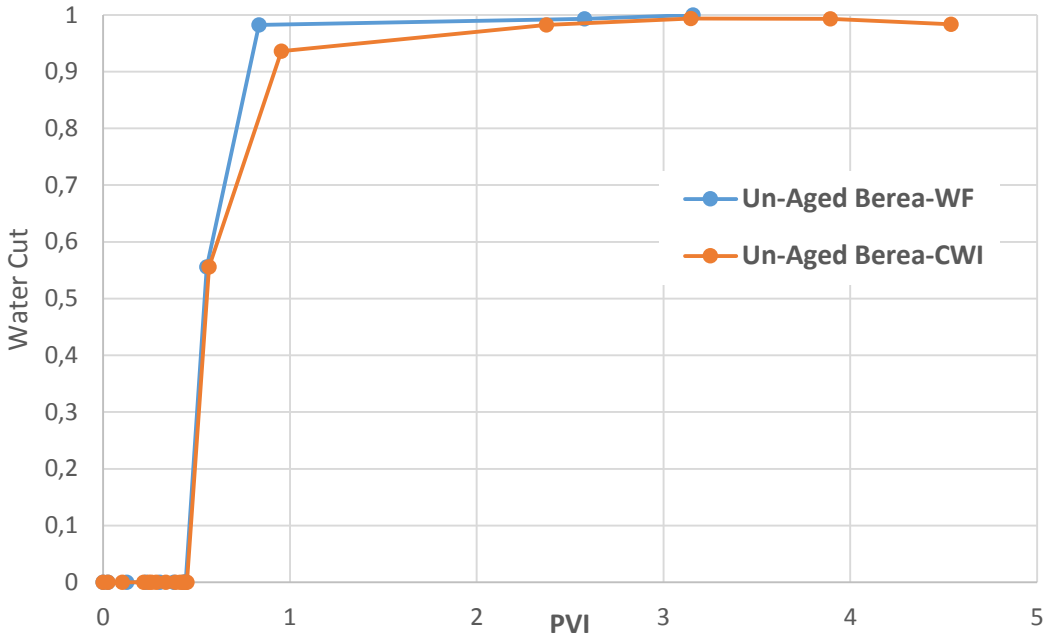

Figure 4-9 Comparison of water cut during secondary CWI with its secondary waterflooding counterpart in water-wet systems

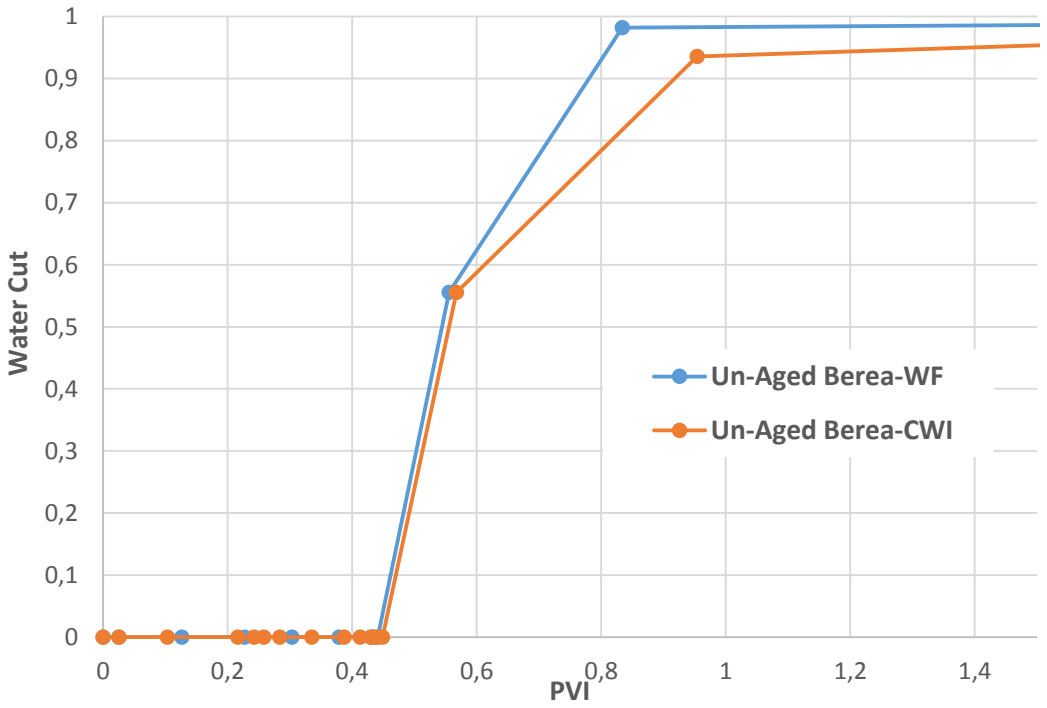

Figure 4-10 Comparison of water cut during secondary CWI with its secondary waterflooding counterpart in water-wet systems

4.3.1.2 Aged Berea System

In the second series of coreflood experiments, the performance of secondary CWI is compared to the performance of conventional waterflooding in aged Berea cores. The cores were aged for three weeks at high temperature to alter their wettability states toward mixed-wet to oil-wet conditions. Figure 4-11 presents the recovery during both conventional waterflooding and secondary CWI in the aged Berea cores. The long tail of oil production during conventional waterflood reveals the aging process was effective, and the system is in mixed-wet to oil-wet conditions. On the other hand, for the case of un-aged system (Figure 4-5), the amount of oil production after water BT was negligible compared to the aged system (Figure 4-11) that indicates the system was more water-wet. As depicted in this figure, CWI had a better performance compared to conventional waterflooding and led to 11.4% additional oil recovery. Figure 4-12 shows recovery around BT time, during both coreflood experiments in aged Berea system. As can be seen, the BT time in the instance of CWI in oil-wet Berea is higher than the one during conventional waterflood. In the case of waterflooding, BT happened at around 0.45 PVI; however, BT during secondary CWI took place at around 0.5 PVI. The oil recovery at BT time of CWI is also 4.6% higher than the oil recovery obtained at BT time of conventional waterflood. Comparing this figure with Figure 4-6 reveals that for the oil-wet systems the additional oil recovery by CWI took place sooner than in the water-wet systems where the additional oil recovery took place gradually after the BT. As it was shown in Chapter 3 (section 3.3.2.1), CW can change the wettability state of mixed-wet quartz toward more water-wet conditions. Wettability alteration by CW can affect the pore displacement mechanism and fluid distribution inside the porous medium. Therefore, for the mixed-wet system (aged Berea) both wettability alteration; nucleation and growth of the new phase are the active recovery mechanisms by CWI. This explains why the improvement in oil recovery by CWI is higher in the mixed-wet system (aged Berea) i.e. by 11.4%, as opposed to only 6.2% in the water-wet system (un-aged Berea). Comparing the results of the water-wet and mixed-wet system reveals that between the wettability alteration and the nucleation of the new phase during CWI the predominant recovery mechanism is nucleation and growth of the new phase inside the oil. These observations are critical for the application of CWI since most oil reservoirs have mixed-wet to oil-wet wettability state, and reservoir oils normally have a significant amount of dissolved gases.

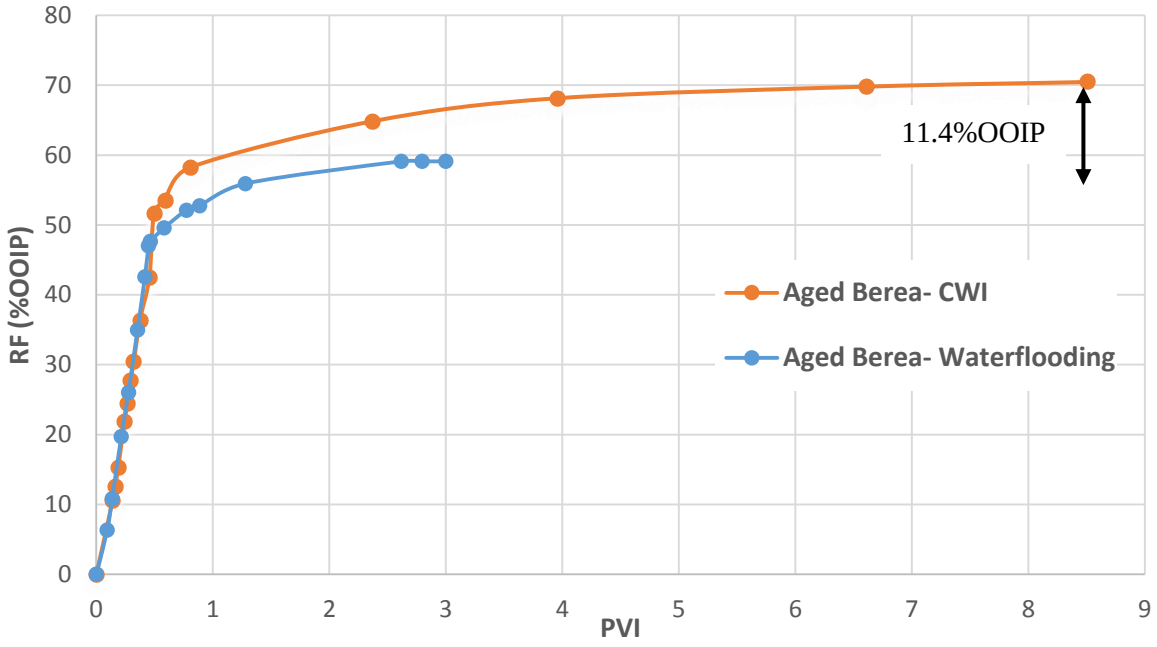

Figure 4-11 Recovery during both conventional waterflooding and secondary CWI in aged Berea (mixed-wet) cores

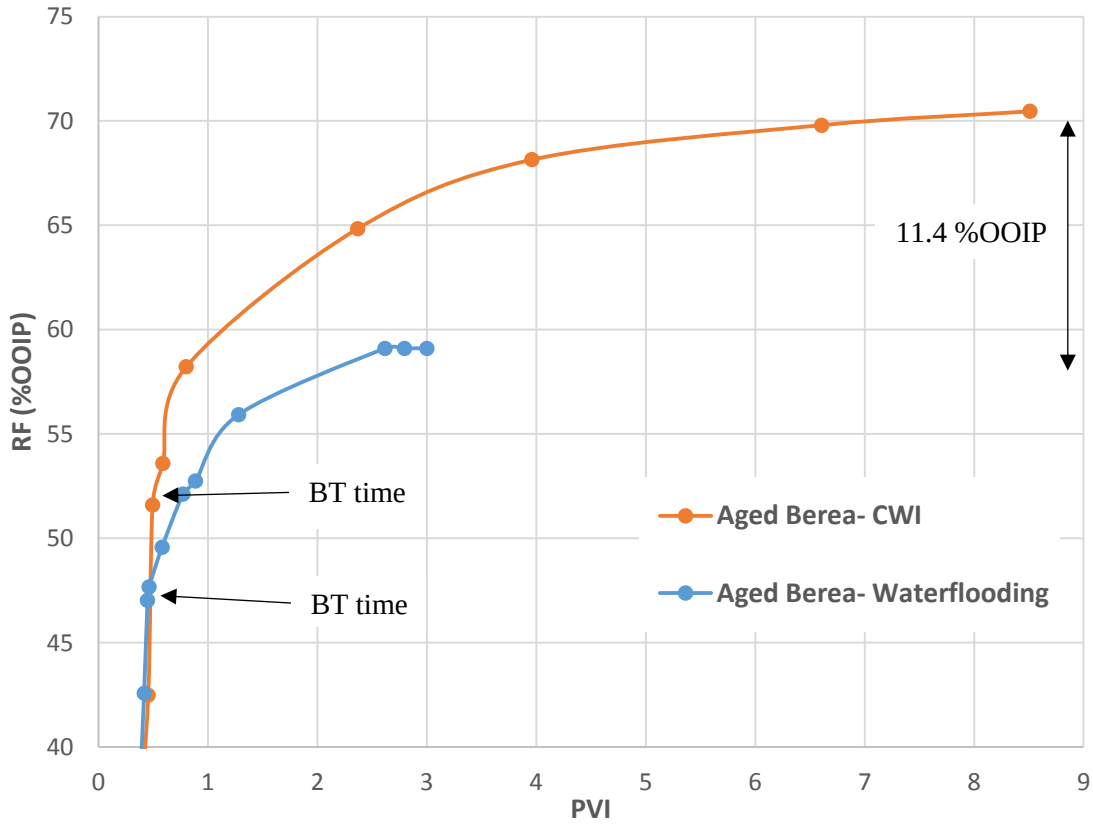

Figure 4-12 Recovery during both conventional waterflooding and secondary CWI in aged Berea (mixed-wet) cores

Figure 4-13 shows the differential pressure (dP) across the core during both experiments in the aged (mixed-wet) system. Figure 4-14 shows the dP behaviour during first pore volume of injection (PVI). Based on Figures 4-13 and 4-14, shortly after water flows into the rock, there was oil production, the dP started to decrease and after around one pore volume of brine injection, the dP became stable. This is the typical dP behaviour during waterflooding in mixed-wet to oil-wet systems where water is displacing a heavier fluid. For the case of CWI, compared to waterflooding, less entry pressure was observed. As previously mentioned in Chapter 3 (section 3.3.2.1), for the case of oil-wet quartz, low pH of CW can alter the wettability of the system toward more water-wet conditions. This wettability alteration would directly affect the dP and oil displacement during CWI. As depicted in Figure 4-14, shortly after CW touched the core, the dP started to increase to 2.5 psia. Although there was oil production, the dP during CWI was almost stable up to the time of BT, then gradually increased. This trend of dP is attributed to both wettability alteration and formation of the new phase inside the oil during CWI.

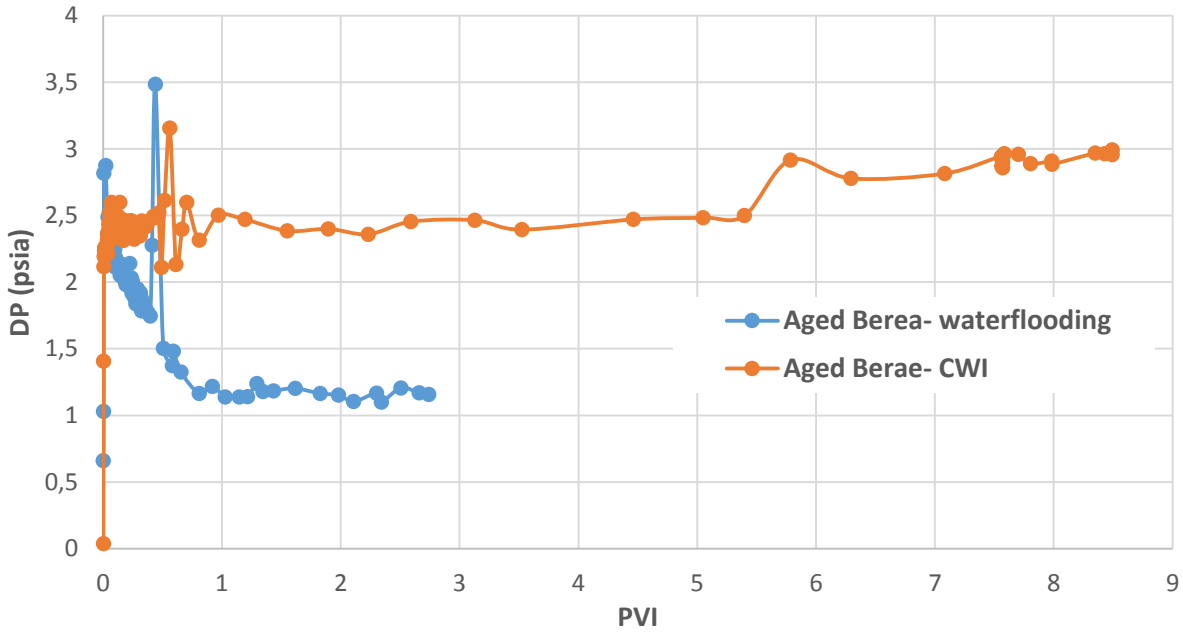

Figure 4-13 Differential pressure across the cores during both conventional waterflooding and secondary CWI in aged Berea (mixed-wet) rocks

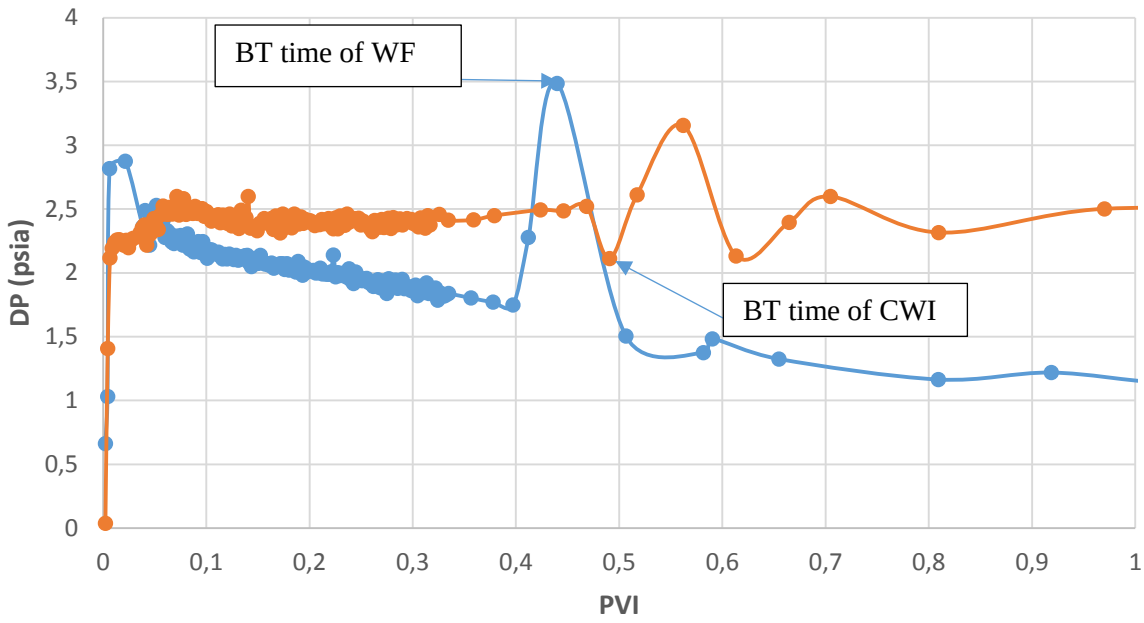

Figure 4-14 Differential pressure across the cores during both conventional waterflooding and secondary CWI in aged Berea (mixed-wet) rocks

Figure 4-15 compares water cut during both waterflooding and secondary CWI in the aged system. As can be seen from this figure, water cut during CWI is less than the one during waterflood. Figure 4-16 presents a blown up version of the data shown in Figure 4-15 which highlights the BT time of the brine and the better conformance control during CWI compared to the waterflood.

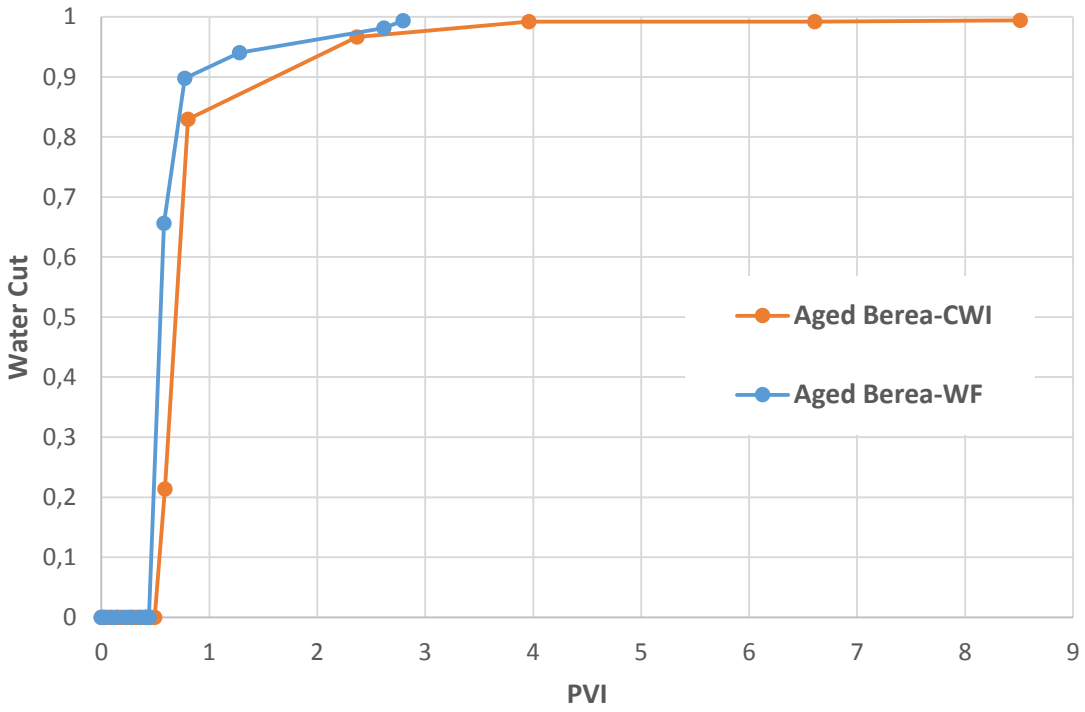

Figure 4-15 Comparison of water cut during secondary CWI with its secondary waterflooding counterpart in mixed-wet system

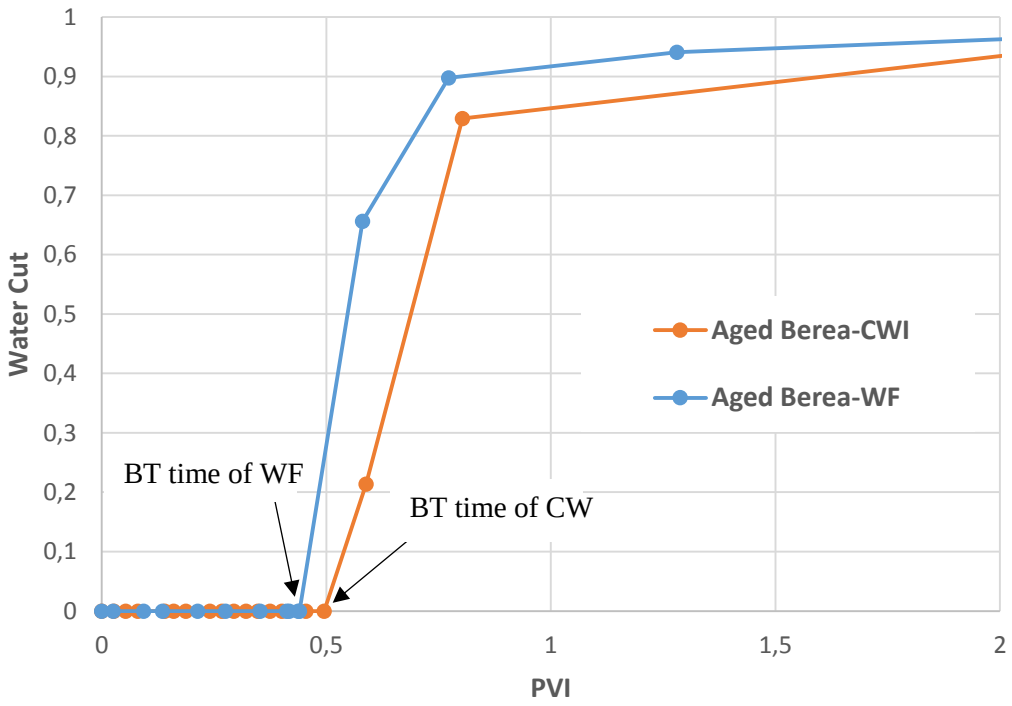

Figure 4-16 Comparison of water cut during secondary CWI with its secondary waterflooding counterpart in mixed-wet system

4.3.1.3 CO_2 Storage

To assess the CO_2 delivery potential of CWI as well as the potential for CO_2 storage in oil reservoirs, the gas production rate and CO_2 production rate in the water-wet system were measured. Figure 4-17 depicts the gas rates during both secondary WF and CWI. As this figure shows, up to the time of BT, the gas rates for both experiments were identical and equal to the original GOR of the live oil which was 50 scc CH_4/scc oil. This figure confirms similar BT times for both experiments as seen by a sharp drop in gas rate, for the same pore volume injected in both experiments. The sharp drop in gas rate indicates the BT of the displacing fluids. For the case of WF, since there were small oil production and high value of water cut after the BT time, the gas rate after the BT decreases with time then finally converges to the initial GOR of CH_4-saturated brine which was 3 scc CH_4/ scc brine. However, for the case of CWI since there was more oil production after the BT compared to the WF case and also since the GOR of CW is much higher than the GOR of CH_4-saturated brine, the gas rate after BT of CW is higher than the one for WF. As time passes and more CW was injected into the core, the gas rate after the BT of CW increases and finally after a long injection time, when residual oil inside the core becomes fully saturated with CO_2, it will converge to the original GOR of CW (26 scc CO_2/scc brine).

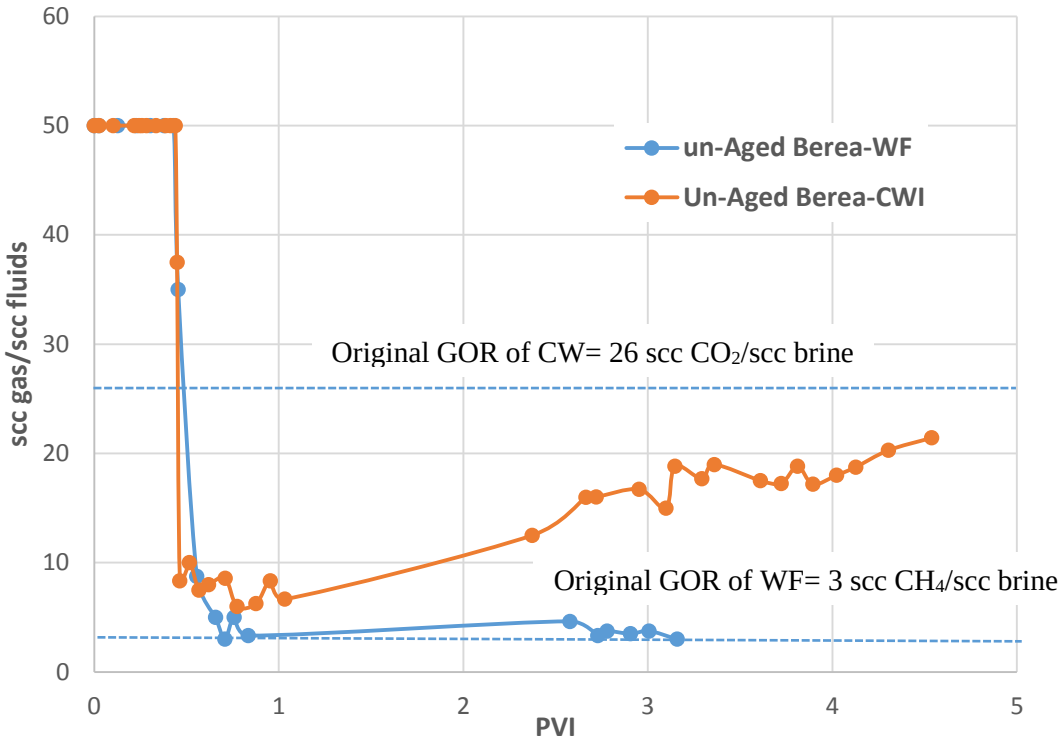

Figure 4-17 Gas rate during secondary CWI and its secondary waterflooding counterpart in water-wet system

During CWI, when CW comes into contact with the oil in a porous medium, due to the higher solubility of CO_2 in oil rather than brine, CO_2 will transfer from CW into the oil. Therefore, it is possible that the production of oil bank ahead of the CW front leads to earlier BT of CO_2 compared to the brine. To study whether CO_2 BT happened sooner than brine BT or not, the gas rate and CO_2 rate during CWI are shown in Figure 4-18. The BT of CW happened at around 0.45 pore volume of injection (PVI). Figure 4-19 shows a blown up version of the data presented in Figure 4-18 which highlights the BT time of CO_2. As depicted in this figure, the CO_2 BT happened around 0.41 PVI which is slightly earlier than the water BT time (0.45 PVI); however, the rate of CO_2 production up to one pore volume of injection is negligible. This is due to strong mass transfer happening between the trapped oil and CW. The earlier BT of CO_2 indicates good delivery of CO_2 into the oil; however, it should be noted that this earlier CO_2 BT might not necessarily be the case over longer porous mediums. As can be seen from Figure 4-18, even after an extended period of CWI (4.5 PVI), the measured CO_2 rate is 75% of the initial CO_2 content of the injected CW. This shows that the residual oil is not still saturated with CO_2 and yet taking up the CO_2 in the injected CW.

The total amount of trapped CO_2 during CWI was measured and was around 42% of the total injected CO_2. This shows strong potential for this method of CO_2 storage in oil reservoirs. The trapped CO_2 is under CO_2 dissolution trapping mechanism which is one the safest method for underground CO_2 storage. Since CO_2 is not in the form of free-phase CO_2, the risk of leakage is lower. This is of great importance for the final fate of a CO_2 geological storage project.

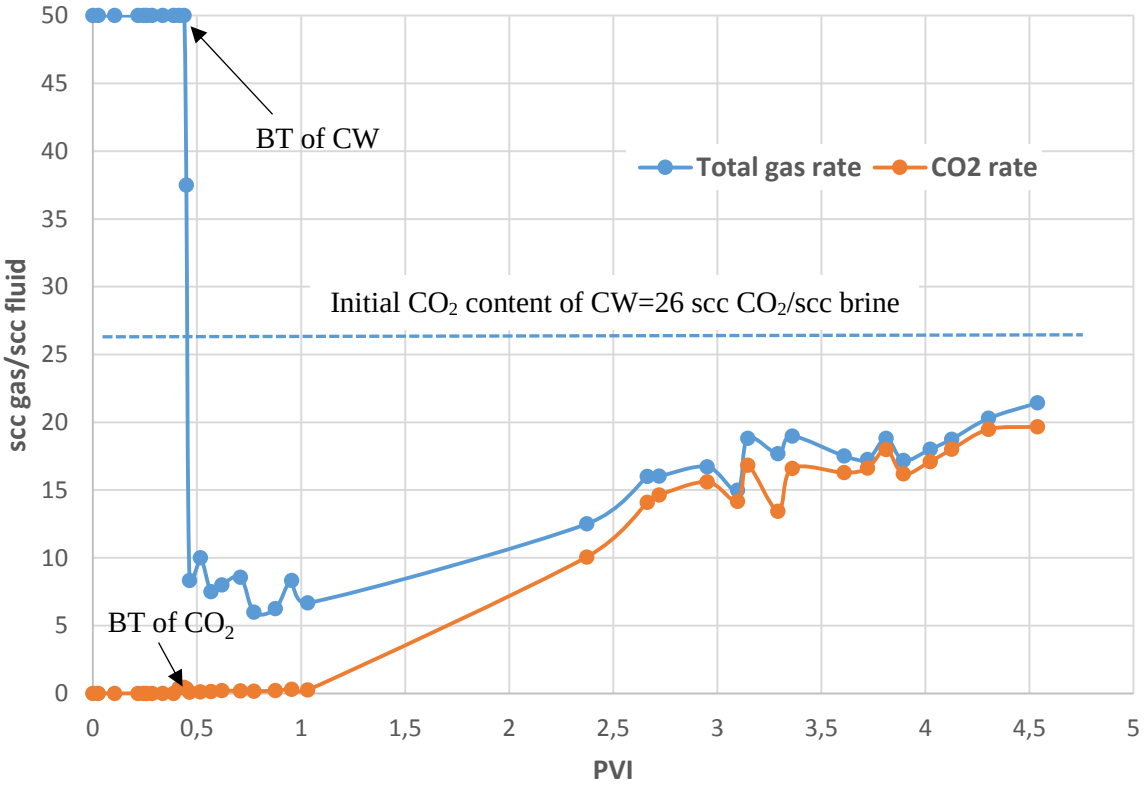

Figure 4-18 Gas rate and CO_2 rate during secondary CWI in water-wet system

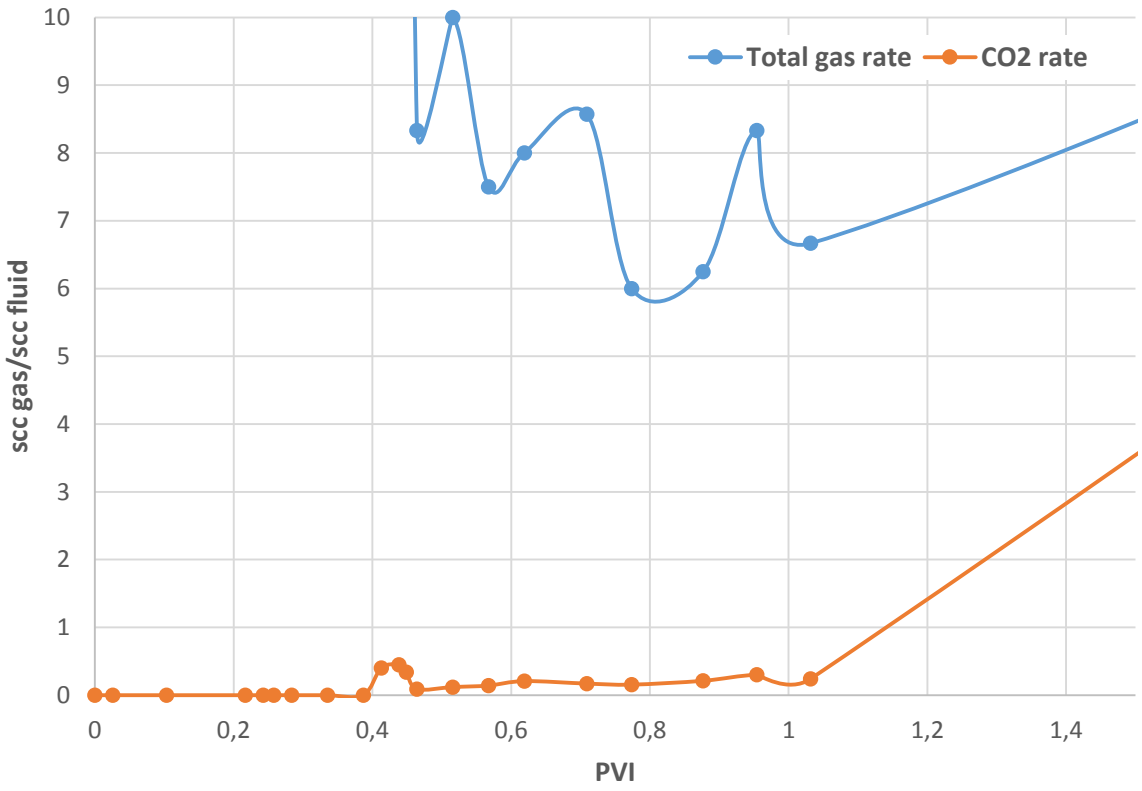

Figure 4-19 Gas rate and CO_2 rate during secondary CWI in water-wet system

4.3.2 Impact of Carbonation Level of CW

To investigate the impact of carbonation level of CW on its performance, the sea brine used in this study (see Table 4-2) was diluted by adding distilled water until its salinity reached to 500 ppm. It is well known that the solubility of CO_2 in lower salinity brine is higher than high salinity brine. The carbonation level of CW prepared with the diluted brine, at the experimental conditions of 2500 psia and 100 °F, was 27% higher than the one prepared with sea brine.

Having prepared the CW with higher carbonation level, it was injected into the core as the secondary CWI scenario and oil production was recorded. The results were compared with the results of experiments number 4 and 3 where the aged cores were flooded by CW and CH_4-saturated brine respectively. Figure 4-20 shows oil recoveries versus pore volumes of injected fluids during experiments 3, 4 and 5. As can be seen from this figure, CW with 27% higher carbonation level led to 15.8% (OOIP%) additional oil recovery compared to the conventional waterflooding and also 4.5% (OOIP%) additional oil recovery compared to the CW with lower carbonation level (experiment number 4). The water breakthrough (BT) time for the CWI with 27%

higher carbonation level was same as the BT time of CWI (0.5 PVI) in experiment number 4 and slightly later than the breakthrough time of waterflooding (0.45 PVI) in experiment number 3. As depicted in Figure 4-20, the 4.5% additional oil recovery obtained by this method took place after the BT.

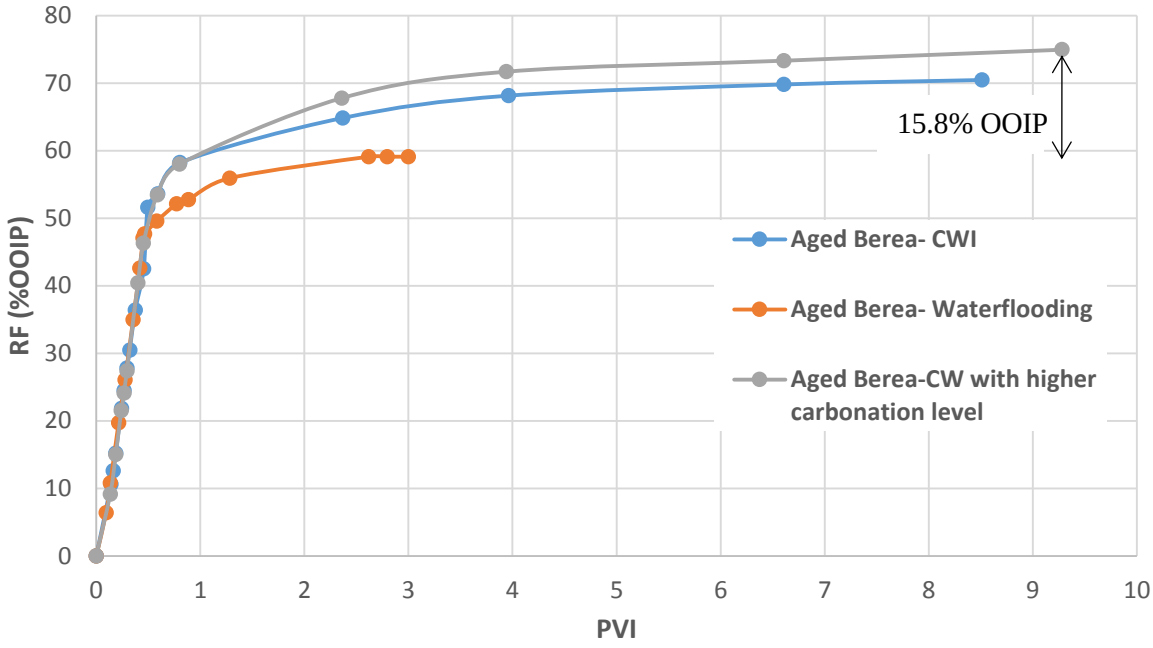

Figure 4-20 Oil recovery through secondary conventional waterflooding, CWI, and CW with 27% higher carbonation level at pressure and temperature of 2500 psi and 100 °F

Based on Figure 4-20, higher carbonation level of CW favourably impacts the performance of CWI. As CW with higher carbonation level has more CO_2 in itself, more CO_2 will be available for transferring into the oil which leads to stronger new phase formation and hence stronger oil swelling which leads to better oil displacement and recovery.

As can be seen from the slopes of oil recovery curves in Figure 4-20, as the injection of both CW with 27% higher carbonation level and original CW (blue curve) continued, oil production continued too and yet after injection of several pore volumes of either of them, oil was still being produced. This behaviour is mainly attributed to the formation and growth of the new phase. As it was shown in micromodel experiments reported in Chapter 2 (Section 2.3.2.3, Figure 2-24), as time elapses and more CW comes in contact with live oil, the saturation of the new phase inside the isolated oil ganglions increases that leads to much stronger overall oil swelling which in turn leads to further oil

reconnection and production. In Chapter 6 the characteristic of the new phase and how it evolves with time will be discussed in details.

4.3.3 CWI Potential in a Heterogeneous and Longer Porous Media

One factor that adversely affects the performance of waterflooding is the heterogeneity of the porous media which leads to an early breakthrough of water. As a result, vast amounts of oil remain in place. In this part, the aim is to study the potential of CWI in a heterogeneous and longer porous medium than previous experiments. For this objective, experiments number 6 and 7 (Table 4-3) were carried out in using a 30 cm long heterogeneous core. First, a secondary conventional waterflooding (WF) followed by a tertiary carbonated water injection (CWI) were carried out. In the second test performance of secondary CWI was investigated.

4.3.3.1 Conventional WF Followed by Tertiary CWI

To simulate conventional waterflooding (WF) in an oil reservoir, a period of methane-saturated brine injection (WF) was conducted until no more oil was produced. Through this stage, the volumes of effluent fluids were recorded to calculate the recovery of WF as a secondary recovery scenario. The conditions of the core at this stage of the test would resemble a waterflooded heterogeneous oil reservoir where significant amounts of oil still exist in the form of immobile disconnected patches of oil. Next, to quantify the level of additional oil recovery by CWI as the tertiary injection method, after the WF period, CWI began with the same injection rate (5 cm^3/hr) and from the same end of the core as the preceding WF. The obtained oil recoveries are indicated in Figure 4-21. As can be seen from this figure, around two pore volumes methane-saturated brine injection, recovered 34.9% of the original oil in place (OOIP) and left 0.46 pore volume (PV) of residual oil after waterflooding. The water breakthrough (BT) happened at early pore volumes of injection (PVI), i.e. 0.21 PVI. The main reason for this early breakthrough of brine is the rock heterogeneity. Reservoir heterogeneity led to the early breakthrough of the injected brine. Due to the presence of high permeability layer in the rock, water tended to flow through the theft zone (high permeability layer) and tended to reduce front advancement in the lower permeability layer. As a result, BT happened during early stages of the injection, and a large volume of bypassed or virgin oil (untouched oil) remained in the rock.

As can be seen from Figure 4-21, although the breakthrough happened at early times of the injection, there was yet oil recovery after the breakthrough. Since after water breakthrough, the viscous forces between oil and water are yet active, the recovery factor after the BT has increased from 27.8% of the OOIP to 34.9% of the OOIP. Due to the presence of viscous forces, some part of the bypassed oil was produced after the breakthrough. However, the amount of produced oil after one pore volume of injection is minuscule and converged to zero at around 1.5 pore volume of injection.

Having no more oil production, CW was injected as the tertiary injection scenario. The oil recovery by tertiary CWI is reported in Figure 4-21. As can be seen from this figure, tertiary CWI in the waterflooded heterogeneous rock led to additional oil recovery of 10% of the OOIP. The obtained additional oil recovery by CW reveals the strong potential of CWI as a tertiary injection scenario in waterflooded heterogonous reservoirs where the direct displacement of oil by water is usually poor. The main reasons for this additional recovery are:

(i) Formation and growth of the new phase. Based on the results of high-pressure micromodel experiments presented in Chapter 2, when CW comes in contact with the bypassed ‘’live’’ oil in the porous medium, due to CO_2 exchange between the CW and trapped ‘’live’’ oil phase, a new phase rapidly forms inside the oil that boosts the performance of CWI. With time as more CW comes in contact with oil, the saturation of the new phase increases. Formation and growth of the new phase inside the trapped live oil leads to oil production through; (i) reconnection of the trapped oil and oil displacement, (ii) creating a favourable three phase flow region with less residual oil saturation, and (iii) restricting the flow path of CW and diverting CW toward the unswept areas of the porous medium.

(ii) Wettability alteration. Based on the results of high-pressure high-temperature contact angle measurements presented in Chapter 3 (section 3.3.2.1), CW has this potential to alter the wettability of mixed-wet quartz toward more water-wet conditions. As mentioned earlier in this chapter, the main component of the core used for these experiments is quartz. Wettability alteration by CW can directly affect the pore displacement mechanism and fluid distribution inside the porous medium and therefore leads to better oil recovery.

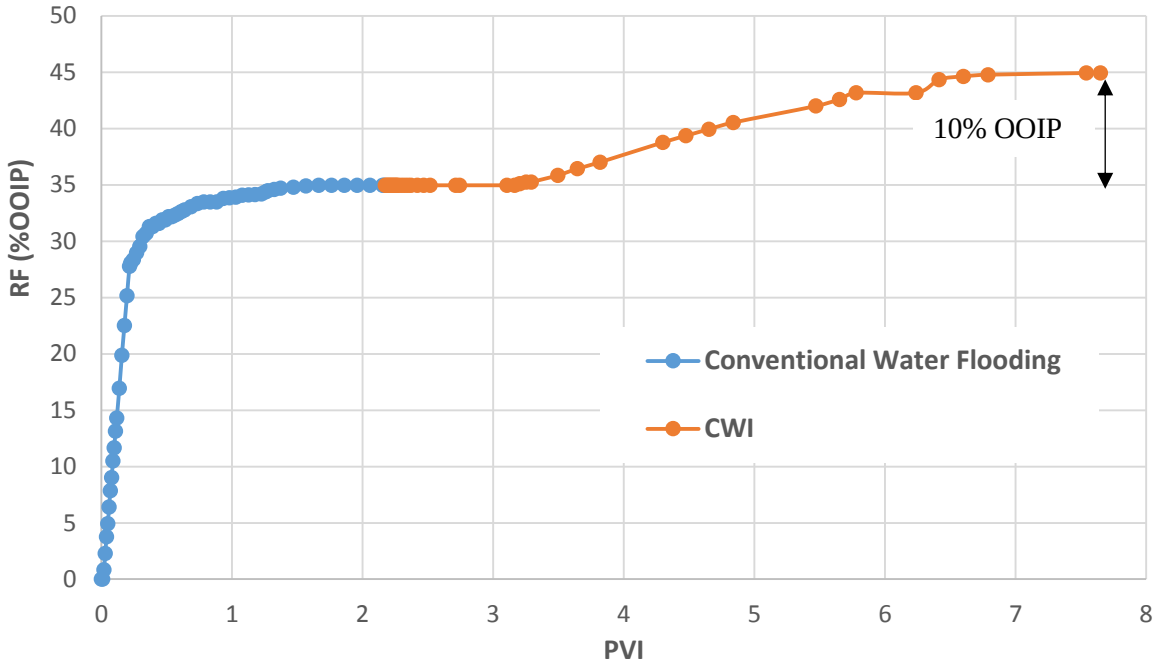

Figure 4-21 Measured cumulative oil recovery in the tertiary carbonated water injection (CWI) in a heterogeneous sandstone core at 100 °F and 2500 psia

4.3.3.2 Secondary CWI

As it was shown in Table 4-3, in experiment number 7 potential of secondary CWI on a heterogeneous sandstone core was studied. Figure 4-23 compared oil recovery profiles obtained by the secondary water injection (Experiment 6) and secondary carbonated water injection, keeping all other parameters the same. As it is depicted in Figure 4-22, secondary water injection in experiment number 6 resulted in oil recovery of 34.9% of the original oil in place. However, CWI as a secondary recovery method in experiment number 7 led to oil recovery of 48.4% of the OOIP. These results clearly verified the strong potential of CWI as a secondary recovery method compared to waterflooding in heterogeneous reservoirs.

The breakthrough (BT) for both cases happened at 0.21 PVI. The main reason for these early breakthroughs is the rock heterogeneity. Reservoir heterogeneity led to the rapid breakthrough of both water and carbonated water. Due to the presence of high permeability layer in the rock, water or carbonated water tended to flow through it. As a result, BT happened at early times of the injection and a large volume of bypassed or virgin oil (untouched oil) remained in the rock. Although in both experiments the BT

happened at early times of the injection, there were still oil productions in both experiments after the BT time. As it is depicted in Figure 4-22, for the case of conventional waterflooding, recovery factor after the BT increased by 7% of the OOIP. However, for the case of secondary CWI recovery factor after the BT increased by 18.8% of the OOIP. The same reasons that led to better oil recovery by tertiary CWI in experiment number 6, i.e. formation and growth of the new phase and wettability alteration, are applied for this significant increase in oil recovery after carbonated water BT and finally, this led to better performance of secondary CWI compared to the secondary conventional waterflooding counterpart.

Figure 4-23 summarized the strong potential of CWI for improving oil recovery either as a secondary or tertiary injection method. Based on this figure, CWI in a heterogeneous sandstone rock, compared to conventional waterflooding, improved oil recovery in both secondary (pre-waterflood) and tertiary (post-waterflood) injection scenarios. However, similar to micromodel results presented in Chapter 2 (section 2.3.2), coreflood results confirm the better performance of secondary carbonated water injection compared to the tertiary carbonated water injection. This is because of the higher oil saturation and better oil connectivity during secondary carbonated water injection compared to the tertiary carbonated water injection. It should be noticed that the total amount of injected CW during secondary scenario was less than the total amount of injected CW during the tertiary scenario.

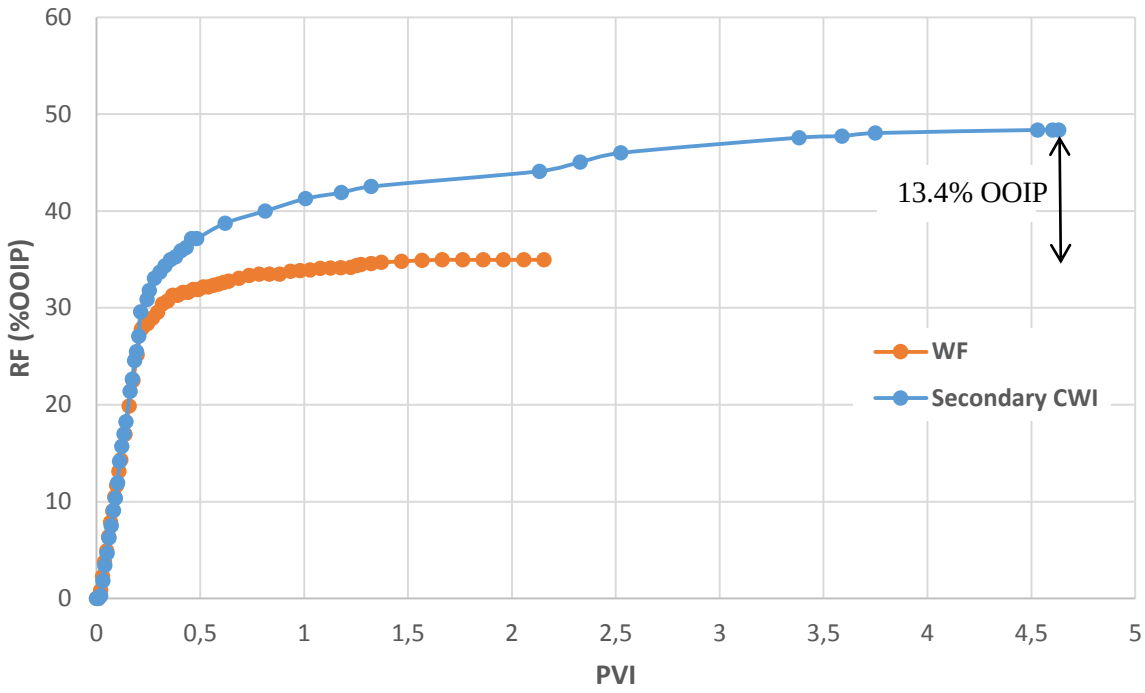

Figure 4-22 Comparison of the performance of the secondary CWI in an aged heterogeneous sandstone core with its secondary water injection counterpart

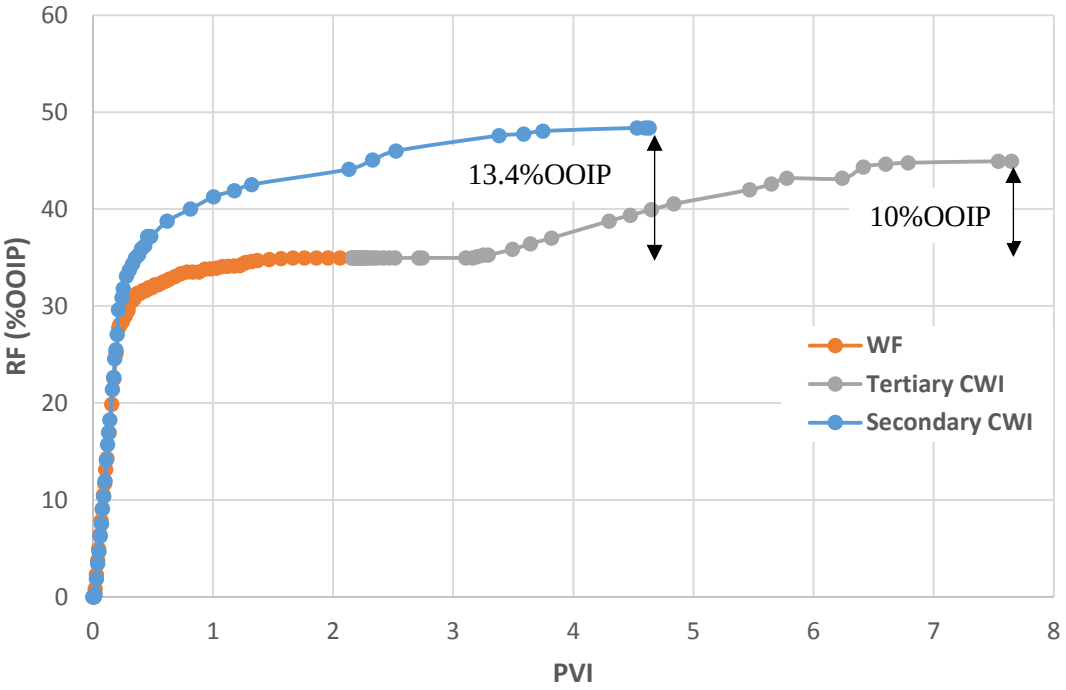

Figure 4-23 Oil recovery through experiments 6 and 7 in an aged heterogeneous sandstone core

Figure 4-24 compares the water cut during secondary CWI in the heterogeneous core with its secondary water injection counterpart. As can be seen from this figure, CWI reduced the water cut and improved the conformance. Figure 4-25 shows a blown up version of the data presented in Figure 4-24 which highlights the differences between the water cuts during secondary CWI and conventional waterflooding after the water BT. This figure clearly shows a better conformance control for the case of secondary CWI.

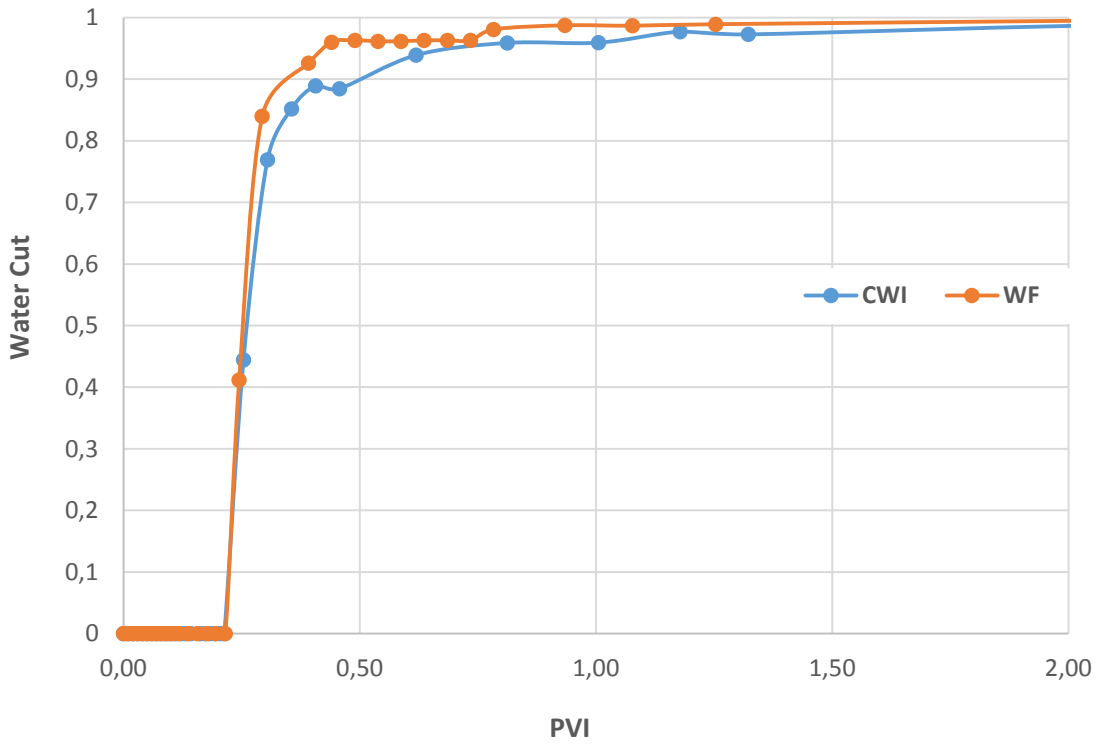

Figure 4-24 Comparison of the water cut during secondary CWI in the heterogeneous core with its secondary water injection counterpart

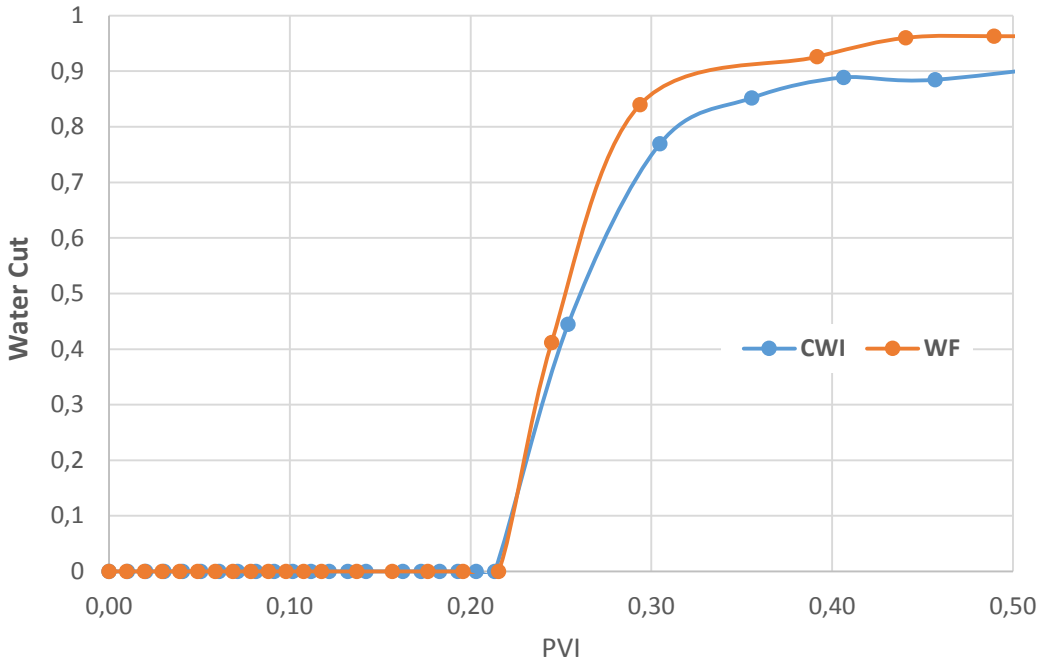

Figure 4-25 Comparison of the water cut during secondary CWI in the heterogeneous core with its secondary water injection counterpart around water breakthrough time

4.3.3.3 CO_2 Storage

To study the CO_2 storage potential of CWI, the gas rate during experiments number 6 and 7 were recorded, and CO_2 production was monitored. Figure 4-26 depicted the gas rate during conventional waterflooding. As can be seen from this figure, the initial gas rate is constant and is equal to the gas oil ratio (GOR) of the live oil (50 scc CH_4/ cc oil). After breakthrough, the gas rate dropped, and as time passes, it converged to a constant value of 3.3 which is the original gas content of methane-saturated brine. The reason that the gas rate exactly after the breakthrough is not equal to the initial gas content of methane-saturated brine is the production of oil after the breakthrough. As a result, the amount of produced gas at early times after the breakthrough was slightly more than the original gas content of CH_4-saturated brine. However, as time elapses, the oil production reaches to zero; therefore, the gas rate finally converges to the initial gas content of CH_4-saturated brine.

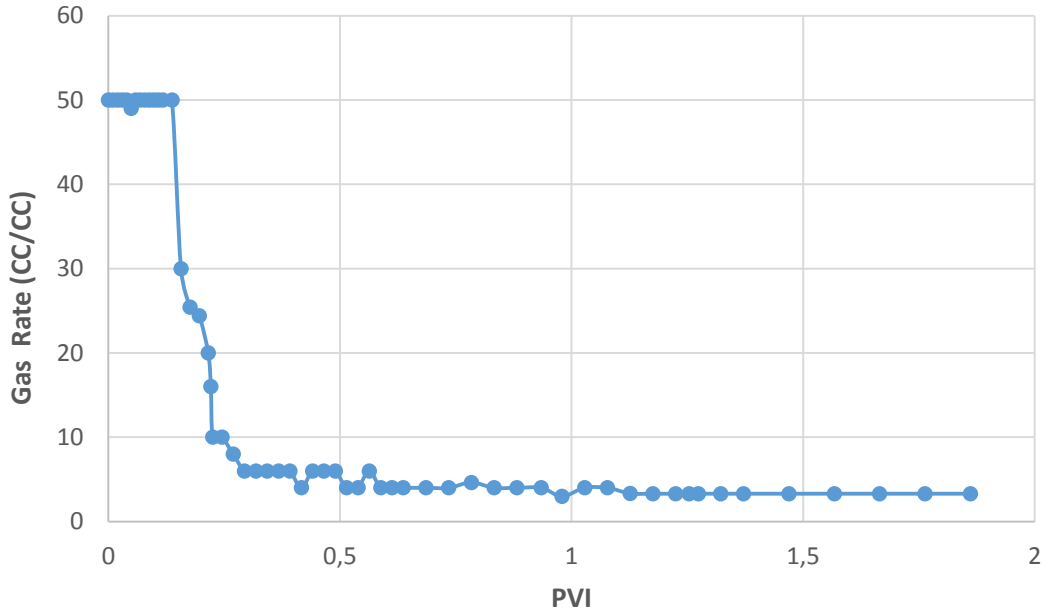

Figure 4-26 Gas rate during water injection in the heterogeneous sandstone core

Figure 4-27 depicted the rate of gas production and the calculated rate of CO_2 production during the period of WF and tertiary CWI performed in experiment number 6. This figure represents the substantial potential of CWI for safe storage of CO_2. Based on the material balance conducted over gas production data, about 44% of the total injected CO_2 in CW was stored at the end of tertiary CWI. This proof the potential of CWI for CO_2 storage in waterflooded oil reservoirs. The trapping mechanism is dissolution trapping; i.e. dissolution of CO_2 in both resident brine and oil in the porous medium, which is one of the safest methods for safe underground storage of CO_2.

Figure 4-28 depicted the rate of gas production and the calculated rate of CO_2 production during tertiary carbonated water injection. As mentioned earlier, the original CO_2 content of CW was 26 scc CO_2/scc brine. This ratio was monitored through the test and after 5.4 pore volumes of CWI, the ratio reached 80% of the original value. This indicates that the remained oil in the core is still taking up CO_2 from the injected CW. It is desirable to stop the injection of CW when the residual oil in the core is almost saturated with CO_2, i.e. when CO_2 gas rate reaches close to its injected value. This would represent the maximum oil that can be recovered from the process implementation as well as the maximum CO_2 that can be stored in the oil and brine within the core.

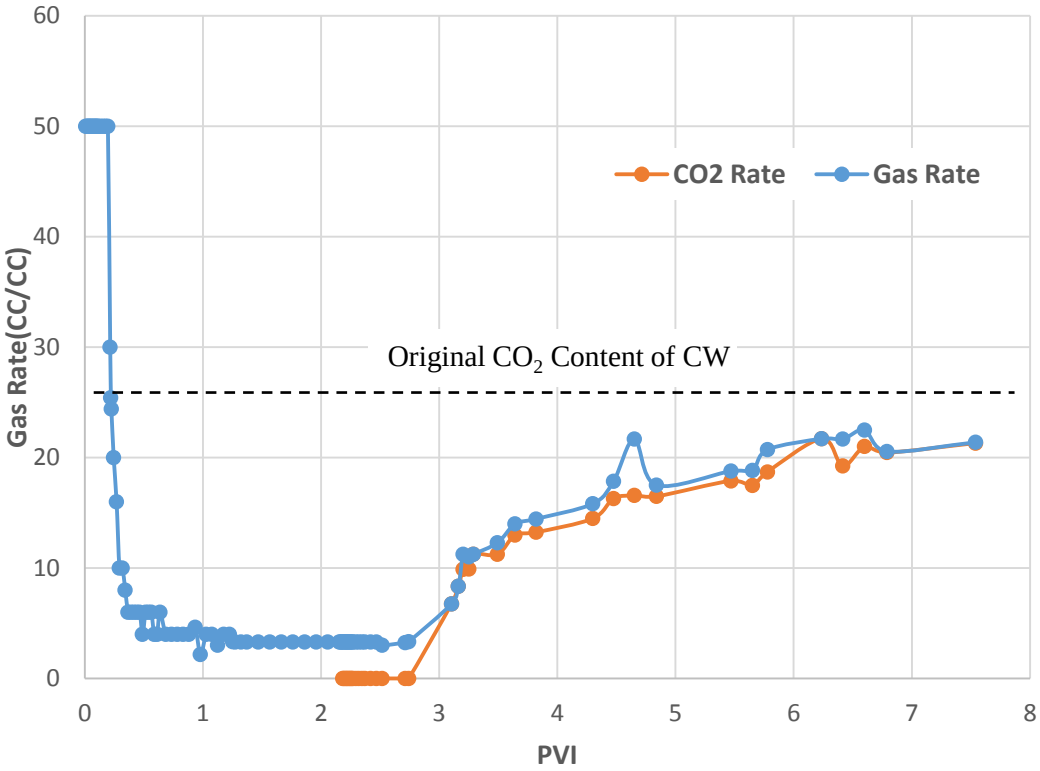

Figure 4-27 Rate of gas production and calculated rate of CO_2 production during WI and tertiary CWI in the heterogeneous sandstone core

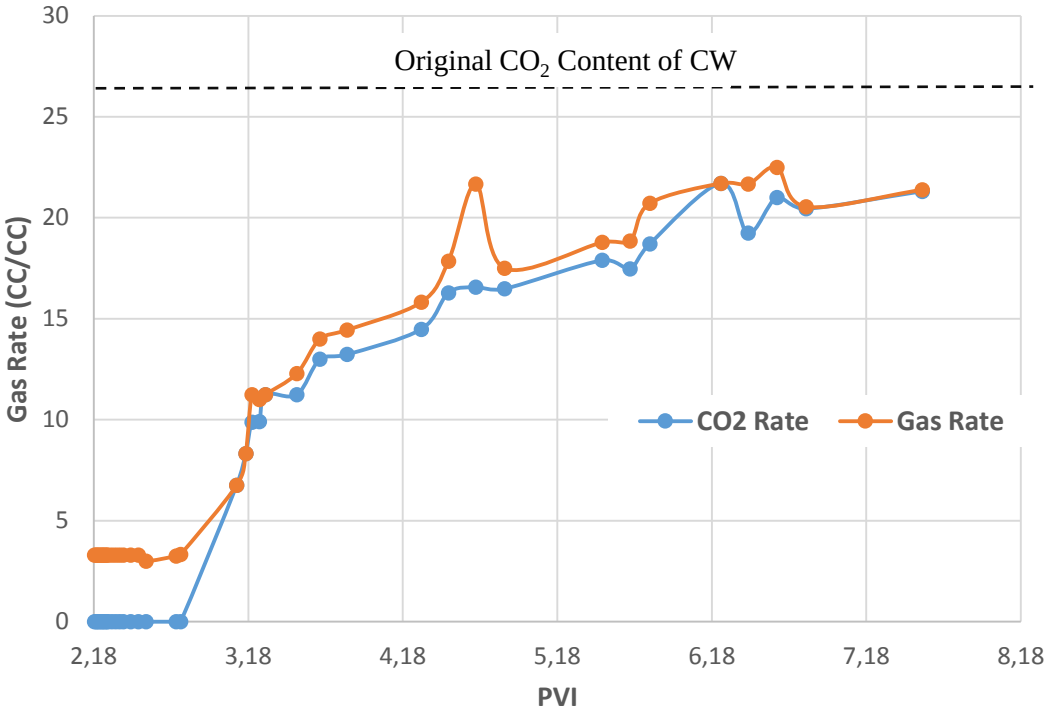

Figure 4-28 Rate of gas production and calculated rate of CO_2 production during tertiary carbonated water injection in the heterogeneous sandstone core

Figure 4-29 depicted the rate of gas production and the estimated rate of CO_2 production during secondary carbonated water injection in the heterogeneous sandstone core (experiment number 7). As can be seen from this figure, the initial gas rate was constant and was equal to gas oil ratio (GOR) of the live oil. After the breakthrough (BT), the gas rate dropped and then gradually increased. Since after the BT still there was some oil production, and also CW production, the released methane, and CO_2 gases from the produced oil and CW leads to a gradual increase in the gas rate. As time passes and more CW was injected into the core, the gas rate after the BT of CW increases and finally after a long injection time, when the residual oil inside the core becomes fully saturated with CO_2, it will converge to the original GOR of CW (26 scc CO_2/scc brine).

According to Figures 4-29 and 4-30, secondary CWI demonstrated an excellent potential for safe CO_2 storage. Based on the performed material balance, about 47.5% of the total injected CO_2 in CW was stored at the end of secondary CWI. This value for the tertiary CWI was 44% of the total injected CO_2 in CW. These results verified the potential of CWI for safe storage of CO_2 in oil reservoirs.

As mentioned earlier, the original CO_2 content of CW was 26 scc CO_2/cc brine. This ratio was monitored through the experiment and after 4.63 pore volume of secondary CWI the ratio reached 78.8% of the original value. This reveals that the bypassed oil in the porous medium is not yet saturated and therefore taking up CO_2 from the injected CW.

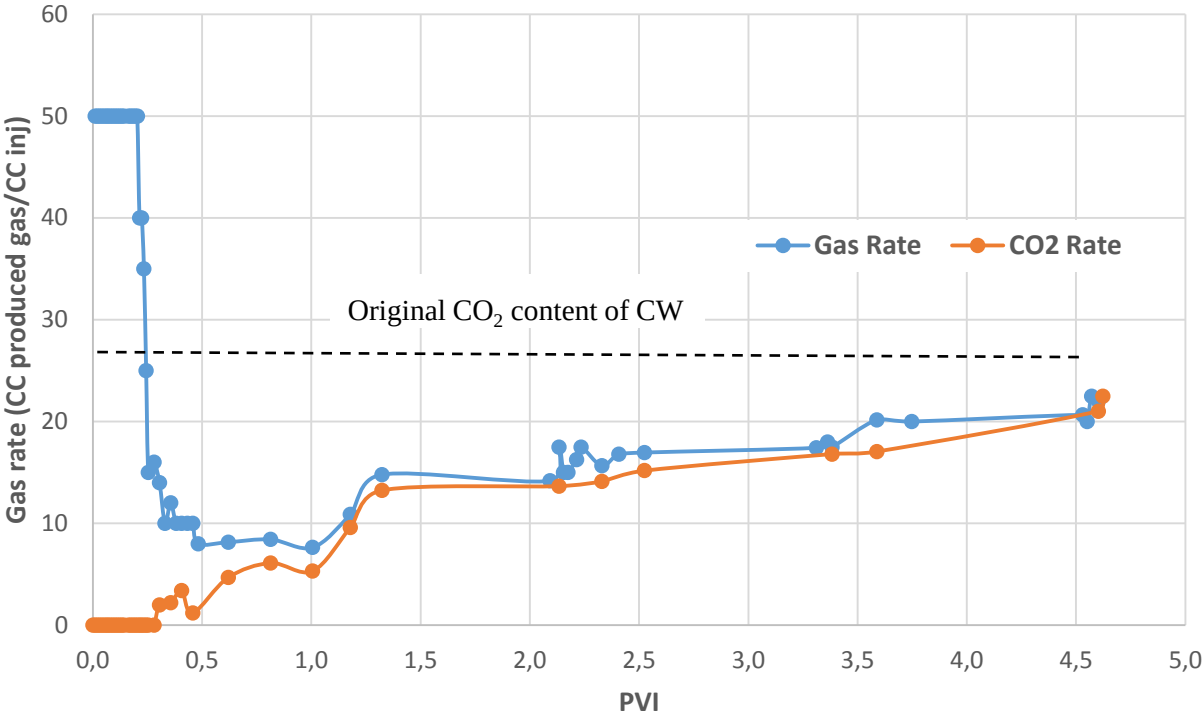

Figure 4-29 Gas rate during secondary carbonated water injection in a heterogeneous sandstone core

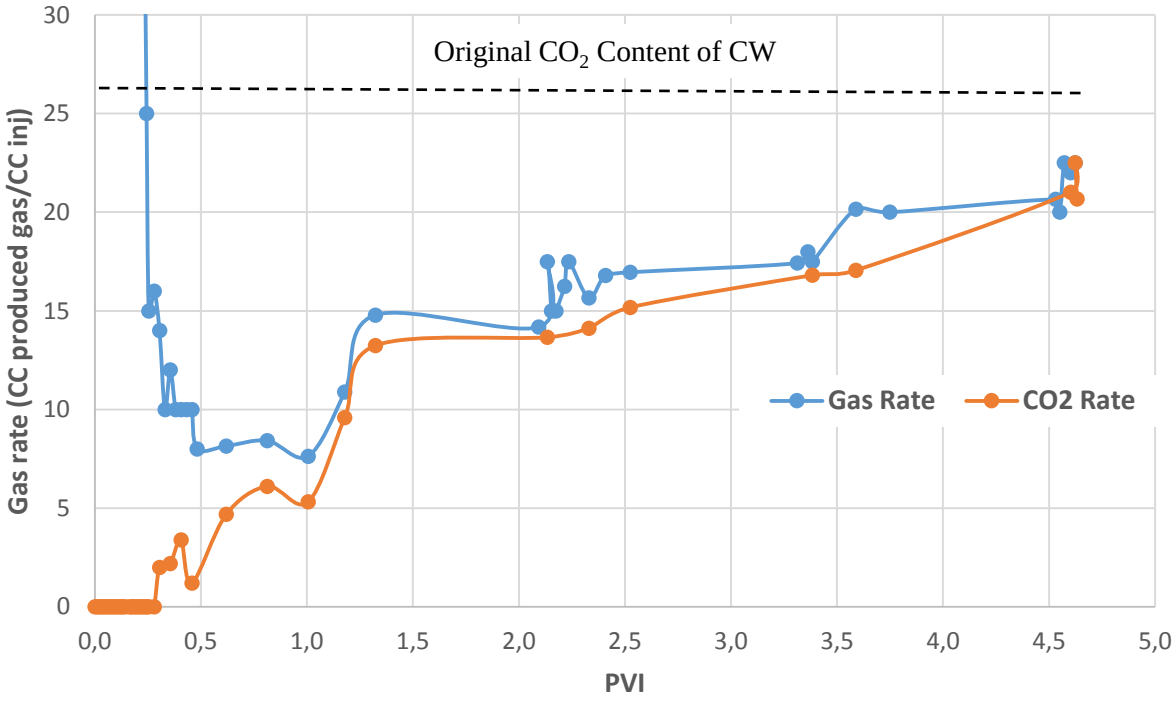

Figure 4-30 Gas rate during secondary carbonated water injection in a heterogeneous sandstone core

4.3.4 Repeatability of Coreflood Experiments

Each of the reported coreflood experiments was performed with the maximum accuracy and the process of running each of them was on average around two to three months. Figures 4-31 and 4-32 show the results of repeated measurements for two different experiments (experiments number 1 and 2 in Table 4-3) including secondary waterflooding and CWI in un-aged Berea cores. As can be seen from these figures, a minor difference was observed between the curves in each figure. The recovery curves in each figure show a same trend and a same ultimate oil recovery. This behaviour clearly confirms the repeatability and reliability of the reported recovery measurements.

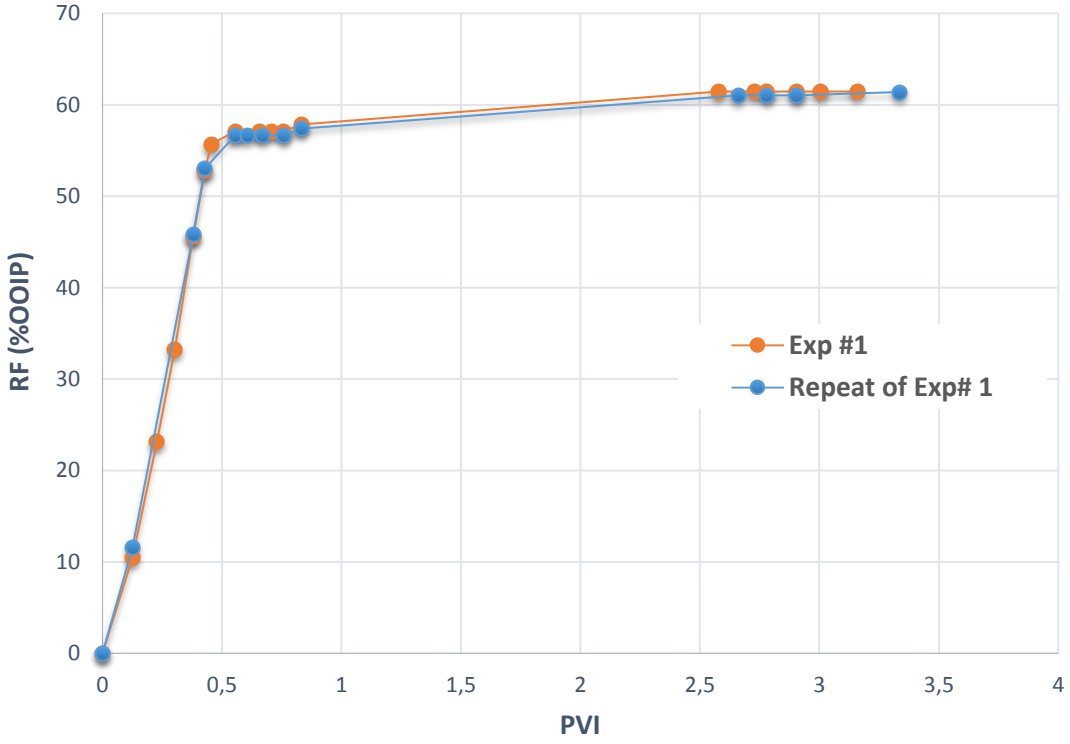

Figure 4-31 Reproducibility of experiment number 1 (waterflooding in un-aged Berea core)

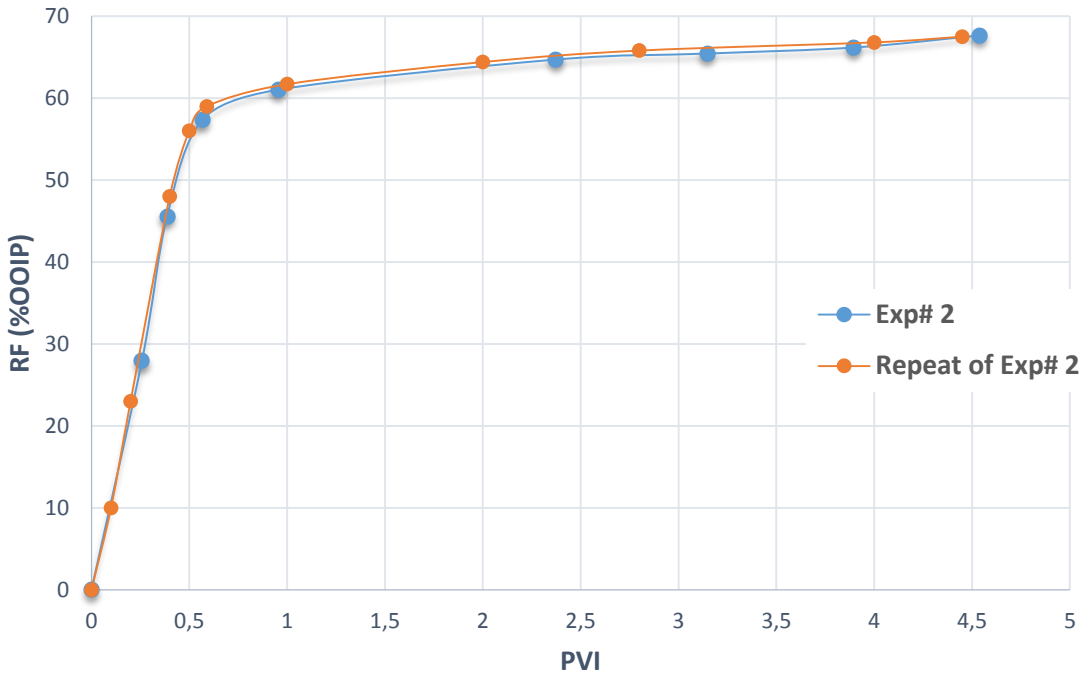

Figure 4-32 Reproducibility of experiment number 2 (CWI in un-aged Berea core)

4.4 Conclusion

A series of high-pressure high-temperature coreflood experiments were performed to study; (i) the coupling impacts of new phase formation and wettability alteration on improved oil recovery by CWI under realistic reservoir conditions (ii) the impact of carbonation level of CW on its performance and (iii) the potential of CWI either as secondary or tertiary injection scenario in heterogeneous reservoirs. Two separate systems were considered; mixed-wet system and water-wet system, using ‘’live’’ crude oil. Based on this study the following conclusions can be made:

1. Results of the coreflood experiments in both water-wet and mixed-wet systems revealed the strong potential of secondary CWI compared to that of waterflooding.
2. The native wettability state of the rock affects the performance of CWI. Secondary CWI in the mixed-wet system led to higher and earlier incremental oil recovery than the water-wet system.
3. The main recovery mechanism for the case of the water-wet system is the formation of the new phase. However, in mixed-wet to oil-wet systems, both wettability alteration and the formation of the new phase contribute to improved

oil recovery by CWI. Based on the results, the formation and growth of the new phase play a more dominant role.

4. In all the performed experiments the water cut during CWI was less than the one shown during waterflood. This indicates better water conformance control of CWI in comparison to conventional waterflood.
5. CWI shows good potential for CO_2 storage in oil reservoirs. Between 42 to 47.5% of the total injected CO_2 was stored by the end of CWI.
6. Earlier BT of CO_2 compared to the brine during CWI indicates good delivery of CO_2 from CW into the oil. However, over longer porous mediums this might not be the case.
7. Increasing carbonation level of CW has a favourable impact on the performance of CWI, which is due to the presence of more CO_2 in the injected CW. As a result, more CO_2 will be available for transferring into the oil which leads to stronger new phase formation and hence stronger oil swelling which leads to better oil displacement and recovery.
8. Results of the coreflood experiments performed in the heterogeneous core revealed the strong potential of CWI either as secondary or tertiary injection scenario for producing the bypassed oil and improving oil recovery. However, similar to micromodel results presented in Chapter 2 (Section 2.3.2), the coreflood results confirmed the better performance of secondary CWI compared to the tertiary CWI.

Chapter 5: Enhancing Water Imbibition Rate and Oil Recovery by Carbonated Water

5.1 Introduction

Spontaneous imbibition refers to the process of a wetting fluid being spontaneously drawn into a porous medium by the capillary forces and displacing a non-wetting fluid. The resultant displacement could be counter-current (in the opposite direction) or co-current (in the same direction). The positive role of this mechanism during waterflood (WF) has been recognised, in particular, in heterogeneous and fractured reservoirs where large permeability variations usually make the direct displacement of oil by water inefficient. In the presence of high permeability layers or fractures, injection water will tend to flow into the high permeability areas bypassing the low permeability zones; therefore, the oil located in the low permeability parts would not be displaced. Due to the preferential flow of water in the high permeability layers, the differential pressure across the reservoir would be limited and, as a result, viscous forces would be weak for oil production during waterflood. This would lead to poor sweep efficiencies and low recoveries.

Several field applications [74], [75] have shown the importance of spontaneous water imbibition as a mechanism for oil production. However, spontaneous imbibition can be a relatively slow process. As a result, oil recovery from the reservoirs that are dominated by this process can be slow [74]. One way to increase the rate of water imbibition and thereby oil recovery is to change the wettability preference of the rock surface. By changing the wettability of the rock surface from oil-wet toward more water-wet conditions, the amount of imbibed water and the rate of imbibition would increase which would have a positive impact on oil recovery. Several researchers have conducted imbibition experiments using surfactant [75]–[77] and it has been shown that chemicals such as surfactants have the potential to change the wettability toward water-wet [76], [78]–[83]. However, surfactants application is limited due to some reasons including high cost and adsorption onto the rock surfaces. Surfactants performance is also significantly reduced in high-temperature reservoirs and reservoirs with high salinity formation water. It has also been reported that under certain conditions seawater

may act as a wettability modifying fluid for weakly water-wet chalks leading to improved oil recovery by spontaneous imbibition [67], [71], [84]–[86].

The aim of this chapter is to investigate the potential of carbonated water (CW) for speeding up the rate of water imbibition from high permeability zones into low permeability parts.

In an experimental study, Perez et al. [87] reported the effects of carbonated water on oil recovery by spontaneous counter-current imbibition using limestone and sandstone cores. Oil recovery was increased by carbonated water imbibition in comparison to water imbibition. Grape et al. [88] performed imbibition tests involving CO_2-enriched water (carbonated water) and showed that the inclusion of CO_2 into the imbibed water improved both the imbibition rate and the recovery efficiency. In these studies, instead of using an actual crude oil, synthetic/white oil was used. Furthermore, they did not study the recovery mechanisms of CWI and the impact of wettability and aging on the imbibition rate and oil recovery. Fjelde et al. [89] studied the potential of CW (carbonated water) to improve the spontaneous imbibition of water in fractured chalk. They concluded that CW can improve spontaneous imbibition and oil recovery. The impact of rock type and native wettability state of the rock were not studied in their work. In this chapter, we are aiming to study the CWI potential on improving the spontaneous imbibition rate while addressing these issues. Therefore, the objectives of this chapter include:

(i) To evaluate the potential of carbonated water (CW) for improving the spontaneous imbibition of water in both carbonate and sandstone rocks.
(ii) To understand the effective mechanisms responsible for possible additional oil recovery during spontaneous CW imbibition.
(iii) To evaluate the effect of wettability and aging on spontaneous imbibition.
(iv) To investigate the effect of rock type on CW imbibition.

5.2 Experimental Setup and Procedure

5.2.1 Imbibition Rig

Figure 5-1 depicts the experimental setup used in this study. Conventional spontaneous imbibition cells normally used in laboratories are made of glass and can only operate at atmospheric pressure (Figure 5-2). Therefore, conventional imbibition cells would not

be suitable for this study as the experiments have to be performed under high pressure (2500 psia) in order to experiment with carbonated water (CW). The imbibition rig used in this study was specifically designed to conduct spontaneous experiments at high pressures and consisted of the following components: an imbibition cell, pump, injection cell, pressure transducers, back pressure regulator, a fluid separator, and a gasometer. The rig was kept at room temperature (T=68 ^{0}F) for the experiments reported in this chapter. During the experiments, the effluent fluids passed through a back pressure regulator where the pressure would drop to atmospheric pressure and hence, any dissolved CO_2 would be liberated. The separated liquid would then be collected in a graduated cylinder while the liberated CO_2 would pass through a gasometer.

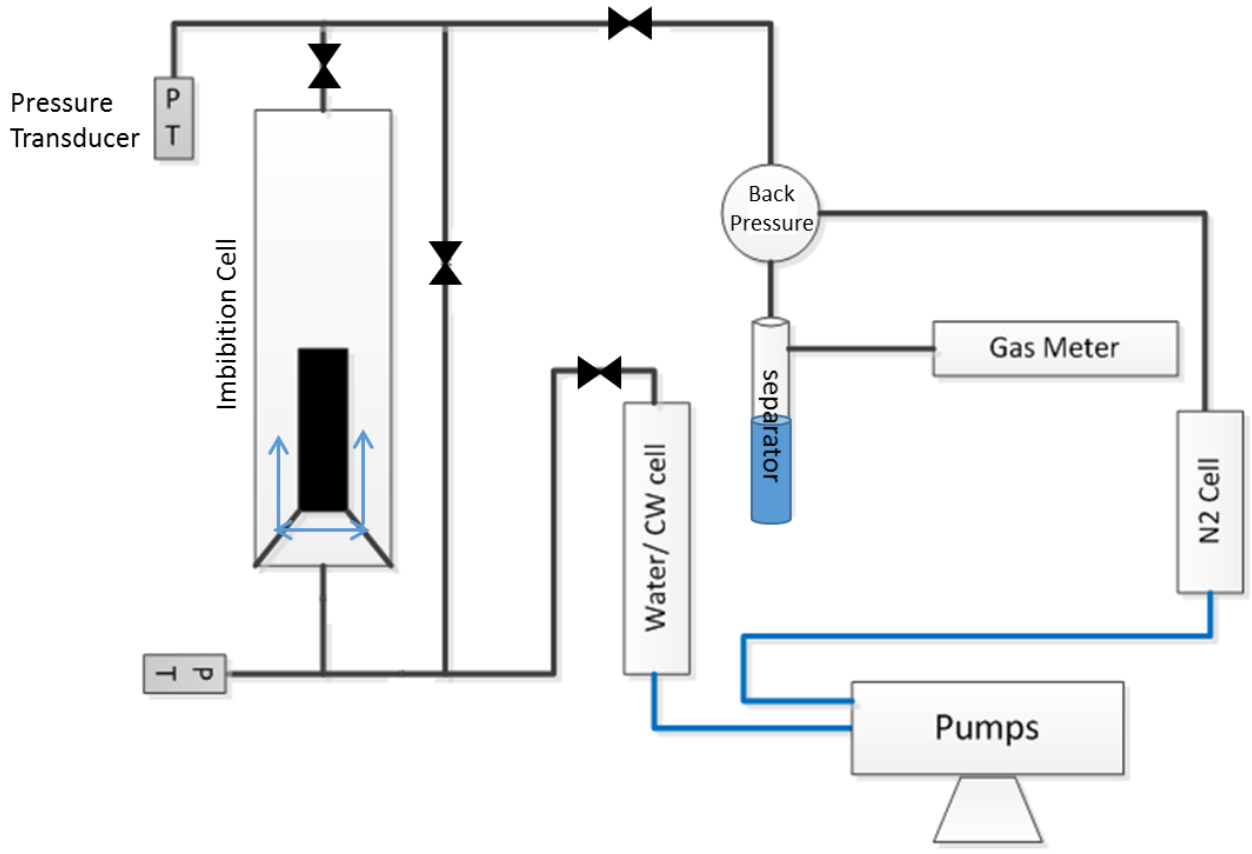

Figure 5-1 Schematic of the high-pressure spontaneous imbibition rig

Figure 5-2 Conventional imbibition cell

5.2.2 Fluids Properties

The crude oil used in the experiments had an API gravity of 26.9° at room temperature. Table 5-1 shows the properties of the crude oil. The brine that was used in the spontaneous imbibition experiments represents seawater with a total salinity of 54,540 ppm. The brine composition is shown in Table 5-2.

To make the carbonated brine, CO_2 was mixed with the brine (seawater) at a pressure of 2500 psi and room temperature. At the pressure and temperature of the imbibition experiments, the carbonated water contained 30.3 cm^3 of CO_2 per every cm^3 of the brine.

Table 5-1 Crude oil properties

Crude ID	API	Density (gr/cm^3)	Saturates (%wt.)	Aromatics (%wt.)	TAN (mg KOH/gr Oil)	TBN (mg KOH/gr Oil)
B	26.9	0.8915	43.8	25.86	0.35	4.9

Table 5-2 Sea brine Components

Ion	ppm
Na	16844
Ca	664
Mg	2279
SO_4^{-2}	3560
Cl	31107
HCO_3^{-1}	193

5.2.3 Core Properties

Two types of outcrop cores (one carbonate and one sandstone) were used for these experiments. The dimensions and some of the physical properties of the cores are given in Table 5-3. The XRD analysis of the carbonate cores showed that 99% of the rocks were made of calcite ($CaCO_3$). For the sandstone core, the XRD analysis showed that 98% of the core was made of Quartz.

Table 5-3 Dimensions and properties of the cores used in this study

experiments	core ID	length (cm)	diameter (cm)	porosity%	absolute k (mD)	pore volume	S_{wi} %
1 & 2 (WF→ CW)	Desert Pink (Carbonate)	14.9	3.82	29.07	47.24	48.512	8
3 & 4 (WF→ CW)	Desert Pink (Carbonate)	14.5	3.77	29.43	41.89	46.841	6.9
5 & 6 (WF→ CW)	Clashach (Sandstone)	15	4	23.77	1637	46.808	9.9

5.2.4 Methodology

After cleaning the cores, their pore volume and porosity and permeability were measured. The pore volumes of the cores were determined as the total volume of fluid used to saturate the core. The porosity was calculated as the ratio of pore volume and the bulk volume of the core. The permeabilities of the cores were measured at the test pressure and temperature using brine (Table 5-3). Next, the initial water saturation (S_{wi}) was established in the cores through a drainage process of the brine-saturated cores with oil. Then, the sandstone core and one of the carbonate cores were aged in crude B for a month at a temperature of 158 ^{0}F. A higher temperature was chosen for ageing (compared to the test temperature) to accelerate the aging process. After completing the aging process, the aged core was placed inside the high-pressure imbibition cell. The design of the imbibition cell allowed a gap to exist between the outside diameter of the core and the inside diameter of the cell (see Figure 5-1). In order to investigate the effect of ageing and the role of wettability, the other carbonate core was not aged in crude oil prior to the imbibition test. This core was placed in the imbibition cell as soon as its initial water saturation was established.

Having placed the core inside the imbibition cell, the cell was filled with the brine from the bottom. Next, the pressure inside the cell was increased to 2500 psi. Then, the brine (either carbonated or plain brine) was injected into the imbibition cell at a very low rate only to gradually transfer the produced oil from the cell towards the separator. The pressures at the inlet and outlet of the imbibition cell were continuously monitored and recorded to ensure that there was no differential pressure across the cell. For all of the spontaneous imbibition tests reported here, first, a spontaneous imbibition of plain brine (seawater) was performed, and then potential additional oil recovery by tertiary spontaneous imbibition of CW was investigated.

5.3 Results and Discussion

As shown in Table 5-3, two different types of rocks were used in this chapter. In this section, the results of the carbonate cores are discussed and in the next section, the results of the sandstone core will be presented.

5.3.1 Spontaneous Imbibition in Carbonate Rock

It is estimated that more than half of the world's oil reserves are held in carbonate reservoirs. Most carbonate reservoirs show low oil recovery factor due to the heterogeneous distribution of porosity and permeability; therefore, spontaneous imbibition is a key recovery mechanism for waterflooding in this type of reservoirs. However, the majority of carbonate reservoirs are believed to be oil-wet. To study the effect of the initial rock wettability on the imbibition rate and oil recovery by brine and carbonated brine, two situations were considered using two cores taken from the same block of carbonate rock; an un-aged core and an aged core.

5.3.1.1 Aged Carbonate Rock

5.3.1.1.1 Imbibition Experiments

In this section, the results of the aged rock system are discussed (Experiments number 1 and 2). The spontaneous imbibition experiments were carried out at room temperature and pressure of 2500 psi using plain brine and CW as test fluids on one aged carbonate core. The core had been aged in crude oil to allow its wettability to change to oil-wet naturally by being in contact with crude oil. First, a spontaneous (plain) brine imbibition was studied for a period of time; next the additional oil recovery by tertiary spontaneous CW imbibition was tested.

During the spontaneous imbibition of plain brine, the aged core was in the imbibition cell for 31 days; however, no oil recovery was observed during this relatively long period of time. This result indicates that the aging process had been very effective, and the core was strongly oil-wet. An oil-wet condition caused a negative capillary pressure; therefore, brine could not imbibe into the oil-wet carbonate rock spontaneously. As mentioned before, the majority of the carbonate reservoirs are oil-wet. The result of this experiment demonstrates clearly the poor performance of spontaneous brine imbibition as a method of oil recovery from oil-wet carbonate rocks.

Having finished the spontaneous imbibition of brine, without touching the core or changing any other parameter of the test, CW was injected into the imbibition cell from the bottom to replace the plain brine used in the previous brine imbibition test. When the brine had been replaced by CW for approximately four days, oil production started. Figure 5-3 summarises the results of both stages of this spontaneous imbibition test.

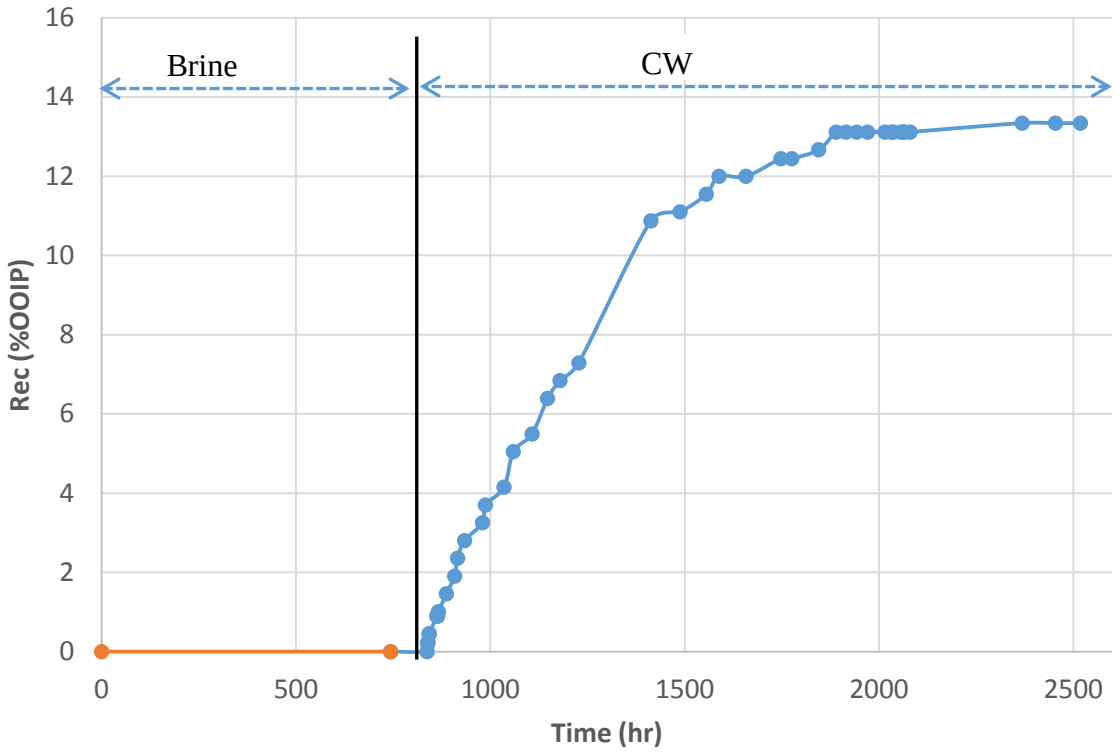

Figure 5-3 Cumulative oil production during spontaneous imbibition of brine and CW into an aged carbonate rock at room temperature and pressure of 2500 psi. CW improved the rate of spontaneous imbibition and led to 13.3% additional oil recovery

As can be seen from Figure 5-3, while there was absolutely no oil recovery during the whole period that the aged carbonate rock was in contact with seawater, the spontaneous imbibition of CW led to an oil recovery factor of 13.3% of the original oil in place (OOIP). This result reveals the potential of CW for improving oil recovery from oil-wet carbonate reservoir by significantly enhancing the process of spontaneous imbibition.

5.3.1.1.2 Oil Recovery Mechanisms – Oil-Wet Carbonate Rock

As it was observed from Figure 5-3, the spontaneous imbibition of (plain) seawater did not lead to any oil production. This is attributed to the wettability state of the rock

which was oil-wet. On the other hand, spontaneous imbibition of CW resulted in an oil recovery of 13.3% of the original oil in place (OOIP). It should be noted that dead crude oil had been used for all reported experiments in this chapter. As a result, formation and growth of the gaseous new phase would not be the active oil recovery mechanism in here. The main mechanisms leading to oil recovery by CW are as follows:

1) CW favourably changes the wettability of the oil-wet carbonate rock towards water-wet conditions. This wettability alteration by CW has been observed in the wettability studies that were reported in Chapter 3 (section 3.3.2.3). It should be noted that the type of oil and brine that was used in this study was the same as those that had been used in wettability study that was investigated in Chapter 3. Therefore, the results of Chapter 3 can be applied for this investigation. Based on the XRD analysis 99% of the carbonate core was made of calcite. As it was reported in Chapter 3 (Figure 3-14), for an aged calcite CW has this potential to change the wettability toward more water-wet conditions. The wettability alteration from oil-wet toward water-wet has a strong effect on imbibition process since the amount of water imbibed depends on the capillary pressure curve, which is a function of wettability of the rock.

2) CW can lead to carbonate rock dissolution, which can help with the alteration of wettability from oil-wet toward water-wet by detaching the oil aggregate from the rock surfaces. This mineral dissolution has been observed during the coreflood and contact angle experiments. Figure 5-4 shows the inlet section of a reservoir carbonate core before and after CWI (carbonated water injection). As can be seen, CW caused some mineral dissolution. 0.5% (wt%) of the rock was dissolved when the core came in contact with CW. Furthermore, the permeability of the rock was increased by 16.5%.

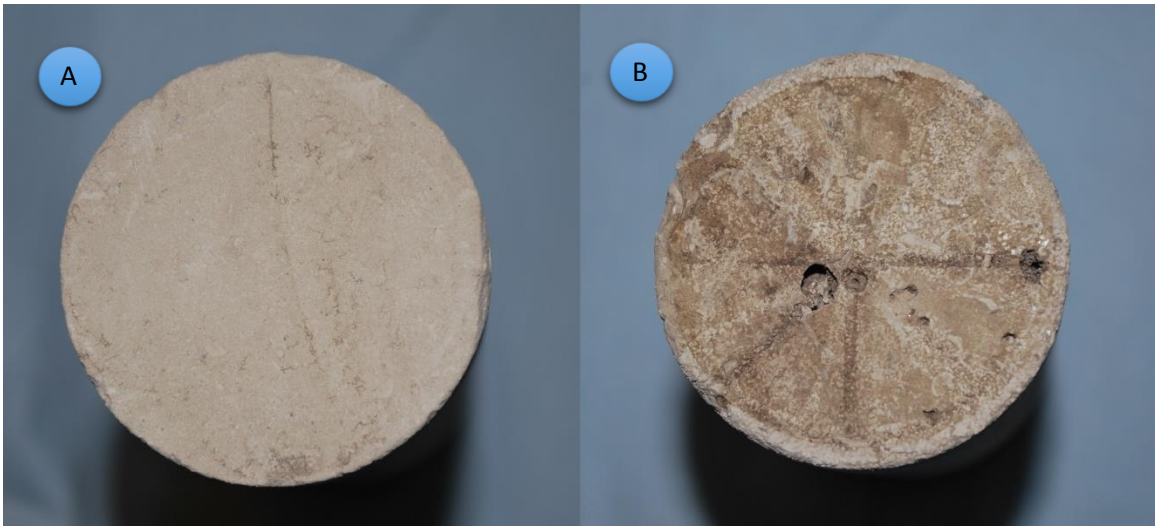

Figure 5-4 Inlet of a reservoir carbonate core A) before and after B) CWI

3) When CW comes in contact with the oil in the porous medium, CO_2 from the imbibed CW will diffuse into the oil and oil swelling would happen. This oil swelling was reported in the micromodel investigations in Chapter 2 (see Figures 2-11 and 2-17). This oil swelling expels the oil from the rock and can lead to additional oil recovery.
4) As a result of CO_2 transfer from the imbibed CW into the oil, the viscosity of the oil reduces. The oil viscosity reduction by CW was observed in the reported micromodel investigations in Chapter 2 (see Figures 2-12 and 2-18). Since less viscous oil needs less driving force for flow, the viscosity reduction by CW can help improving recovery.
5) Transfer of CO_2 from CW into the oil also may lead to some reductions of the interfacial tension (IFT) between the oil and water [90], [91].

5.3.1.1.3 ICP Analysis

To further improve our understanding of the effects of CW on the rock and mineral dissolution, ICP (Inductively Coupled Plasma) analyses were performed on the effluent brine samples that had been taken during both seawater imbibition and the subsequent CW imbibition.

Figure 5-5 presents the results of the ICP analysis for Ca, Mg, and S. The y-axis in this figure shows the ratio of the concentration of each ion to its original concentration (C/Co) and the x-axis shows the effluent sample numbers that had been taken during the

experiments. Based on this data, during the seawater spontaneous imbibition period; the concentration of the ions did not change. However, during CW spontaneous imbibition, the concentration of Ca increased. The increase in Ca concentration is due to rock dissolution that happened during spontaneous CW imbibition. XRD results of the core show that 99% of the core is made of calcite ($CaCO_3$). When CW comes in contact with carbonate rock, due to its lower pH, calcite dissolution takes place. This effect has been observed in the flooding experiment (Figure 5-4) as well as the wettability studies reported in Chapter 3 (see Figure 3-10). As a result of this mineral dissolution, the concentration of Ca in the effluent increased during spontaneous imbibition of CW, as shown in Figure 5-5.

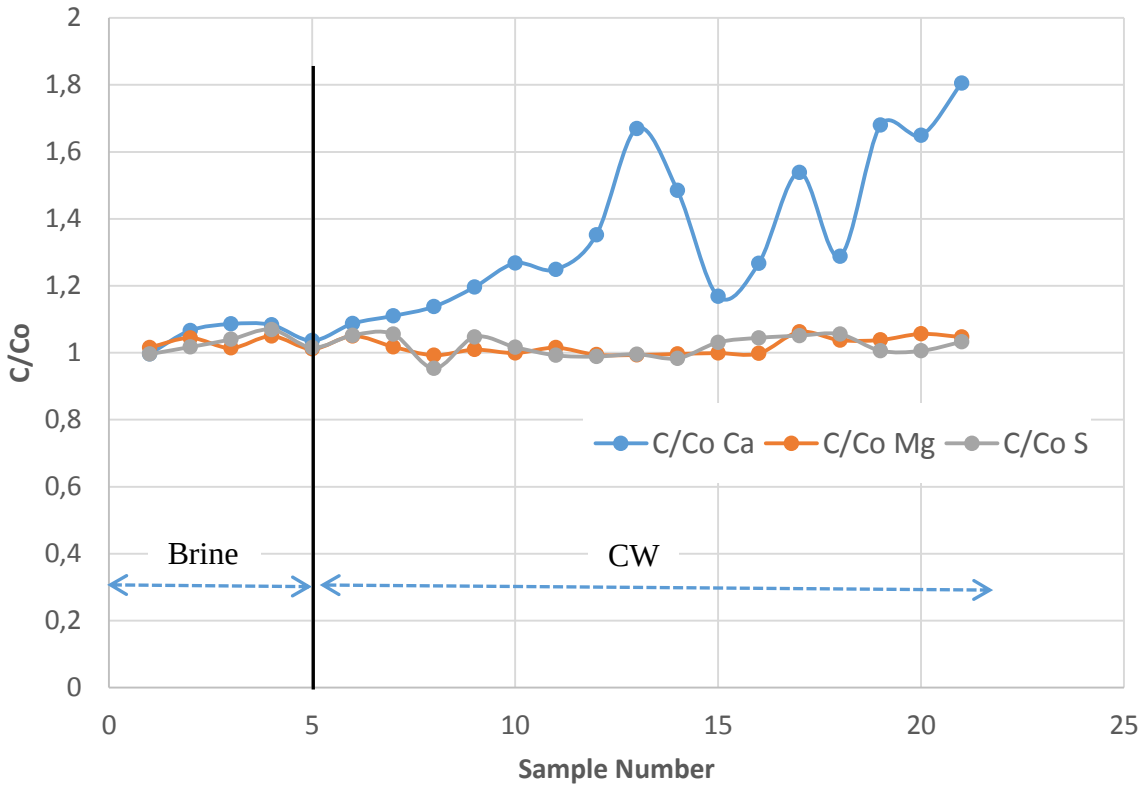

Figure 5-5 ICP analysis of the effluent brine samples taken during spontaneous imbibition of brine and CW into an aged carbonate rock

5.3.1.2 Un-Aged Carbonate Rock

5.3.1.2.1 Imbibition Experiments

In order to study the effect of initial wettability of the rock on spontaneous imbibition and oil recovery by CW, two more experiments (experiments 3 and 4) were designed and performed on an un-aged carbonate rock. The core that was used in these two

experiments was very similar to the one that was utilized in the experiments reported above. The main properties of the cores are listed in Table 5-3. As can be seen, the initial water saturations and permeabilities of these carbonate cores were quite similar to each other. The only main difference was the initial wettability state of the two cores due to one not undergoing the ageing process in the crude oil. For the un-aged core, after establishing the initial water saturation, the core was immediately assembled in the imbibition setup for spontaneous brine imbibition, and it was not aged in crude oil. Therefore, the core's initial wettability was expected to be water-wet. The test pressure and temperature were kept the same as those of the aged system (2500 psi and room temperature), and the same fluids were used in the experiments (see Tables 5-1 and 5-2).

For the un-aged system, similarly to the aged system, first, a secondary spontaneous imbibition of plain brine (seawater) was performed, and then the additional oil recovery by a subsequent (tertiary) spontaneous CW imbibition was investigated. Figure 5-6 presents the results of the spontaneous brine imbibition in the un-aged carbonate rock. As can be seen from this figure, the oil recovery due to spontaneous brine imbibition started after around 50 hours and resulted in 5.3% (OOIP%) oil recovery. Spontaneous imbibition by brine was continued until the curve of the oil recovery reached a plateau. This test clearly shows the crucial impact of the initial wettability of the rock on the rate of spontaneous imbibition and the resultant oil recovery from carbonate rocks. By comparing the results of this test with the results of the spontaneous brine imbibition test in the aged rock presented in Figure 5-3, one can conclude that the wettability of the rock has a crucial role in the amount of imbibed water and hence, on oil recovery. By changing the wettability from oil-wet toward water-wet, 5.3% (OOIP%) oil recovery was obtained during plain brine imbibition period.

After 35 days, when oil production reached a plateau, the plain brine was displaced very slowly by CW without changing any other parameter of the test and the tertiary spontaneous imbibition of CW was started. When the resident brine was replaced by CW, after approximately 26 hours, oil production started again (Figure 5-7).

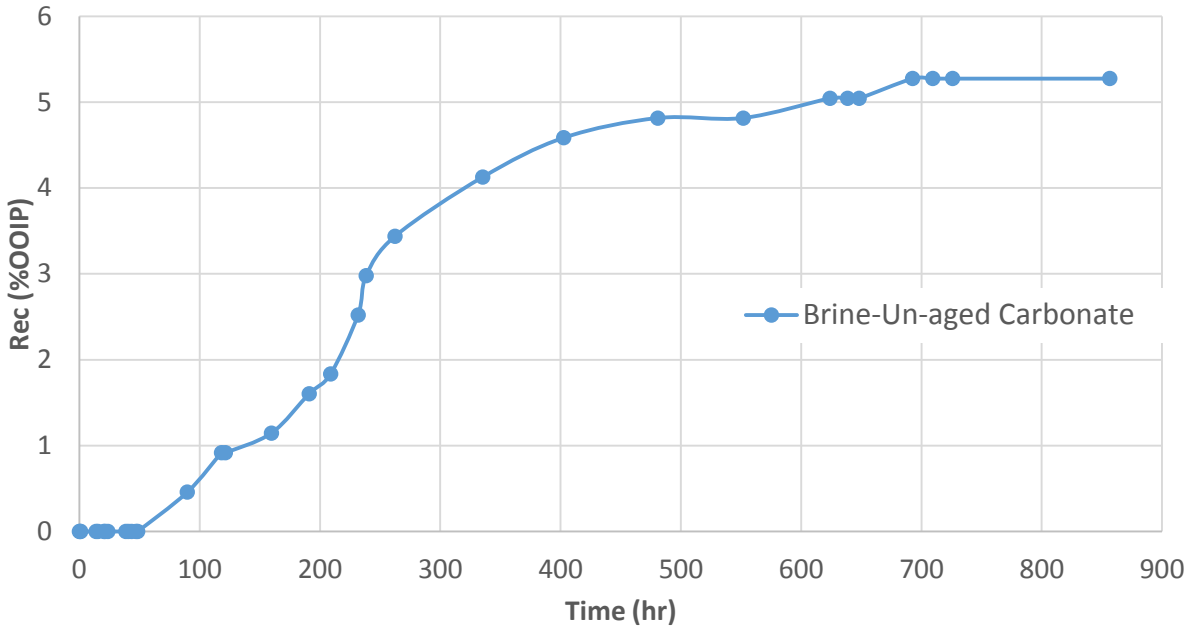

Figure 5-6 Cumulative oil production during spontaneous imbibition of brine into an un-aged carbonate rock at room temperature and pressure of 2500 psi

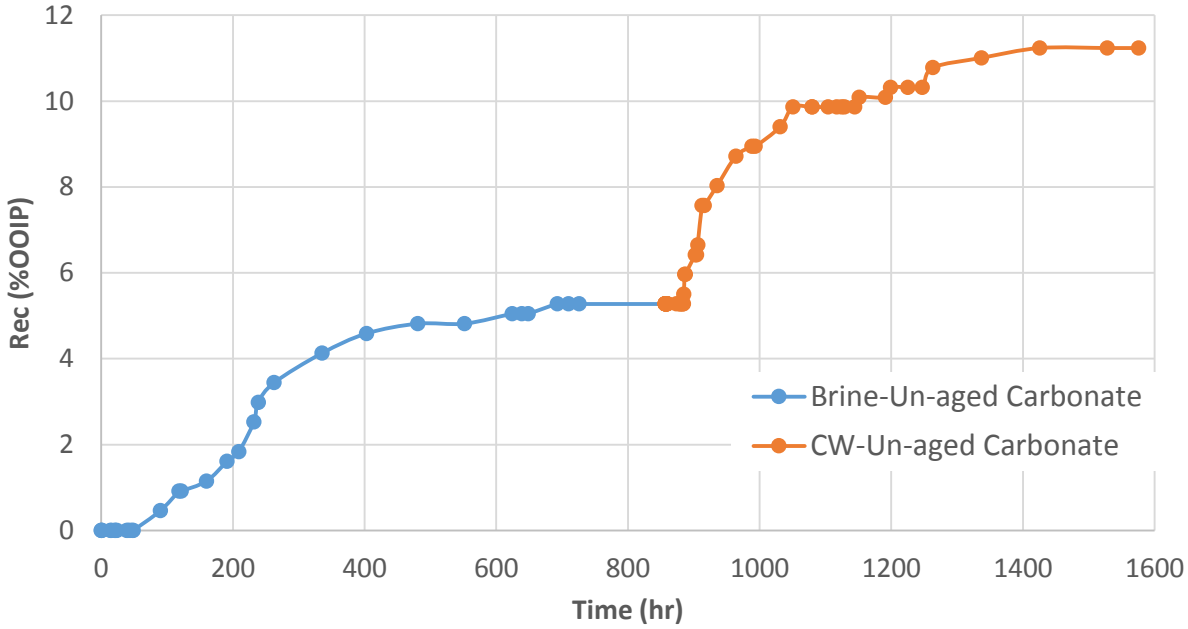

Figure 5-7 Cumulative oil production during spontaneous imbibition of brine and CW into an un-aged carbonate rock at room temperature and pressure of 2500 psi

As can be seen from Figure 5-7, imbibition of CW enhanced oil recovery by 6% of the OOIP. It should be noted that the rate of imbibition and oil production during tertiary spontaneous CW imbibition is much higher than spontaneous brine imbibition (Figure 5-7). This demonstrates the potential of CW for accelerating the imbibition rate and

therefore oil recovery even for the water-wet rocks. Imbibition by CW was continued for 30 days.

5.3.1.2.2 Oil Recovery Mechanisms -Water-Wet Carbonate Rock

Since the core used in experiments shown in Figure 5-7 had not been aged, it can be assumed that the initial wettability state of the core remained mostly water-wet, and that was the reason why brine could imbibe into the rock, which resulted in 5.3% (OOIP%) oil recovery. Comparison of the results of the seawater imbibition period in the unaged core with that of its aged counterpart demonstrates the importance of wettability on oil recovery by water imbibition.

As depicted in Figure 5-7, the spontaneous imbibition of CW accelerated the rate of imbibition and therefore oil recovery. Based on the results, it is believed that oil swelling, oil viscosity reduction, and reduction of IFT between the oil and brine were, to varying degree, the main mechanisms of the observed additional oil recovery during spontaneous CW imbibition in the un-aged carbonate rock. As shown by the reported wettability studies in Chapter 3 (see Figure 3-14), CW can change the wettability of the weakly water-wet carbonate rocks toward more water-wet conditions; however, the extent of this wettability alteration is much less than what has been observed for oil-wet systems. Figure 3-14 depicted the extent of wettability alteration for both water-wet and oil-wet calcite. As can be seen, for the case of an oil-wet system, CW led to 47 degrees change in the contact angle toward water-wet; however, for the case of the un-aged (water-wet) calcite, the extent of wettability alteration by CW was equivalent to 4 degrees. Based on this, it is expected that the wettability alteration by CW in the un-aged rock would not to be the dominant mechanism for the observed additional oil recovery.

Figure 5-8 depicts the results of both plain brine and carbonated brine imbibition into the un-aged and aged carbonate rocks. As can be seen from this figure, during the secondary plain water spontaneous imbibition stage of the tests, due to the initial difference in the wettability state of the rocks, while 5.3% of oil was recovered from the water-wet (un-aged) rock, no oil recovery was obtained from the oil-wet (aged) rock. Since there was not any oil production during secondary brine imbibition in the aged carbonate rock, the subsequent tertiary CW imbibition in this rock can be considered as secondary imbibition too. Comparing the results of oil recovery in the aged rock system

with that of the un-aged rock reveals the good potential of CW for changing the wettability of the oil-wet carbonate rock towards water-wet conditions and thereby resulting in the observed better performance of spontaneous imbibition and additional oil recovery.

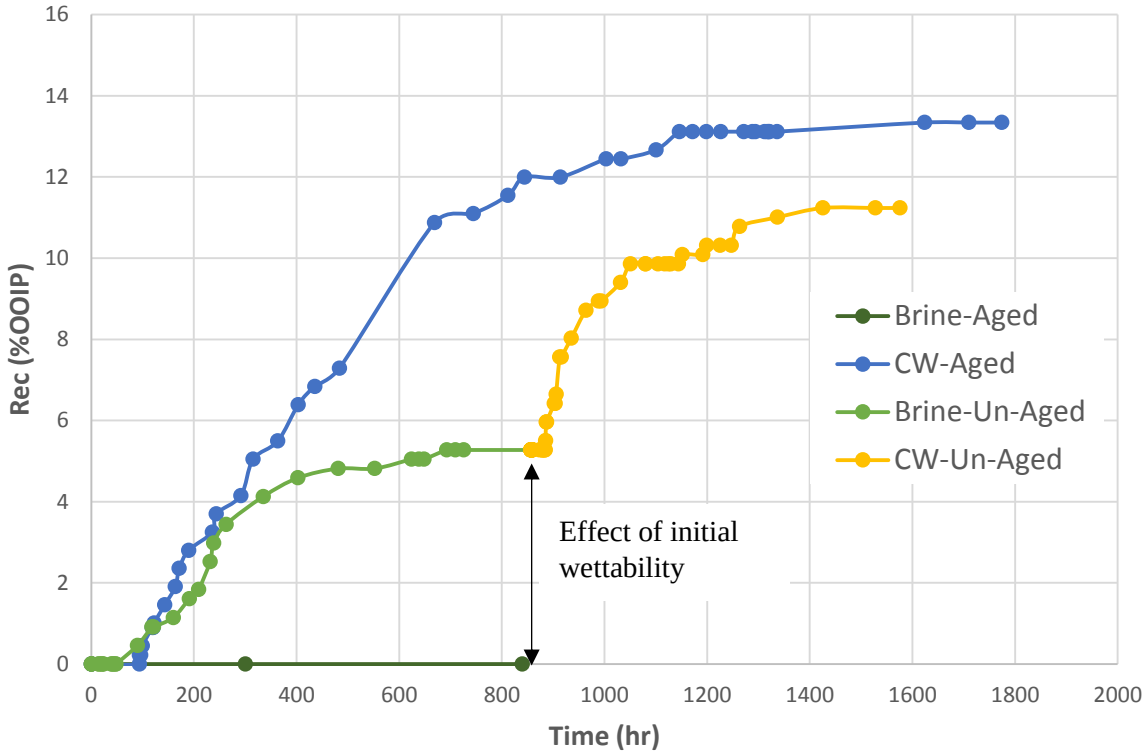

Figure 5-8 Cumulative oil production during spontaneous imbibition of brine and CW into aged and un-aged carbonate rocks at room temperature and pressure of 2500 psi

As can be seen from Figure 5-9, in the oil-wet system, imbibition by CW led to higher oil recovery (7% of the Remaining Oil in Place, ROIP) compared to un-aged system, this shows under more realistic reservoir conditions where the reservoir rock is usually mixed wet or oil-wet, CW has a higher potential to change the wettability of the oil-wet system toward water-wet conditions and improve water and oil recovery.

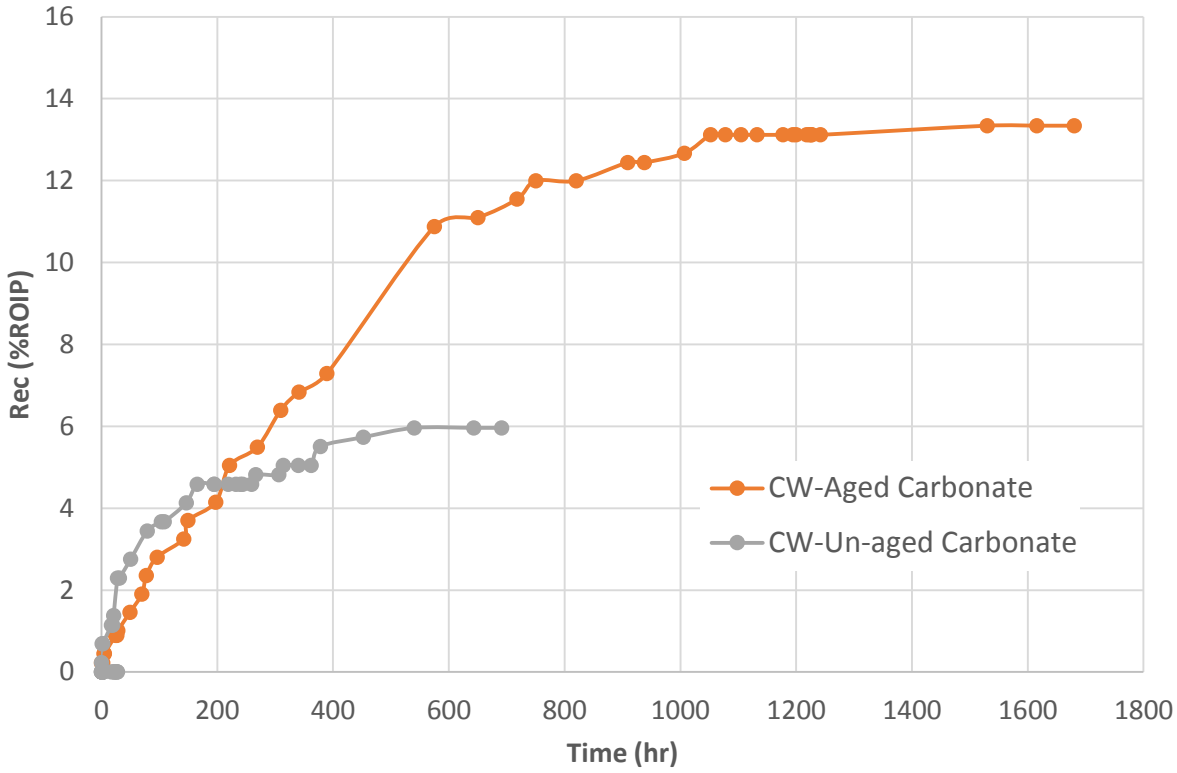

Figure 5-9 Tertiary spontaneous imbibition of CW in aged rock system and un-aged rock system at pressure of 2500 psi and room temperature

5.3.2 Spontaneous Imbibition in Sandstone Rock

So far, the potential of CW for accelerating the rate of imbibition and consequently oil recovery in carbonate rocks were discussed. Here in this section, the impact of CW on the imbibition rate in oil-wet sandstone rock is investigated (experiments 5 and 6 in Table 5-3). Similarly to the study of carbonate rocks, the study on sandstone was also carried out at a pressure of 2500 psi and room temperature.

5.3.2.1 Imbibition Experiment

After aging the sandstone core for a period of a month, the aged core was placed in the imbibition cell, and spontaneous imbibition of brine at a pressure of 2500 psi and room temperature was started. The experiment was continued for a month; however, no oil was produced during this time (see Figure 5-10). This shows that the aging process had been effective, and it had changed the wettability of the rock toward oil-wet and therefore, the brine could not imbibe into the rock. Next, the brine was displaced by CW and the spontaneous imbibition of CW in tertiary mode started. When the brine had been replaced by CW for approximately three days, oil production started.

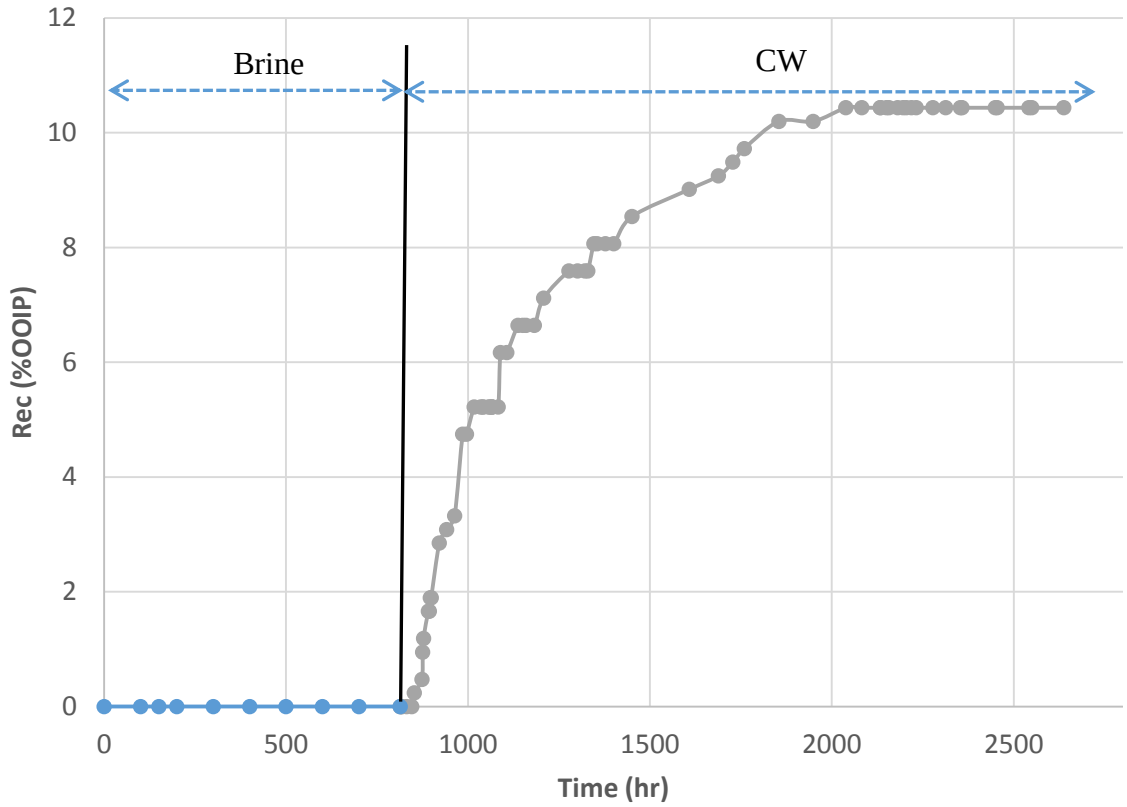

Figure 5-10 Cumulative oil production during spontaneous imbibition of brine and CW into an aged sandstone rock at room temperature and pressure of 2500 psi

As can be seen from Figure 5-10, although no oil was produced during 30 days of spontaneous brine imbibition, spontaneous CW imbibition led to 10.2% (OOIP%) oil recovery. This improvement in oil recovery is a good indication of the positive impact of CW on spontaneous imbibition of water and oil recovery from oil-wet sandstone rocks.

5.3.2.2 Oil Recovery Mechanisms –Oil-Wet Sandstone

The improvement in oil recovery observed for the sandstone rock is attributed to oil swelling, oil viscosity reduction, reduction of IFT between the oil and brine, and also wettability alteration. For the case of sandstone rocks, mineral dissolution is not as strong as in carbonate rocks. As it was shown in Chapter 3 (see Figure 3-12), CW had the potential to change the wettability of aged quartz toward a more water-wet state. Quartz is the main component of sandstone rocks. Figure 3-12 shows the contact angle measurements indicating the effect of CW on altering the wettability of aged quartz substrates toward more water-wet. As can be seen, for aged quartz, when CO_2 was

added to the brine, the contact angle reduced around 15 degrees toward more water-wet conditions. This wettability alteration toward more water-wet conditions will have a direct effect on the amount of imbibed water and oil recovery during spontaneous CW imbibition.

Figure 5-11 compares the oil recovery obtained during spontaneous imbibition of CW in aged sandstone and aged carbonate rock. Although the permeability of the sandstone rock is much higher than that of the carbonate rock (see Table 5-3), which directly helps water imbibition and oil recovery, the recovery by CW for the sandstone rock is 3% less than the recovery for the carbonate rock. If we ignore the positive effect of higher permeability of the sandstone rock on its imbibition rate and oil recovery, since the fluids that were used for all the experiments were the same and the only differences were rock type and rock properties (e.g., permeability), it can be assumed that the effects of oil swelling, oil viscosity reduction and decrease in the IFT between the oil and brine on oil recovery by spontaneous CW imbibition for both the aged sandstone and carbonate rock are the same. However, as can be seen from Figure 5-11, oil recovery by spontaneous CW imbibition in the aged carbonate rock was higher than that for the aged sandstone. The reason for this better oil recovery is the stronger potential of CW for changing the wettability of the carbonate rock compared to the sandstone rock. This result is consistent with the results of wettability studies reported in Chapter 3 (Section 3.3.2). Comparison of the results presented in Figures 3-14 and Figure 3-12 shows that CW has a stronger potential for changing the wettability of the aged calcite compared to aged quartz. This means that CW will have a higher potential for enhancing the imbibition rate and thereby oil recovery in oil-wet carbonate rocks compared to oil-wet sandstone rocks as was confirm by the results of the imbibition tests.

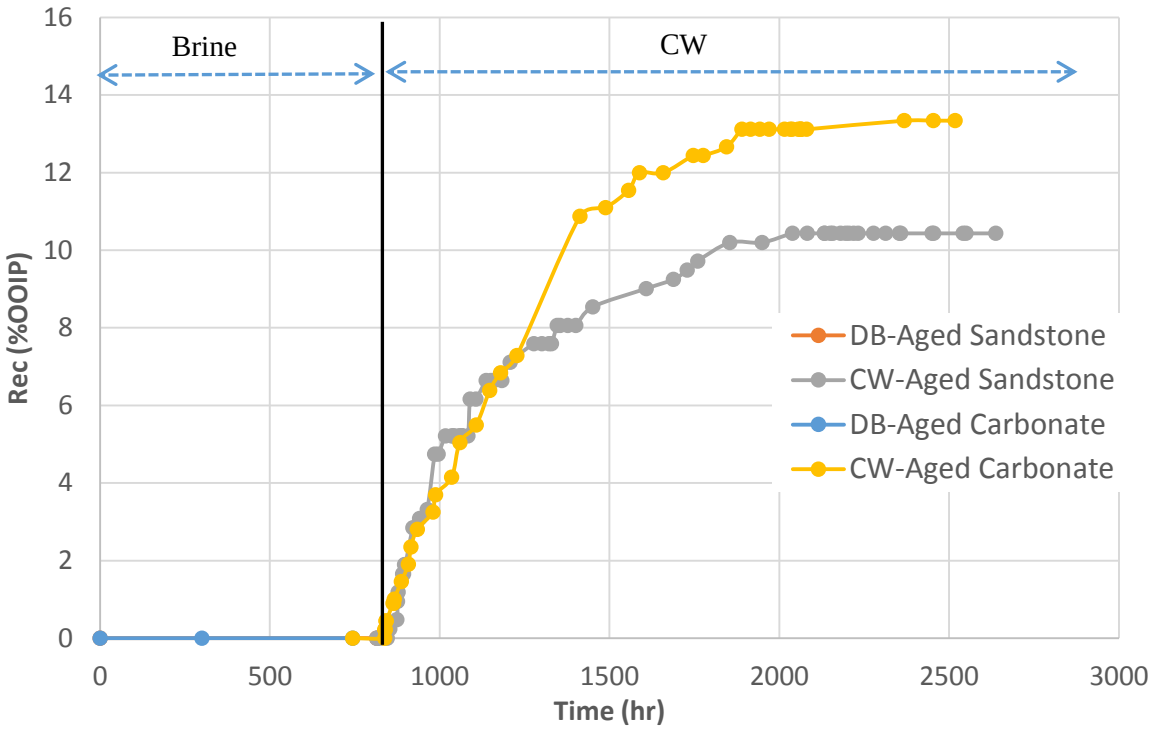

Figure 5-11 Cumulative oil production during spontaneous imbibition of brine and CW into aged sandstone and carbonate rocks at room temperature and pressure of 2500 psi

5.3.2.3 ICP Analysis

As mentioned above, mineral dissolution was not considered as an oil recovery mechanism during CW spontaneous imbibition in sandstone rock. To check this assumption, ICP analysis was performed on the effluent brine samples that had been taken during both brine imbibition and CW imbibition in sandstone rock. Figure 5-12 presents the changes in the concentration of Ca, Mg, and S in the collected brine samples. As can be seen, during both water imbibition and carbonated water imbibition period; the concentration of the ions in the brine samples is close to their original concentration. Since the XRD analysis of the rock shows that rock is mainly made of silica, the concentration of silica in brine samples was also analysed. Figure 5-13 demonstrates the change in the concentration of silica. The red curve illustrates the concentration of silica in effluent brine. It should be noted that the initial concentration of silica in the brine used in this study (Table 5-2) was zero. As can be seen, the change in concentration of silica was also negligible. The slight increase in the silica concentration might be due to the glass tubes that were used for keeping the brine samples. Based on Figures 5-12 and 5-13, CWI had no effect over the mineralogy of our

sandstone rock and therefore, mineral dissolution cannot be regarded as an oil recovery mechanism for this type of rock. On the other hand for the case of carbonate rock, we faced a strong mineral dissolution (see Figure 5-5). That might be another reason for higher oil recovery by spontaneous imbibition of CW in the carbonate core compared to the sandstone one (Figure 5-11). The strong mineral dissolution by CW for the case of carbonate rock can cause the fresh surface of the rock to come in contact with oil resulting in a more wettability alteration for carbonate rock and therefore better imbibition and oil recovery.

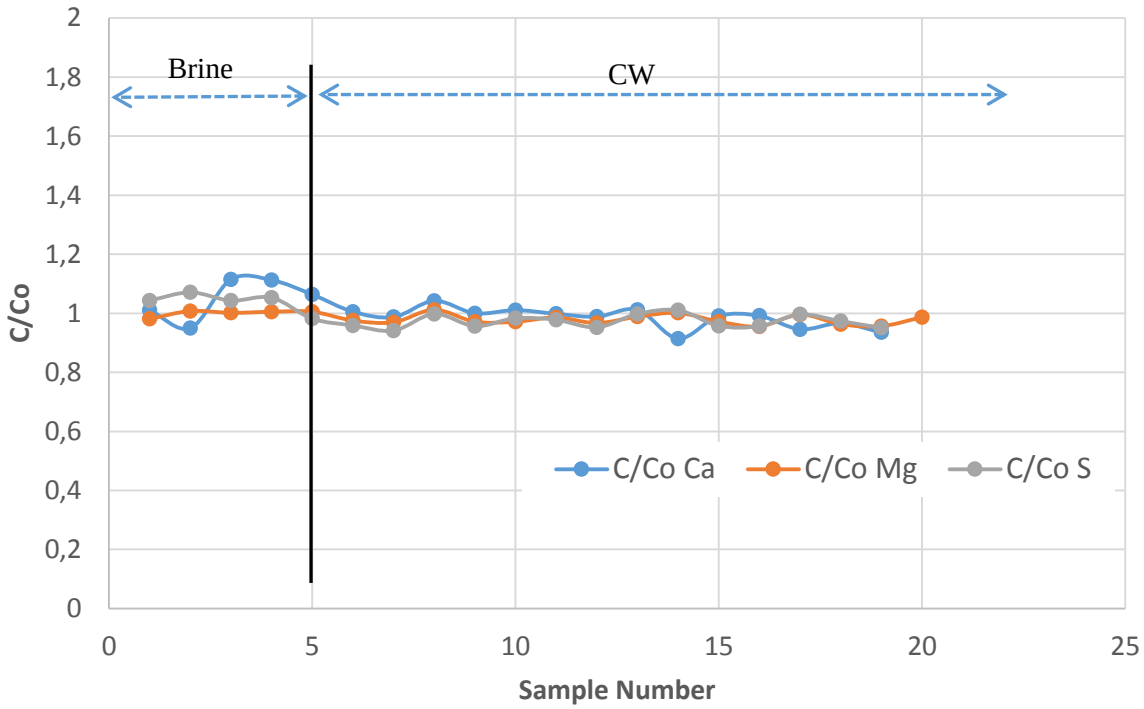

Figure 5-12 ICP analysis of the effluent brine samples taken during spontaneous imbibition of brine and CW into an aged sandstone rock

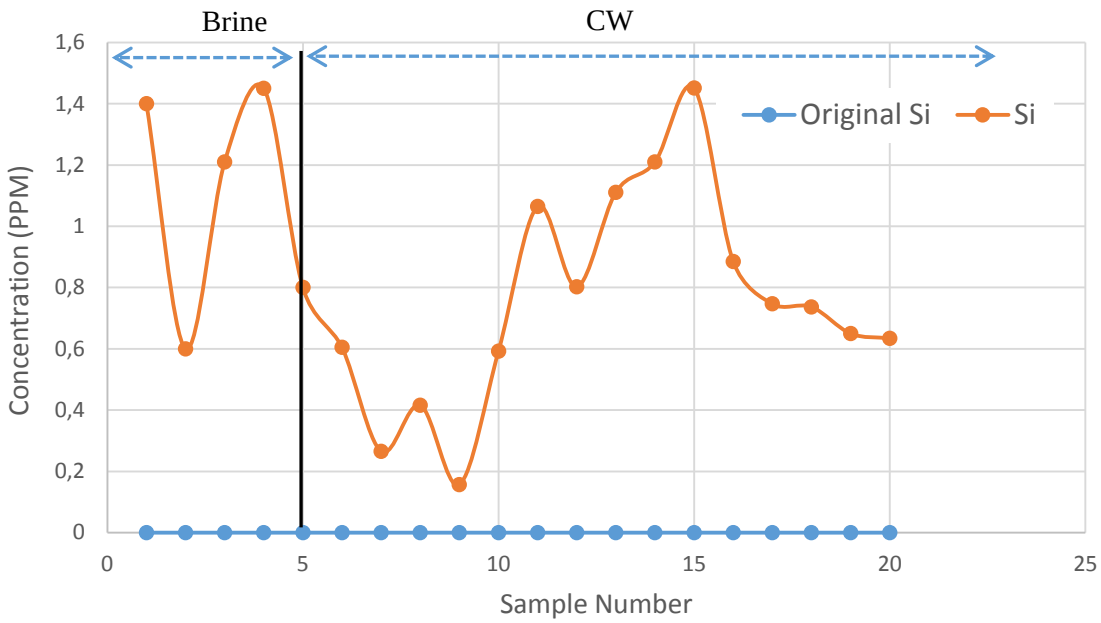

Figure 5-13 Changes in concentration of Silica in the effluent brine samples collected during spontaneous imbibition studies on aged sandstone rock

5.4 Conclusion

The potential of CW (CO_2-enriched water) for improving the rate of brine imbibition and therefore oil recovery in carbonate and sandstone rocks has been studied in this chapter. The following conclusions can be drawn from this chapter:

1. CW has a significant potential for increasing the amount of imbibed water and consequently oil recovery for both sandstone and carbonate rocks.
2. The initial wettability state of the rock has a strong effect on the oil recovery factor. No oil recovery by spontaneous brine imbibition was observed for aged (oil-wet) sandstone or aged (oil-wet) carbonate rocks.
3. The principal mechanisms of improving oil recovery by spontaneous CW imbibition are oil swelling, oil viscosity reduction, reduction of interfacial tension between brine and oil, mineral dissolution and wettability alteration toward more water-wet conditions.
4. Comparing the results of oil recovery in the aged and un-aged carbonate rocks reveals the high potential of CW for changing the wettability of the oil-wet system toward water-wet conditions which directly leads to improved imbibition and oil recovery.

5. Wettability alteration by CW in carbonate rock was stronger than sandstone rock which resulted in better imbibition and oil recovery in carbonate compared to sandstone rocks.

Chapter 6: Characterization of Fluids-Fluids Interactions Leading to EOR by Carbonated Water Injection

6.1 Introduction

As it was discussed in details in Chapter 1 (see Table 1-2), in all the previously published studies [6]–[27] either model oil or dead crude oil was used, which would not represent real reservoir conditions where the oil normally contain a significant amount of dissolved gases. In Chapters 2 and 4 of this study, through performing a series of high-pressure high-temperature micromodel as well as coreflood experiments, the author revealed the great importance of dissolved gas in oil on the performance of CWI. The reported results showed that CO_2 transfer from CW into the ‘’live’’ oil (oil with dissolved gases) trigger the formation and growth of a new gaseous phase. As time elapses and more CW comes in contact with live oil, the saturation of the new phase increases. Based on these findings, the formation and growth of the new gaseous phase would play a critical role on the efficiency of CWI to improve oil recovery. The observed formation and continuous growth of the new gaseous phase would boost the performance of CWI significantly and represents a game-changer for this EOR technique and a massive improvement in our understanding of the mechanisms of oil recovery by CWI at real reservoir conditions. Therefore, characterization of this new phase would have significant implications for identifying the suitable conditions at which CWI would displace the oil more efficiently.

To have a comprehensive analysis of the new phase and its characteristics and properties, here is this chapter, a series of high-pressure high-temperature fluid characterization tests were carried out in which multiple batches of CW were sequentially brought into contact with a specific volume of a ‘’live’’ oil in a PVT cell. After each contact, the resultant phases, i.e. aqueous/oil/gas, were analysed to track the CO_2 partitioning and the consequent changes in the properties and compositions of each phase.

Furthermore, in all previously reported studies [6]–[9], [13], [17]–[23] cores with a maximum length of 30 cm were used to examine CWI potential. CWI potential and CO_2-water front movements at such small length cannot be a good representative of

CWI behaviour in a reservoir at a considerable distance from the injection well. Also, displacement tests performed in core plugs can be influenced by heterogeneities which may control the propagation of carbonated water and hence CO_2 transfer. In this study, a 60 ft slim tube packed with 80-140 Ottawa sand was used to investigate the significance of the new phase formation on additional oil recovery by CWI in live crude oil systems. To the best of author's knowledge, this is the first time that the performance of CWI has been studied using a long porous medium, i.e. 60 ft, which would shed some lights on CO_2 and water frontal advancements.

To summarize, in this chapter, through a series of multiple-contact (PVT) tests linked to slim tube experiments, it has been aimed to comprehensively investigate;

(i) CW-oil phase behaviour
(ii) The characteristic of the new phase
(iii) Impact of gaseous new phase on oil recovery by CWI
(iv) CW displacement front propagation inside the reservoir as CW moving far from the injection well.

6.2 Experimental Setup and Procedure

6.2.1 PVT and Slim Tube Rigs

Figures 6-1 and 6-2 show the schematic of the PVT and slim tube set-ups, respectively. Both rigs can work at high pressure and high temperature and consist of the following components: a high-pressure PVT cell, a Hassler-type slim tube, pump, pressure transducers, backpressure regulator (BPR), separator, gasometer, and an in-line CO_2 analyser. The high-pressure PVT cell is equipped with a heating jacket that enables the author to perform the experiments at the desired temperature (100 °F). The slim tube rig is housed inside an oven at a constant temperature of 100 °F. While running an experiment, the fluids would pass through a backpressure regulator where the pressure would drop to atmospheric pressure and hence, any dissolved CO_2 will be liberated and measured. The separated liquid would then be collected in a graduated cylinder while the CO_2 will pass through CO_2 analyser and then gasometer.

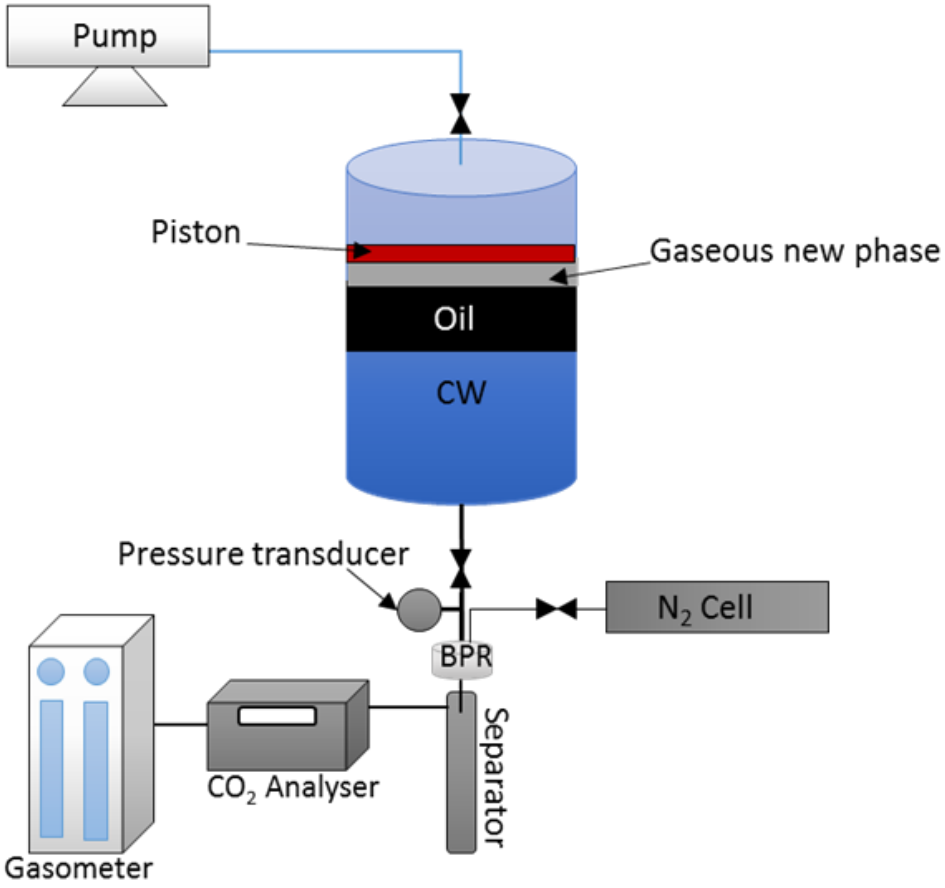

Figure 6-1 Schematic of PVT rig

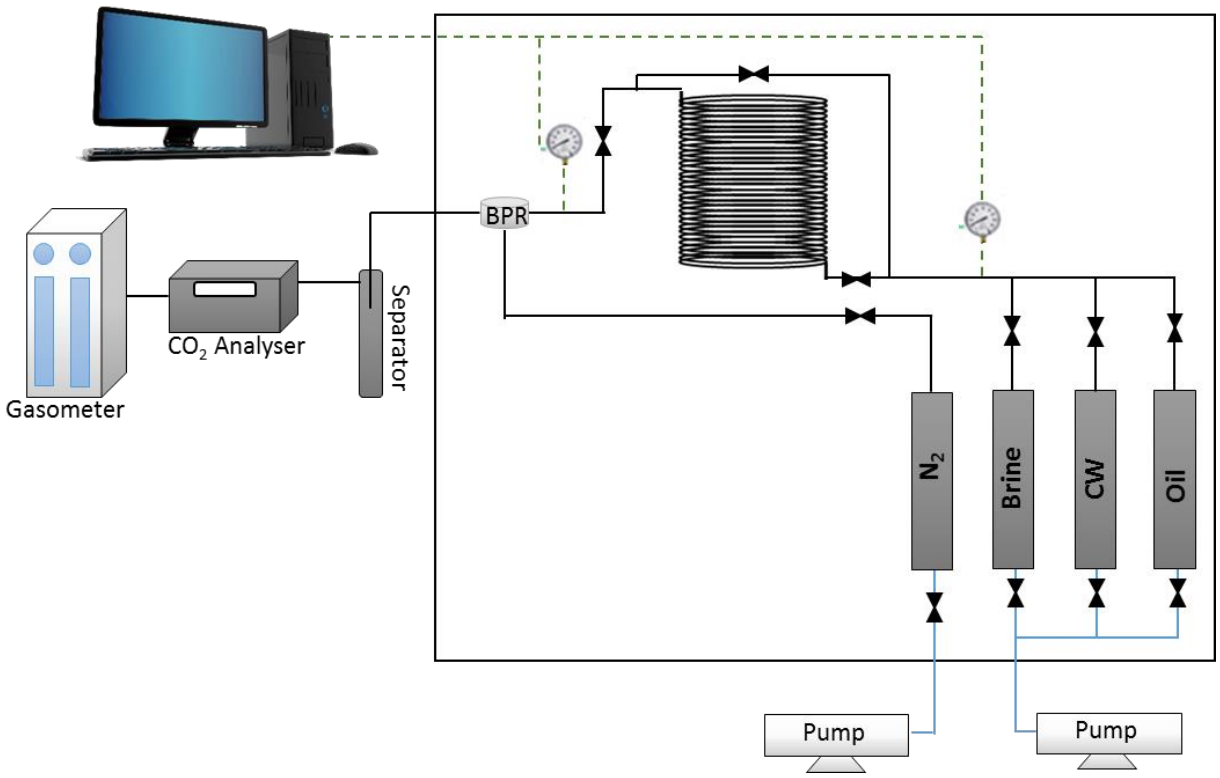

Figure 6-2 Schematic of slim tube rig

6.2.2 Fluids Properties

It should be noted that to have a consistency with the performed micromodel and coreflood experiment in Chapters 2 and 4, the same type of fluids were used under same experimental conditions. As a result, to prepare live oil used in the experiments, crude ‘’J’’ was mixed with CH_4 at pressure and temperature of 2500 psia and 100 °F. The API and density of this crude at dead condition are respectively 20.87° and 0.9247 gr/cm^3. The other properties of the crude are shown in Table 6-1. The carbon number distribution of crude J obtained by high-resolution gas chromatograph (HRGC) with flame ionization detector (FID) was reported in Figure 2-7. As can be seen from this figure, Crude J is mainly made of medium to heavy components.

Table 6-1 Crude J properties

crude ID	API	saturates (wt. %)	aromatics (wt. %)	resins (wt. %)	asphaltenes (wt. %)
Crude J	20.87	30.00	40.10	24.20	5.70

To prepare the CW (CO_2-enriched water), CO_2 was mixed with high salinity seawater at pressure and temperature of the experiments (2500 psi and 100 °F). The seawater sample had a salinity of 54,540 ppm. The brine composition is shown in Table 6-2. The viscosity of brine was 0.789 cp at test conditions.

Table 6-2 Sea brine components

ion	ppm
Na	16844
Ca	664
Mg	2279
SO_4^{-2}	3560
Cl	31107
HCO_3^{-1}	193

6.2.3 Methodology

6.2.3.1 PVT Experiments

To mimic the dynamic mass transfer taking place between crude oil and CW in a porous medium, a series of contact tests were performed between the crude oil and CW. In the first part, dead oil was brought in contact with CW and in the second part; live crude oil was put in contact with CW to study the mass transfer between the oil and CW.

For the live oil experiment, 400 cc of crude ‘’J’’ was mixed with CH_4 inside a rocking cell at pressure and temperature of 2500 psia and 100 °F until it became fully saturated with CH_4. Next, the CH_4 gas cap was removed from the cell, and the GOR of the live oil was measured, which was 50 scc CH_4/scc oil.

Having prepared the live oil, CW (CO_2-enriched water) was prepared at same experimental conditions. The GOR of CW was 26 scc CO_2/scc brine. Next, CW was transferred into the mixing cell. During transferring care was taken to maintain the pressure always above the saturation pressure which was 2500 psia. Having transferred a specific amount of CW into the mixing cell, the cell was gently rocked until equilibrium was reached. During the whole time that the test was in progress, the water side of mixing cell (bottom of mixing cell), was connected to a pump to keep the

pressure inside the mixing cell at a constant value of 2510 psia (10 psia higher than mixing pressure). One good indication that equilibrium between the oil and CW in the cell had been achieved was the pressure of the pump connected to the mixing cell. As long as the oil and CW continue mass exchange, oil swelling would continue to happen, and the pump would continue retraction to keep the pressure constant. When finally equilibrium is achieved, there would be no further mass transfer and the pump would not retract anymore.

Having reached equilibrium between CW and live oil, all of the transferred CW, as well as 10 cc of the oil, was taken out of the cell, and their compositions were analysed.

Having finished the first contact, a new batch of CW was prepared and transferred into the mixing cell where it came in contact with the oil remaining from the previous contact. The same procedure was followed for the second contact and again after reaching equilibrium, CW as well as 10 cc of the oil were removed from the cell and were analysed. This procedure was continued for several contacts until the oil inside the cell was almost fully saturated with CO_2. In each contact, the composition of fluids that were taken out of the cell was analysed in order to trace the transfer and distribution of CO_2 between different fluid phases. A total of 16 contacts were performed. The multiple-contact test was designed to replicate the dynamic interactions between the oil in a reservoir rock, and the flowing carbonated water in which the oil would be contacted by fresh CW leading to further CO_2 transfer. Table 6-3 shows the ratio of the volume of CW to live oil in each contact.

Table 6-3 Ratio of the volume of CW to live oil in each contact

contact	ratio (cc CW/cc oil)	contact	ratio (cc CW/cc oil)
1	1	9	3
2	1	10	2.75
3	1	11	3.64
4	1	12	4.44
5	1	13	5.45
6	1	14	6.7
7	2	15	8.25
8	2.5	16	12.5

For the dead oil system, similarly to the live oil tests, first a specific volume of dead oil (100 cc) was transferred into the mixing cell under identical experimental conditions (2500 psia and 100 °F). Next, 350 cc CW was prepared and transferred into the mixing cell. Having reached equilibrium, the resultant phases were removed from the cell and analysed to determine the partition coefficient and track CO_2 mass transfer.

6.2.3.2 Slim Tube Experiments

To investigate the performance of CWI at a considerable distance from the injection point and to study the impact of the influence of the new phase formation on CWI performance, two slim tube experiments were performed. The unique characteristic of slim tube setup is the very long length of it which allows evaluating whether the positive effects of CWI observed in our conventional coreflood experiments could still be seen a long distance away from the injection point. The slim tube properties are shown in Table 6-4. In both experiments, first, the slim tube was fully saturated with oil, then live oil was injected to displace the dead oil. Having completely displaced the dead oil by live oil, without aging the slime tube, the experiments were performed. In the first test, a conventional waterflood was carried out. To minimise the CH_4 transfer between CH_4-saturated oil (live oil) and brine, the brine was pre-equilibrated with CH_4 gas at experimental conditions. The CH_4 content of CH_4-saturated brine was 3 scc CH_4/scc brine. In the second experiment, a secondary CWI was performed. The rate of injection in both experiments was 1 cc/hr. During the experiments, the differential pressure across the slim tube, oil, CO_2, and gas productions were recorded.

Table 6-4 Dimensions and properties of the slim tube

length (ft)	inner diameter (in)	packing material	K (D)	pore volume (cc)	porosity %
60	1/8	80-140 mesh Ottawa sand Coil	6	44	30

6.3 Experimental Results and Discussion

6.3.1 PVT Experiments

6.3.1.1 Dead Oil-CW Interactions

100 cc dead crude oil was brought in contact with 350 cc CW at pressure and temperature of 2500 psia and 100 °F. The PVT cell was gently rocked to facilitate the process of reaching equilibrium. The total expansion of the fluids as CW came in contact with dead oil, was detected from the pump. CO_2 partitioning between CW and oil phase happened which in turn led to oil swelling. Having reached equilibrium (no more expansion), samples of the contacted CW and oil were analysed. Due to CO_2 mass transfer from CW into the dead oil, the GOR of the CW was dropped from 26 to 13 scc CO_2/scc brine, on the other hand, the GOR of the oil increased from zero to 37.38 scc CO_2/scc oil. This would result in a partitioning coefficient value of 2.85. However, it should be reiterated that the behaviour observed for dead oil systems cannot represent realistic reservoir conditions where crude oil always has some dissolved gas.

6.3.1.2 Live Oil-CW Interactions

Live oil was sequentially brought into contact with CW until it became almost fully saturated with CO_2. In terms of changes that happened to the contacted carbonated water, Figure 6-3 shows the variation in the CO_2 and CH_4 content of CW in each contact. As can be seen, as carbonated water came in contact with the live oil, partitioning of CO_2 and CH_4 between live oil and CW happened which led to the transfer of CO_2 from CW to the oil and also the transfer of CH_4 from live oil into the CW (albeit to a much lesser extent). A sharp drop in the CO_2 content of CW was observed at the first contact with the live oil which indicates significant CO_2 transfer from CW into the oil. Even after 16 contacts, which would represent infinite cell volume contacted, the results of the experiment demonstrates clearly that carbonated water would lose some of its CO_2 content gradually, which implies a steady transferring of CO_2 to the hydrocarbon phase (oil + gas) and hence a steady oil expansion and oil recovery. Therefore, in porous media flooded by CW, oil ganglia would expand continuously leading to high overall swelling. On the other hand, based on Figure 6-3, we have had CH_4 mass transfer from live oil into the CW. However, this CH_4 mass transfer to CW was much less than the CO_2 transfer to oil, and the reason is the lower solubility of CH_4 in brine compared to CO_2. The maximum solubility of CH_4 in our

brine at the experimental conditions is 3 scc CH_4/scc brine. In this experiment, the maximum value of 2.64 scc CH_4/scc brine was reached and after contact number 13 the CH_4 content of brine was negligible (almost zero). From this point onward, only CO_2 was transferred from CW into the oil. Figure 6-4 shows the changes in the GOR of CW during the whole time of the experiment. As can be seen from this figure, the GOR of CW has a sharp drop in the first contact and then starts to increase, however, it did not reach to its original value even by the last contact.

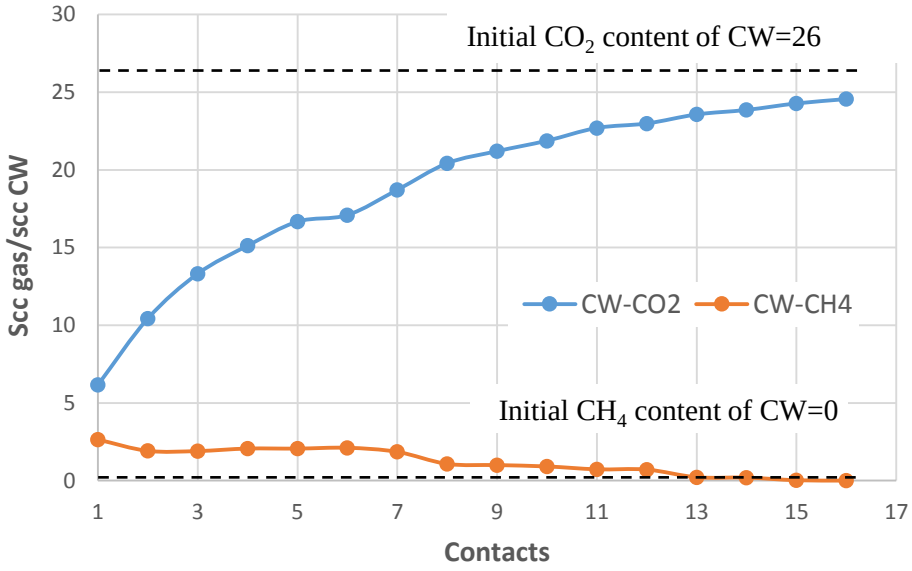

Figure 6-3 CO_2 and CH_4 contents of equilibrated CW in each contact. The dashed lines represent the original (initial) conditions of the fluid before it comes in contact with any other fluid. The sharp drop in the CO_2 content of CW indicates strong CO_2 partitioning

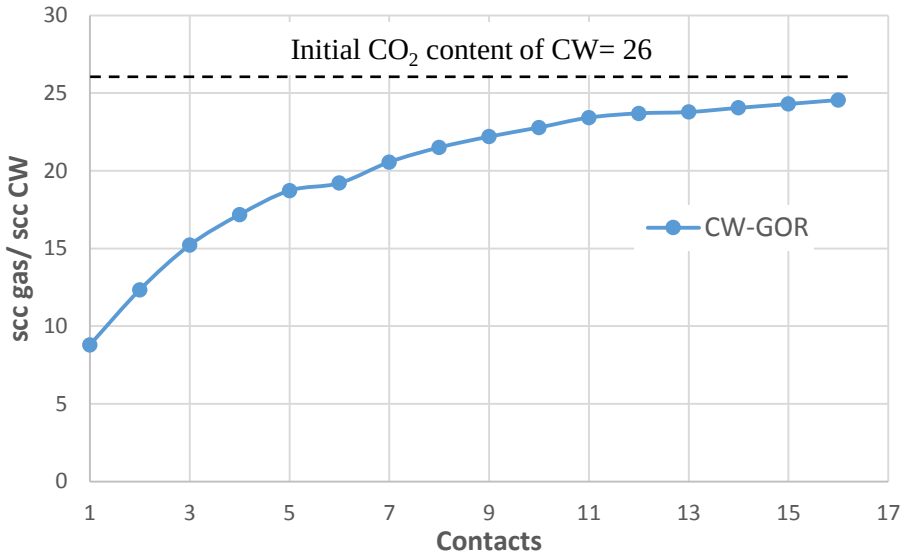

Figure 6-4 GOR of equilibrated CW in each contact. The strong decline in the GOR of CW indicates strong CO_2 partitioning between CW and live oil

To have a better understanding of CO_2 and CH_4 mass transfer between live oil and CW, the GOR, CO_2 and CH_4 contents of equilibrated oil was measured in each contact. Figure 6-5 shows the GOR of live oil in each contact. As can be seen, the GOR of the live oil increased in the progressive contacts with CW due to the increasingly higher concentration of CO_2 dissolved in the oil. In the latter contacts, the GOR of oil reached to around 133 scc CO_2/ scc oil. This value is around 2.6 times higher than the original GOR (based on dissolved CH_4) of the live oil.

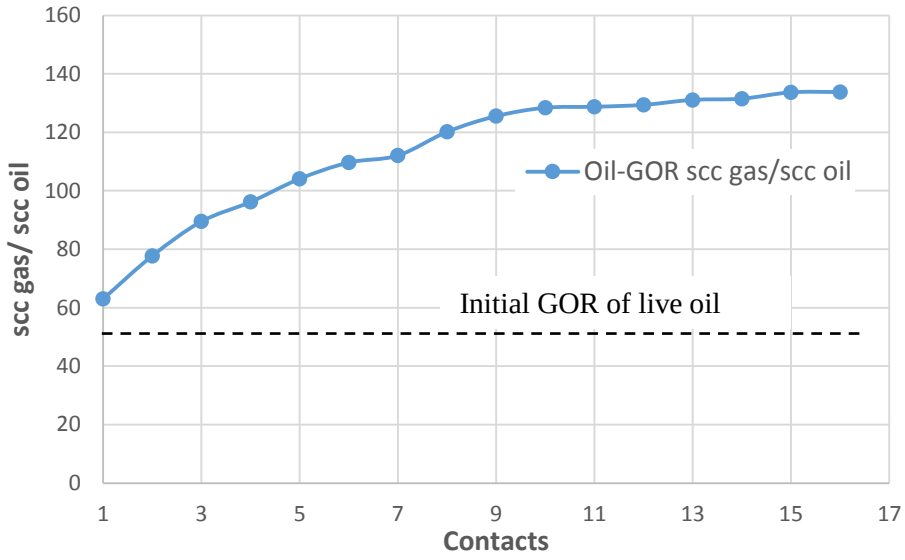

Figure 6-5 GOR of the equilibrated liv oil in each contact. CO_2 exchange between CW and live oil led to an increase in the GOR of live oil by around 2.6 times

The original CH_4 content (GOR) of live oil was 50 scc CH_4/scc oil, and its CO_2 content was zero. When live oil was brought into contact with CW since the solubility of CO_2 in oil is higher than that in brine, CO_2 went from CW into the oil; this mass transfer can be seen in Figure 6-6. Based on this figure, in addition to continuous CO_2 transfer, CH_4 loss from the live oil was also observed. The CH_4 content of the live oil had a decreasing trend approaching zero, which indicates a unique behaviour of CO_2 in expelling lean gases. One source of methane loss from oil was the gain of CH_4 by the carbonated water (as highlighted in Figure 6-3) but, the material balance cannot explain this loss and gain and hence there should be another source of methane transfer, which is the formation of the new phase.

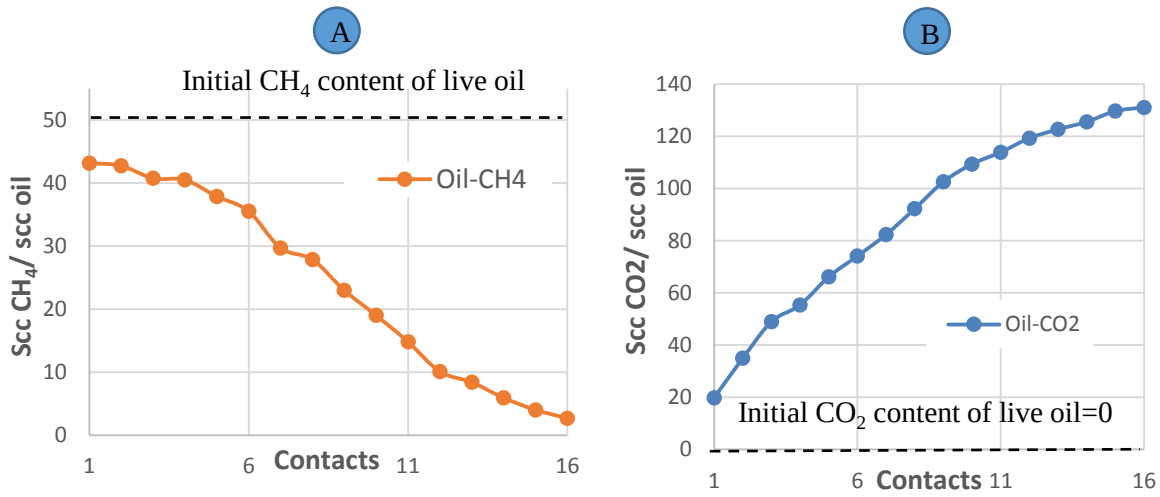

Figure 6-6 CH_4 and CO_2 contents of the gas separated from equilibrated live oil in each contact. CO_2 exchange between CW and live oil led to decrease in the CH_4 content of live oil and increase in its CO_2 content

The same as the dead oil test, in the live oil test, the PVT cell was connected to a pump to keep the pressure of the cell constant. As CW was brought in contact with the live oil in the cell for the first time (contact =1), the pump immediately started to retract. Although the ratio of CW to oil in the dead oil system was 3.5 times higher than the one in the live oil system, the volume of pump retraction in live oil system was four times higher than the pump retraction volume that was observed for the dead oil system. Interestingly, the analysis of the results of both live and dead oil tests after the first contact showed almost the same oil swelling factor, which indicates the same expansion for live and dead oleic phase due to CO_2 dissolution. This reveals that another phenomenon had been happening for the live oil system when it came in contact with CW that led to a much stronger pump retraction. It is believed that this sudden pump retraction is due to the formation of the new gaseous phase when CW contacts live oil, which would be in line with the previous micromodel (visual) results reported in Chapter 2 (Section 2.3.2). Therefore, a gaseous phase was formed in the PVT cell and accumulated at the top of the oil. To verify this, the new gaseous phase accumulated at the top of the cell was completely taken out and separated at two different points during the multiple-contact experiment. The first sample was taken at an early stage of the experiment (after 3rd contact) and the second sample was taken after the last contact. The gaseous phase was analysed by using high-resolution gas chromatograph, which reveals that the new phase is a multi-component mixture of hydrocarbons starting from CH_4 and CO_2 at early stages and becoming richer with CO_2 towards the next contacts.

Table 6-5 shows the composition of the new gaseous phase at two different stages of the experiment. Evidently, the gaseous new phase is mainly composed of methane in early stages, and high concentration of CO_2 was observed in the latter stages. Therefore, the presence of lean gases in the oil is crucial as the triggering factor but, the growth of the new phase mainly occurs due to CO_2 transfer into the gaseous new phase.

Table 6-5 Gas composition results of new phase

component	first sample mole%	second sample mole%
Methane	63.59	6.561
CO_2	36.333	93.277
Ethane	0.00035	0
Propane	0.00384	0
i-Butane	0.00369	0.002
n-Butane	0.00797	0.008
i-Pentane	0.06185	0
Pentane	0	0.147
Hexane	0	0.001
Heptane	0	0.004

The amount of produced gaseous phase after 3rd contact was 15.1 cc gas and from 3rd to the end of the experiment was 46.396 cc gas at reservoir conditions. The total amount of produced new gaseous phase during this test was around 61.496 cc gas at reservoir conditions which is a significant value. The formation volume factor (Bg) of third gaseous phase was also measured, and it was 0.0031 cc gas/scc gas for the first sample and 0.0026 cc gas/scc gas for the second sample. Based on the definition of Bg, these values confirm that at later times the gaseous phase became richer with CO_2 which was also confirmed by the gas composition measurement results.

It was identified that the presence of CO_2 in the new gaseous phase led to a slight extraction of the intermediate components of the oil and gradually the new gaseous phase became richer in composition. Through the process of separating the second sample of the new phase from the PVT cell, around 2.8 scc of condensate was produced

along with the gas. The condensate had a light colour. Figure 6-7 shows the carbon number distribution of the condensate obtained by high-resolution gas chromatograph with flame ionization detector. The condensate is made of light to intermediate components of the oil between C_7 to C_{23}.

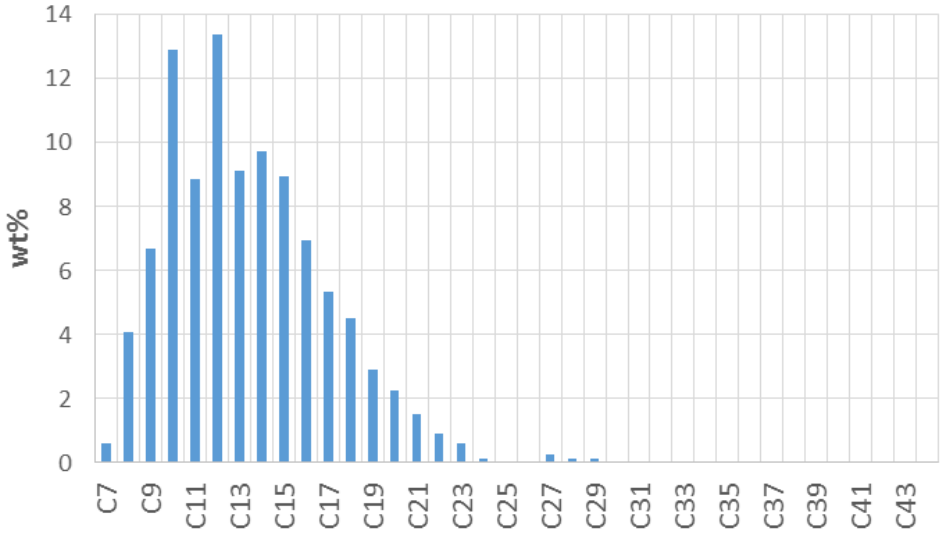

Figure 6-7 Composition of the condensate. Presence of CO_2 in the new gaseous phase led to an insignificant extraction of the light components of oil

The condensate was observed only during the separation of the second gaseous sample, not the first one. Based on this observation, as the new phase gets richer with CO_2, CO_2 can extract some light components of the oil. It should be noted that contrary to the very fast formation of new gaseous phase, the formation of condensate happened very late and only after many cell volumes of CW came in contact with the live oil. Furthermore, its volume is very small compared to the volume of new gaseous phase that was observed during this study.

6.3.1.3 New Phase Characteristics

To comprehensively grasp the characterization of the new gaseous phase and how it evolves as CW comes in contact with live oil, material balance calculations were performed over the experimental data. The CO_2 and CH_4 contents of live oil (Figure 6-6) and CW (Figure 6-3) in each contact was used to carry out the material balance and the difference between CO_2 moles in the live oil and CW would be considered as the composition of the new phase. As a validating measure, the material balance

calculations should honour the measured composition of gaseous new phase as illustrated in Table 6-5. Table 6-6 compares the predicted values obtained by the material balance with the experimentally measured values, which exhibits an acceptable degree of agreement. Therefore, having validated the material balance calculations, the compositional trends of two nominal components (CH_4 and CO_2) in new phase can be estimated.

Table 6-6 Predicted and actual values of composition of the new gaseous phase

	first sample mole%	second sample mole%
CH_4 measured value	63.59	6.56
CH_4 predicted value	63.2	8.54
CO_2 measured value	36.33	93.28
CO_2 predicted value	36.86	91.45

Figure 6-8 depicts the compositions of new gaseous phase predicted by the material balance method versus cell volume of CW that was brought in contact with live oil inside the PVT cell. CO_2 dissolution into the live oil, at early stages, could liberate the CH_4 of the live oil, which triggered the formation of the new phase, which brings about a system under liquid-liquid-vapour equilibria (two immiscible liquid phases and a gas phase). The presence of CH_4 in the gaseous new phase causes the CO_2 transfer from oil phase into the gaseous new phase. As CO_2 comes into the new phase, the potential of gaseous phase for vaporising the carbon dioxide and some light components of the oil from the oil phase would become stronger. As a result, with time, and as the oil phase became richer with CO_2, the gaseous new phase would be enriched in CO_2. Transfer of CO_2 from oleic phase into the new phase would create a CO_2-enriched gas phase with a tendency towards extracting intermediate components of oil, which was observed in the form of condensate phase (very light brown colour) rich in intermediate compounds (Figure 6-7). However, it should be pointed out that the extraction of the intermediate compounds was not an intense mass transfer (like a plain CO_2 injection) that can cause a significant degree of compositional changes to the oil in the cell. In next section, the properties of the contacted oil are measured to examine the extent of compositional changes happened to the oil.

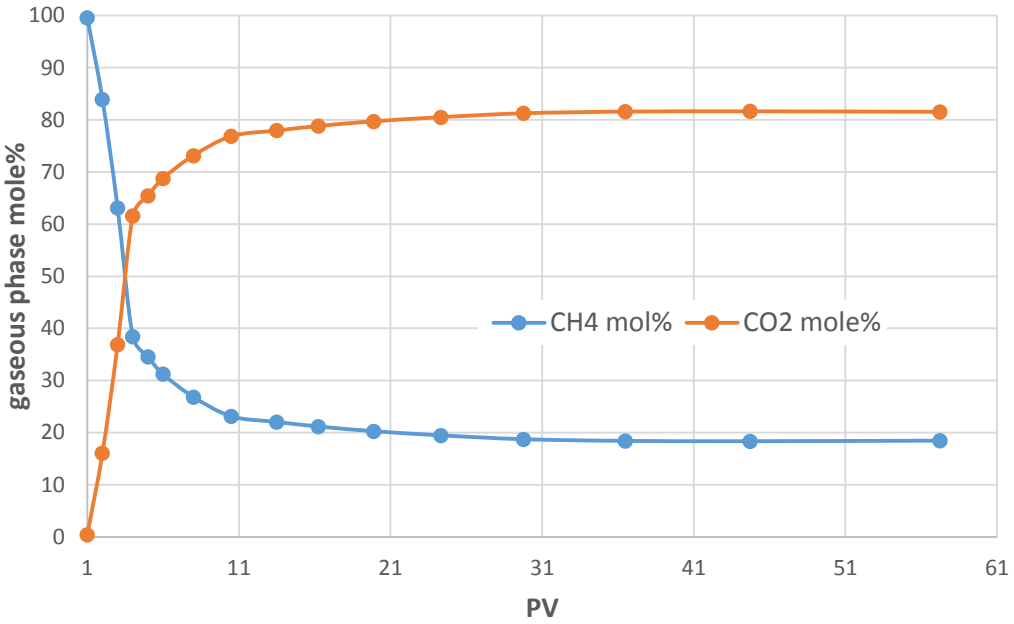

Figure 6-8 Composition of the new gaseous phase versus pore volumes of CW that brought in contact with live oil. The gaseous phase is mainly composed of CH_4 at the first contact and it became richer with CO_2 in subsequent contacts

6.3.1.4 Oil Density and Viscosity

Due to the formation of the new phase and the associated liquid-liquid-vapour equilibria conditions, the compositional effects of carbonated water injection in live oil systems is substantially complex, however, this would not necessarily lead to high compositional "changes" in the oil. On the other hand, in bulk CO_2 injections (conventional CO_2 flood), significant compositional changes take place between the injection carbon dioxide and the oil. This often includes intense extraction of the intermediate components of the oil, which would have an adverse effect on oil recovery due to downgrading the oil to a heavier hydrocarbon. Therefore, to study the significance of changes in the oil quality due to the formation of the new gaseous phase and CO_2 mass transfer, the densities and viscosities of the oil samples (after separating from its dissolved gas) that had been taken in each contact were measured. Figures 6-9 and 6-10 show the changes in the density and viscosity of the oil in each contact as the main properties that could affect the oil flow. The dashed lines show the original values before oil came in contact with any fluid. The original density and viscosity of dead oil were 0.9254 gr/cm^3 and 83 cp, respectively. Based on Figures 6-9 and 6-10, the density and viscosity values were fairly constant around their original value. This demonstrates

that formation of the new phase and the associated mass transfer did not adversely affect the oil quality. The red points in these figures represented the density and viscosity of crude J when it was pre-equilibrated with CO_2 gas under same experimental conditions (2500 psia and 100 °F). This condition represents the last contact (contact= 16) in the multiple-contact experiment when the oil was almost fully saturated with CO_2. However, comparing the density and viscosity of the oil, when it was pre-equilibrated with CO_2 (red point), with the density and viscosity of the oil at contact 16 reveals that formation of the gaseous new phase has less effect on the oil quality compared to the CO_2. It has been well documented in the literature that supercritical CO_2 can extract the intermediate components of the oil [92]–[96] which in turn leads to increase in oil density and viscosity.

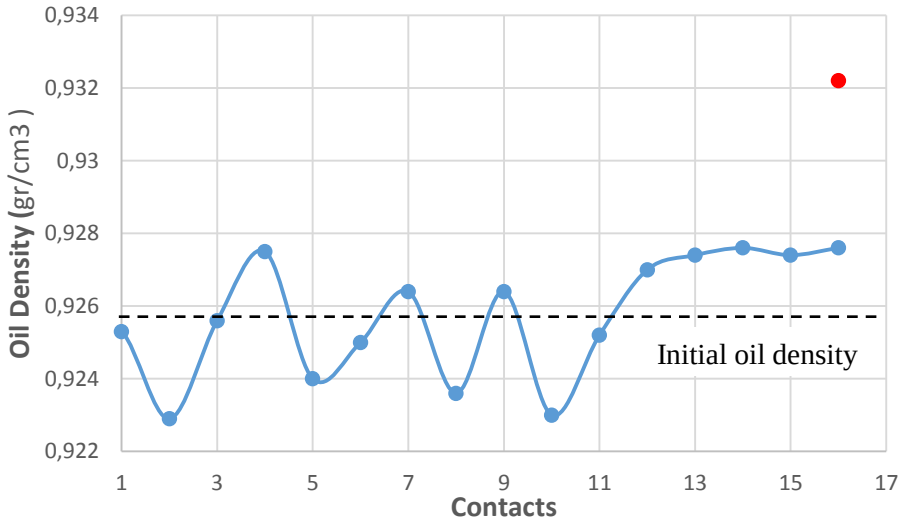

Figure 6-9 Blue curve presents the changes in the density of dead oil taken out in each contact. Red point represents the density of crude J when it was pre-equilibrated with CO2 gas under same experimental conditions.

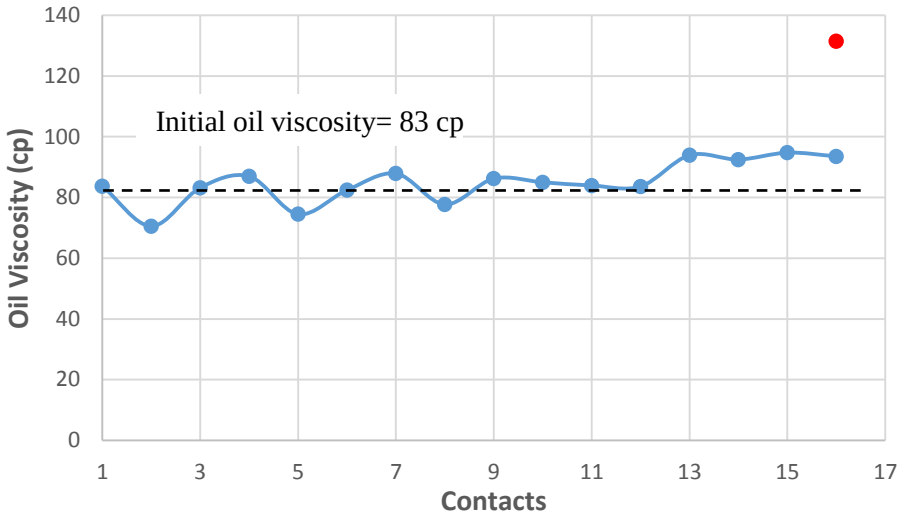

Figure 6-10 Blue curve shows the changes in the viscosity of dead oil taken out in each contact. Red point represents the viscosity of crude J when it was pre-equilibrated with CO2 gas under same experimental conditions.

6.3.1.5 Oil Swelling Factor and CO_2 Partitioning

CO_2 exchange between CW and oil phase causes oil swelling which is regarded as one of the oil recovery mechanisms of CWI. To quantify the effect of CW on oil swelling factor (SF, ratio of oil volumes at elevated conditions to flashed oil), the SF was measured in live oil tests. In the case of the live oil system, swelling factor of oil in each contact was measured and presented in Figure 6-11. This figure shows that as CO_2 from CW transfers into the oil, the swelling factor of oil increases (the original value is 1.04) and after 8 contacts converges to a value of around 1.2 (15.4% increase in swelling factor). This result is of great importance since it would directly affect the recovery factor calculation during CWI.

Figure 6-12 shows the swelling factor of oil versus CO_2 content of oil (scc CO_2/ scc oil). Based on this figure, as the CO_2 content of oil increases, the swelling factor increases too, however, from the CO_2 content of 86 scc CO_2/ scc oil onward the swelling factor is almost constant around the value of 1.2.

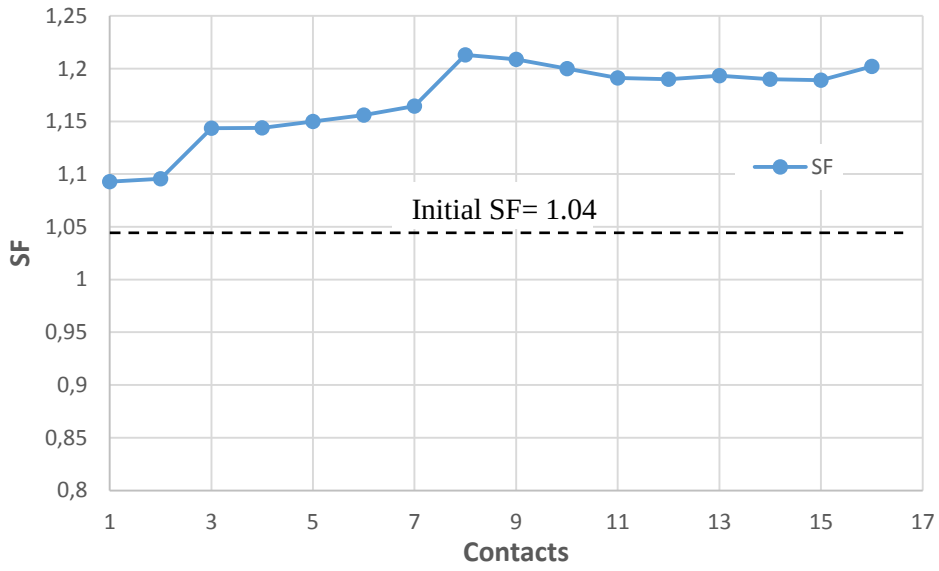

Figure 6-11 Swelling factor (SF) of the oil in each contact

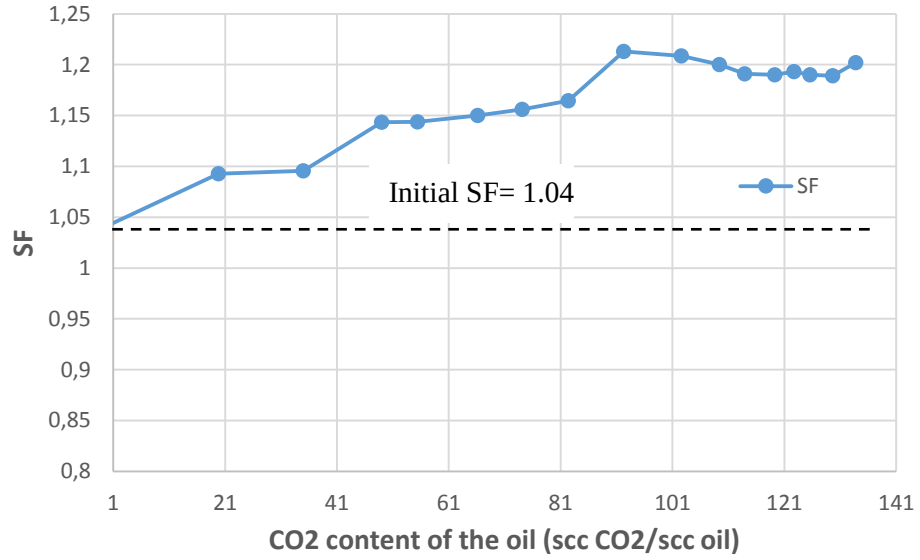

Figure 6-12 Swelling factor (SF) of the oil versus the CO_2 content of oil. The SF increases as the CO_2 content of oil increases until the CO_2 content of oil reaches to around 90 scc CO_2/scc oil. From that point onward the swelling factor is almost constant

As CW comes in contact with oil, CO_2 partitioning between CW and oil takes place which leads to oil swelling. Partition coefficient is defined as the ratio of equilibrium CO_2 concentration in oil to that in water.

$$C_{CO2(oil)} = (K_{CO2}) * C_{CO2(CW)} \quad \text{Eq. 1}$$

where K_{CO2} is the CO_2 partition coefficient of binary CW and oil system. For the case of dead oil, in this work, CO_2 partition coefficient was 2.85. However, CO_2 transfer for the case of live oil leads to nucleation and growth of a new gaseous phase inside the oil. Therefore, a three-phase liquid-liquid-gas equilibrium would form whereby a portion of the CO_2 transferred from CW sub-partitions to the new phase. As a result, contrary to dead oil systems, where CO_2 only partitioned between CW and oil phase, for live oil systems, CO_2 partitioning would take place between CW and the oil plus the gas phase. This will result in stronger partitioning of CO_2 and therefore stronger oil swelling for live oil system. Therefore, the above conventional definition (Eq. 1) of partition coefficient could not be of use for live oil system. Therefore, another definition should be put forward (pseudo-partition coefficient) which is the ratio of equilibrium CO_2 concentration in the hydrocarbon (oil +gas) phases to that in the water phase.

$$C_{CO2(oil+\text{gas})} = (K^{ps}{}_{CO2}) * C_{CO2(CW)} \qquad \text{Eq. 2}$$

Figure 6-13 shows the changes in the value of pseudo-partition coefficient at different contacts for the live oil test. The value of CO_2 pseudo-partition coefficient was measured to be around 3.3 in the first three contacts and in the subsequent contacts, it exhibited an increasing trend, which plateaued to a value of around 5.4. This indicates as more CW comes in contact with the live oil, the saturation of the new phase and its CO_2 content increases, which in turn leads to stronger CO_2 partitioning. Based on these results, CO_2 partitioning for the case of live oil system would be stronger than dead oil system and thereby, it is expected that CWI would be more effective for the case of live oil system compared to the dead oil system. Also, contrary to a constant partition coefficient for dead oil and water systems, the pseudo-partition coefficient has demonstrated a dynamic characteristic, in which its value would increase in progressive contacts.

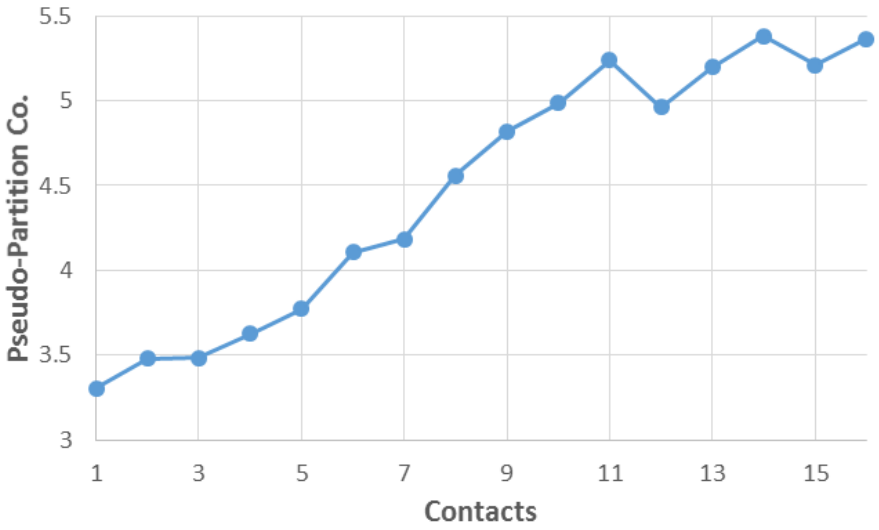

Figure 6-13 CO_2 pseudo-partition coefficient in each contact. The increase in the value of CO_2 pseudo-partition coefficient indicates the growth in CO_2 content of the new phase

6.3.2 Slim Tube Experiments

A series of two slim tube experiments were designed and performed at the conditions of the multiple-contact experiment, which enable the author linking the findings of the multiple-contact test to improved oil recovery by CWI in a porous medium. As a long homogeneous porous medium, the unique advantage of slim tube apparatus is its one-dimensional characteristic that allows continuous dynamic interactions of injected CW and the live oil to take place. In all previously reported studies [6]–[9], [13], [17]–[23], either small cores or sand packs with the maximum length of 30 cm were used. CWI behaviour and its front propagation at such a short length cannot be representative of its behaviour at a significant distance from the injection well as it flows inside the main body of oil reservoirs. As CW flows inside the reservoir and comes in contact with the reservoir oil, it would deliver its CO_2 to the oil and hence there would be a possibility of CW becoming depleted. An in-depth understanding of the behaviour of CW in a longer porous medium is of great importance to elaborate on CO_2 dissipation and improved oil recovery. In these slime-tube experiments, to exclude the wettability effects on oil displacement, no initial water saturation was established and no aging period was considered for wettability restoration in the slim tube.

To study the performance of CWI in this very long porous medium, a series of two experiments were performed; one plain waterflood and the other being a carbonated water injection, both in secondary mode.

Figure 6-14 depicts the oil recovery during both experiments, i.e. plain water injection and the carbonated water injection. Compared to plain waterflood, secondary CWI led to significant additional oil recovery of 24% of the original oil in place (OOIP). The additional oil recovery by CWI takes place at earlier pore volume of injection that highlights better oil displacement by CWI compared to waterflood. It is well known that CO_2 dissolution in oil can lead to oil viscosity reduction. However, at experimental conditions used in this study, the CO_2 solubility in the brine is 26 scc CO_2/scc brine. Therefore, with such relatively small quantity of CO_2 in brine, the oil viscosity reduction by CW, would not happen during early pore volumes of injection and it would only be expected to happen after an extended injection of CW. Furthermore, the viscosity of live oil used in this study is around 14 cp and when it becomes fully saturated with CO_2, its viscosity reduces to around 5.4 cp at test conditions. For such a relatively low initial oil viscosity, the difference in viscosities is not very high. As a result, for the period of CWI in this study (5 PVI), viscosity reduction by CW cannot be responsible for the observed additional oil recovery. As it was shown in micromodel studies reported in Chapter 2 (Figure 2-24), the total increase in the volume of the live crude oil J (overall oil swelling) was around 35% with greater than 60% of that due to the formation of the new phase. As can be seen from Figure 2-24, shortly after the start of CWI, there is the (normal) oil swelling which stops relatively quickly but the increase in the oil volume due to the formation of the new phase continues. This confirms that the main oil recovery mechanism in here was formation and growth of the new gaseous phase that led to 24% additional oil recovery.

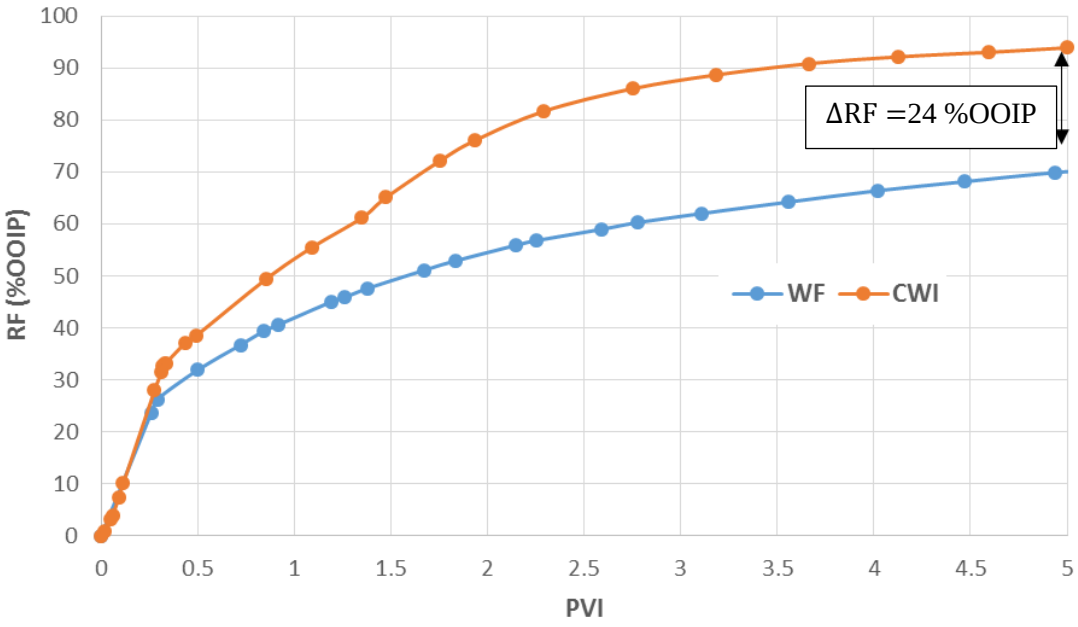

Figure 6-14 Comparison of oil recovery obtained by CWI with the one from conventional waterflood

Figure 6-15 compares the differential pressure (dP) behaviour across the slim tube during both experiments. As can be seen, from the first pore volume of CWI onward the differential pressure across the slim tube is almost equal to that obtained from the conventional waterflood test. This indicates that the relative permeabilities of water at the end of both experiments are the same; therefore, the water saturations, at the end of both experiments, are almost the same. Consequently, the residual total hydrocarbon saturations, at the end of both experiments, are expected to be similar. However, based on the material balance results, the residual oil saturation at the end of CWI is 24% smaller than that obtained at the end of the conventional waterflood experiment. This is in line with the visual, i.e. micromodel experiments performed in Chapter 2 (section 2.3.2), and PVT (multiple-contact) experiments and reveals that for the case of CWI, as CW is injected and starts contacting the live oil in the porous medium, a new phase (gaseous new phase) evolves inside the porous medium that creates a favourable three phase flow region with less residual oil saturation. In other words, when the tail of the dP curve stayed identical in both experiments in the absence of wettability effects (wettability was the same in both experiments), it can be inferred that same water saturation existed in both experiments. Therefore, the total ultimate hydrocarbon saturation was similar in both waterflood and carbonated waterflood but, as significant

additional oil recovery was observed in CWI (significantly lower residual oil saturation), the produced oil must have been replaced by the new phase formed as a result of CWI. From Figures 6-14 and 6-15, it can be concluded that the saturation of the new phase at the end of CWI was around 24% of the OOIP. In here, the formation and growth of the new phase can lead to improved oil recovery by; (i) reconnection of the trapped oil and oil displacement, (ii) creating a favourable three phase region which results in lower residual oil saturation.

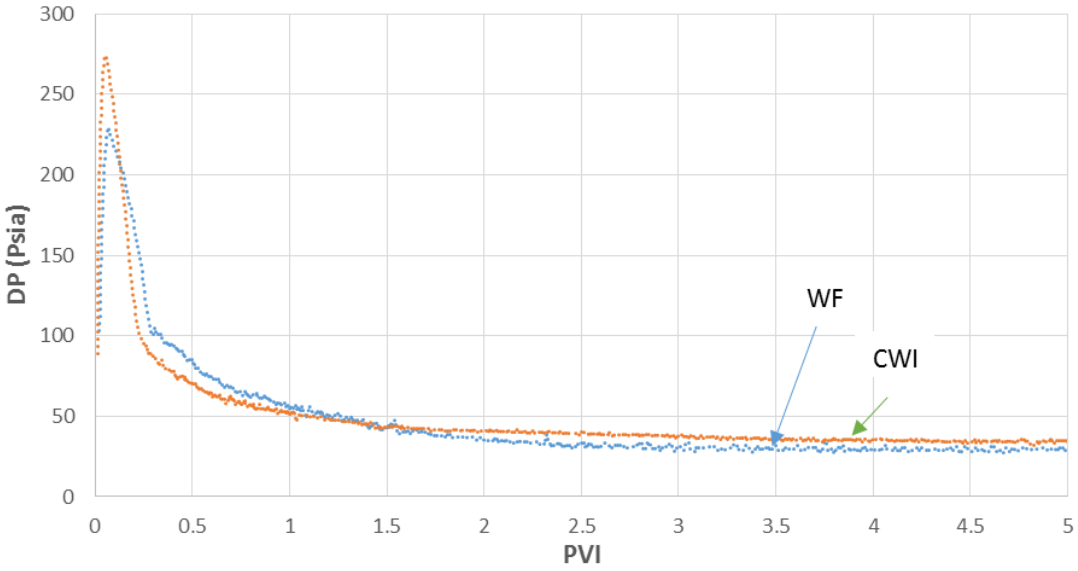

Figure 6-15 Differential pressure behaviour during both conventional waterflooding (blue curve) and secondary CWI (orange curve). Although the residual oil saturation at the end of CWI was 24% lower than the one in WF, the differential pressures were the same

6.3.3 Displacement Front Propagation

The other objective of performing the slim tube tests was to study the CO_2 and waterfront movements during CWI at longer lengths (than the normal corefloods) and better understand the behaviour of the CO_2 dissolved in CW and its interactions with the oil inside the reservoir away from the wellbore. The brine and CO_2 breakthrough times were carefully recorded and compared during secondary CWI. Figure 6-16 depicts the CO_2 rate (scc CO_2/scc effluent fluids) and water cut during the secondary CWI. The water breakthrough took place at around 0.31 PVI; however, the CO_2 breakthrough happened at around 0.6 PVI. The CO_2 production rate was almost negligible up to 1.5 PVI and after that it started to increase. These results reveal that at longer lengths as

CW moves away from the injection well, due to continuous CO_2 transfer from the CW front to the oil, the waterfront would be depleted from CO_2. This behaviour occurs due to the stronger CO_2 solubility in crude oil than in water, which caused significant CO_2 transfer to the oil phase and the additional oil recovery of 24% of the original oil in place.

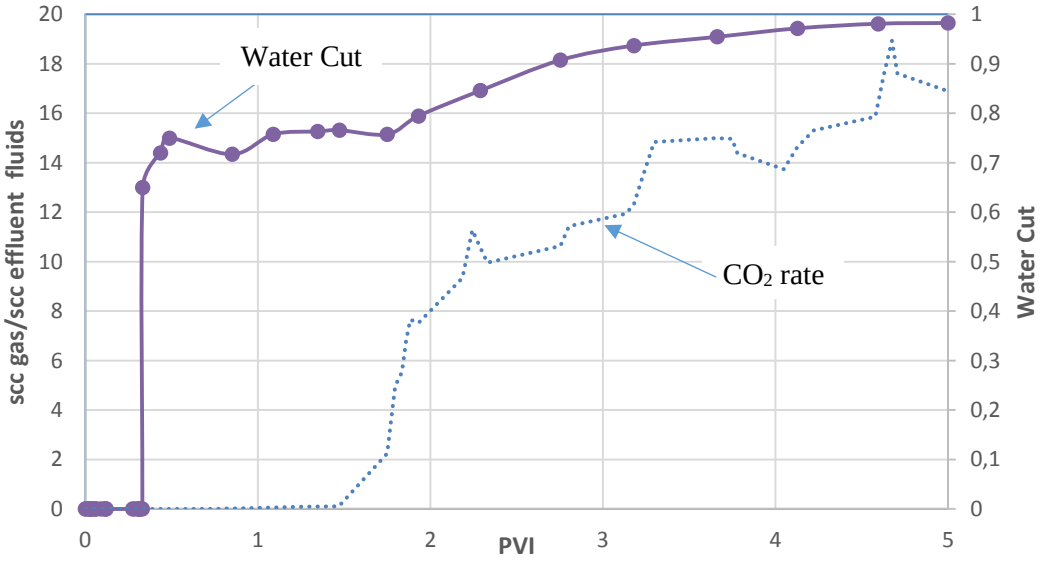

Figure 6-16 Breakthrough times of water and CO_2 during secondary CWI. The water breakthrough happened at earlier times compared to CO_2 breakthrough

6.3.4 Discussion

Based on the series of integrated PVT and slim tube experiments, immediately after CW comes in contact with live oil, CO_2 moves from CW into the oil pushing the dissolved gas out of solution to form a gaseous new phase. The formation and growth of this new phase would be a dominant mechanism behind the efficiency of a carbonated water injection scheme for improving oil recovery. The competition between various oil components to dissolve CO_2 and methane would be the factor controlling the extent of this phenomenon, which can be linked to different binary interaction coefficients of methane and CO_2 with hydrocarbon compounds.

In the multiple-contact test, the gaseous new phase was completely taken out of the PVT cell at the third contact, and it was observed that the separated gas of the oil had a CO_2 concentration of 54%. After that contact, the test continued with more sequential

contacts (between CW and oil), and the formation of the new phase continued with a similarly stable trend. If the oil after the third contact is considered as a new oil sample with a 54% CO_2 content, which is then contacted with fresh carbonated water, the test reveals that the high CO_2 content of live oil would not adversely affect the dominant mechanism behind CWI, i.e. formation and growth of the gaseous new phase. In other words, in those reservoirs that there is already some CO_2 in the oil, the CO_2 dissolved in the reservoir oil is not a limiting factor for this mechanism to effectively improve oil recovery by CWI. From the multiple-contact test, a unique and distinct difference between carbonated water and conventional CO_2 (CO_2 flood) can be identified; in conventional CO_2 flooding, the nature of the mass transfer between CO_2 and the oil is a two-way process where the intermediate hydrocarbons would be extracted from the oil and CO_2 dissolves in the oil, which would consequently create a vaporising/condensing process. However, in carbonated water injection, a one-way mass transfer takes place in which CO_2 from CW would be dissolved in the oil and liberates lean gases from the oil, which results in an improvement in oil properties. It should be noted that due to the enrichment of the new phase with CO_2, slight vaporization of light components of the oil after infinite cell volume contacted was observed, however, this does not affect the oil quality. On the other hand, in bulk CO_2 injections (conventional CO_2 flood), significant compositional changes take place between the injection CO_2 and the oil that would adversely affect the oil quality. Carbonated water injection would not adversely affect the properties of remaining oil and after CWI other enhanced oil recovery techniques can be implemented too.

6.4 Conclusions

In this chapter, through a series of integrated multiple-contact test as well as slim tube experiments, it was attempted to comprehensively investigate the characteristic of the new phase forms in the oil due to the competition between CO_2 and dissolved hydrocarbon gas, its impact on oil recovery by CWI, and CWI behaviour and performance over a long distance. The following conclusions can be made:

1. CO_2 transfer from CW to live oil leads to a rapid nucleation and growth of a new gaseous phase. The formation of the new gaseous phase happened immediately after CW comes in contact with live oil. This finding form PVT experiment was

confirmed with the direct visualization experiments performed in Chapter 2 (section 2.3.2).

2. It was revealed that the new gaseous phase is a multi-component mixture of hydrocarbons starting with CH_4 and CO_2 at early stages and becoming richer towards the latter contacts. As the new phase gets richer with CO_2, the CO_2 can extract some intermediate components of the oil. Also, it was demonstrated that formation of new gaseous phase would not have an adverse effect on the oil density and viscosity.
3. CO_2 partitioning during CWI in live oil systems is much stronger than the one in dead oil systems due to formation and growth of the new phase, which would contribute to CO_2 transfer from carbonated water and hence a pseudo-partition coefficient was defined.
4. CW-oil phase behaviour is completely different from CO_2-oil phase behaviour. In CW-oil systems, there is a one-way mass transfer taking place where CO_2 is gradually transferred to the oil liberating lean gases inside the oil, which results in an improvement in oil properties. This is in contrast with the mutual mass transfer taking place between the free CO_2 and oil in a typical CO_2 flood which results in the remaining oil being heavier than the original oil.
5. Based on the multiple-contact experiment, even after infinite cell volume contacted, carbonated water would lose its CO_2 content gradually, which implies a steady transferring of CO_2 to the hydrocarbon phase (oil + new phase) and hence a steady oil expansion and oil recovery. Therefore, in porous media flooded by CW, oil ganglia would expand continuously leading to high overall swelling.
6. As a one-dimensional porous medium, the slim tube was found to be a valuable tool for studying the behaviour of CWI and its front propagation at considerable distances from the injection point. The one-dimensional characteristic of slim-tube would resemble the multiple contact tests in a way that the true pore-scale efficiency of CWI for recovering oil can be evaluated. CWI in slim tube experiment led to much stronger and earlier additional oil recovery compared to plain water injection. The additional oil recovery of 24% by CWI was shown to be due to formation and growth of new gaseous phase rather than other factors such as oil viscosity reduction.

7. The CO_2 breakthrough happened after the water breakthrough during CWI in a 60 ft long slim tube. This reveals that, as CW penetrates inside the reservoir, it can transfer its CO_2 till it becomes depleted from CO_2.

Chapter 7: Conclusions and Recommendations

7.1 Conclusions

The two main objectives on this thesis were to comprehensively investigate the underlying oil recovery mechanisms by CWI under realistic reservoir conditions and to quantify the level of additional oil recovery by CWI. For this aim, integrated experimental investigations including high-pressure high-temperature micromodel, contact angle, coreflood, imbibition, multiple-contact (PVT) and slim tube experiments were carried out. Followings are the main conclusions of this study:

7.1.1 Oil Recovery Mechanisms by CWI

7.1.1.1 Fluid-Fluid Mechanisms

a. Dead Oil System

Based on the observed pore-scale results, for the case of the dead oil system, CO2 mass transfer from CW into the oil leads to normal oil swelling and oil viscosity reduction, which in turn lead to oil reconnection, re-distribution and better oil recovery.

b. Live Oil System

In addition to normal oil swelling and oil viscosity reduction, which are the common mechanisms during CWI, the CO2 partitioning between CW and live oil leads to a new crucial phenomenon. The results of high-pressure high-temperature micromodel experiments revealed that the presence of associated (dissolved) gas in oil has a crucial role on the performance and oil recovery mechanisms by CWI. Based on the reported results, CO_2 partitioning between CW and ‘’live’’ oil (oil with dissolved gases) leads to rapid formation and growth of a new gaseous phase inside the oil phase that leads to better oil recovery by CWI under realistic reservoir conditions where oil has plenty amounts of dissolved gases. The rapid formation and growth of the new gaseous phase is a novel oil recovery mechanism of CWI introduced in this study.

Based on the visualization results, formation and continues growth of the new gaseous phase in the oil phase lead to better oil recovery through; (i) reconnection of the trapped oil and oil displacement, (ii) restricting the flow path of CW and diverting CW toward unswept areas of the porous medium, and (iii) creating a favourable three phase flow region with less residual oil saturation. Formation and growth of the new gaseous phase

is a game-changer in our understanding of how CW performs at real reservoir conditions where oil has dissolved gases.

To understand the characteristic of the new gaseous phase a series of PVT experiments were carried out. The results of multiple-contact (PVT) experiments revealed that the new gaseous phase is a multi-component mixture of hydrocarbons starting with CH_4 and CO_2 at early stages and becoming richer towards the latter contacts. As the new phase gets richer with CO_2, the CO_2 can extract some intermediate components of the oil. Also, it was demonstrated that formation of the new gaseous phase would not have an adverse effect on the oil density and viscosity.

Based on the results of multiple-contact (PVT) experiments, CW-oil phase behaviour is completely different from CO_2-oil phase behaviour. In CW-oil systems, there is one-way mass transfer taking place where CO_2 is gradually transferred into the oil liberating lean gases inside the oil, which results in an improvement in oil properties. This is in contrast with the mutual mass transfer taking place between the free CO_2 and oil in a typical CO_2 flood which results in the remaining oil being heavier than the original oil.

Based on the multiple-contact (PVT) experiment, even after infinite cell volume contacted, carbonated water would lose its CO_2 content gradually, which implies a steady transferring of CO_2 to the hydrocarbon phase (oil + new phase) and hence a steady oil expansion and oil recovery. This was the reason for the steady increase (growth) in the saturation of the new gaseous phase during CWI in the micromodel experiments. Therefore, in porous media flooded by CW, oil ganglia would expand continuously leading to high overall swelling.

7.1.1.2 Rock-Fluids Mechanisms

The results of a series of high-pressure high-temperature contact angle measurements at two different wettability states (water-wet and oil-wet) showed that CW has a promising potential for changing the wettability state of the oil-wet rock toward more water-wet conditions. It was observed that the extent of this wettability alteration is a direct function of the native (initial) wettability state of the rock and the saturation pressure of CW (or in another word CO_2 concentration in brine). Based on our wettability study, the extent of wettability alteration on the aged Calcite was higher than that on the aged Mica and Quartz. This is attributed to the dissolution of Calcite by the low-pH

carbonated water as well as the desorption of the adsorbed oil wetting layer that also took place in the Quartz and Mica measurements. Wettability alteration from oil-wet toward more water-wet conditions can affect the fluids distributions inside the porous medium and therefore oil recovery. Wettability alteration by CW is another oil recovery mechanisms of CWI that was introduced in this study.

7.1.2 Potential of CWI for Enhancing Oil Recovery

7.1.2.1 Coreflood Experiments

A series of coreflooding experiments were conducted using live oil to study the potential of CWI at core scale. The results of coreflood experiments confirmed the strong potential of CWI for improving oil recovery either as a secondary or tertiary injection scenario with the better performance of secondary. This is because of the higher oil saturation and better oil connectivity during secondary CWI compared to the tertiary CWI. Based on the results, carbonation level of CW has a positive impact on the performance of CWI.

Furthermore, the coreflooding results indicated that the native wettability state of the rock affects the performance of CWI. Secondary CWI in the mixed-wet system led to higher and earlier incremental oil recovery than the water-wet system. Based on the results, for the case of the water-wet system, the main oil recovery mechanism is the formation of the new gaseous phase, however, for the case of mixed to the oil-wet system the recovery mechanisms are both wettability alteration toward more water-wet conditions and formation of the new gaseous phase. As a result, under realistic reservoir conditions where the reservoir rock is mostly mixed-wet to oil-wet and the oil has plenty amounts of dissolved gases, CWI performs better and can improve the oil recovery more strongly. Furthermore, the coreflood results revealed that CWI is a good strategy for storing CO_2 in underground oil reservoirs.

7.1.2.2 Imbibition Experiments

To study the potential of CWI in fractured or heterogeneous oil reservoirs, where the viscous forces are negligible and the oil recovery is mainly happening due to the spontaneous imbibition mechanism, a series of high-pressure imbibition tests were conducted in this study. Based on the performed experiments, CW has a significant

potential for increasing the amount of imbibed water and consequently oil recovery for both sandstone and carbonate rocks.

The results of performed imbibition experiments indicated the better spontaneous imbibition of CW for the case of oil-wet carbonate rock compared to the oil-wet sandstone rock. The reasons for such behavior are i) stronger wettability alteration toward more water-wet conditions for the case of aged carbonate rock compared to the aged sandstone one, and ii) presence of mineral dissolution for the case of carbonate rock.

7.1.2.3 Slim Tube Experiment

To study the behaviour of CWI and its front propagations at considerable distances from the injection point slim tube was utilised in this study. CWI in slim tube experiment led to much stronger and earlier additional oil recovery (24% of the OOIP) compared to plain water injection that indicates its strong potential for improving oil recovery. The CO_2 breakthrough happened after water breakthrough during CWI in a 60 ft long slim tube. This behaviour occurs due to the stronger CO_2 solubility in crude oil than in water, which caused significant CO_2 transfer to the oil phase and the additional oil recovery of 24% of the original oil in place (OOIP).

To conclude, this study revealed two new and important oil recovery mechanisms of CWI, i.e. nucleation and growth of the gaseous new phase and wettability alteration. It also revealed the promising potential of CWI for improving oil recovery from oil reservoirs, where the reservoir rock is usually mixed-wet to oil-wet and oil has significant amounts of dissolved gases. The new oil recovery mechanisms of CWI introduced in this study can be game-changers in our understanding of how CWI performs at real reservoir conditions which would help us in identifying and targeting suitable oil reservoirs for this EOR technique.

7.2 Recommendations

To further investigate the potential of CWI and role of newly introduced oil recovery mechanisms by CWI and to improve our knowledge of this injection strategy some recommendations are made for future work.

7.2.1 Effect of Dissolved Gases Type

As it was revealed in this study, the presence of dissolved gases in oil is of great importance, and it significantly affects the performance of CWI under realistic reservoir conditions. Based on the results of this study, as carbonated water (CW) comes in contact with live oil (oil with dissolved gas) due to CO_2 exchange between CW and oil phase, a new phase nucleates inside the oil. As time elapses and more CW comes in contact with the oil, the saturation of the new phase increases. The results of the multiple-contact (PVT) experiment reveals that the new phase is initially made of CH_4 and with time it is getting richer with CO_2. However, to prepare the live oil (oil with dissolved gas) in this study, the reservoir oil was saturated with CH_4 at experimental conditions. The presence of other hydrocarbon gases or even CO_2 in the dissolved gases in the reservoir oil is quite usual. The presence of these gases in oil might affect the effectiveness of new phase and its saturation. This would directly affect the performance of CWI. As a result, performing a series of high-pressure high-temperature micromodel and multiple-contact experiment to investigate the impact of dissolved gases type on the effectiveness of the new phase and therefore on oil displacement efficiency by CWI is necessary.

7.2.2 Coupling the Low Salinity Brine Injection with CWI

Through this method not only the carbonation level of CW will be improved, which directly favours the performance of CWI, but also we might take advantage of the EOR mechanisms of low salinity brine injection. The positive impact of increasing carbonation level of CW was reported in Chapter 4 of this study. By increasing the carbonation level of CW, more CO_2 will be available for transferring into the oil and therefore formation of the new phase, oil swelling, and oil viscosity reduction will be stronger. This leads to stronger and earlier oil reconnection and distribution inside the porous medium that causes better oil production by CWI. Furthermore, it has been shown in the literature that low salinity brine injection in oil-wet sandstone reservoirs has the potential to improve oil recovery compared to high salinity brine injection [97]–[100]. Therefore, by combining low salinity brine injection with CWI, in addition to increasing CO_2 solubility, which is essential for the mechanisms of CWI, we may also take advantage from the positive impact of low salinity water injection.

7.2.3 Improving the Carbonation Level of CW by using Co-solvent

Through improving the carbonation level of CW, more CO_2 will be available for transferring into the oil; therefore, nucleation and growth of the new phase, oil swelling, and oil viscosity reduction will be stronger. This leads to stronger and earlier oil reconnection, distribution and displacement. The solubility of CO_2 in water can be improved by adding co-solvents to the water phase. In the literature, the use of some of these co-solvent materials has been reported. It should be noted that CO_2 co-solvents can be divided into two groups: physical and chemical absorbent agents. Chemical absorption is characterized by the occurrence of a chemical reaction between the gas (CO_2) component and a component in the liquid (water) phase. However, use of such co-solvents (chemical absorption) would not readily allow CO_2 to diffuse into the oil phase.

A physical absorbent, on the other hand, does not react chemically with the absorbed CO_2 and hence allows the partitioning of CO_2 when it comes in contact with oil. Below are some examples of physical absorbent materials for CO_2 [101]–[107]:

- Tributyl phosphate (TBP)
- Propylene carbonate (PC)
- Normal Methyl Pyrrolidone (NMP)
- Dimethyl Ether of Polyethylene Glycol (Selexol)
- Mixture of Polyethylene Glycol Dialkyl Ethers (Sepasolv)
- Methanol
- Acetone
- Hexamethyl phosphorotriamide
- Alkanes such as n-C_4 and n-$C1_0$ for the oil phase

7.2.4 Investigating Performance of CWI in Heterogeneous Carbonate Rocks

It is estimated that more than 60% of the world's oil and 40% of the world's gas reserves are held in carbonate reservoirs. The Middle East, for example, is dominated by carbonate fields, with around 70% of oil and 90% of gas reserves held within these reservoirs. Carbonate reservoirs are well known for their heterogeneous nature of the rock containing the fluids and their native initial wettability state which are mainly mixed-wet to oil-wet.

Based on the performed wettability and imbibition studies in this thesis, CW has this potential to change the wettability state of oil-wet carbonate rocks toward more water-wet conditions that favour oil recovery by CWI. Furthermore, the results of the micromodel experiments reveal that formation and growth of the new phase can lead to better oil recovery through restricting the flow path of carbonated brine and diverting it toward the unswept areas of the reservoir. This is of great importance for heterogeneous reservoirs where water is mainly flowing in the high-permeability or theft zoon and bypassing huge amount of oil in place. By restricting the flow path of water and diverting it into the unswept areas of reservoir some part of the untouched oil can be produced. In this study, through a coreflood experiment in a heterogeneous sandstone rock, the better performance of CWI compared to waterflooding was investigated. However, to further investigate the potential of CWI in heterogeneous reservoirs and to improve our knowledge of this injection scenario in heterogeneous carbonate reservoirs, performing more experiments is necessary.

7.2.5 Using a Nano-CT scanner

The best way to directly study the fluid's saturations and distributions inside the core and also the underlying physical processes involved in CWI, while running coreflood experiments, is to use a CT scanner. It is highly recommended that for the future works to utilize a nano-CT scanner to further study the role of newly introduced oil recovery mechanisms by CWI; i.e. formation of the new gaseous phase and wettability alteration, at core scale to further improve our knowledge of this injection strategy.

7.2.6 Developing a Numerical Model

To study the potential of CWI at real reservoir scale a reliable numerical model is needed to be developed. The model should be able to include the recovery mechanisms by CWI in particular wettability alteration and formation of the new gaseous phase. A reliable numerical simulation would help us in upscaling the experimental results to a real field application; therefore for field application of this EOR scenario having an accurate model is necessary.

References:

[1] F. F. C. Jr., *The Reservoir Engineering Aspects of Waterflooding.* SPE Monograph Series, 1993.

[2] G. P. Willhite, *Waterflooding*. SPE Textbook Series, 1986.

[3] J. F. B. and R. J. W. Stephen C. Rose, *The Design Engineering Aspects of Waterflooding*. SPE Monograph Series Vol. 11.

[4] L. W. Lake, *Enhanced Oil Recovery*. Prentic Hall, Englewood Cliffs, New Jersey 07632., 1989.

[5] B. V. Thomas F.S., Qin D., Plattner G., Tignor M., Allen S., Judith B., Xia Y., *IPCC-Intergovernmental Panel on Climate Change.* 2013.

[6] J. W. Martin, "Additional oil production through flooding with carbonated water," *Prod.Mon.*, 1951.

[7] J. W. and N. Y. T. Martin, "Process of recovering oil from oil fields involving the use of critically carbonated water," 1959.

[8] Johnson, W.E., "Laboratory experiments with carbonated water and liquid carbon dioxide as oil recovery agents.," *Prod. Mon.*, vol. 17, no. 1, 1952.

[9] L. Holm, "Carbon dioxide solvent flooding for increased oil recovery," *Trans., AIME*, vol. 216, pp. 225–231, 1959.

[10] M. Sohrabi, M. Riazi, M. Jamiolahmady, S. Ireland, and C. Brown, "Carbonated Water Injection for Oil Recovery and Co2 Storage," no. April 2014, pp. 1–30, 2008.

[11] M. Sohrabi, M. Riazi, M. Jamiolahmady, and S. Ireland, "Carbonated Water Injection (CWI) Studies," no. June, pp. 1–14, 2011.

[12] M. Sohrabi, M. Riazi, and M. Jamiolahmady, "Mechanisms of oil recovery by carbonated water injection," *SCA.* January, pp. 1–12, 2009.

[13] M. Sohrabi, N. I. Kechut, M. Riazi, M. Jamiolahmady, S. Ireland, and G. Robertson, "Safe storage of Co2 together with improved oil recovery by Co2-enriched water injection," *Chem. Eng. Res. Des.*, vol. 89, no. 9, pp. 1865–1872,

2011.

[14] M. Sohrabi, M. Riazi, M. Jamiolahmady, N. I. Kechut, S. Ireland, and G. Robertson, “Carbonated Water Injection (CWI) - A productive way of using CO2 for oil recovery and CO2 storage,” *Energy Procedia*, vol. 4, pp. 2192–2199, 2011.

[15] M. Riazi, M. Sohrabi, M. Jamiolahmady, S. Ireland, and C. Brown, “SPE 121170 Oil Recovery Improvement Using CO2 — Enriched Water Injection,” *Proc. Int. Pet. Technol. Conf.*, p. 14070, 2009.

[16] M. Riazi, M. Sohrabi, and M. Jamiolahmady, “Experimental Study of Pore-Scale Mechanisms of Carbonated Water Injection,” *Transp. Porous Media*, vol. 86, no. 1, pp. 73–86, 2011.

[17] M. Sohrabi, M. Tavakolian, A. Emadi, M. Jami, and S. Ireland, “Improved Oil Recovery and Injectivity By Carbonated Water Injection,” pp. 1–12, 2012.

[18] M. Sohrabi, N. I. Kechut, M. Riazi, M. Jamiolahmady, S. Ireland, and G. Robertson, “Coreflooding Studies to Investigate the Potential of Carbonated Water Injection as an Injection Strategy for Improved Oil Recovery and CO2 Storage,” *Transp. Porous Media*, vol. 91, no. 1, pp. 101–121, 2012.

[19] Y. Dong, C. Ishizawa, E. Lewis, and B. Dindoruk, “Carbonated Water Flood: What We Observed in Sand Pack Experiments,” *Int. Symp. Soc. Core Anal. held Austin, Texas, 18-21 Sept.*, pp. 1–12, 2011.

[20] N. Mosavat and F. Torabi, “Experimental evaluation of the performance of carbonated water injection (CWI) under various operating conditions in light oil systems,” *Fuel*, vol. 123, pp. 274–284, 2014.

[21] N. I. Kechut, M. Riazi, M. Sohrabi, and M. Jamiolahmady, “Tertiary Oil Recovery and CO2 Sequestration by Carbonated Water Injection (CWI),” *SPE Int. Conf. CO2 Capture, Storage, Util.*, 2013.

[22] N. I. Kechut, M. Sohrabi, and M. Jamiolahmady, “Experimental and numerical evaluation of carbonated water injection (CWI) for improved oil recovery and CO2 storage,” *SPE Eur. Annu. Conf. Exhib.*, 2011.

[23] M. Shakiba, S. Ayatollahi, and M. Riazi, “Investigation of oil recovery and CO2

storage during secondary and tertiary injection of carbonated water in an Iranian carbonate oil reservoir," *J. Pet. Sci. Eng.*, vol. 137, pp. 134–143, 2016.

[24] G. Shu, M. Dong, S. Chen, and P. Luo, "Improvement of CO2 EOR performance in water-wet reservoirs by adding active carbonated water," *J. Pet. Sci. Eng.*, vol. 121, pp. 142–148, 2014.

[25] L. Zuo and S. M. Benson, "Exsolution enhanced oil recovery with concurrent CO2 sequestration," *Energy Procedia*, vol. 37, pp. 6957–6963, 2013.

[26] L. Zuo, C. Zhang, R. W. Falta, and S. M. Benson, "Micromodel investigations of CO2 exsolution from carbonated water in sedimentary rocks," *Adv. Water Resour.*, vol. 53, pp. 188–197, 2013.

[27] N. Mosavat and F. Torabi, "Micro-optical analysis of carbonated water injection in irregular and heterogeneous pore geometry," *Fuel*, vol. 175, pp. 191–201, 2016.

[28] C. W. Hickok, R. J. Christensen, and H. J. Ramsay, "Progress Review of the K&S Carbonated Waterflood Project," *J. Pet. Technol.*, vol. 12, no. 12, pp. 20–24, 2013.

[29] C. Hickok and H. R. Jr, "Case Histories of Carbonated Waterfloods in Dewey-Bartlesville Field," *SPE Second. Recover. Symp.*, 1962.

[30] R. J. Christensen, "Carbonated Waterflood Results--Texas and Oklahoma," *Annu. Meet. Rocky Mt. Pet. Eng. AIME*, 1961.

[31] J. O. Scott, C. E. Forrester, and others, "Performance of Domes Unit Carbonated Waterflood-First Stage," *J. Pet. Technol.*, vol. 17, no. 12, pp. 1–379, 1965.

[32] A. B. Tumasyan, "Results of Field Experiment on Pumping Carbonated Water in the Stratum. Neft Khoz," vol. 12, pp. 31–35, 1973.

[33] H. J. J. Ramsay and F. Small, "Use of carbon dioxide for water injectivity improvement," *J. Pet. Technol.*, 1964.

[34] M. C. C. Kraus, A.D., C.M. Mendoza, "Injection of Acidulated Water of Carbonated Water," *ING Pet.*, vol. 10, no. 1, pp. 17–21, 1970.

[35] G. A. B. Y.P. Kislyakov, K.I. Kovalenko, "Treatment of well-Bore Area of

Injection Wells with Carbonated Water," *Neft Khoz*, vol. 45, no. 4, pp. 41–44, 1967.

[36] L. Nelson, J. Barker, T. Li, N. Thomson, M. Ioannidis, and J. Chatzis, "A field trial to assess the performance of CO2-supersaturated water injection for residual volatile LNAPL recovery," *J. Contam. Hydrol.*, vol. 109, no. 1–4, pp. 82–90, 2009.

[37] W. G. Anderson, "Wettability Literature Survey Part 3: The Effects of Wettability on the Electrical Properties of Porous Media," *J. Pet. Technol.*, vol. 38, no. 12, pp. 1371–1378, 1986.

[38] W. G. Anderson, "Wettability Literature Survey- Part 4: Effects of Wettability on Capillary Pressure," *J. Pet. Technol.*, vol. 39, no. 10, pp. 1605–1622, 1987.

[39] S. K. Masalmeh, "The effect of wettability heterogeneity on capillary pressure and relative permeability," *J. Pet. Sci. Eng.*, vol. 39, no. 3–4, pp. 399–408, 2003.

[40] J. R. Christensen, E. H. Stenby, and a. Skauge, "Review of WAG Field Experience," *SPE Reserv. Eval. Eng.*, vol. 4, no. January, pp. 3–5, 2001.

[41] N. R. Morrow, "Wettability and Its Effect on Oil Recovery," *J. Pet. Technol.*, vol. 42, no. 12, pp. 1476–1484, 1990.

[42] M. Alotaibi, R. Azmy, and H. Nasr-El-Din, "Wettability Challenges in Carbonate Reservoirs," *SPE Improv. Oil Recover. ...*, no. April, pp. 24–28, 2010.

[43] A. Y. Zekri, S. A. Shedid, and R. A. Almehaideb, "Possible alteration of tight limestone rocks properties and the effect of water shielding on the performance of supercritical CO2 flooding for carbonate formation," *SPE 15th Middle East Oil Gas Show Conf. MEOS 2007*, vol. 1, pp. 156–170, 2007.

[44] I. Fjelde, S. M. Asen, I. F. Iris, and S. M. A. Iris, "Wettability Alteration During Water Flooding and Carbon Dioxide Flooding of Reservoir Chalk Rocks (SPE-130992)," *Eage*, no. June 2010, pp. 14 – 17, 2010.

[45] N. Siemons, H. Bruining, H. Castelijns, and K. H. Wolf, "Pressure dependence of the contact angle in a CO2-H2O-coal system," *J. Colloid Interface Sci.*, vol. 297, no. 2, pp. 755–761, 2006.

[46] R. Sakurovs and S. Lavrencic, “Contact angles in CO2-water-coal systems at elevated pressures,” *Int. J. Coal Geol.*, vol. 87, no. 1, pp. 26–32, 2011.

[47] N. Shojai Kaveh, E. S. J. Rudolph, K. H. A. A. Wolf, and S. N. Ashrafizadeh, “Wettability determination by contact angle measurements: HvbB coal-water system with injection of synthetic flue gas and CO 2,” *J. Colloid Interface Sci.*, vol. 364, no. 1, pp. 237–247, 2011.

[48] P. Chiquet, D. Broseta, and S. Thibeau, “Wettability alteration of caprock minerals by carbon dioxide,” *Geofluids*, vol. 7, no. 2, pp. 112–122, 2007.

[49] J. Wan, Y. Kim, and T. K. Tokunaga, “Contact angle measurement ambiguity in supercritical CO2-water-mineral systems: Mica as an example,” *Int. J. Greenh. Gas Control*, vol. 31, pp. 128–137, 2014.

[50] J. Jung and J. Wan, “Supercritical CO2 and Ionic Strength E ff ects on Wettability of Silica Surfaces : Equilibrium Contact Angle Measurements,” *Energy & Fuels*, vol. 26, pp. 6053–6059, 2012.

[51] R. Farokhpoor, “CO2 Wettability Behavior During CO2 Sequestration in Saline Aquifer -An Experimental Study on Minerals Representing Sandstone and Carbonate,” *Energy Procedia*, vol. 37, pp. 5339–5351, 2013.

[52] D. Yang, Y. Gu, and P. Tontiwachwuthikul, “Wettability determination of the crude oil− reservoir brine− reservoir rock system with dissolution of CO 2 at high pressures and elevated temperatures,” *Energy & Fuels*, vol. 22, no. 4, pp. 2362–2371, 2008.

[53] N. Shojai Kaveh, E. S. J. Rudolph, P. Van Hemert, W. R. Rossen, and K. H. Wolf, “Wettability evaluation of a CO2/water/bentheimer sandstone system: Contact angle, dissolution, and bubble size,” *Energy and Fuels*, vol. 28, no. 6, pp. 4002–4020, 2014.

[54] a. Ameri, N. S. Kaveh, E. S. J. Rudolph, K. Wolf, R. Farajzadeh, and J. Bruining, “Investigation on Interfacial Interactions among Crude Oil–Brine–Sandstone Rock–CO 2 by Contact Angle Measurements,” *Energy & Fuels*, vol. 27, no. 2, pp. 1015–1025, 2013.

[55] C. Chalbaud, M. Robin, J. M. Lombard, F. Martin, P. Egermann, and H. Bertin,

"Interfacial tension measurements and wettability evaluation for geological CO2 storage," *Adv. Water Resour.*, vol. 32, no. 1, pp. 98–109, 2009.

[56] J. L. Dickson, G. Gupta, T. S. Horozov, B. P. Binks, and K. P. Johnston, "Wetting phenomena at the CO_2/water/glass interface," *Langmuir*, vol. 22, no. 5, pp. 2161–2170, 2006.

[57] S. M. Al-Mutairi, S. A. Abu-Khamsin, T. M. Okasha, S. Aramco, and M. E. Hossain, "An experimental investigation of wettability alteration during CO2 immiscible flooding," *J. Pet. Sci. Eng.*, vol. 120, pp. 73–77, 2014.

[58] W. G. Anderson, "Wettability Literature Survey- Part 1: Rock/Oil/Brine Interactions and the Effects of Core Handling on Wettability," *J. Pet. Technol.*, vol. 38, no. 10, pp. 1125–1144, 1986.

[59] P. Recovery and K. Takamura, "Influence of Electrical Surface Charges on the Wetting Properties of Crude Oils," no. August, pp. 332–340, 1989.

[60] G. Vigil, Z. Xu, S. Steinberg, and J. Israelachvili, "Interactions of Silica Surfaces," *Journal of Colloid and Interface Science*, vol. 165, no. 2. pp. 367–385, 1994.

[61] P. M. Dove and C. M. Craven, "Surface charge density on silica in alkali and alkaline earth chloride electrolyte solutions," *Geochim. Cosmochim. Acta*, vol. 69, no. 21, pp. 4963–4970, 2005.

[62] E. V Gribanova, "Dynamic contact angle23 temperature dependence and the influence of the state of the adsorption film," vol. 39, pp. 235–255, 1992.

[63] L. Liu and J. S. Buckley, "Alteration of wetting of mica surfaces," *J. Pet. Sci. Eng.*, vol. 24, no. 2–4, pp. 75–83, 1999.

[64] M. V. Maslova, L. G. Gerasimova, and W. Forsling, "Surface properties of cleaved mica," *Colloid J.*, vol. 66, no. 3, pp. 322–328, 2004.

[65] D. P. C.A.J. Appelo, *Geochemistry, Groundwater and Pollution*. CRC Press, 2005.

[66] M. M. Thomas, J. A. Clouse, and J. M. Longo, "Adsorption of organic compounds on carbonate minerals. 1. Model compounds and their influence on

mineral wettability," *Chem. Geol.*, vol. 109, no. 1–4, pp. 201–213, 1993.

[67] T. Austad, S. Strand, E. J. Høgnesen, and P. Zhang, "Seawater as IOR Fluid in Fractured Chalk," *2005 SPE Int. Symp. Oilf. Chem.*, no. 3, pp. 1–10, 2005.

[68] T. Austad, S. Strand, M. Madland, T. Puntervold, and R. Korsnes, "Seawater in Chalk: An EOR and Compaction Fluid," *SPE Reserv. Eval. Eng.*, vol. 11, no. August, pp. 648–654, 2008.

[69] S. Strand, E. J. Høgnesen, and T. Austad, "Wettability alteration of carbonates - Effects of potential determining ions (Ca2+ and SO42-) and temperature," *Colloids Surfaces A Physicochem. Eng. Asp.*, vol. 275, no. 1–3, pp. 1–10, 2006.

[70] P. Zhang and T. Austad, "Wettability and oil recovery from carbonates: Effects of temperature and potential determining ions," *Colloids Surfaces A Physicochem. Eng. Asp.*, vol. 279, no. 1–3, pp. 179–187, 2006.

[71] P. Zhang, M. T. Tweheyo, and T. Austad, "Wettability alteration and improved oil recovery by spontaneous imbibition of seawater into chalk: Impact of the potential determining ions Ca2+, Mg2+, and SO42-," *Colloids Surfaces A Physicochem. Eng. Asp.*, vol. 301, no. 1–3, pp. 199–208, 2007.

[72] J. J. M. Werner Stumm, *aquatic Chemistry: Chemical Equilibria and Rates in Natural Waters*. New York.: JohnWiley & Sons, 1995.

[73] M. Riazi and M. Sohrabi, "Oil recovery improvement using CO2-enriched water injection," *SPE Eur. Annu. Conf. Exhib.*, 2009.

[74] B. J. Bourblaux and J. Kalaydjlan, "Experimental Study of Cocurrent and Countercurrent Flows in Natural Porous Media," *Soc. Pet. Eng. J.*, no. August, pp. 361–368, 1990.

[75] G. Hirasaki and D. L. Zhang, "Surface Chemistry of Oil Recovery From Fractured, Oil-Wet, Carbonate Formations," *SPE J.*, vol. 9, no. 02, pp. 151–162, 2004.

[76] A. Seethepalli, B. Adibhatla, and K. Mohanty, "Physicochemical Interactions During Surfactant Flooding of Fractured Carbonate Reservoirs," *SPE J.*, vol. 9, no. 4, pp. 17–21, 2004.

[77] B. Adibhatla and K. Mohanty, “Oil Recovery From Fractured Carbonates by Surfactant-Aided Gravity Drainage: Laboratory Experiments and Mechanistic Simulations,” *SPE Reserv. Eval. Eng.*, vol. 11, no. 1, pp. 119–130, 2008.

[78] T. Austad, B. Matre, J. Milter, A. Sævareid, and L. Øyno, “Chemical flooding of oil reservoirs 8. Spontaneous oil expulsion from oil- and water-wet low permeable chalk material by imbibition of aqueous surfactant solutions,” *Colloids Surfaces A Physicochem. Eng. Asp.*, vol. 137, no. 1–3, pp. 117–129, 1998.

[79] D. L. Zhang, “Wettability alteration and instantaneous imbibition in oil-wet carbonate formation,” in *Proceedings of 8th International Symposium on Reservoir Wettabilit*, 2004.

[80] X. Xie, W. W. Weiss, Z. Tong, and N. R. Morrow, “Improved Oil Recovery From Carbonate Reservoirs by Chemical Stimulation,” *SPE J.*, no. May, pp. 1–10, 2005.

[81] P. Chen and K. K. Mohanty, “Surfactant-Mediated Spontaneous Imbibition in Carbonate Rocks at Harsh Reservoir Conditions,” *SPE J.*, vol. 18, no. 1, pp. 1–13, 2013.

[82] G. Sharma and K. K. Mohanty, “Wettability alteration in high temperature and high salinity carbonate reservoirs,” *SPE Annu. Tech. Conf. Exhib. 2011, ATCE 2011*, vol. 5, no. 2010, pp. 4092–4106, 2011.

[83] L. Wang and K. Mohanty, “Enhanced oil recovery in gas-flooded, carbonate reservoirs by wettability-altering surfactants,” *Proc. - SPE Annu. Tech. Conf. Exhib.*, vol. 3, no. October 2013, pp. 2448–2464, 2013.

[84] and T. A. E.J. Høgnesen, S. Strand, “Waterflooding of preferential oil-wet carbonates: oil recovery related to reservoir temperature and brine composition,” in *14th SPE Europec Biennial Conference*, 2005.

[85] K. J. Webb, C. J. J. Black, and G. Tjetland, “IPTC 10506 A Laboratory Study Investigating Methods for Improving Oil Recovery in Carbonates,” *Int. Pet. Technol. Conf.*, pp. 1–7, 2005.

[86] P. Zhang, M. T. Tweheyo, and T. Austad, “Wettability alteration and improved

oil recovery in chalk: The effect of calcium in the presence of sulfate," *Energy and Fuels*, vol. 20, no. 5, pp. 2056–2062, 2006.

[87] J. M. Perez, S. W. Poston, and Q. J. Sharif, "Carbonated Water Imbibition Flooding: An Enhanced Oil Recovery Process for Fractured Reservoirs," *Proc. SPE/DOE Enhanc. Oil Recover. Symp.*, 1992.

[88] J. S. O. Grape, and S.W. Poston, "Imbibition Flooding with CO2-Enriched Water," in *SCA*, 1990.

[89] I. F. M. A. A. Zuta, "Improvement of Spontaneous Imbibition in Carbonate Rocks by CO2- saturated Brine," in *16th European Symposium on Improved Oil Recovery*, 2011.

[90] D. Yang and Y. Gu, "Interfacial Interactions of Crude Oil-Brine-CO2 Systems under Reservoir Conditions," *SPE Annu. Tech. Conf. Exhib. Houston, Texas, 26-29 Sept.*, 2004.

[91] D. Yang, P. Tontiwachwuthikul, and Y. Gu, "Interfacial Tensions of the Crude Oil + Reservoir Brine + CO 2 Systems at Pressures up to 31 MPa and Temperatures of 27 °C and 58 °C," *J. Chem. Eng. Data*, vol. 50, no. 4, pp. 1242–1249, 2005.

[92] R. Grigg, "Dynamic phase composition, density, and viscosity measurements during CO2 displacement of reservoir oil," *SPE International Symposium on Oilfield Chemistry*. 1995.

[93] M. Ding, X.-A. Yue, H. Zhao, and W. Zhang, "Extraction and Its Effects on Crude Oil Properties During CO $_2$ Flooding," *Energy Sources, Part A Recover. Util. Environ. Eff.*, vol. 35, no. 23, pp. 2233–2241, 2013.

[94] K. D. Hagedorn and F. M. Orr, "Component Partitioning in CO2/Crude Oil Systems: Effects of Oil Composition on CO2 Displacement Performance," *SPE Adv. Technol. Ser.*, vol. 2, no. 02, pp. 177–184, 1994.

[95] L. Holm and V. Josendal, "Effect of Oil Composition on Miscible-Type Displacement by Carbon Dioxide," *Soc. Pet. Eng. J.*, vol. 22, no. 1, 1982.

[96] U. W. R. Siagian and R. B. Grigg, "SPE 39684 The Extraction of Hydrocarbons from Crude Oil by High Pressure C02," 1998.

[97] M. Cissokho, S. Boussour, P. Cordier, H. Bertin, and G. Hamon, “Low salinity oil recovery on clayey sandstone: Experimental study,” *Petrophysics*, vol. 51, no. 5, pp. 305–313, 2010.

[98] R. A. Nasralla, M. B. Alotaibi, and H. A. Nasr-El-Din, “Efficiency of Oil Recovery by Low Salinity Water Flooding in Sandstone Reservoirs,” *SPE West. North Am. Reg. Meet.*, no. 1967, 2011.

[99] R. A. Nasralla, M. A. Bataweel, and H. A. Nasr-El-Din, “Investigation of Wettability Alteration by Low Salinity Water in Sandstone Rock,” *SPE Offshore Eur. Oil Gas Conf. Exhib.*, p. 12, 2011.

[100] R. Nasralla and H. Nasr-El-Din, “Coreflood Study of Low Salinity Water Injection in Sandstone Reservoirs,” *Proc. SPE/DGS Saudi Arab. Sect. Tech. Symp. Exhib.*, no. May, pp. 15–18, 2011.

[101] O. O. Blanc, C., J. Y. Chenard, J. J. Delpuech, “Physical solvent absorption of carbon dioxide and hydrogen sulphide for the deacidification of industrial gaseous mixtures,” 1979.

[102] J. Xia, M. Jödecke, A. P. S. Kamps, and G. Maurer, “Solubility of CO2 in (CH3OH + H2O),” *J. Chem. Eng. Data*, vol. 49, no. 6, pp. 1756–1759, 2004.

[103] M. Jödecke, Á. Pérez-Salado Kamps, and G. Maurer, “Experimental Investigation of the Solubility of CO_2 in (Acetone + Water),” *J. Chem. Eng. Data*, vol. 52, no. 3, pp. 1003–1009, 2007.

[104] Á. Pérez-Salado Kamps, R. Sing, B. Rumpf, and G. Maurer, “Influence of NH 4 Cl, NH 4 NO 3 , and NaNO 3 on the Simultaneous Solubility of Ammonia and Carbon Dioxide in Water,” *J. Chem. Eng. Data*, vol. 45, no. 5, pp. 796–809, 2000.

[105] V. Abovsky and S. Watanasiri, “Equation of state mixing rule based on activity coefficient model: Explicit solution for ‘finite pressure approach,’” *Fluid Phase Equilib.*, vol. 158–160, pp. 259–269, 1999.

[106] L. L. Williams, E. M. Mas, and J. B. Rubin, “Vapor - Liquid Equilibrium in the Carbon Dioxide - Propylene Carbonate System at High Pressures,” pp. 282–285, 2002.

[107] M. Jödecke, J. Xia, Á. Pérez-Salado Kamps, and G. Maurer, “Solubility of carbon dioxide in aqueous, salt-containing solutions of methanol or acetone,” *Chem. Eng. Technol.*, vol. 27, no. 1, pp. 31–34, 2004.